**♻EPA**

# Evaluation of Unsaturated/Vadose Zone Models for Superfund Sites

**♻EPA**

# EVALUATION OF UNSATURATED/VADOSE ZONE
# MODELS FOR SUPERFUND SITES

by

D. L. Nofziger, Jin-Song Chen, and C. T. Haan
Oklahoma Agricultural Experiment Station
Oklahoma State University
Stillwater, Oklahoma 74078

CR-818709

## Project Officer

Joseph R. Williams
Extramural Activities and Assistance Division
Robert S. Kerr Environmental Research Laboratory
Ada, Oklahoma 74820

ROBERT S. KERR ENVIRONMENTAL RESEARCH LABORATORY
OFFICE OF RESEARCH AND DEVELOPMENT
U.S. ENVIRONMENTAL PROTECTION AGENCY
ADA, OKLAHOMA 74820

♻ Printed on Recycled Paper

## DISCLAIMER NOTICE

Margins for all numbered pages:

- $1''$ foot
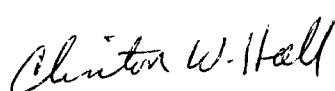-center PAGE NUMBER side to side.

# FOREWORD

EPA is charged by Congress to protect the Nation's land, air, and water systems. Under a mandate of national environmental laws focused on air and water quality, solid waste management and the control of toxic substances, pesticides, noise and radiation, the Agency strives to formulate and implement actions which lead to a compatible balance between human activities and the ability of natural systems to support and nurture life.

The Robert S. Kerr Environmental Research Laboratory is the Agency's center of expertise for investigation of the soil and subsurface environment. Personnel at the laboratory are responsible for management of research programs to: (a) determine the fate, transport and transformation rates of pollutants in the soil, unsaturated and the saturated zones of the subsurface environment; (b) define the processes to be used in characterizing the soil and subsurface environment as a receptor of pollutants; (c) develop techniques for predicting the effect of pollutants on ground water, soil and indigenous organisms; and (d) define and demonstrate the applicability and limitations of using natural processes, indigenous to the soil and subsurface environment, for the protection of this resource.

Mathematical models are useful tools for evaluating potential remediation treatments. However, models require users to specify various parameters characteristic of the site and chemical of interest. These parameters are not known without error. Many parameters vary over time and space in manners which are unknown. This is especially true when models are used to predict future events. This uncertainty in input parameters is associated with an uncertainty in model output which should be recognized by the model user. This research analyzes several transport models for unsaturated soils and quantifies the sensitivity and uncertainty of model outputs to changes in input parameters. This information will help users understand the importance of different parameters, identify parameters which must be determined at the site, interpret model results and apply their findings to specific problems.

Clinton W. Hall
Director
Robert S. Kerr Environmental
Research Laboratory

# ABSTRACT

Mathematical models of water and chemical movement in soils are being used as decision aids for defining ground water protection practices for superfund sites. Numerous transport models exist for predicting movement and degradation of hazardous chemicals through soils. Many of these require extensive input parameters which include uncertainty due to soil variability and unknown future weather. The impact of uncertain model parameters upon the model output is not known. Model users need an understanding of this impact so they can measure the appropriate parameters for the site and incorporate the uncertainty in the model predictions into their decisions. This report summarizes research findings which address the sensitivity and uncertainty of model output due to uncertain input parameters.

The objective of the research was to determine the sensitivity and uncertainty of travel time, concentration, mass loading and pulse width of contaminants at the water table. The four models selected for this analysis were RITZ, VIP, CMLS and HYDRUS. All of the models are designed to estimate movement of solutes through unsaturated soils. The models span a considerable range in detail and intended use. This report presents information on the sensitivity of these models to changes and uncertainties in input parameters. It does not intend to assess the appropriateness of any model for a particular use nor uncertainty due to the model chosen.

Model parameters investigated include soil properties such as organic carbon content, bulk density, water content, hydraulic conductivity. Chemical properties examined include organic carbon partition coefficient and degradation half-life. Site characteristics such as rooting depth, recharge rate, weather, evapotranspiration and runoff were examined when possible in the models. Model sensitivity was quantified in the form of sensitivity and relative sensitivity coefficients. The sensitivity coefficient is useful when calculating the absolute change in output due to a known change in a single parameter. Relative sensitivity is useful for determining the relative change in an output corresponding to a specified relative change in one input parameter. Relative sensitivity can also be used to compare the sensitivity of different parameters. Results are presented in graphical and tabular forms.

The study found that large uncertainty exists in many model outputs due to the combination of sensitivity and high parameter variability. The study found that predicted movement of contaminants was greater when the natural variability of rainfall was incorporated into the model than when only average fluxes were used. This is because major rainstorms that result in large fluxes of water and high leaching are essentially ignored when average flux values are used. The study reaffirms that uncertainty is pervasive in natural systems and that results of modeling efforts presented in a deterministic fashion may be misleading. Rather than presenting absolute predictions of solute movement, results of model studies should present the probabilities of various outcomes.

This report evaluates model sensitivity for a specific scenario. There is abundant evidence that the sensitivity and uncertainty are highly dependent on the scenario being modeled and the parameters used. Therefore these results will not serve to define sensitivity for the general model user. That need can only be met by incorporating algorithms into each computer code to enable the user to obtain these sensitivity and uncertainty estimates for the specific conditions and parameters of interest.

# SYMBOLS

| | |
|---|---|
| b | Clapp-Hornberger constant |
| CV | coefficient of variation |
| $C_a$ | concentration of contaminant in air |
| $C_o$ | concentration of contaminant in oil |
| $C_s$ | concentration of contaminant adsorbed on soil phase |
| $C_w$ | concentration of contaminant in water |
| cov(x) | (k x k) covariance matrix of the input parameters |
| cov(y) | (n x n) covariance matrix of model outputs |
| var(x) | (k x 1) vector of variances of parameters |
| $D_{ew}$ | effective diffusion-dispersion coefficient of the solute in water |
| $D_{ea}$ | effective diffusion-dispersion coefficient of the solute in air |
| d | soil depth |
| f | model output |
| $f(m_x)$ | (n x 1) vector of model outputs where the model is evaluated at $\underline{m}_x$ |
| h | soil-water pressure head |
| $h_0$ | osmotic head |
| $h_{50}$ | pressure head at which transpiration is reduced by 50% |
| K | unsaturated hydraulic conductivity function |
| $K_d$ | partition coefficient between the solid phase and the water phase |
| $K_{oc}$ | organic carbon partition coefficient |
| $K_s$ | saturated hydraulic conductivity |
| $K_{\alpha,w}$ | linear partition coefficients between the $\alpha$ phase (air, soil, or oil) and the water, w, phase |
| k | number of model input parameters in uncertainty analysis |
| L | distance |
| m | empirical constant, $m = 1 - 1/\beta$ |
| $\underline{m}_y$ | (n x 1) vector of mean model outputs |
| $\underline{m}_x$ | (k x 1) vector of mean parameter values |
| n | number of model outputs |
| OC | organic carbon content |
| PET | potential evapotranspiration |
| Q | sink or source term |
| p | power constant in stress response function |
| $q_a$ | flux of air |
| q | steady-state flux of water |
| $q_w$ | flux of water |
| R | retardation factor |
| $r_w, r_a, r_o$ | sink/source terms for contaminant uptake, decay, and production in water, air and oil |
| S | model sensitivity |
| $\underline{S}$ | (n x k) matrix of sensitivity coefficients of model outputs to input parameters |
| $S_r$ | relative sensitivity |
| T | travel time |
| t | time |
| v | pore water velocity |
| x | model input parameter in the matrix $\underline{x}$ |
| $\underline{x}$ | (k x 1) vector of model parameters |
| z | position coordinate |

## SYMBOLS (continued)

| | |
|---|---|
| $\alpha$ | van Genuchten (shape) parameter |
| $\beta$ | van Genuchten (shape) parameter |
| $\mu_{\alpha}$ | degradation rate constant for the contaminant in $\alpha$ phase (water, soil, air, or oil) |
| $l$ | pore-connectivity factor |
| $\phi$ | porosity |
| $\rho$ | soil bulk density |
| $\sigma$ | stress-response function |
| $\theta_a$ | volume fraction of air in the soil |
| $\theta$, $\theta_w$ | water content of soil on a volume basis |
| $\theta_s$ | saturated water content |
| $\theta_r$ | residual water content |
| $\theta_o$ | volume fraction of oil in the soil |
| $\varsigma$ | normalized root uptake distribution function |

# CONTENTS

# SECTION 1

## INTRODUCTION

Mathematical models of water and chemical movement in soils are being used as decision aids for defining remediation practices for Superfund sites. Numerous transport models exist for predicting movement and degradation of hazardous chemicals through soils. Many of these require extensive input parameters which are often not measured and which include uncertainty due to inherent soil variability at the site and due to unknown future weather patterns. Little information exists on impact of uncertain input data on outputs from these models. Model users want guidelines for the selection and use of models under these conditions. This report summarizes research findings which address these issues of uncertainty.

One objective of this research was to determine the sensitivity of several transport model outputs to changes in values of input parameters required by the models. Sensitivity as used here refers to the change in model output resulting from a specified change in an input parameter. We can observe the sensitivity of an output by examining differences in graphs of the model outputs for different inputs in the expected range. If differences in output are large, we conclude the output is sensitive to these changes in inputs. If differences in output are small, we conclude the output is not sensitive to these changes in inputs. Quantitative definitions of sensitivity are given later in this report.

In order to use models in making decisions about remediation practices appropriate for Superfund sites, the model must predict the future behavior of the contaminant. The use of models in a predictive manner introduces added uncertainty. For example, chemical leaching depends upon water movement through the unsaturated soil. This water movement is dependent upon the amount and distribution of water entering the soil and hence upon future weather. Since we do not know future weather, there is an uncertainty in that model input. As a result, there is an uncertainty in the model output. Natural variability of the soil parameters within the area of interest is another source of input parameter uncertainty. The second part of this report computes the uncertainty in model outputs due to uncertainty in one or more model inputs. This uncertainty can be incorporated into decisions utilizing model predictions.

The sensitivity of a particular output to changes in model inputs depends upon the entire set of parameters used in the model and upon the total system being analyzed. The general scenario modeled in this study was that of a site containing an initial contaminant layer near the soil surface. The thickness of that layer is known. None of the contaminant is present below this layer. No more contaminant enters the soil profile during the simulation period. Model outputs of interest include (1) the time at which the contaminant reaches the water table, (2) the amount of contaminant entering the saturated zone, (3) the width of the contaminant pulse at the water table, and (4) the concentration of the contaminant entering the ground water.

This report presents results for four models. The models differ substantially in their intended use, assumptions and processes included, input data requirements, computer requirements, and ease of use. Model selection is a critical step in model use. Each of these models is appropriate for certain uses. None of them are appropriate for all uses. Results of the sensitivity and uncertainty analyses are presented for the models. It is not our intent to compare the predictive ability of the models. The cited references for each model should be consulted for detail on the formulation of the various models.

1

# SECTION 2

## MODEL DESCRIPTIONS

The four models selected for this analysis are RITZ, VIP, CMLS, and HYDRUS. Overviews of the models are presented in Tables 2.1 to 2.4. RITZ, VIP, and CMLS were written as management tools. HYDRUS is better suited for detailed research use by scientists. All four models include sorption of the contaminant by soil and advection or movement of the contaminant with water. RITZ and VIP include sorption on an immobile oil phase as well as a vapor transport component. RITZ and VIP assume uniform soil properties and steady water flow. CMLS and HYDRUS can be used in layered soils and unsteady, unsaturated water flow. HYDRUS includes hydrodynamic dispersion. This section presents the common general governing equations which form the framework for the models. The models are then described along with assumptions inherent in them.

RITZ and VIP were developed for use at waste disposal sites where oil can be mixed with the contaminant and where movement of the contaminant in the vapor phase may be significant. If we assume the flow and transport processes are one dimensional and the oil phase is immobile, the governing transport equation in unsaturated soil is given by

$$\theta_w \frac{\partial C_w}{\partial t} + \rho \frac{\partial C_s}{\partial t} + \theta_o \frac{\partial C_o}{\partial t} + \theta_a \frac{\partial C_a}{\partial t} = \theta_w D_{ew} \frac{\partial^2 C_w}{\partial z^2}$$
$$+ \theta_a D_{ea} \frac{\partial^2 C_a}{\partial z^2} - q_w \frac{\partial C_w}{\partial z} - q_a \frac{\partial C_a}{\partial z} + r_w + r_a + r_o$$

(1)

where $C_w$ is the concentration of contaminant in water, $C_a$ is the concentration of contaminant in air, $C_o$ is the concentration of contaminant in oil, $C_s$ is the concentration of contaminant adsorbed on soil phase, $\rho$ is the soil bulk density, $\theta_w$ is the water content of the soil on a volume basis, $\theta_a$ is the volume fraction of air in the soil, $\theta_o$ is the volume fraction of oil in the soil, $q_a$ is the flux of air, $q_w$ is the flux of water, $D_{ew}$ is effective diffusion-dispersion coefficient of the solute in water, $D_{ea}$ is effective diffusion-dispersion coefficient of the solute in air, and $r_w$, $r_a$, $r_o$ represent sink/source terms for contaminant uptake, decay, and production in water, air and oil, respectively. In equation 1, z is the position coordinate and t is time. Partitioning of the contaminant between the phases is approximated by the equation

$$C_\alpha = K_{\alpha,w} C_w$$

(2)

where $K_{\alpha,w}$ is the linear partition coefficients between the $\alpha$ phase (air, soil, or oil) and the water phase. First-order degradation of the chemical is generally assumed in each phase so

$$\frac{dC_\alpha}{dt} = -\mu_\alpha C_\alpha$$

(3)

where $\mu_\alpha$ is the degradation rate constant for the contaminant in $\alpha$ phase (water, soil, air, or oil). Physical constraints imply the sum of the volume fractions of air, water, and oil must equal the porosity of the soil, $\phi$, or

$$\phi = \theta_a + \theta_w + \theta_o$$

(4)

2

Table 2.1. Characteristics of the Regulatory and Investigative Treatment Zone (RITZ) model (Nofziger, Williams, and Short, 1988).

Intended Use:
    Estimate movement and fate of hazardous chemicals during land treatment of oily wastes

Processes Included:
    Mass flow of chemical with soil water
    Linear reversible sorption of chemical on soil and oil
    Partitioning of chemical to vapor and diffusion from soil
    Degradation of hazardous chemical and oil

Data Requirements:
    Soil Properties (Assumed constant with depth)
        Organic carbon content
        Bulk density
        Saturated water content
        Saturated hydraulic conductivity
        Clapp - Hornberger constant (water characteristic parameter)
    Site Characteristics
        Plow zone and Treatment zone depths
        Recharge rate (Assumed constant over time)
        Evaporation rate (Assumed constant over time)
        Air temperature (Assumed constant over time)
        Relative humidity (Assumed constant over time)
        Sludge application rate
        Concentration of pollutant in sludge
        Diffusion coefficient of water vapor in air
    Pollutant Properties
        Organic carbon partition coefficient
        Oil-water partition coefficient
        Henry's law constant
        Diffusion coefficient in air
        Degradation half-life (Assumed constant with depth and time)
    Properties of Oil
        Concentration of oil in sludge
        Density of oil
        Degradation half-life of oil

Model Outputs:
    Fraction of pollutant degraded, leached, and volatilized
    Flux density and total mass of pollutant lost to atmosphere
    Flux density and total mass of pollutant leached
    Location of pollutant as a function of time
    Concentration of pollutant in liquid, solid, vapor, and oil phases as functions of time
    Concentration of oil as a function of time

Computer Requirements:
    DOS-based computer with math coprocessor. The model requires only a few seconds to simulate the movement and degradation of the chemical through the plow zone and treatment zone.

3

Table 2.2. Characteristics of the Vadose Zone Interactive Processes (VIP) model
(Stevens, Grenney, and Yan, 1989).

Intended Use:
Evaluate the fate of a hazardous substance in the unsaturated zone of the soil for land treatment of oily wastes

Processes Included:
Transport of the contaminant by advection with soil water
Transport of the contaminant by advection and dispersion in the air phase (Note: advection was not implemented in the source code)
Transport of the oxygen (diffusion only) in the air
Linear reversible sorption of chemical on soil and oil
Partitioning of the contaminant between air, oil, soil, and water
Partitioning of oxygen between air, oil, and water
Oxygen-limited degradation in air, water, oil, and soil

Data Requirements:
Soil Properties
Soil porosity
Bulk density
Saturated hydraulic conductivity
Clapp and Hornberger constant

Site Characteristics
Plow zone depth
Treatment zone depth
Mean daily recharge rate during each month
Temperature during each month in plow zone
Temperature during each month in treatment zone
Temperature correction coefficient for each month of the year
Sludge application rate
Pollutant concentration in the sludge
Weight fraction of oil in waste
Weight fraction of water in sludge
Density of sludge
Application period
Application frequency within application period

Pollutant Properties
Oil-water partition coefficient for plow zone and lower treatment zone
Air-water partition coefficient for plow zone and lower treatment zone
Soil-water partition coefficient for plow zone and lower treatment zone
Degradation constant in oil for plow zone and lower treatment zone
Degradation constant in water for plow zone and lower treatment zone
Dispersion coefficient in unsaturated pore space
Adsorption/desorption rate constant between water and soil
Adsorption/desorption rate constant between water and oil
Adsorption/desorption rate constant between water and air

4

Table 2.2. Continued.

Data Requirements (Continued)

Oxygen Properties
    Oil-air partition coefficient for plow zone and lower treatment zone
    Water-air partition coefficient for plow zone and lower treatment zone
    Oxygen half-saturation constant with respect to the oil degradation
    Oxygen half-saturation constant in air phase in the plow zone
    Oxygen half-saturation constant in air phase in the treatment zone
    Oxygen half-saturation constant in oil phase in the plow zone
    Oxygen half-saturation constant in oil phase in the treatment zone
    Oxygen half-saturation constant in water phase in the plow zone
    Oxygen half-saturation constant in the water phase in treatment zone
    Stoichiometric ratio of the oxygen to the pollutant consumed
    Stoichiometric ratio of the oxygen to the oil consumed
    Oxygen transfer rate coefficient between the oil and air phases
    Oxygen transfer rate coefficient between the water and air phases

Properties of Oil
    Density of oil
    Degradation rate constant of oil

Model Outputs:
    Concentration of pollutant in air, water, oil, and soil as function of depth and time
    Concentration of oxygen in air, water, oil, and soil as function of depth and time
    Concentration of oil in air, water, and soil as function of depth and time
    Amount of pollutant remaining in the plow zone and treatment zone
    Amount of pollutant leached below treatment zone
    Fraction of pollutant in air, water, oil, and soil phases
    Fraction of pollutant in plow zone and treatment zone

Computer Requirements:
    DOS-based computer. The model requires a few seconds to simulate 10 years of movement and degradation.

**Table 2.3. Characteristics of Chemical Movement in Layered Soils (CMLS) model (Nofziger and Hornsby, 1986, 1988)**

**Intended Use:**

Estimate the movement and degradation of pesticides through unsaturated soils; Serve as a management tool for managing soil applied chemicals.

**Processes Included:**

Mass flow of chemical with soil water
Sorption of chemical on soil
Degradation of chemical

**Data Requirements:**

Soil Properties (required for each soil layer)
    Depth of bottom of soil layer
    Organic carbon content
    Bulk density
    Saturated water content
    Water content at "field capacity"
    Water content at "permanent wilting point"

Site Characteristics
    Daily infiltration (can be estimated in model from daily weather, supplemental irrigation, and SCS curve number)
    Daily evapotranspiration (can be estimated in model from daily weather or pan evaporation)

Chemical Properties
    Organic carbon partition coefficient (or actual partition coefficient for each soil layer)
    Degradation half-life for each soil layer
    Amount of chemical applied
    Depth of chemical at application
    Date of chemical application

**Model Outputs:**

Depth of center of mass of chemical as a function of time
Amount of chemical in the soil profile as a function of time
Amount of chemical passing specified depth as function of time
Travel time of chemical to specified depth
Probability of exceeding different depths at a specified time
Probability of exceeding different amounts passing specified depth

**Computer Requirements:**

DOS or UNIX based computer. Movement and degradation are calculated on a daily time step to accommodate dynamic changes in infiltration and evapotranspiration. A single simulation requires approximately one second per year on a 80386/387 DOS-based computer. Computational time may increase to several hours when using Monte Carlo techniques and making hundreds of simulations.

## Table 2.4. Characteristics of the HYDRUS model (Kool and van Genuchten, 1991).

**Intended Use:**

To simulate the movement of water and dissolved solutes in one-dimensional variably saturated and layered porous media

**Processes Included:**

Transient, unsaturated water flow with hysteresis in the soil hydraulic properties
Root water uptake
Transport of chemical by advection, molecular diffusion and hydrodynamic dispersion
Linear or non-linear reversible sorption
First-order degradation

**Data Requirements:**

Soil Properties (for each soil layer)
    Depth of soil layers
    Saturated water content
    Saturated hydraulic conductivity
    Bulk density
    Retention parameters for main water desorption and wetting curves
    Residual water content

Site Characteristics
    Uniform or step-wise rainfall intensity

Pollutant Properties (for each soil layer)
    Molecular diffusion coefficient
    Dispersivity
    Decay coefficient for dissolved phase
    Decay coefficient for adsorbed phase
    Freundlich isotherm coefficients

Root Water Uptake Parameters:
    Power constant in stress-response function
    Pressure head at which transpiration is reduced by 50%
    Root density as a function of depth

**Model Outputs:**

Water content and pressure head distribution with time
Concentration of chemical as a function of time and depth
Cumulative infiltration and drainage
Cumulative root water uptake from the soil profile
Cumulative amount of chemical entering the soil profile
Cumulative amount of chemical leaving the soil profile
Amount of chemical remaining in the soil

**Computer Requirements:**

DOS-based computer. The numerical solution requires 4 to 24 hours on a 80386/387 based computer to simulate transport for ten years.

Water flow is described using the equation

$$\frac{\partial \theta_w}{\partial t} = \frac{\partial}{\partial z}[K(\frac{\partial h}{\partial z} - 1)] - Q \tag{5}$$

where K is the unsaturated hydraulic function, h is the water pressure head, and Q is the sink or source term. Equations 1 to 5 can be used to estimate contaminant fate with advection, dispersion, sorption, root solute uptake, evaporation, partitioning to oil and vapor phases, degradation, water flow, and evapotranspiration. They serve as a general framework for discussing equations used in the RITZ, VIP, CMLS, and HYDRUS models. The specific governing equation for each model can be derived after incorporating model-specific assumptions.

RITZ Model: The conceptual framework of RITZ was developed by Short (1985) and implemented as an interactive program by Nofziger et al. (1988). It was created to predict the fate of contaminants mixed with oily wastes and applied to land treatment sites. RITZ considers the soil to be made up of two parts as shown in Figure 2.1. The upper region is called the plow zone. The sludge containing contaminant and oil are mixed uniformly within this depth. Below the plow zone is the treatment zone which contains no oil. The model simulates movement of the contaminant through both zones. For this study, the plow zone represents the portion of soil containing the contaminant at the beginning of the simulation. The bottom of the treatment zone represents the water table depth.

RITZ contains many simplifying assumptions. (1) Soil properties are assumed to be uniform throughout the profile. (2) The flux of water through the soil is assumed to be constant with depth and with time. (3) Oil is assumed to be immobile so it does not move out of the plow zone. (4) Both oil and contaminant degrade as first-order processes. (5) Partitioning of the contaminant between phases is linear, instantaneous, and reversible. (6) Dispersion in water phase is small and can be ignored. (7) The soil water content and unsaturated hydraulic conductivity can be described by the Clapp and Hornberger equation (1978).

Assumption 7 above is used to determine the soil water content, $\theta_w$, from the saturated conductivity, $K_s$, and the average recharge rate, q, using the equation

$$\theta_w = \phi[\frac{q}{K_s}]^{\frac{1}{2b + 3}} \tag{6}$$

where $\phi$ is the soil porosity or saturated water content and b is the Clapp-Hornberger constant (which depends on soil properties). Incorporating these simplifications into equation 1 results in

$$\theta_w\frac{\partial C_w}{\partial t} + \rho\frac{\partial C_s}{\partial t} + \theta_o\frac{\partial C_o}{\partial t} + \theta_a\frac{\partial C_a}{\partial t} = -q\frac{\partial C_w}{\partial z} \tag{7}$$

Short (1985) derived analytical solutions for the total concentration in plow zone, the total concentration in the treatment zone, the time at which the top and bottom of the solute slug reaches a specific depth, and the amount lost due to volatilization.

VIP Model: This model was developed by Stevens et al. (1989) to solve the same general problem as that of RITZ. Thus Figure 2.1 describes the conceptualized soil system for VIP. Again, a sludge containing a contaminant and oil are uniformly mixed into the plow zone and the movement of the contaminant is predicted. Several assumptions made in RITZ are modified in VIP. For example, VIP considers the dynamics of sorption rather than assuming instantaneous equilibrium between phases. It also simulates
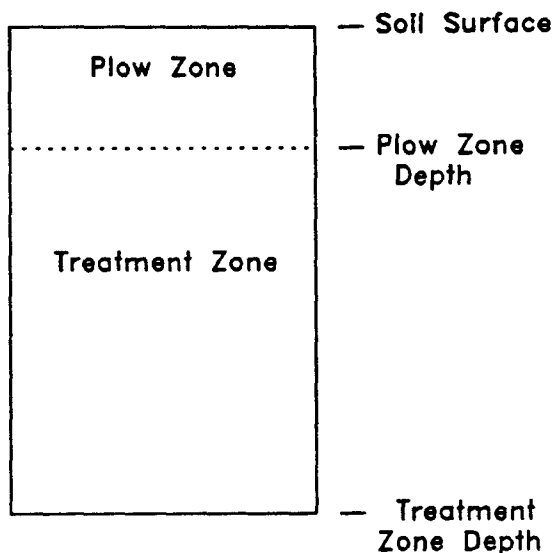
8

```
                    ┌──────────────┐    ── Soil Surface
                    │   Plow Zone   │
                    │              │
                    │··············│    ── Plow Zone
                    │              │        Depth
                    │              │
                    │Treatment Zone│
                    │              │
                    │              │
                    │              │
                    │              │
                    └──────────────┘    ── Treatment
                                           Zone Depth
```

Figure 2.1. Conceptualized soil system for RITZ and VIP models.

oxygen diffusion in the air-phase and oxygen-limited degradation of the contaminant, and diffusion of contaminant in air phases. When oxygen is not limiting, sorption is instantaneous, and diffusion of contaminant is negligible, the equations in VIP are essentially the same as those in RITZ. VIP solves the differential equations numerically. As a result, the recharge rate or flux of water passing through the soil can change with time on a monthly basis.

CMLS Model: Nofziger and Hornsby (1986) developed CMLS to describe the movement and degradation of pesticides in layered soils. The model was intended as a management tool. It was designed to utilize parameters which are readily available to most users. In CMLS, the soil profile is composed of up to 20 layers. Soil and chemical properties are constant within a layer, but may change from layer to layer. Water balance is computed on a daily basis to account for infiltration and evapotranspiration. To apply this model to the problem of interest in this study, the initial distribution of the chemical was divided into a series of thin layers. Movement of each chemical layer was then simulated. The amount of chemical entering the water table was the sum of the amounts for all the layers.

Simplifying assumptions made in the development of CMLS include: (1) Chemicals move in the liquid phase with the soil water only. Movement in the vapor phase can be ignored. (2) Partitioning of chemicals between the soil solids and water can be described by the linear, reversible model with instantaneous equilibrium as in equation 2. (3) Dispersion and diffusion of the chemical can be ignored. (4) Degradation can be described as a first-order process (Eqn. 3). The degradation constant can vary with depth, but not with time. (5) Water moves through the soil system in a piston-like manner. All water in the soil is pushed ahead of new water entering the soil. (6) The soil drains instantly to the "field capacity" water content after each infiltration event. (7) Water is removed from each layer in the root zone in proportion to the available water stored in that layer. (8) Chemicals move downward in the soil system. Upward movement of chemicals is ignored. (9) No oil is present in the soil system.

The CMLS model estimates the amount of chemical at a particular position as a function of time. It does not calculate concentrations. If concentrations are needed, the user must estimate the mass of water in

which the chemical is mixed and then calculate the concentration from this mass of water and the mass of chemical leached.

Incorporating the assumptions listed above into equation 1 we obtain

$$R\frac{\partial C}{\partial t} = -\frac{q_w}{\theta}\frac{\partial C}{\partial z}$$

(8)

where $R = (1 + \rho K_d)/\theta_w$ is the retardation factor and $q_w$ is the flux of water. Bond and Phyllips (1990) proved that this equation implies that the solute velocity or the rate of change in position of a constant concentration, $\partial z/\partial t \mid_C$, under unsteady flow conditions is given by

$$\frac{\partial z}{\partial t}\bigg|_C = \frac{q_w}{\theta_w + \rho K_d}$$

(9)

or

$$\frac{\Delta z}{\Delta t}\bigg|_C = \frac{q_w}{\theta_w + \rho K_d}$$

(10)

Equation 10 is used in CMLS to calculate the change in position of the contaminant on a daily basis. The water content, $\theta_w$, is replaced by the water content at field capacity, and $q_w$ is the daily flux passing the current solute position.

HYDRUS Model: HYDRUS is a finite element model developed by Kool and van Genuchten (1991). The model makes fewer simplifying assumptions than the other models and is the most computationally demanding. In this model the soil is described by properties at a series of points. Soil and chemical properties can vary from one location to another. The user has great flexibility to define initial conditions to represent the site of interest. Assumptions incorporated into HYDRUS include the following: (1) Partitioning of chemical between solid and water can be described by the linear, reversible model with instantaneous equilibrium between phases; (2) Movement in the vapor phase can be ignored; (3) No oil is present in the system.

Applying these assumptions to equation 1 yields

$$R\frac{\partial C_w}{\partial t} = D_{ew}\frac{\partial^2 C_w}{\partial z^2} - v\frac{\partial C_w}{\partial z}$$

(11)

where $C_w$ is the concentration of the contaminant in water at time t and position z, R is the retardation factor defined previously and v is the pore water velocity ($v = q_w/\theta_w$).

10

The root water uptake, Q, (Eqn. 5) for HYDRUS is given by

$$Q(z,t) = PET(t) \cdot \varsigma(z)\sigma(h,h_0)$$ (12)

where $\varsigma(z)$ is a normalized root uptake distribution function, $PET(t)$ is the potential evapotranspiration and $\sigma$ is the stress-response function. The stress response function is given by

$$\sigma = \frac{1}{1 + [(h + h_0)/h_{50}]^p}$$ (13)

where $h_{50}$ is the pressure head at which transpiration is reduced by 50%, $h_0$ is the osmotic head, and p, is a power constant. The osmotic head is proportional to the solute concentration, $C_w$. HYDRUS solves equations 11-13 with equation 5 using a finite element method with mass-lumping and upstream-weighting techniques (Kool and van Genuchten, 1991).

# SECTION 3

## SENSITIVITY AND UNCERTAINTY

Sensitivity: As explained in the introduction, the sensitivity of a model refers to the change in a selected model output resulting from a specified change in an input parameter. Mathematically the sensitivity coefficient, S, is defined as

$$S = \frac{\partial f}{\partial x} \tag{14}$$

where f represents the output of interest and x represents the input parameter (McCuen, 1973). If the model output can be written in a nice symbolic form, the sensitivity can be applied by differentiating f symbolically. Often the models are too complex for this approach. In that case the sensitivity can be calculated using the difference equation

$$S = \frac{\Delta f}{\Delta x} \tag{15}$$

Model sensitivity, S, as defined by equations 14 and 15 is the change in model response per unit change in the input parameter. The change in model output due to a small change in input parameter is given by

$$\Delta f = S \Delta x \tag{16}$$

where Δf is the change in output f due to a change of Δx in the input parameter. That is, the product of the sensitivity, S, and the change in input parameter is the change in model output.

The value of S calculated from these equations has units associated with it. This makes it difficult to compare sensitivities for different input parameters. This problem can be overcome by using the relative sensitivity, $S_r$, given by

$$S_r = \frac{\partial f}{\partial x} \frac{x}{f} = S \frac{x}{f} \tag{17}$$

or

$$S_r = \frac{\Delta f}{\Delta x} \frac{x}{f} = S \frac{x}{f} \tag{18}$$

12

where f is the value of the model output and x is the value of the input parameter. The relative sensitivity can be used to estimate the relative change in model output, $\Delta f/f$, from the relative change in input parameter, $\Delta x/x$, using the equation

$$\frac{\Delta f}{f} = S_r \frac{\Delta x}{x} \qquad (19)$$

So the relative sensitivity is a measure of the relative change in model output corresponding to a relative change in the input parameter. In other words, $S_r$ gives the percentage change in model response for each one percent change in the input parameter. If the absolute value of $S_r$ is greater than 1, the absolute value of the relative change in model output will be greater than the absolute value of the relative change in input parameter. If the absolute value of $S_r$ is less than 1, the absolute value of the relative change in model output will be less than the absolute value of the relative change in input. Note that the sensitivity coefficient reflects the change in output function due to a single input parameter. Uncertainty analysis is used to incorporate simultaneous changes in more than one parameter and variability of the parameters.

Uncertainty: Two approaches are frequently used for determining model uncertainty. The first approach, a deterministic approach, is most applicable to models in which explicit equations can be written for model outputs as functions of input parameters. The first-order second-moment uncertainty analysis is the most used technique in this approach. It provides a method of calculating the mean, variance, and covariance of model outputs from means, variances, covariances and sensitivity coefficients for the model inputs. The following equations are used to determine these quantities (Dettinger and Wilson, 1981).

$$\underline{y} = \underline{f}(\underline{x}) \qquad (20)$$

$$\underline{m}_y = \underline{f}(m_x) + \frac{1}{2}\frac{\partial^2 f}{\partial x^2} var(x) \qquad (21)$$

$$\underline{cov(y)} = \underline{S}\ \underline{cov(x)}[\underline{S}]^T \qquad (22)$$

where n is the number of model outputs, k is the number of model input parameters, $\underline{y}$ is a (n x 1) vector of model outputs, $\underline{f}(\underline{x})$ is the (n x 1) vector of model outputs with inputs of $\underline{x}$, $\underline{x}$ is a (k x 1) vector of model parameters, $\underline{m}_y$ is a (n x 1) vector of mean model outputs, $\underline{f}(\underline{m}_x)$ is a (n x 1) vector of model outputs where the model is evaluated at $\underline{m}_x$, $\underline{m}_x$ is a (k x 1) vector of mean parameter values, $\partial^2 f/\partial x^2$ is a (n x k) matrix of 2nd partial derivatives of $\underline{f}(\underline{m}_x)$, $\underline{cov(x)}$ is a (k x k) covariance matrix of the input parameters, $\underline{cov(y)}$ is a (n x n) covariance matrix of model outputs, $\underline{var(x)}$ is a (k x1) vector of variances of parameters, and $\underline{S}$ is a (n x k) matrix of sensitivity coefficients of model outputs to input parameters. First-order second-moment analysis is most appropriate when the model is not too nonlinear in its parameters and the coefficients of variation of the parameters are small.

The second approach is a stochastic approach. It is often used when the explicit formula for a complex system can not be obtained or the equations are too cumbersome. Monte Carlo simulation is an example of this approach. The Monte Carlo technique requires knowledge of the frequency distribution of each input parameter and the correlations among these parameters. Input parameters are generated at random from

13

the parameter populations so that means and correlations are preserved. Each set of inputs is used in the model to compute the outputs of interest. This process is repeated many times until the probability distribution of the model outputs is defined. Summary statistics of the outputs are then computed or the entire distribution is used in the analysis.

Previous Work: Knopman and Voss (1987, 1988) conducted a sensitivity analysis of one-dimensional solute transport in steady water flow. They presented implications for parameter estimation and sampling design. Jarvis (1991) developed a deterministic model of non-steady state water flow and solute transport in soils containing macropores. He found that pesticide leaching was sensitive to soil hydraulic properties defining the macropore region and to pesticide properties. Recently, Cawlfield and Wu (1993) used probabilistic approach to examine the sensitivity to transport parameters in 1-d steady water flow. They indicated that the probabilistic outcome is most sensitive to likely changes in flow velocity and the reaction terms. Diffusion coefficient can also be an important uncertain variable but only when it has significantly higher uncertainty than any other variables. Skyes et al. (1985) determined the relative sensitivity of performance to various parameters. Sensitivity analyses have been performed to guide a gradient search algorithm for parameter estimation (Newman, 1980). Dettinger and Wilson (1981) used a sensitivity analysis as the framework for first and second-order, second-moment uncertainty analysis.

While the sensitivity of model output to the input parameters is of importance, the overall uncertainty of the model prediction is of concern to model users. Burges and Lettenmaier (1975) subdivided uncertainty into two categories. Type I uncertainty is the result of the use of an incorrect model which has correct (deterministic) parameters. This uncertainty can be subdivided into inappropriate model selection and inherent modeling error. Type II uncertainty results from the choice of the correct model with incorrect, or uncertain parameters (including data used for estimating parameters, initial and boundary conditions, and sink/source terms). These two types of uncertainty define the total uncertainty of the model, measured by the mean square error or variance in output variable. The uncertainty analysis incorporated in this report is primarily limited to Type II uncertainty. This is particularly relevant when using models as decision-making tools for remediation practices appropriate for Superfund sites since the model must predict the future behavior of the contaminant when inputs such as future weather at the site are unknown.

Dettinger and Wilson (1981) used the first-order second-moment techniques to estimate the uncertainty of ground-water flow due to uncertain flow parameters. Loague et al. (1990) used the same technique to investigate the impact of data uncertainty in soil, climatic, and chemical information on assessment of pesticide leaching. Zhang et al. (1993) used the Monte Carlo method to characterize the uncertainty of solute movement through soils. They found the uncertainty resulting from weather variability at a site was approximately the same as that due to uncertainty in soil and chemical parameters.

Illustration: This section illustrates the use of the sensitivity coefficient, S, and the relative sensitivity, $S_r$, by applying them to a simplified transport equation. The illustration is informative in itself and it forms a basis for understanding results for more complex models which follow. If we assume that the soil is uniform, that it contains no oil, that dispersion and movement in the vapor phase are negligible, and that water is flowing at a constant rate through the soil, the time, T, required for a solute to move a distance L is given by

$$T = L\frac{(\theta + \rho K_d)}{q} \tag{23}$$

where q is the steady-state flux of water, $\rho$ is the bulk density, $K_d$ is the partition coefficient ($K_d$ is the product of the organic carbon partition coefficient, $K_{oc}$, and the organic carbon content, OC, or $K_d = K_{oc}OC$), and $\theta$ is the soil water content. Table 3.1 lists the sensitivity and relative sensitivity of the travel time to the parameters in the model. These expressions were obtained by applying equations 14 and 17 to

14

Table 3.1. Sensitivity and relative sensitivity of predicted travel time to different variables based on equation 23.

| Parameter | Sensitivity, $S$ | Relative Sensitivity, $S_r$ |
|-----------|------------------|-----------------------------|
| $q$ | $\dfrac{-L(\theta + \rho K_{oc}OC)}{q^2}$ | $-1$ |
| $\theta$ | $\dfrac{L}{q}$ | $\dfrac{\theta}{\theta + \rho K_{oc}OC}$ |
| $\rho$ | $\dfrac{LK_{oc}OC}{q}$ | $\dfrac{\rho K_{oc}OC}{\theta + \rho K_{oc}OC}$ |
| $K_{oc}$ | $\dfrac{L\rho OC}{q}$ | $\dfrac{\rho K_{oc}OC}{\theta + \rho K_{oc}OC}$ |
| $OC$ | $\dfrac{L\rho K_{oc}}{q}$ | $\dfrac{\rho K_{oc}OC}{\theta + \rho K_{oc}OC}$ |
| $K_d$ | $\dfrac{L\rho}{q}$ | $\dfrac{\rho K_d}{\theta + \rho K_d}$ |

equation 23. Examination of Table 3.1 reveals that the relative sensitivity for bulk density, $\rho$, partition coefficient, $K_d$, organic carbon partition coefficient, $K_{oc}$, and organic carbon content, OC, are identical.

Figure 3.1 shows graphs of travel time, sensitivity, and relative sensitivity of the travel time to the flux of water, q (Equations in Table 3.1). The lower graph is a plot of equation 23 for different values of recharge rate. The middle graph is a plot of sensitivity to recharge rate. The upper figure is a plot of the relative sensitivity which has a value of -1 for all recharge rates. This relative sensitivity implies that the relative change in travel time is equal in magnitude to the relative change in recharge, but it is opposite in sign. So, if the recharge rate increases by 10%, the travel time decreases by 10%. Figures 3.2 and 3.3 show similar graphs for water content and partition coefficient. In those cases, the relative sensitivities increase as the parameters increase. In both cases the relative sensitivities are less than 1 so the relative change in travel time is less than the relative change in either of these parameters. In each figure, model input parameters were held constant except for the parameter of interest. The standard values used were 1 mm day$^{-1}$ for q, 1.65 Mg m$^{-3}$ for $\rho$, 80 cm$^3$ g$^{-1}$ for $K_{oc}$, 0.14 % for OC, and 0.242 m$^3$ m$^{-3}$ for $\theta$. The value of $K_d$ was 0.112 cm$^3$ g$^{-1}$. The distance, L, was 1.5 m.

Since $S_r$ is dimensionless, it can be used to compare model sensitivity to parameters having different units. For instance, $S_r$ is -1 for recharge rate; $S_r$ is 0.567 for water content, $S_r$ is 0.071 for partition coefficient. So the travel time for the standard input values stated above is most sensitive to recharge rate, and least sensitive to partition coefficient. These results are applicable to the set of input parameters used. Large changes in sensitivity occur as parameters change.

Relative sensitivity can also be used to approximate the required accuracy of a model parameter if the desired accuracy in the model response is known. By rewriting equation 18 as

$$\frac{\Delta x}{x} = \frac{1}{S_r} \frac{\Delta f}{f} \tag{24}$$

we can calculate the required accuracy ($\Delta x/x$) of the input parameter x given the relative sensitivity for x and the required accuracy in the model output ($\Delta f/f$). For example, if we want to estimate T to within 10% of its actual value, then the required accuracy ($\Delta x/x$) for q, $\theta$, and $K_d$ are 10%, 17.6% and 140.8% respectively. Clearly q is the one parameter must be known the most accurately of these three parameters. Note that each of these percentages assume that the other parameters in the model are entered without error. Zhang et al. (1993) demonstrated a technique based on uncertainty analysis, sampling theory, and knowledge of parameter variability for estimating sample size requirements when measuring parameters for simulation models.

Uncertainty analyses of this simplified model was carried out using both first-order second moment and Monte Carlo techniques. The parameters were assumed to be normally distributed and not correlated. Coefficients of variation (CV) of 0.05 for q, 0.05 for $\rho$, 0.20 for $K_{oc}$, 0.40 for OC, and 0.10 for $\theta$ were used. The estimated mean for travel time from equation 21 is 641.0 days with a standard deviation of 134 days. Monte Carlo simulation with 500 runs resulted in a mean value of 642.8 days and standard deviation of 135 days. The two methods are in good agreement for this model and these parameters.

When the sensitivity for each parameter and the covariance matrix cov(x) is known, the ratio of the relative contribution of each parameter to total variance can be used to rank the importance of the input parameter. We illustrate this by using our simplified transport model with five input parameters, q, $\theta$, $\rho$, OC, and $K_{oc}$. Expanding equation 22 for this case yields

16

$$Var(T) = [S_q, S_\theta, S_p, S_{oc}, S_{K_{oc}}] \begin{vmatrix} cov(q,q) & cov(q,\theta) & cov(q,p) & cov(q,oc) & cov(q,K_{oc}) \\ cov(\theta,q) & cov(\theta,\theta) & cov(\theta,p) & cov(\theta,oc) & cov(\theta,K_{oc}) \\ cov(p,q) & cov(p,\theta) & cov(p,p) & cov(p,oc) & cov(p,K_{oc}) \\ cov(oc,q) & cov(oc,\theta) & cov(oc,p) & cov(oc,oc) & cov(oc,K_{oc}) \\ cov(K_{oc},q) & cov(K_{oc},\theta) & cov(K_{oc},p) & cov(K_{oc},oc) & cov(K_{oc},K_{oc}) \end{vmatrix} \begin{vmatrix} S_q \\ S_\theta \\ S_p \\ S_{oc} \\ S_{K_{oc}} \end{vmatrix} \quad (25)$$

where Var(T) is the overall uncertainty or variance of travel time, $S_x$ is the sensitivity of T with respect to parameter x, and $cov(x_1, x_2)$ is the covariance between parameter $x_1$ and $x_2$. The expression

$$\frac{S_q^2(cov(q,q) + cov(q,\theta) + cov(q,p) + cov(q,oc) + cov(q,K_{oc}))}{Var(T)} \quad (26)$$

represents the relative contribution of q to the overall uncertainty of travel time. Using the standard parameter values and CV's listed above, Var(T) is 17902 $day^2$. The relative contributions of $p$, q, $\theta$, $K_{oc}$, and OC to this overall uncertainty are 0.011, 0.057, 0.074, 0.172 and 0.687, respectively. In other words, organic carbon accounts for 68.7% of the total uncertainty, organic carbon partition coefficient 17.2%, water content 7.4%, flux 5.7%, and bulk density 1.1% for this set of parameters and covariances. These results incorporate both sensitivity and parameter variability. Note the much greater contribution of organic carbon than bulk density to the total uncertainty even though the two parameters have the same relative sensitivities. This is due to the much larger natural variation in organic carbon than in bulk density. Nichols and Freshley (1993) used analysis of variance as an alternative method to partition total uncertainty to different parameters in a model.
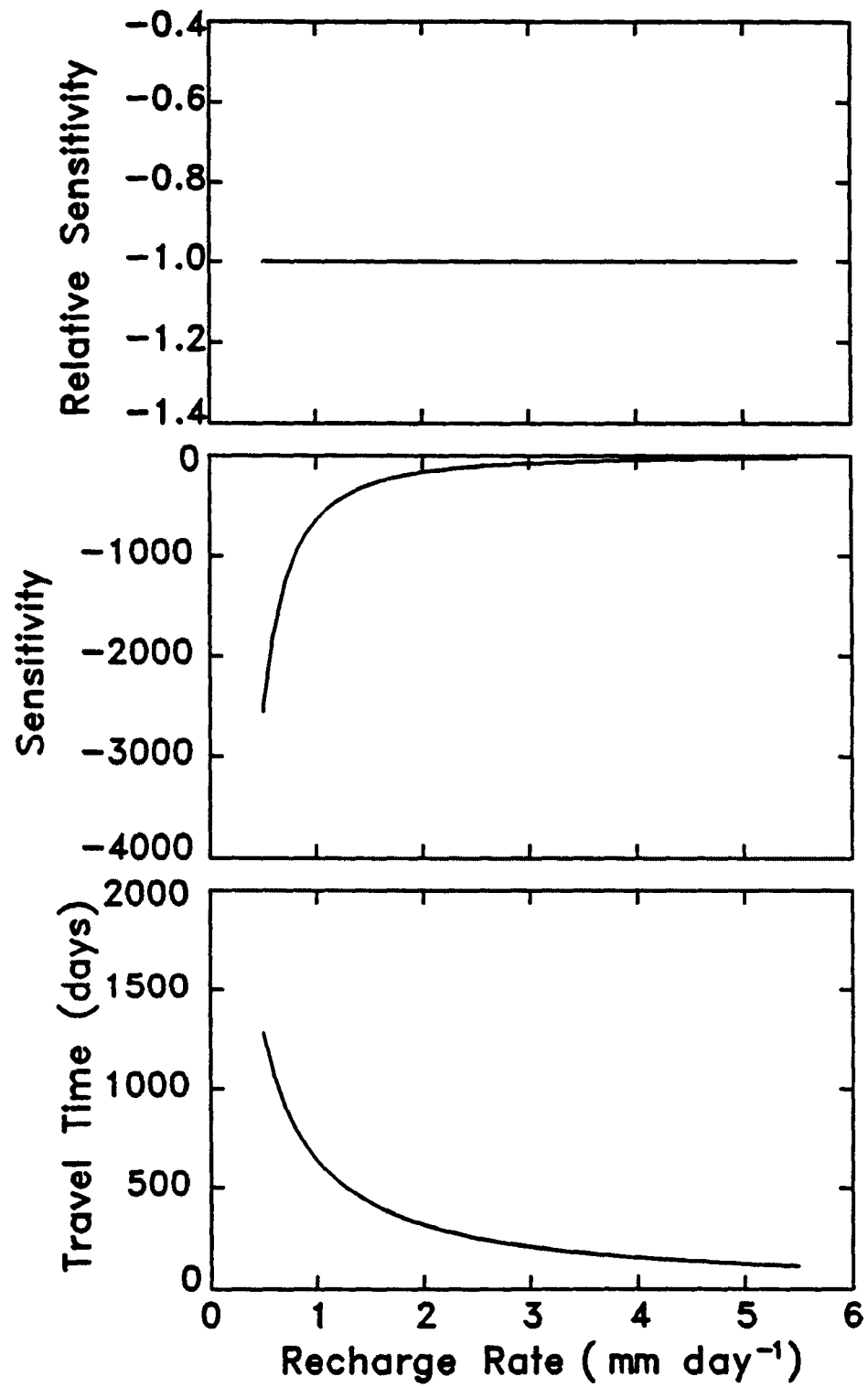
Figure 3.1. Sensitivity of travel time for different values of recharge rate for a simplified model (Eqn. 23).
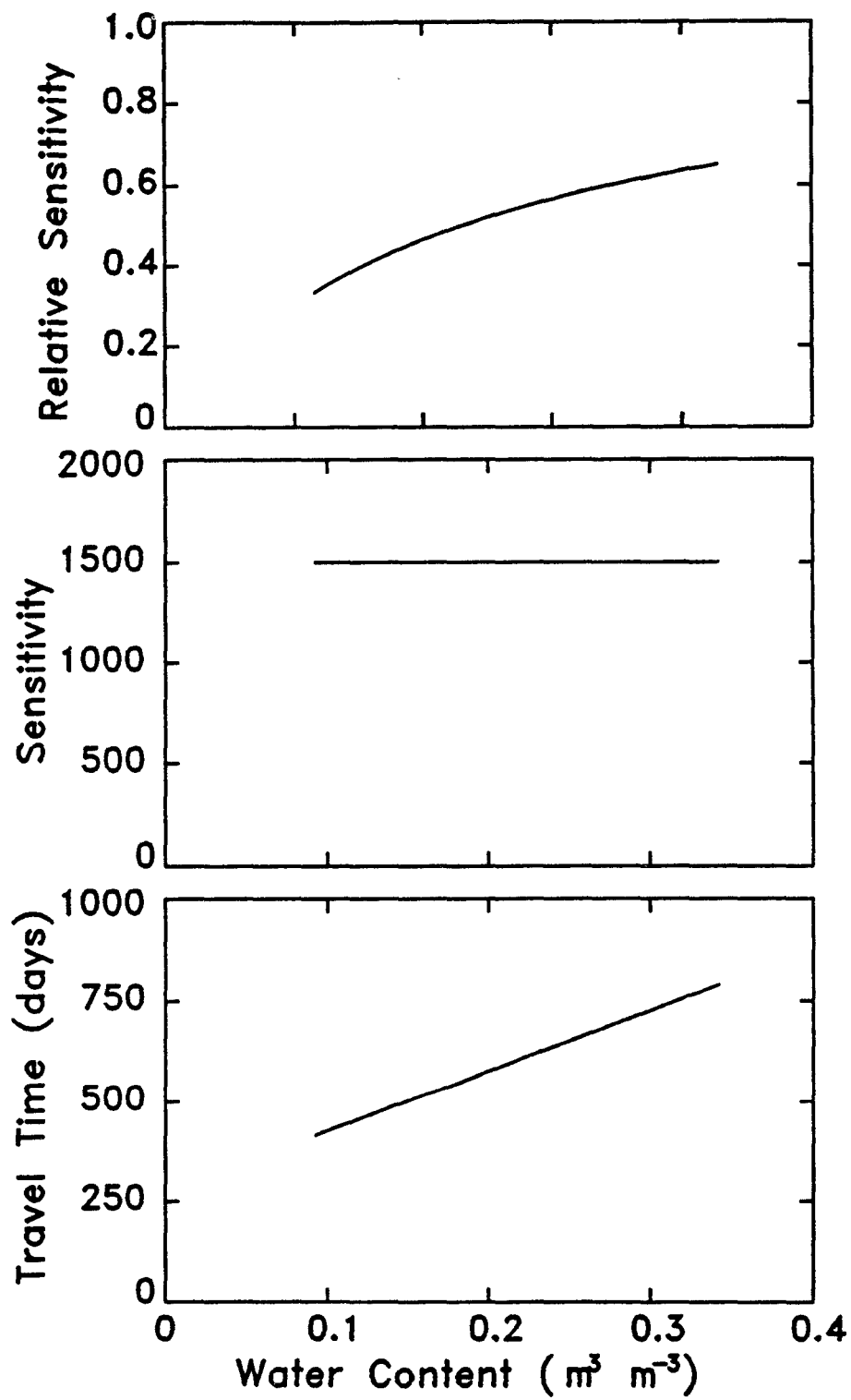
Figure 3.2. Sensitivity of travel time for different values of water contents for a simplified model (Eqn. 23).
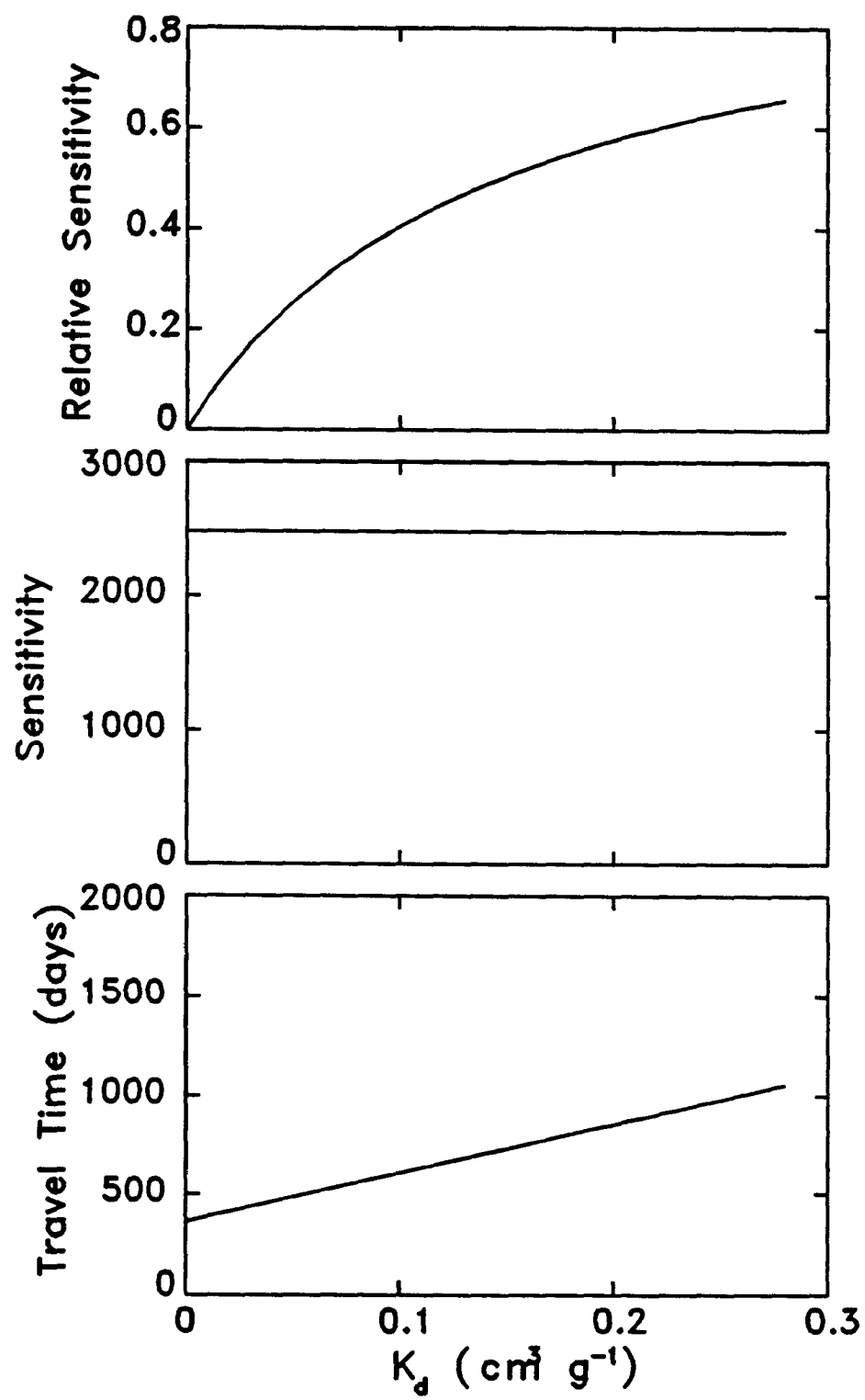
Figure 3.3. Sensitivity of travel time for different values of partition coefficient for a simplified model (Eqn. 23).

## PHYSICAL SETTING

Site Characteristics: The general case study considered was the fate of benzene spilled near Perdido, Alabama. The soil in the area was the Norfolk sand (fine-loamy, siliceous, thermic Typic Paleudult). At the beginning of the simulation, 100 g m$^{-2}$ benzene was assumed to be uniformly distributed in the top 0.5 m of soil. A water table was assumed to be present at a depth of 2 m. The initial water content throughout the soil profile was internally calculated by the RITZ and VIP models from the specified recharge rate, the saturated conductivity, and the Clapp-Hornberger constant. CMLS assumes the initial water content of each soil layer is the field capacity value. An initial water content of 0.15 cm$^3$ cm$^{-3}$ throughout the soil profile was used as the initial condition in HYDRUS. No benzene entered the soil during the simulation.

Soil properties for the top 2 meters of the Norfolk sand were obtained from Quisenberry et al. (1987) for the same soil in Blackville, South Carolina. The basic soil properties used are shown in Table 4.1. Data on the organic carbon content (OC) of the soil were not available in the report. Percent organic carbon content was assumed to decrease with depth according to the equation

$$OC(d) = 1.35e^{-4.0d} \tag{27}$$

where d is the soil depth (m). The organic carbon content determined for the middle of each soil layer was used for that entire layer. Table 4.1 also contains depth-weighted average values used in models requiring uniform soil properties.

The parameters for the van Genuchten closed-form hydraulic functions (van Genuchten, 1980) were obtained from the soil water retention data and unsaturated hydraulic conductivity for sites 5 and 6 found in Tables N5.3 - N6.11 of Quisenberry et al. (1987). The RETC software of van Genuchten et al. (1991) was used to estimate the parameters. Soil porosity was computed from the bulk density. The Clapp-Hornberger constant (Clapp and Hornberger, 1978) required in the RITZ and VIP models was determined by regression. These hydraulic properties are shown in Table 4.2.

Climatological data from the Perdido area of Alabama were obtained for the nearby sites of Fairhope from the SE Regional Climate Center. The only evaporation (ET) data available were from Fairhope. The record period was from 1983 to 1991. Daily weather data from the Fairhope site were used in the simulation runs for HYDRUS and CMLS models. Average recharge rates required for RITZ and VIP were calculated from total rainfall and total evaporation data at these sites. Average rainfall for the area was 5 mm per day. Average evaporation was 4 mm per day. Daily weather data from Caddo County, Oklahoma was also used for some of the analyses using CMLS since the data available for Perdido were not sufficient for the Monte Carlo simulations.

Chemical Properties: The organic carbon partition coefficient for benzene was obtained from $K_{oc}$ values in the literature. Karickhoff and Brown (1979) reported a value of 83 cm$^3$ g$^{-1}$ for benzene in sediment; Rogers et al. (1980) reported 92 cm$^3$ g$^{-1}$; Stuart et al. (1991) reported 18 cm$^3$ g$^{-1}$; and Chen et al. (1992) reported 207 cm$^3$ g$^{-1}$. A value of 80 cm$^3$ g$^{-1}$ was used in this report.

A pseudo zero-order biodegradation rate of benzene has been reported to be 25 mg L$^{-1}$ d$^{-1}$ for a sandy aquifer material by Alvarez and Vogel (1991). Zoetman et al., (1981) published a value of 0.006 d$^{-1}$ (half-life of 116 days) for the first-order coefficient for biodegradation using substrate disappearance in landfill leachate. Goldsmith and Balderson (1988) reported the maximum biokinetic utilization rate (first-order rate) of 0.00667 d$^{-1}$ (half-life of 104 days) in the batch culture. For a modeling study of BTX (benzene, toluene, and xylenes) at a field site, a first-order degradation constant of 0.003 d$^{-1}$ (half-life 231 days) was used by Rifai et al. (1988). A half-life of 100 days was used in this report.

Table 4.1. Soil properties of Norfolk Soil.

| Depth of Bottom m | Bulk Density Mg m$^{-3}$ | Organic Carbon % | Field Capacity m$^3$ m$^{-3}$ | Wilting Point m$^3$ m$^{-3}$ |
|---|---|---|---|---|
| 0.27 | 1.74 | 0.740 | 0.109 | 0.014 |
| 0.40 | 1.79 | 0.270 | 0.230 | 0.104 |
| 0.58 | 1.70 | 0.130 | 0.300 | 0.114 |
| 0.76 | 1.57 | 0.062 | 0.242 | 0.027 |
| 1.06 | 1.52 | 0.035 | 0.300 | 0.114 |
| 1.37 | 1.62 | 0.010 | 0.275 | 0.104 |
| 2.00 | 1.66 | 0.002 | 0.242 | 0.027 |
| Depth-Weighted Average | 1.65 | 0.142 | 0.242 | 0.063 |

Table 4.2. Soil hydraulic properties of Norfolk Soil.

| Depth of Bottom m | $\alpha^1$ m$^{-1}$ | $\beta^1$ | $\theta_s$ m$^3$ m$^{-3}$ | $\theta_r$ m$^3$ m$^{-3}$ | $K_s$ m d$^{-1}$ | Clapp Hornberger Constant |
|---|---|---|---|---|---|---|
| 0.27 | 4.9 | 1.64 | 0.290 | 0.0098 | 0.433 | 2.4 |
| 0.40 | 2.8 | 1.18 | 0.284 | 0.0104 | 0.116 | 4.2 |
| 0.58 | 1.8 | 1.22 | 0.364 | 0.0083 | 0.296 | 8.7 |
| 0.76 | 1.9 | 1.54 | 0.375 | 0.0098 | 0.126 | 8.4 |
| 1.06 | 1.8 | 1.22 | 0.364 | 0.0083 | 0.296 | 14.6 |
| 1.37 | 1.9 | 1.22 | 0.335 | 0.0077 | 0.293 | 11.7 |
| 2.00 | 1.9 | 1.54 | 0.375 | 0.0098 | 0.126 | 9.3 |
| Depth-Weighted Average | 2.3 | 1.40 | 0.349 | 0.0092 | 0.184[2] | 9.1 |

1. Used in hydraulic functions of van Genuchten (van Genuchten et al, 1991) for

Water content, $\theta$:   $(\theta - \theta_r)/(\theta_s - \theta_r) = [1 + (\alpha h)^\beta]^{-m}$

Conductivity, K(h): $K(h) = K_s\{1-(\alpha h)^{m\beta}[1+(\alpha h)^\beta]^{-m}\}^2/[1+(\alpha h)^\beta]^{m\ell}$

   $m = 1 - 1/\beta$;   $\ell = 0.5$

2. Equivalent saturated conductivity (Swartzendruber, 1960).

# SECTION 5

## SENSITIVITY RESULTS FOR RITZ MODEL

### General Impact of Input Parameters

Figures 5.1 to 5.12 illustrate the dependence of chemical concentration in water at the bottom of the treatment zone and the dependence of the position of the pollutant in the soil profile upon different model parameters. The upper graphs in each figure show the concentration of the pollutant in water at a depth of 2 m as a function of time. The lower graphs show the position of the upper and lower edges of the pollutant as functions of time. These bounds define the position of the chemical as it moves through the soil. The solid lines represent estimates from RITZ for benzene movement through the Norfolk soil in Alabama (ignoring movement in the vapor phase). The input parameters are shown in Table 5.1 for the solid lines. These input parameters are the same for all 12 figures. Other lines on a particular figure result from changing only the one parameter listed on the figure. Examining these figures leads us to the following observations:

1. The time required for the pollutant to reach the bottom of the treatment zone is quite dependent upon the recharge rate (Figure 5.1). Decreasing the recharge rate from 1 to 0.5 mm day$^1$ increases the time at which the pollutant reaches the water table from approximately 700 days to 1200 days. The duration of the pulse increases from approximately 900 to 1400 days due to this decrease. The concentration of the pollutant in water decreases 100-fold over this range of recharge rates. As the recharge rate decreases, the travel time increases, the duration of the contaminant pulse increases, the maximum concentration decreases, and the amount of chemical leaching to the ground water decreases.

2. Figure 5.2 shows that increasing the organic carbon partition coefficient, $K_{oc}$, increases sorption of the chemical on the soil solids and increases the time required for the chemical to reach the 2-m depth. This increase in travel time results in an increase in degradation and a decrease in the concentration of the pollutant in water. Little change in the width of the contaminant pulse is visible for these $K_{oc}$ values. The range of values of $K_{oc}$ used in Figure 5.2 is somewhat less than the range found in the literature for benzene.

3. Organic carbon content of the soil has a large impact upon travel time and maximum concentration. This is illustrated in Figure 5.3. Here the solid line for an organic carbon value of 0.14% represents the average organic carbon value for the top 2 meters of the soil. The line for a fraction of 0.8% represents the organic carbon content of the surface horizon. So the difference shown represents the difference between using an average value and the value for the surface layer. The time required for the pulse to reach the water table changes from about 2 years to 6 years due to this change in organic carbon. That corresponds to a 10000-fold difference in concentration. Clearly organic carbon content has a very large and a very significant impact upon chemical movement because of its impact upon sorption and the wide range of organic carbon values which exist in soils.

4. Soil bulk density values seem to have little impact on the parameters of interest (Figure 5.4). Rarely would the uncertainty in bulk density at a site exceed the 0.30 Mg m$^3$ range shown in the figure.

5. One hundred-fold changes in saturated hydraulic conductivity change the travel time by only about 100 days (Figure 5.5). The Clapp-Hornberger constant also has a small impact upon the predictions as seen in Figure 5.6. This is reasonable in that RITZ uses these parameters only to estimate the water content of the soil for a particular recharge rate.

Table 5.1. Values of input parameters used for sensitivity analysis in RITZ model.

| Soil Properties | |
|---|---|
| Organic Carbon (%) | 0.14 |
| Bulk Density (Mg m$^{-3}$) | 1.650 |
| Saturated Water Content (m$^3$ m$^{-3}$) | 0.378 |
| Saturated Hydraulic Conductivity (m day$^{-1}$) | 0.19 |
| Clapp and Hornberger Constant (--) | 4.9 |
| | |
| Site Characteristics | |
| Plow zone depth (m) | 0.5 |
| Treatment zone depth (m) | 2.0 |
| Recharge Rate (mm day$^{-1}$) | 1.0 |
| Evaporation Rate (mm day$^{-1}$) | 4.0 |
| Air temperature (degrees C) | 25 |
| Relative humidity (--) | 0.5 |
| Sludge application rate (Mg ha$^{-1}$) | 250 |
| Concentration of pollutant in the sludge (g kg$^{-1}$) | 4.0 |
| Diffusion coefficient of water vapor in air (m$^2$ day$^{-1}$) | 2.0 |
| | |
| Pollutant properties | |
| Organic carbon partition constant (cm$^3$ kg$^{-1}$) | 80[1] |
| Octanol-water partition coefficient (--) | 700 |
| Henry's law constant (--) | 5.0E-9 |
| Diffusion coefficient in air (m$^2$ day$^{-1}$) | 2.0 |
| Degradation half-life (days) | 104 |
| | |
| Properties of Oil | |
| Concentration of oil in the sludge (g kg$^{-1}$) | 250 |
| Density of the oil (kg m$^{-3}$) | 800 |
| Half-life of the oil (days) | 200 |

1. This partition coefficient was used for the solid lines. The short dashed line represents results for $K_{oc}$ = 20 cm$^3$ g$^{-1}$; the long dashed line represents results for $K_{oc}$ = 110 cm$^3$ g$^{-1}$.

6. The evaporation rate has no detectable impact on the fate of the pollutant in this scenario (Figure 5.7) since the evaporation rate is used in RITZ only to estimate volatile losses of the chemical. If the model parameters were such that volatile losses were appreciable, differences due to evaporation rate would be observed.

7. Figure 5.8 illustrates that decreases in degradation half-life of the pollutant result in large decreases in the concentration of chemical reaching the ground water, but do not effect the rate of chemical movement. RITZ assumes the half-life does not change with depth. Since half-life has a large impact upon concentration and since half-life generally changes with depth, this assumption may produce large errors in predicted concentrations and amounts leached.

8. Henry's constant determines the partitioning of the pollutant between water and air. Figure 5.9 shows its impact upon concentration and pollutant position. As Henry's constant increases above $10^{-3}$, RITZ predicts a substantial decrease in pulse width due to a large increase in loss of pollutant to the vapor phase. The predicted amount of chemical volatilized is so large the pollutant does not reach the water table when Henry's constant is equal to 0.24. The impact of Henry's constant is highly dependent upon the diffusion coefficient of the pollutant.

9. Figures 5.10 and 5.11 illustrate the manner in which the pollutant concentration and pollutant movement depend upon the diffusion coefficient of the pollutant in air. In Figure 5.10, we see no change in predicted concentration and travel time due to changes in diffusion coefficients. In Figure 5.10, Henry's constant is very small so essentially no pollutant is present in the air phase. Therefore changes in the way the pollutant diffuses in air have no impact. The value of Henry's constant used in Figure 5.11 is a reasonable estimate of that for benzene. It is much larger than the value used in Figure 5.10. Figure 5.11 indicates that the diffusion coefficient does not influence the time the pollutant arrives at the water table, but it significantly influences the duration of the pulse and the amount leached. In this case the RITZ model predicts that none of the pollutant will reach the water table if the diffusion coefficient is 2 m$^2$ day$^{-1}$. The curves in Figure 5.11 look quite similar to those in Figure 5.9. This is expected since the equations of RITZ generally include the product of these two parameters. The differences between Figures 5.10 and 5.11 illustrate that all the results of this report are valid for only the set of input parameters used.

10. Figure 5.12 shows predicted results for different oil contents in the sludge. The oil content has no impact upon the time at which the leading edge of the chemical reaches the water table, but it changes the pulse width substantially. The presence of oil in the sludge retards the movement of chemical through the portion of the soil containing oil (the plow zone). This retardation and resulting increase in degradation time causes the concentration of the pollutant at the water table to be much less than that for an oil-free sludge. In Figure 5.12 this change in concentration is approximately 100-fold. The duration of the pulse is greatly reduced when the oil content is reduced.

## Sensitivity Coefficients

Figures 5.13 to 5.24 show the travel time and its sensitivity coefficients for different input parameters of the RITZ model. Each of the figures contains three graphs. The lower graph shows the travel time as a function of the parameter being analyzed. The middle graph shows the sensitivity coefficient, S, (defined in equation 15) as a function of the parameter being analyzed. The upper graph shows the relative sensitivity, $S_r$, as defined in equation 18. Different lines in each graph represent chemicals with different organic carbon partition coefficients as shown on the graph. Input parameters used for these graphs are listed in Table 5.1.

Figure 5.1 illustrated that the pulse of chemical enters ground water at earlier times as the recharge rate increases. This dependency of travel time upon recharge rate is shown in Figure 5.13 for a large range of recharge rates. (We have defined the travel time as the time midway between the time the pollutant reaches the water table and the time all of the pollutant has entered the water table. That is, travel time refers to

the time at the middle of the concentration pulse shown in Figure 5.1.) The middle graph of Figure 5.13 is a graph of the sensitivity coefficient for travel time to recharge rate. This is a graph of the slope of the line in the lower graph. For a recharge rate of 1 mm day$^1$, the sensitivity coefficient is about -1000. This means that an increase in recharge rate of 0.5 mm day$^1$ (recharge goes from 0.75 to 1.25 mm day$^1$) corresponds to a decrease in travel time of -1000 * 0.5 or 500 days. The upper graph of Figure 5.13 shows the relative sensitivity as a function of recharge rate. The relative sensitivity to recharge rate is nearly constant with a value of approximately -0.7 over the range of rates shown. This means that doubling the recharge rate decreases the travel time by a factor of 1.4 (0.7 x 2). If we are concerned about relative changes in travel time, the relative sensitivity is the parameter of interest; if we are interested in absolute changes in travel time, the sensitivity coefficient is the appropriate factor. Since the three lines on each of these graphs are close together, differences between chemicals with $K_{oc}$ values in the range of 20 to 110 cm$^3$ g$^1$ are small. Note that these results are similar to those for the simple case shown in Figure 3.1. Differences are primarily the result of oil in the upper portion of the soil.

Figures 5.14 to 5.24 can be related to Figures 5.2 to 5.12 as was done above. Figures 5.14, 5.15, and 5.16 show that travel time increases as $K_{oc}$, organic carbon content, and bulk density increase just as was observed in the simplified case shown in Figure 5.3. The increase in travel time is nearly linear. The curves are very similar since the product of these factors is the retardation factor, R (Eqn 8), and travel time increases as R increases. Since organic carbon contents commonly vary from near zero to more than 2%, it is a very important parameter for predicting travel time of adsorbed materials.

Figures 5.22 and 5.23 show the sensitivity of travel time to diffusion coefficients. Figure 5.22 shows the travel time is insensitive when Henry's constant is very small just as was shown in Figure 5.10. In Figure 5.23, we see that increasing diffusion coefficients decreases travel time when a larger value of Henry's constant is used.

Travel time predicted by RITZ is not sensitive to evaporation rate, half-life, saturated conductivity, and Clapp-Hornberger constant. Relative sensitivities for travel time are less than 0.20 in absolute value for these scenarios, indicating that the relative change in travel time will be less than 20% of the relative change in the input parameter.

Sensitivities for the concentration of pollutant in water (Figures 5.25 to 5.36) and for the total amount of pollutant leached to ground water (Figures 5.37 to 5.48) are similar in shape but have different scales. Both quantities increase with increasing recharge rate and degradation half-life. The concentration and amount leached decrease with increasing organic carbon content, $K_{oc}$, Henry's constant, Clapp-Hornberger constant, and oil content. Evaporation rate and bulk density have little impact on these predictions. Relative sensitivities are generally greater than 1 in magnitude for recharge rate, organic carbon content, $K_{oc}$, and half-life.

Figures 5.49 to 5.60 present sensitivity graphs for pulse width or the duration of the chemical pulse at the bottom of the treatment zone. This model output is most sensitive to recharge rate, Henry's constant, and oil content for the parameters used here. Relative sensitivities for pulse width are less than 1 in absolute value except for Henry's constant and the diffusion coefficient when the pulse width approaches zero.

Figures 5.61 and 5.62 show the sensitivity of the amount of pollutant volatilized and lost to the atmosphere as functions of Henry's constant and the diffusion coefficient of the pollutant. Clearly RITZ is capable of predicting large losses in the vapor phase. It is interesting to note that differences in $K_{oc}$ do not appear to influence the amount volatilized for the range of parameters shown.

A list of the parameters of RITZ and summaries of sensitivities of travel time, pulse width, and amount leached are given in Tables 5.2, 5.3, and 5.4, respectively. The complete range of values analyzed is broken

Table 5.2. Sensitivity coefficients for travel time using RITZ.

| Input Parameter | | | Travel Time (days) | | |
|---|---|---|---|---|---|
| Name | Range | Value | Value | S | $S_r$ |
| Organic Carbon (%) | 0.02-0.54 | 0.3 | 1500 | 2190 | 0.44 |
| Bulk Density (Mg m$^{-3}$) | 1.35-1.80 | 1.55 | 1130 | 184 | 0.25 |
| Saturated Water Content (m$^3$ m$^{-3}$) | 0.28-0.48 | 0.38 | 1146 | 1094 | 0.36 |
| Saturated Conductivity (m day$^{-1}$) | 0.04-0.59 | 0.34 | 1130 | -91 | -0.027 |
| Clapp and Hornberger Constant | 2.9-14.9 | 4.9 | 1150 | 26.5 | 0.11 |
| Plow zone depth (m) | 0.1-0.6 | 0.5 | 1150 | -310 | -0.14 |
| Treatment zone depth (m) | 1-2.5 | 2.0 | 1150 | 435 | 0.76 |
| Recharge Rate (mm day$^{-1}$) | 0.5-2.2 | 1.0 | 1150 | -820 | -0.72 |
| | 2.2-5.5 | 3.0 | 538 | -121 | -0.67 |
| Evaporation Rate (mm day$^{-1}$) | 1-7 | 3.0 | 1150 | 0.0 | 0.0 |
| Air temperature (degrees C) | 15-35 | 20 | 1150 | 0.0 | 0.0 |
| Relative humidity | 0.2-0.8 | 0.5 | 1150 | 0.0 | 0.0 |
| Sludge application rate (Mg ha$^{-1}$) | 50-450 | 250 | 1120 | 0.64 | 0.14 |
| Conc. pollutant in sludge (g kg$^{-1}$) | 1.5-6.5 | 4.0 | 1146 | 0.0 | 0.0 |
| Diffusion coef. water vapor in air (m$^2$ day$^{-1}$) | 0.4-3.6 | 2.0 | 1146 | 0.0 | 0.0 |
| Partition coefficient (cm$^3$ g$^{-1}$) | 10-150 | 80 | 1150 | 3.81 | 0.27 |
| Oil-water partition coefficient | 100-1300 | 700 | 1120 | 0.24 | 0.15 |
| Henry's law constant | 0-0.4 | 0.05 | 816 | -823 | -0.050 |
| Diffusion coef. in air (m$^2$ day$^{-1}$) | 0.4-3.6 | 2.0 | 1146 | 0.0 | 0.0 |
| Degradation half-life (day) | 24-304 | 104 | 1150 | 0.0 | 0.0 |
| Conc. oil in sludge (g kg$^{-1}$) | 50-450 | 250 | 1150 | 0.54 | 0.12 |
| Density of oil (Mg m$^{-3}$) | 0.4-1.2 | 0.8 | 1150 | 180 | -0.13 |
| Half-life of oil (day) | 25-400 | 200 | 1150 | 1.47 | 0.26 |

into more than one part for parameters with highly nonlinear sensitivity functions. Relative sensitivities for travel time and pulse width are less than 1 in absolute value indicating that a relative change in any parameter will result in a smaller relative change in the travel time or pulse width. Sensitivities for travel time are positive for most input parameters indicating that the travel time increases as those parameters increase. Sensitivities are negative only for saturated hydraulic conductivity, plow zone depth, recharge rate, and Henry's law constant so travel times decrease as each of these parameters increase. The sensitivities for pulse width have the same sign for each parameter as their respective sensitivities for travel time with the exception of plow zone depth. Increasing the plow zone depth increases the pulse width but decreases the travel time for the range of parameters studied here. Relative sensitivities for amount leached are greater in absolute value for many parameters.

Table 5.3. Sensitivity coefficients for pulse width using RITZ.

| Input Parameter | | | Pulse Width (days) | | |
|---|---|---|---|---|---|
| Name | Range | Value | Value | S | $S_r$ |
| Organic Carbon (%) | 0.02-0.54 | 0.3 | 1050 | 412 | 0.12 |
| Bulk Density (Mg m$^{-3}$) | 1.35-1.80 | 1.55 | 982 | 331 | 0.052 |
| Saturated Water Content (m$^3$ m$^{-3}$) | 0.28-0.48 | 0.38 | 986 | 195 | 0.075 |
| Saturated Conductivity (m day$^{-1}$) | 0.04-0.59 | 0.34 | 982 | -16.3 | -0.006 |
| Clapp and Hornberger Constant | 2.9-14.9 | 4.9 | 986 | 4.76 | 0.024 |
| Plow zone depth (m) | 0.1-0.6 | 0.5 | 986 | 250 | 0.13 |
| Treatment zone depth (m) | 1.0-2.5 | 2.0 | 986 | 0.0 | 0.0 |
| Recharge Rate (mm day$^{-1}$) | 0.5-2.2 | 1.0 | 986 | -392 | -0.40 |
| | 2.2-5.5 | 3.0 | 619 | -96 | -0.46 |
| Evaporation Rate (mm day$^{-1}$) | 1-7 | 3.0 | 986 | 0.0 | 0.0 |
| Air temperature (degrees C) | 15-35 | 20 | 986 | 0.0 | 0.0 |
| Relative humidity | 0.2-0.8 | 0.50 | 986 | 0.0 | 0.0 |
| Sludge application rate (Mg ha$^{-1}$) | 50-450 | 200 | 942 | 1.29 | 0.34 |
| Conc. pollutant in sludge (g kg$^{-1}$) | 1.5-6.5 | 4.0 | 986 | 0.0 | 0.0 |
| Diffusion coef. water vapor in air (m$^2$ day$^{-1}$) | 0.4-3.6 | 2.0 | 986 | 0.0 | 0.0 |
| Partition coefficient (cm$^3$ g$^{-1}$) | 10-150 | 80 | 986 | 0.685 | 0.056 |
| Oil-water partition coefficient | 100-1300 | 700 | 927 | 0.488 | 0.37 |
| Henry's law constant | 0-0.4 | 0.05 | 306 | -2026 | -0.33 |
| Diffusion coef. in air (m$^2$ day$^{-1}$) | 0.4-3.6 | 2.0 | 986 | 0.0 | 0.0 |
| Degradation half-life (day) | 24-304 | 104 | 986 | 0.0 | 0.0 |
| Conc. oil in sludge (g kg$^{-1}$) | 50-450 | 250 | 986 | 1.07 | 0.27 |
| Density of oil (Mg m$^{-3}$) | 0.4-1.2 | 0.80 | 1023 | -361 | -0.29 |
| Half-life of oil (day) | 25-400 | 200 | 986 | 2.94 | 0.60 |

Table 5.4. Sensitivity coefficients for amount leached using RITZ.

| Input Parameter | | | Amount Leached (%) | | |
|---|---|---|---|---|---|
| Name | Range | Value | Value | S | $S_r$ |
| Organic Carbon (%) | 0.02-0.14 | 0.10 | 1.1E-1 | -1.4E+0 | -1.66 |
| | 0.14-0.34 | 0.26 | 1.2E-2 | -1.7E-1 | -3.50 |
| | 0.34-0.54 | 0.46 | 8.4E-4 | -1.1E-2 | -6.19 |
| Bulk Density (Mg m$^{-3}$) | 1.35-1.80 | 1.55 | 7.0E-2 | -8.0E-2 | -1.77 |
| Saturated Water Content (m$^3$ m$^{-3}$) | 0.28-0.48 | 0.38 | 6.8E-2 | -4.4E-1 | -2.47 |
| Saturated Conductivity (m day$^{-1}$) | 0.04-0.59 | 0.34 | 7.0E-2 | 3.9E-2 | 0.19 |
| Clapp and Hornberger Constant | 2.9-6.9 | 4.9 | 6.2E-2 | -1.0E-2 | -0.80 |
| | 6.9-14.9 | 8.9 | 4.0E-2 | -2.9E-3 | -0.65 |
| Plow zone depth (m) | 0.1-0.6 | 0.5 | 6.3E-2 | 1.2E-1 | 0.94 |
| Treatment zone depth (m) | 1.0-1.5 | 1.25 | 6.5E-1 | -1.7E+0 | -3.34 |
| | 1.5-2.5 | 2.0 | 1.0E-1 | -2.4E-1 | -4.79 |
| Recharge Rate (m day$^{-1}$) | 0.5-5.5 | 3.0 | 2.9E+0 | 2.3E+0 | 2.33 |
| Evaporation Rate (mm day$^{-1}$) | 1-7 | 3.0 | 6.2E-2 | 0.0E+0 | 0.00 |
| Air temperature (degrees C) | 15-35 | 20 | 6.2E-2 | 0.0E+0 | 0.00 |
| Relative humidity | 0.2-0.8 | 0.5 | 6.2E-2 | 0.0E+0 | 0.00 |
| Sludge application rate (Mg ha$^{-1}$) | 50-200 | 100 | 5.1E-2 | 1.1E-7 | 0.22 |
| | 200-450 | 300 | 6.3E-2 | 2.2E-8 | 0.10 |
| Conc. pollutant in sludge (g kg$^{-1}$) | 1.5-6.5 | 4.0 | 6.2E-2 | 1.6E-2 | 1.00 |
| Diffusion coef. water vapor in air (m$^2$ day$^{-1}$) | 0.4-3.6 | 2.0 | 6.2E-2 | 0.0E+0 | 0.00 |
| Partition coefficient (ml$^3$ g$^{-1}$) | 10-70 | 40 | 1.6E-1 | -3.8E-3 | -0.94 |
| | 70-150 | 110 | 3.1E-2 | -7.2E-4 | -2.59 |
| Oil-water partition coefficient | 100-500 | 300 | 1.6E-1 | -4.6E-4 | -0.87 |
| | 500-1300 | 800 | 6.0E-2 | -5.8E-5 | -0.77 |
| | 250-1300 | 800 | 6.6E-2 | -8.4E-5 | -1.01 |
| Henry's law constant | 0.0-0.17 | 0.10 | 2.6E-2 | -4.1E-1 | -1.56 |
| | 0.17-0.4 | 0.30 | 0.0E+0 | 0.0E+0 | 0.00 |
| Diffusion coef. in air (m$^2$ day$^{-1}$) | 0.4-3.6 | 2.0 | 6.2E-2 | 0.0E+0 | 0.00 |
| Degradation half-life (day) | 24-304 | 104 | 6.2E-2 | 3.6E-3 | 5.98 |
| Conc. oil in sludge (g kg$^{-1}$) | 50-150 | 100 | 1.3E-1 | -1.0E-3 | -0.77 |
| | 150-450 | 300 | 5.3E-2 | -1.6E-4 | -0.89 |
| Density of oil (Mg m$^{-3}$) | 0.4-1.2 | 0.8 | 6.2E-2 | 6.8E-5 | 0.89 |
| Half-life of oil (day) | 25-120 | 75 | 1.4E-1 | -1.8E-3 | -0.94 |
| | 120-400 | 250 | 5.4E-2 | -1.1E-4 | -0.53 |
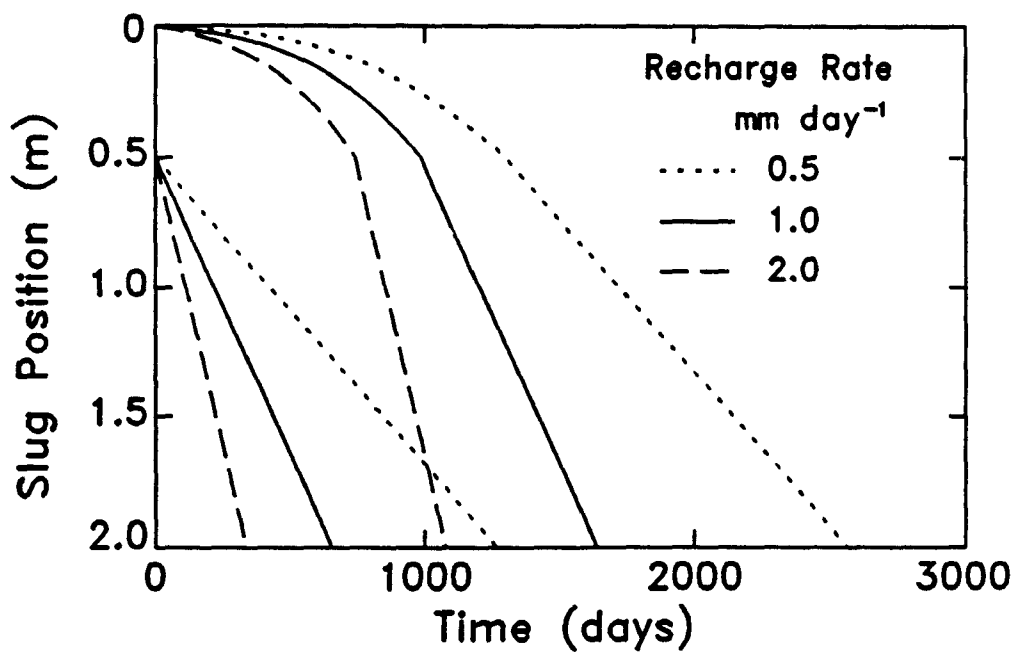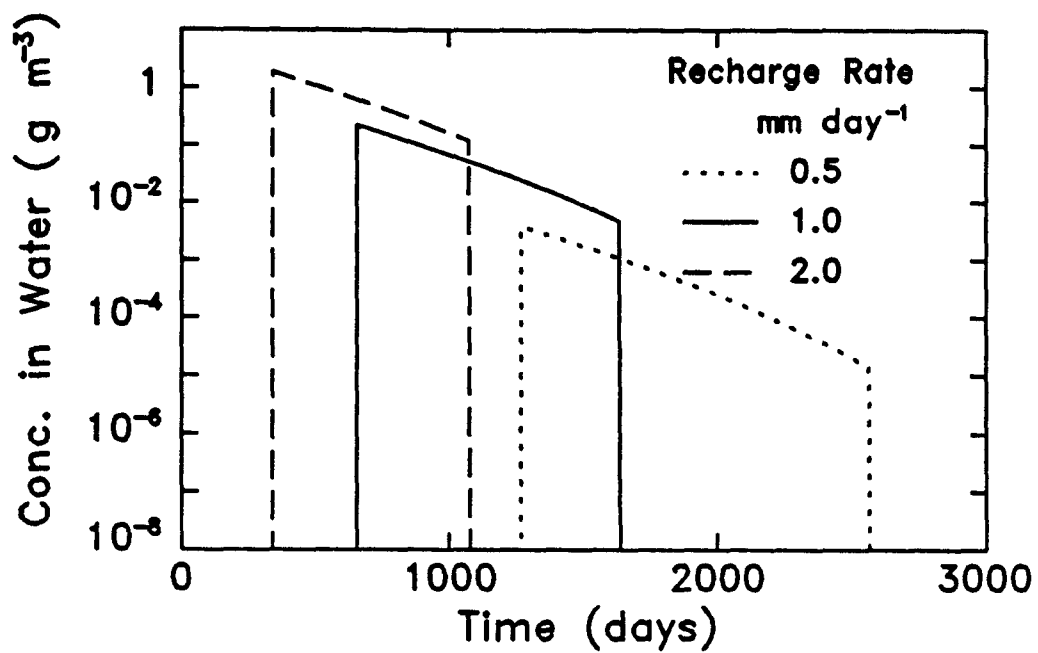
Figure 5.1. Predicted concentration of pollutant in water at 2.0 m and position of the pollutant slug as functions of time for different recharge rates.
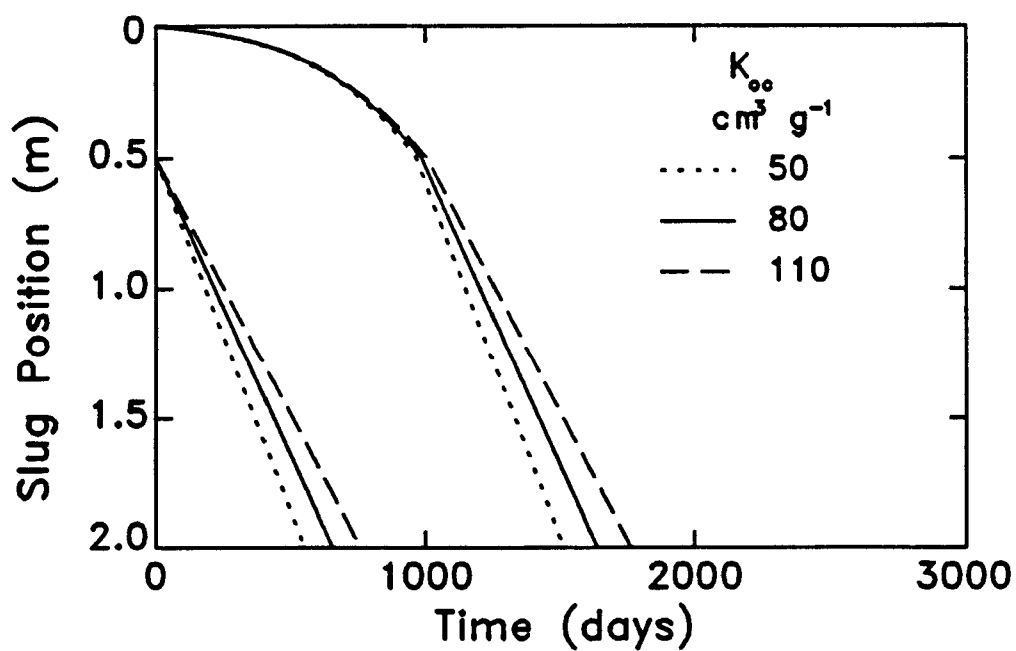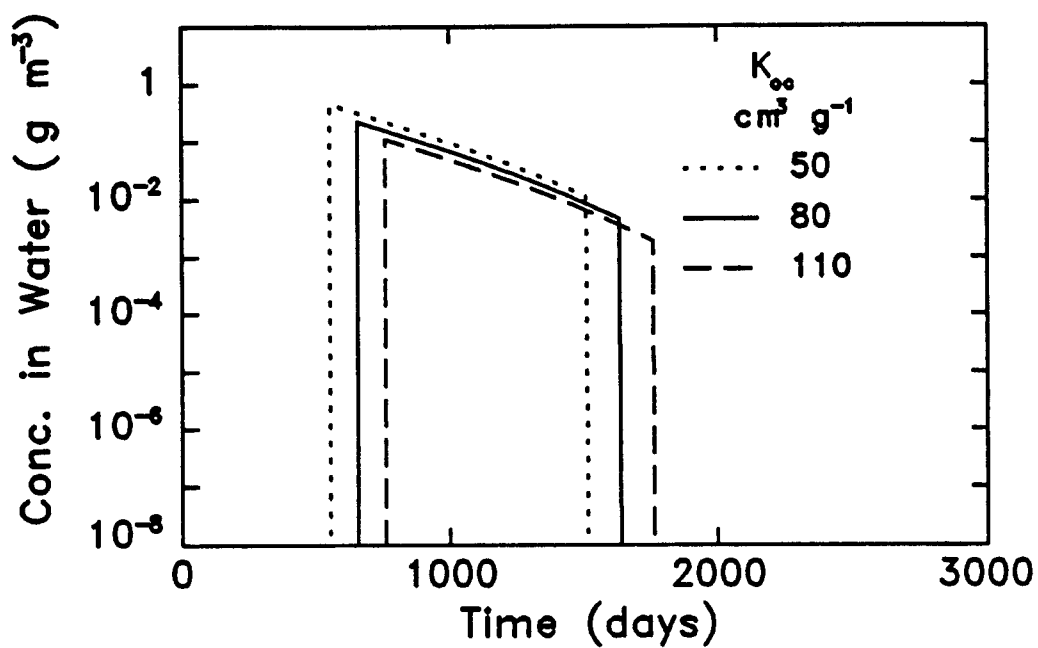
Figure 5.2. Predicted concentration of pollutant in water at 2.0 m and position of the pollutant slug as functions of time for different organic carbon partition coefficients.
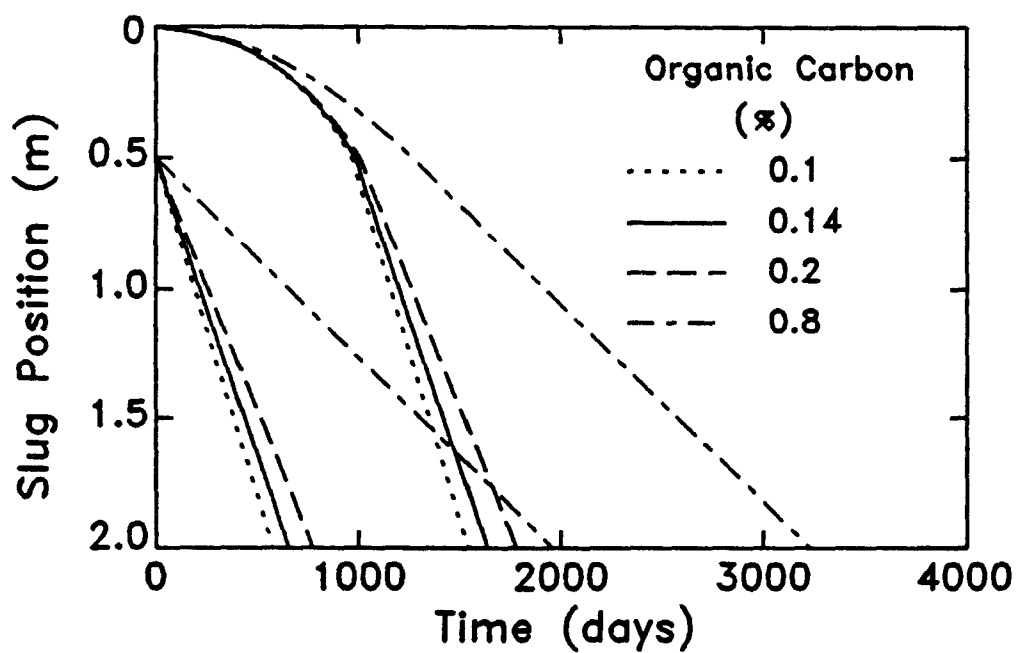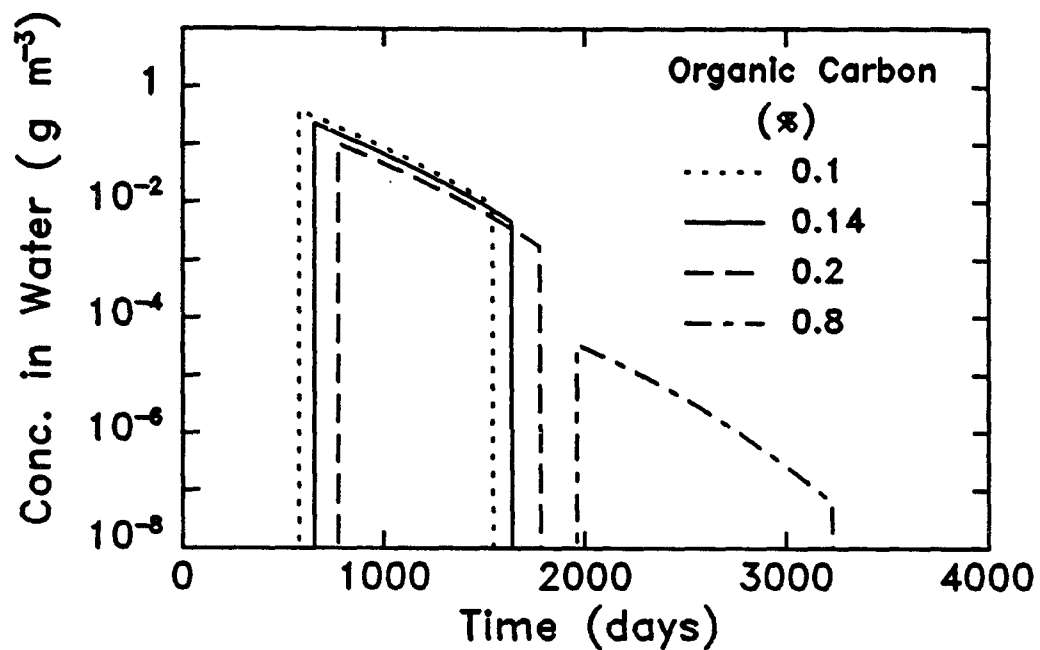
Figure 5.3. Predicted concentration of pollutant in water at 2.0 m and position of the pollutant slug as functions of time for different amounts of organic carbon.
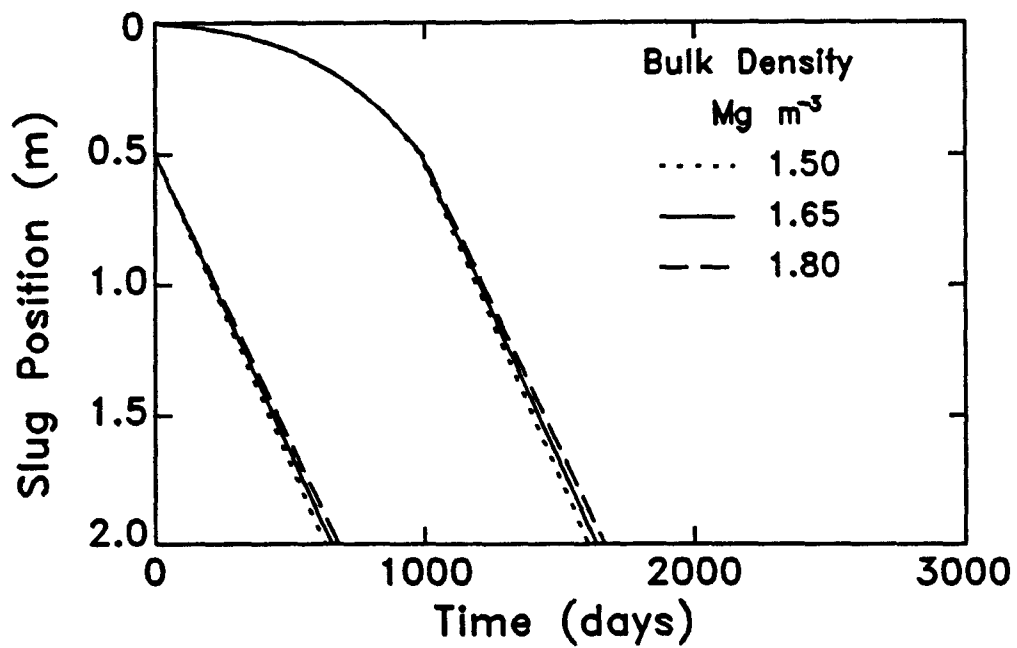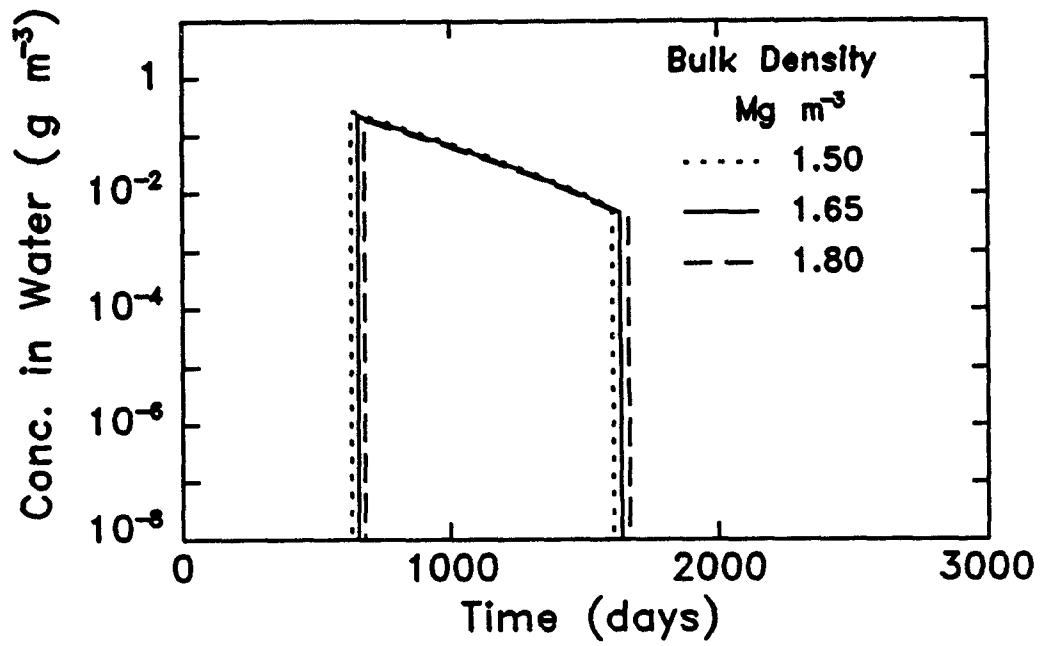
Figure 5.4. Predicted concentration of pollutant in water at 2.0 m and position of the pollutant slug as functions of time for different bulk density values.
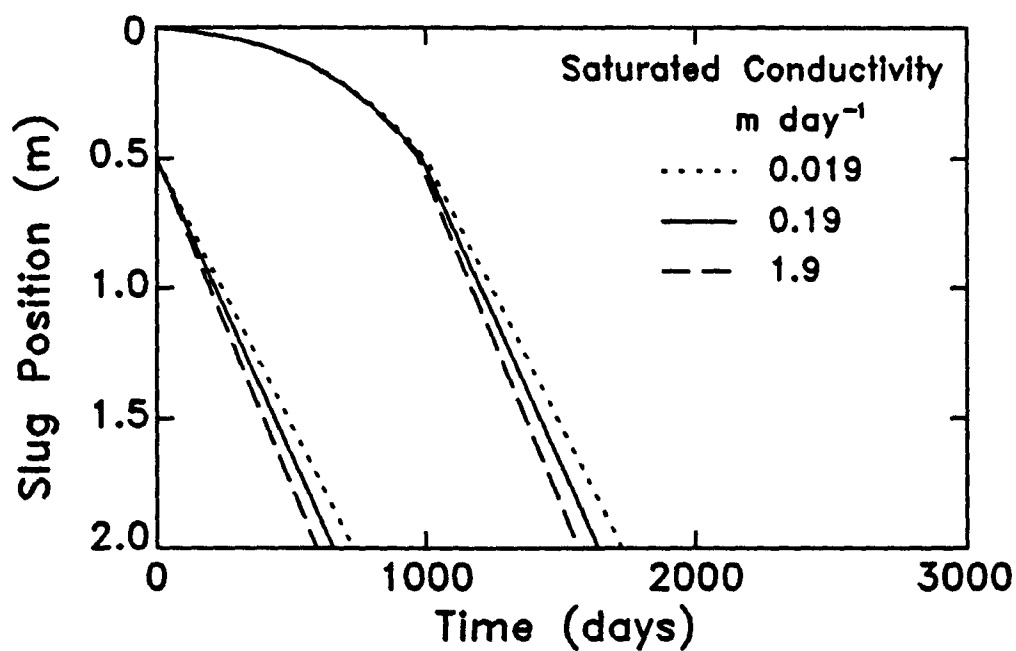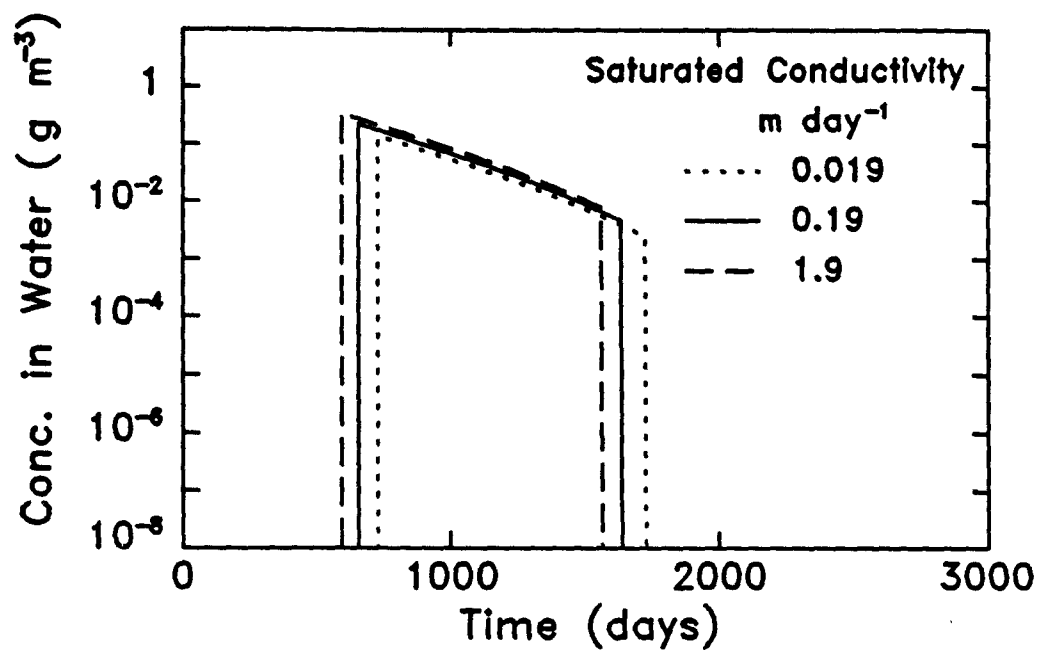
Figure 5.5. Predicted concentration of pollutant in water at 2.0 m and position of the pollutant slug as functions of time for different saturated hydraulic conductivities.
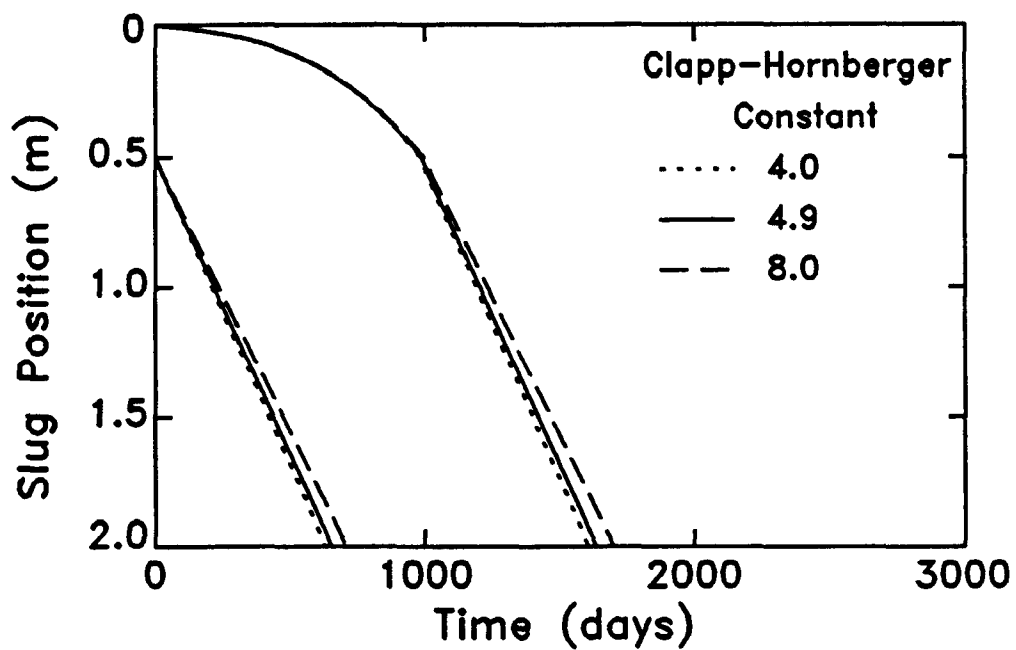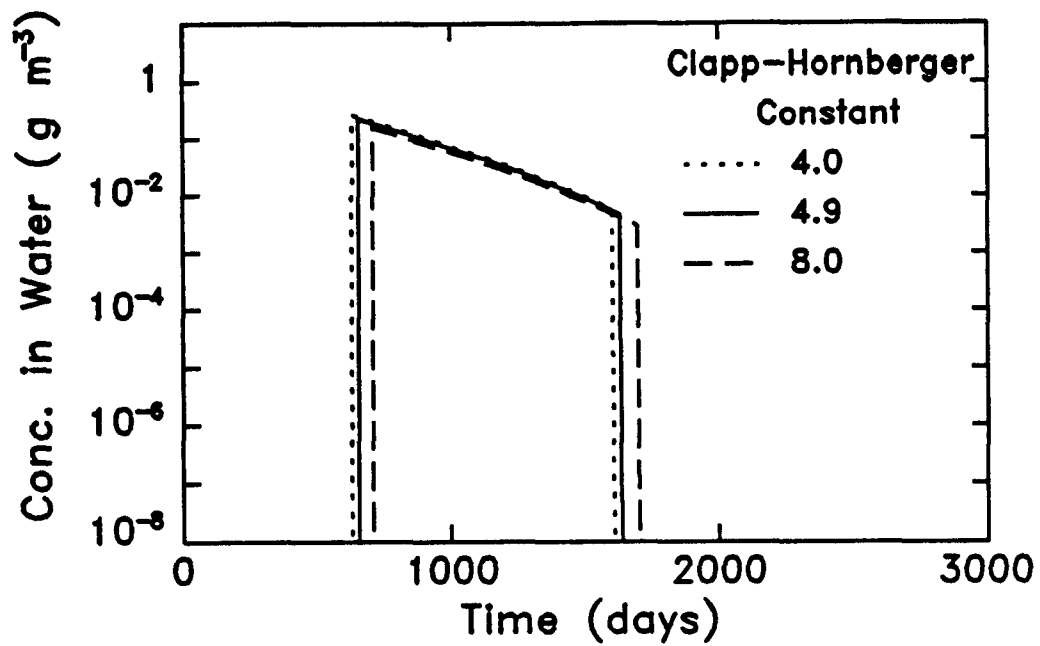
Figure 5.6. Predicted concentration of pollutant in water at 2.0 m and position of the pollutant slug as functions of time for different values of the Clapp-Hornberger constant.
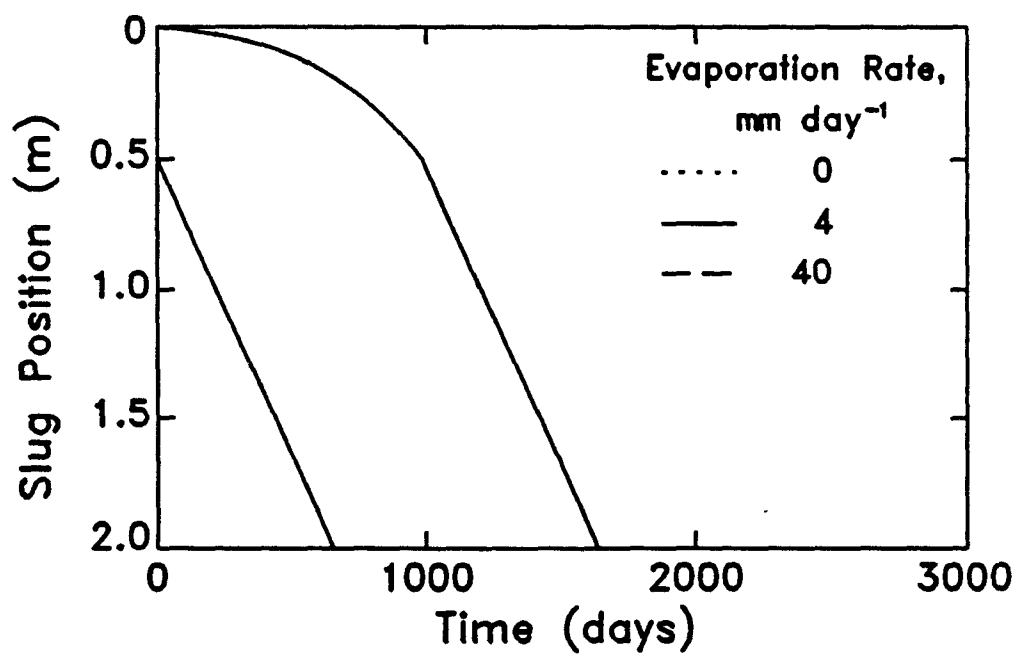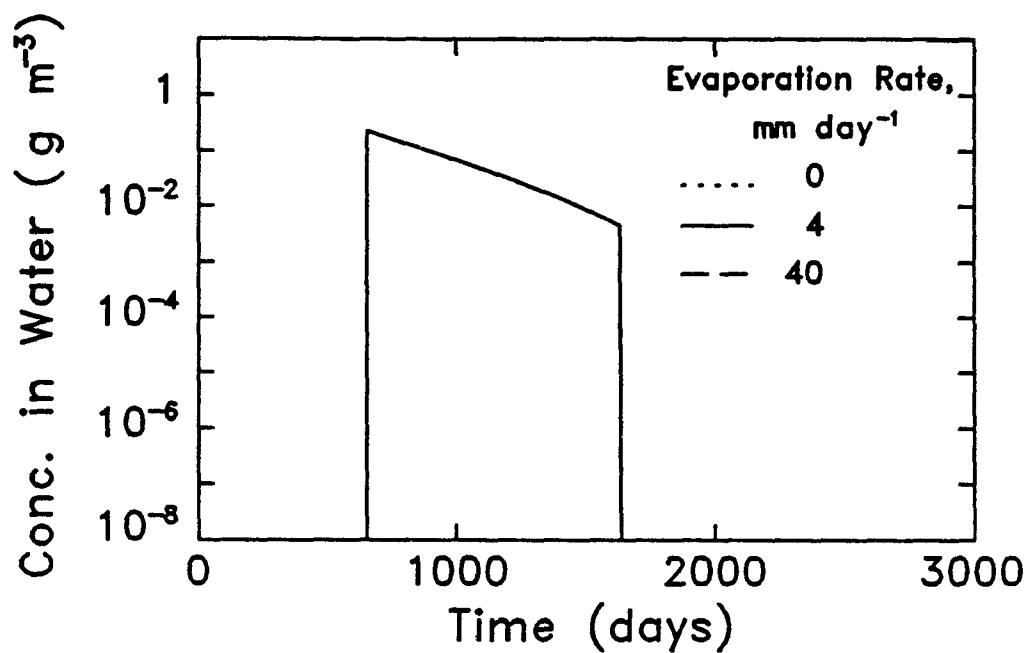
Figure 5.7. Predicted concentration of pollutant in water at 2.0 m and position of the pollutant slug as functions of time for different evaporation rates.
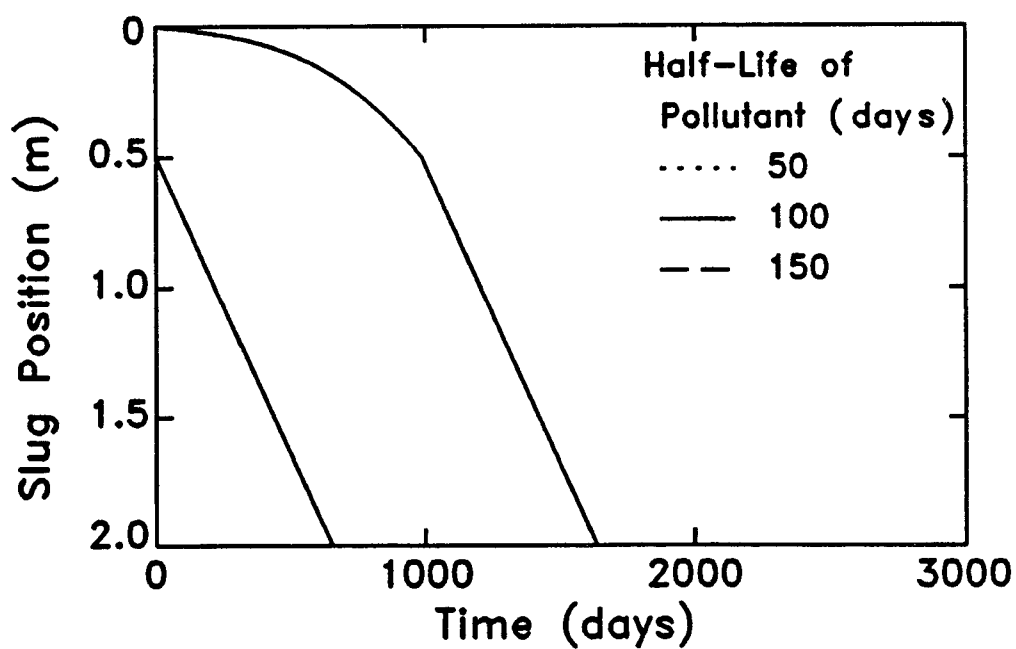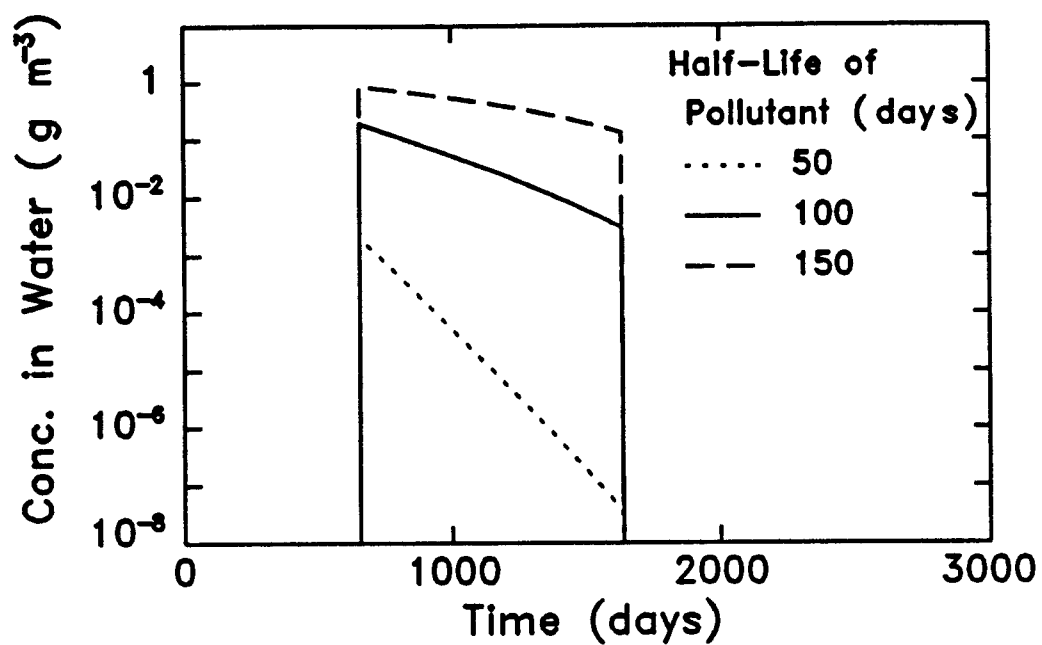
Figure 5.8. Predicted concentration of pollutant in water at 2.0 m and position of the pollutant slug as functions of time for different values of pollutant half-life.
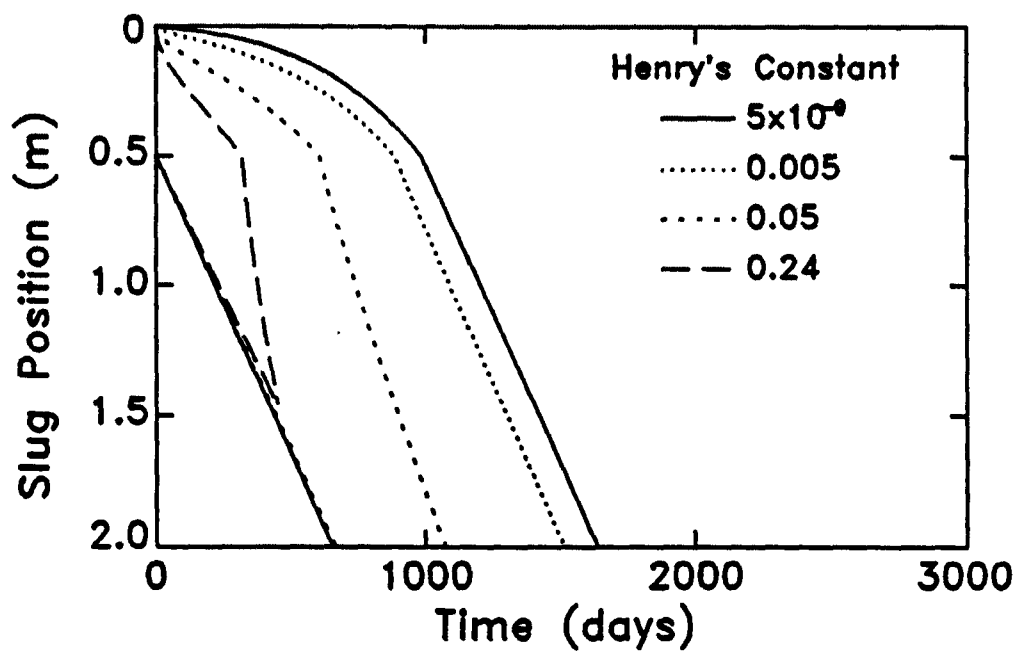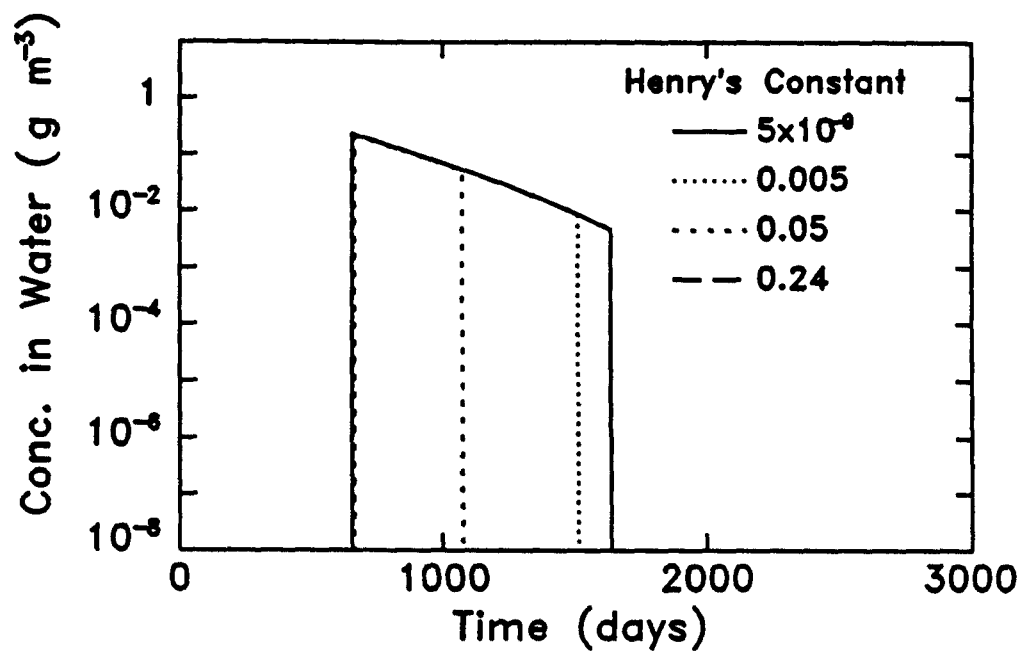
Figure 5.9. Predicted concentration of pollutant in water at 2.0 m and position of the pollutant slug as functions of time for different values of Henry's constant.
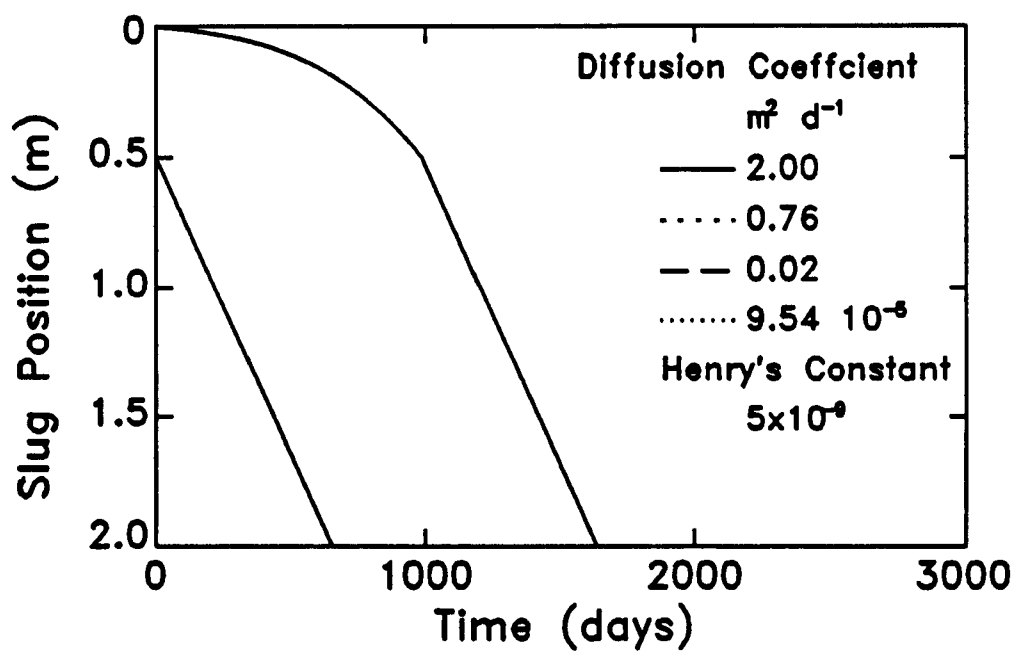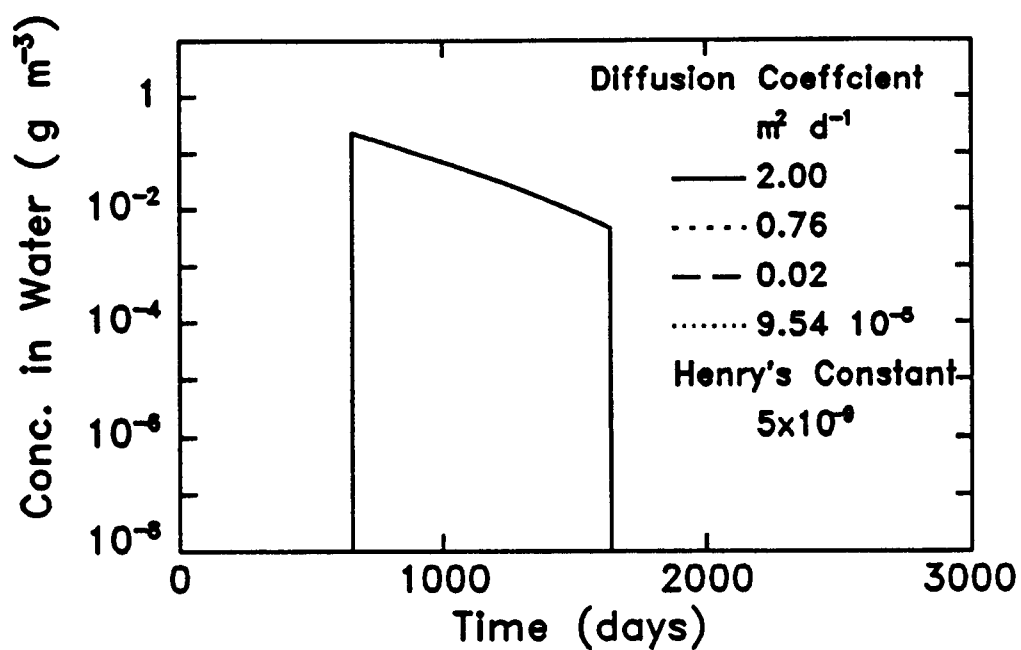
Figure 5.10. Predicted concentration of pollutant in water at 2.0 m and position of the pollutant slug as functions of time for different diffusion coefficients of pollutant in air and a small value of Henry's constant.
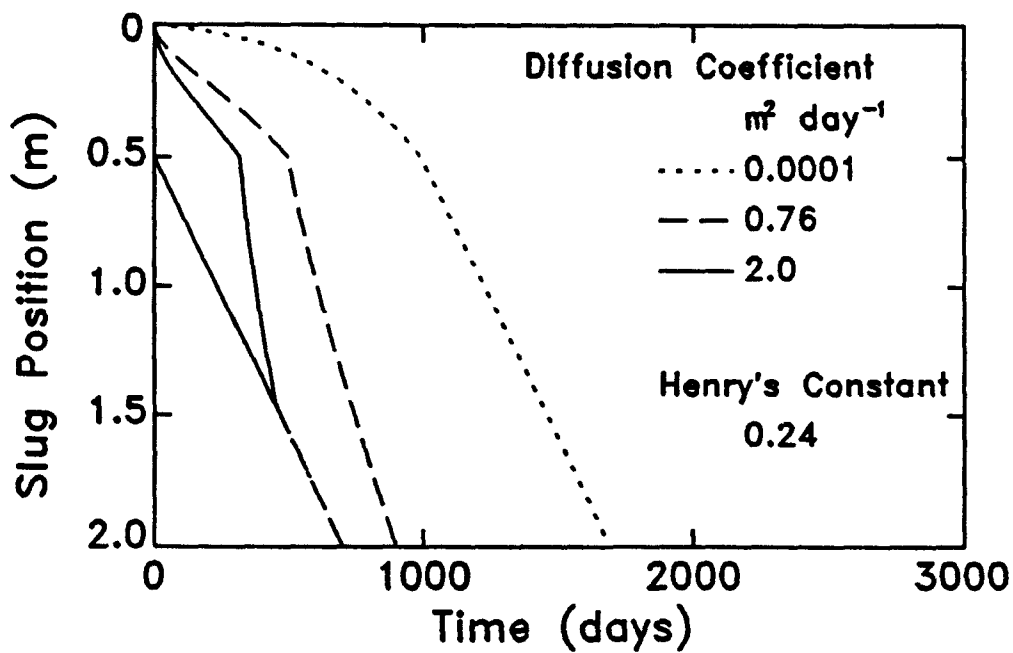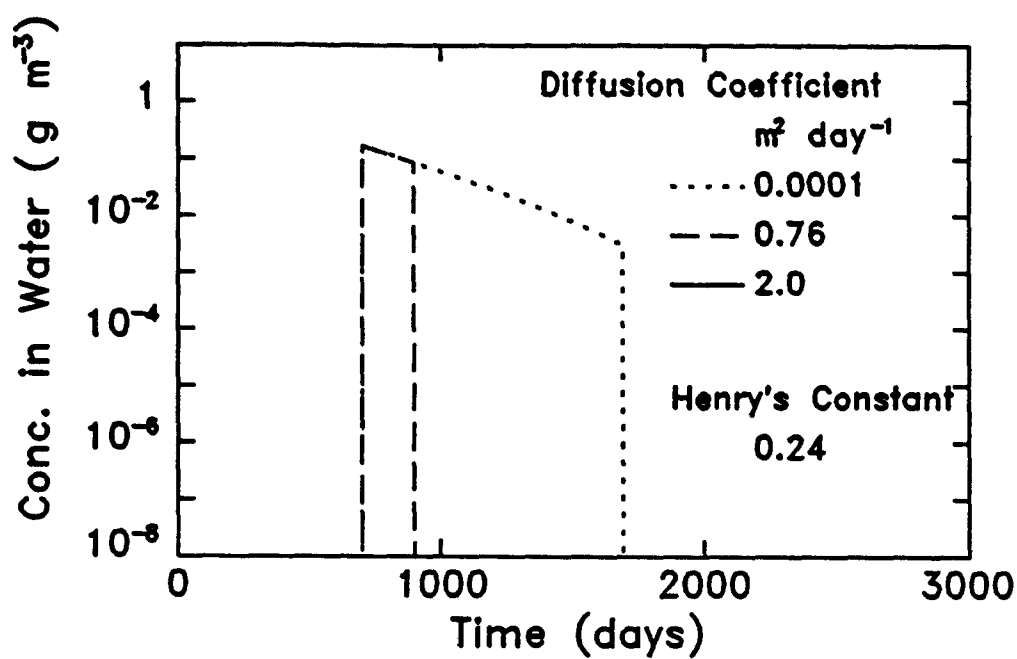
Figure 5.11. Predicted concentration of pollutant in water at 2.0 m and position of the pollutant slug as functions of time for different diffusion coefficients of pollutant in air for Henry's constant for benzene.
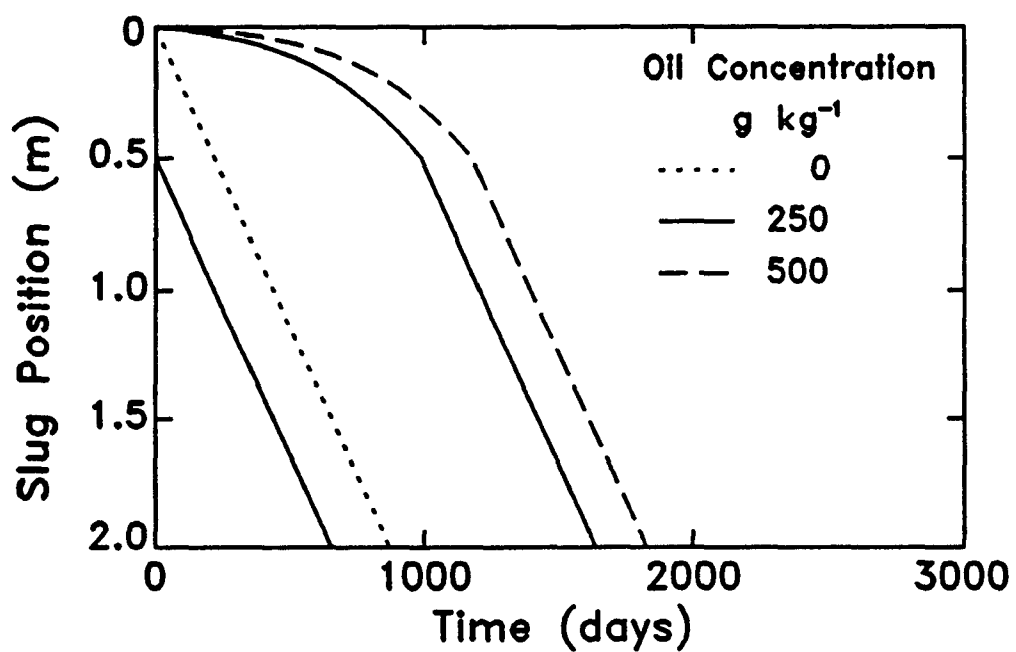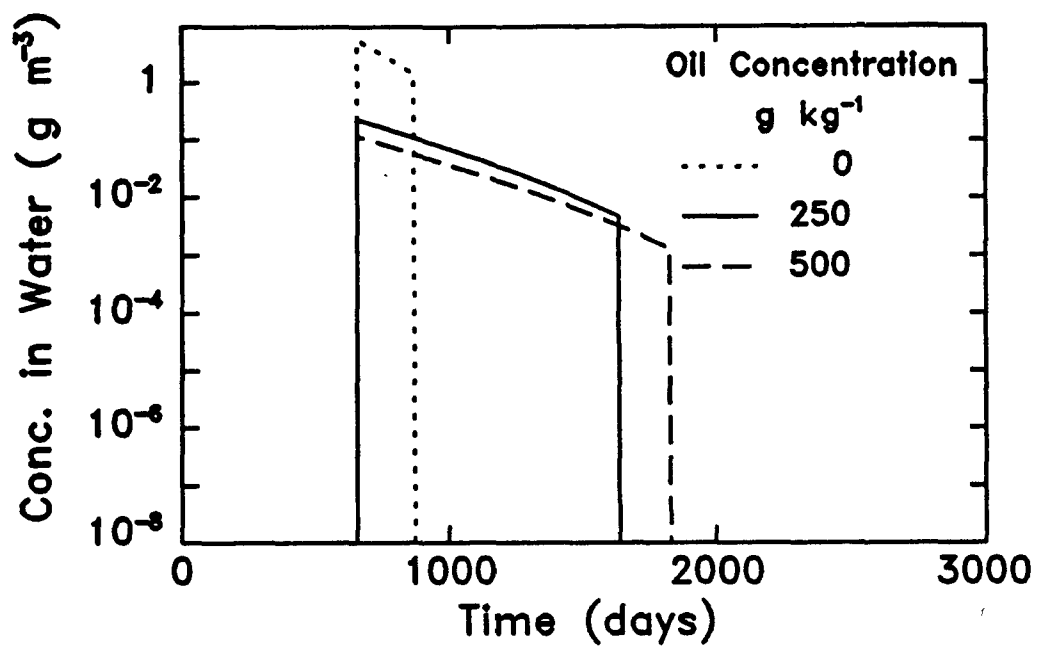
Figure 5.12. Predicted concentration of pollutant in water at 2.0 m and position of the pollutant slug as functions of time for different concentrations of oil in sludge.
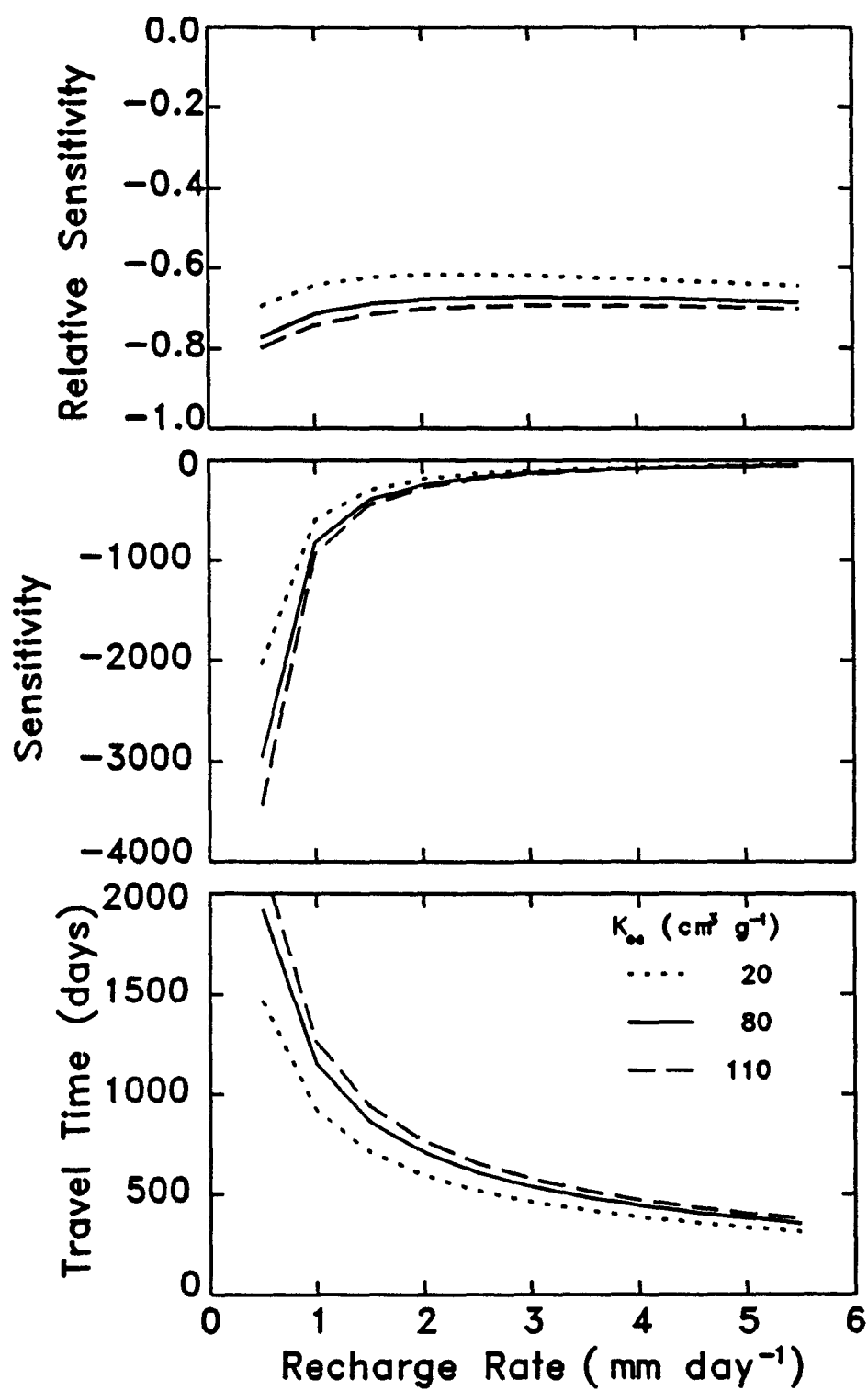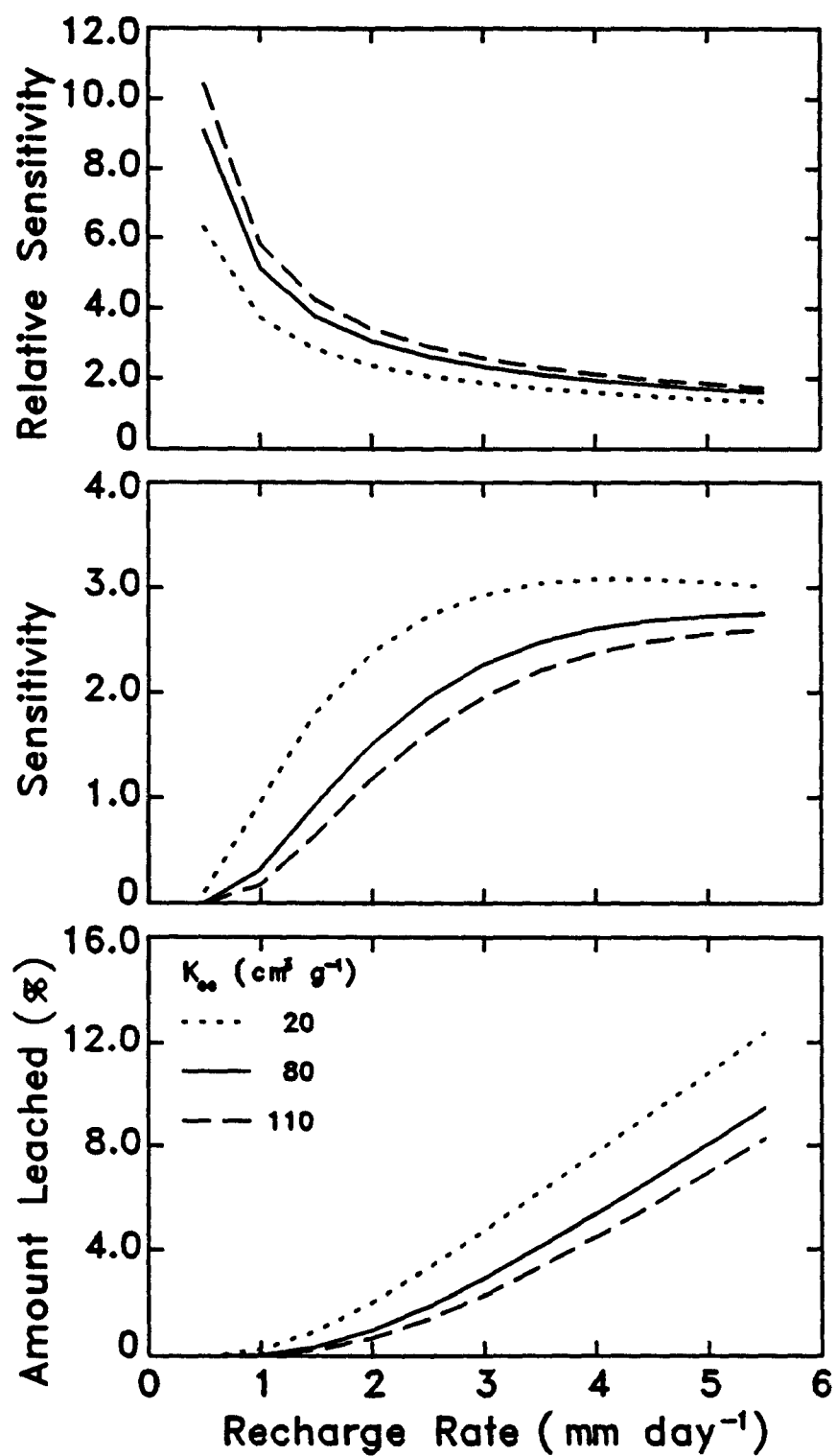
Figure 5.13. Sensitivity of travel time to recharge rate for chemicals with different organic carbon partition coefficients.
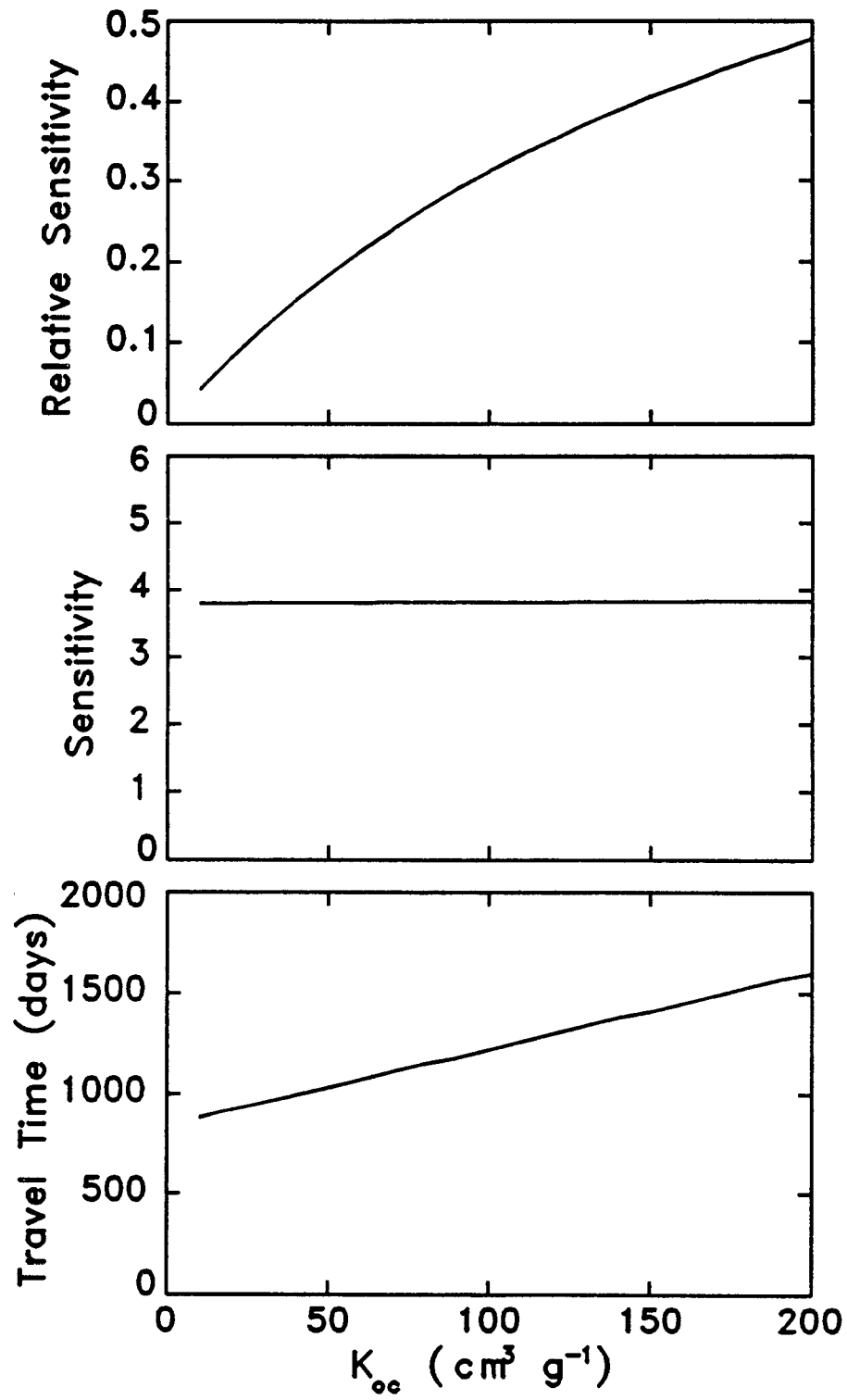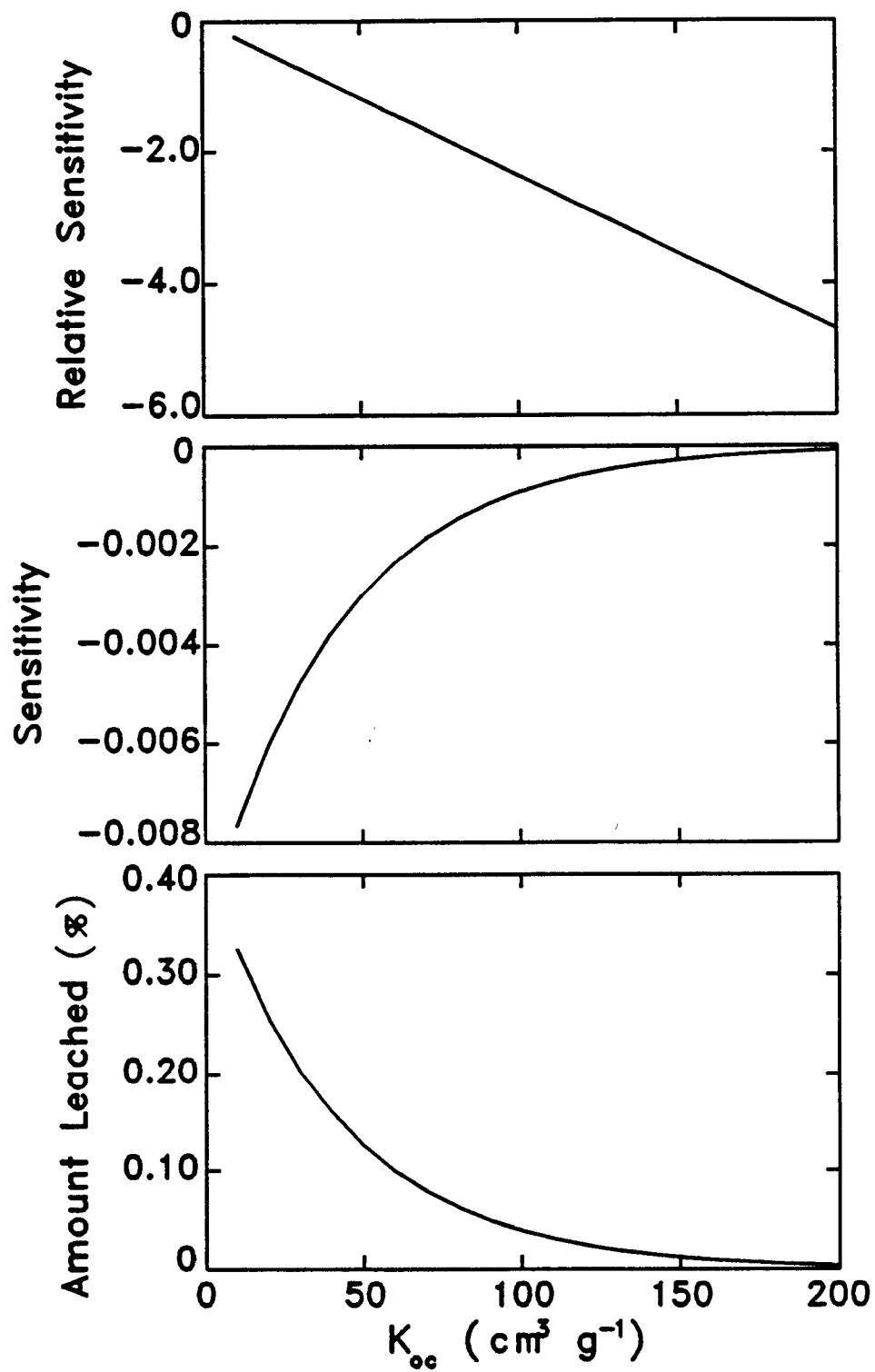
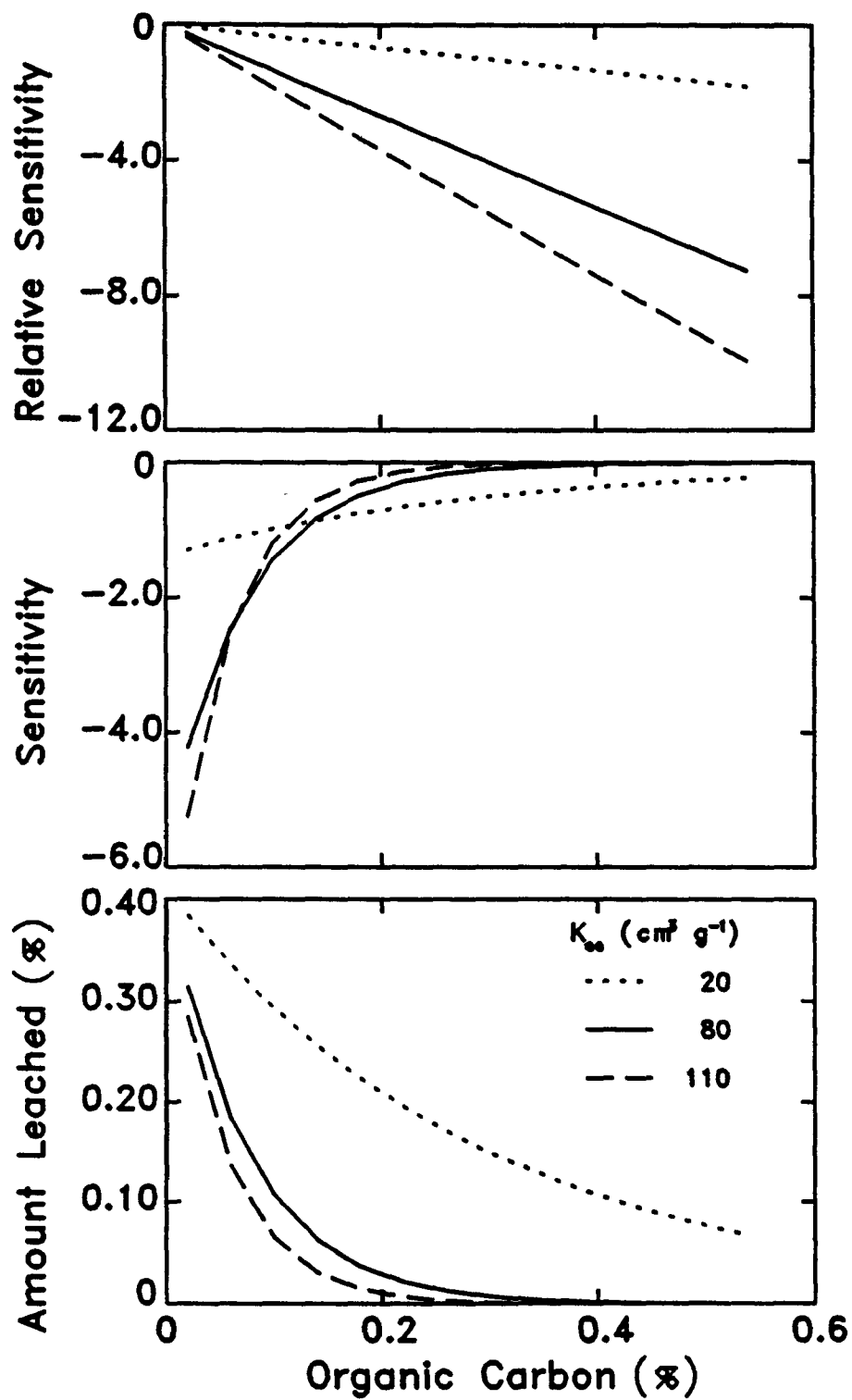Figure 5.14. Sensitivity of travel time to organic carbon partition coefficient.
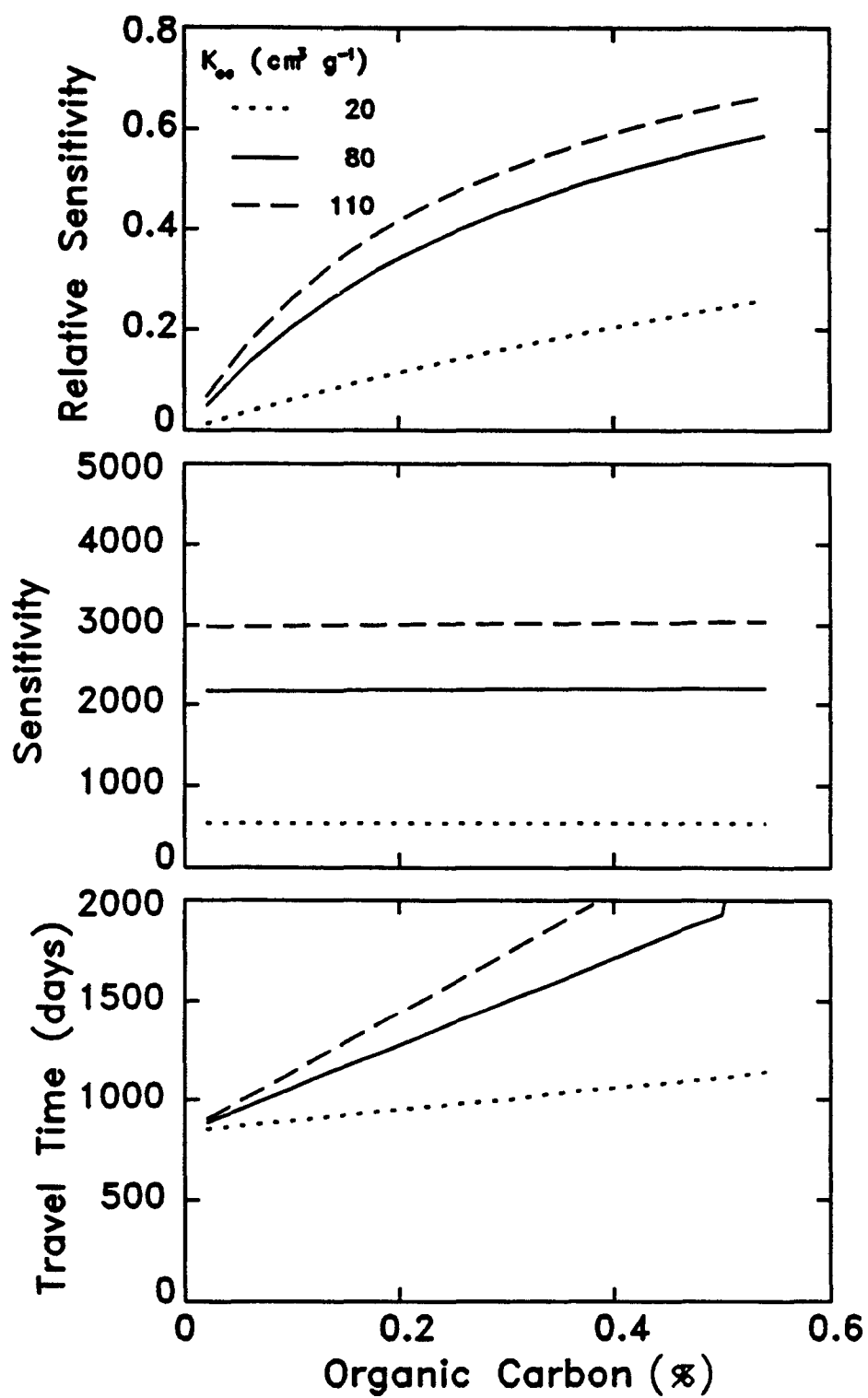
Figure 5.15. Sensitivity of travel time to organic carbon content for chemicals with different organic carbon partition coefficients.
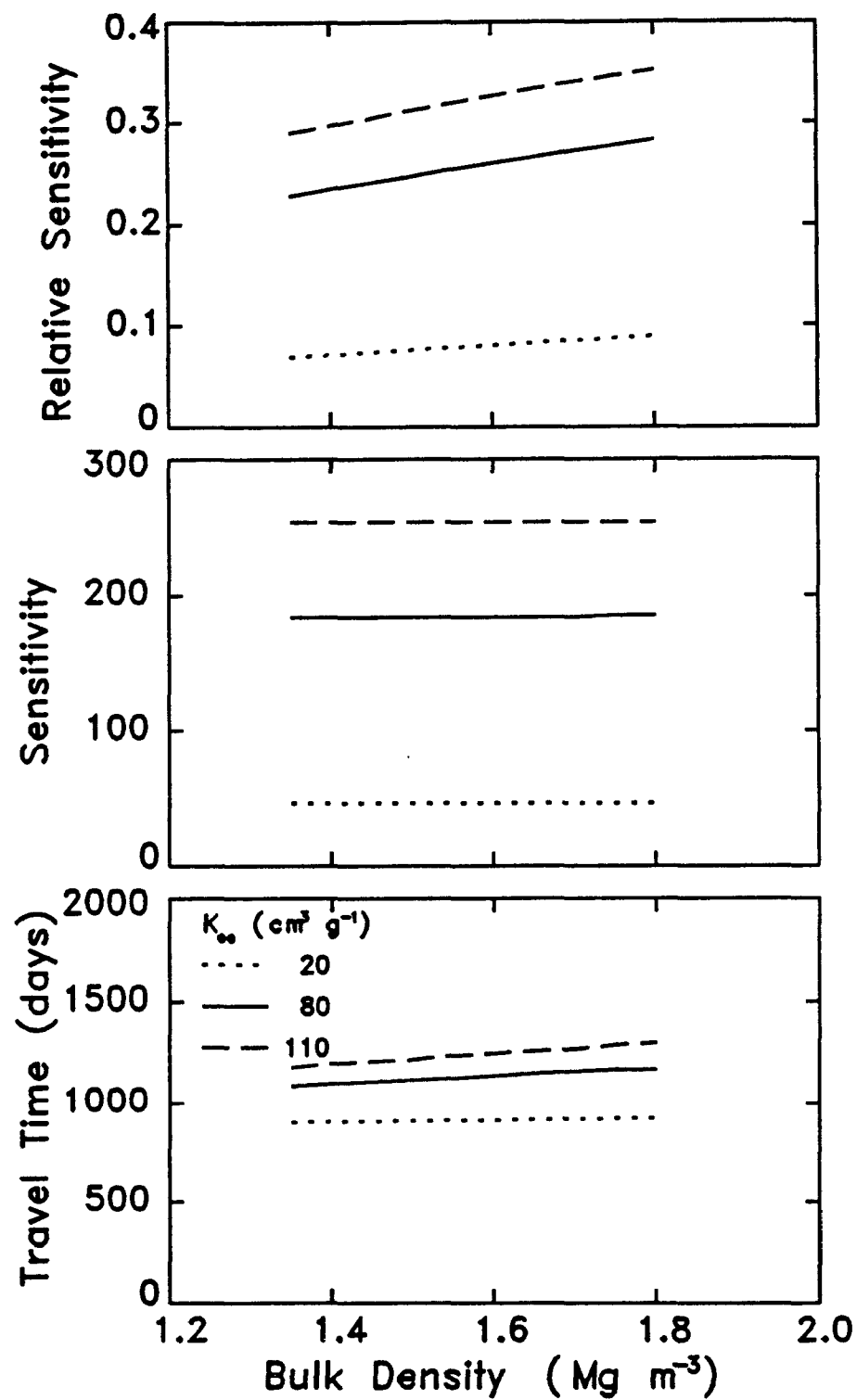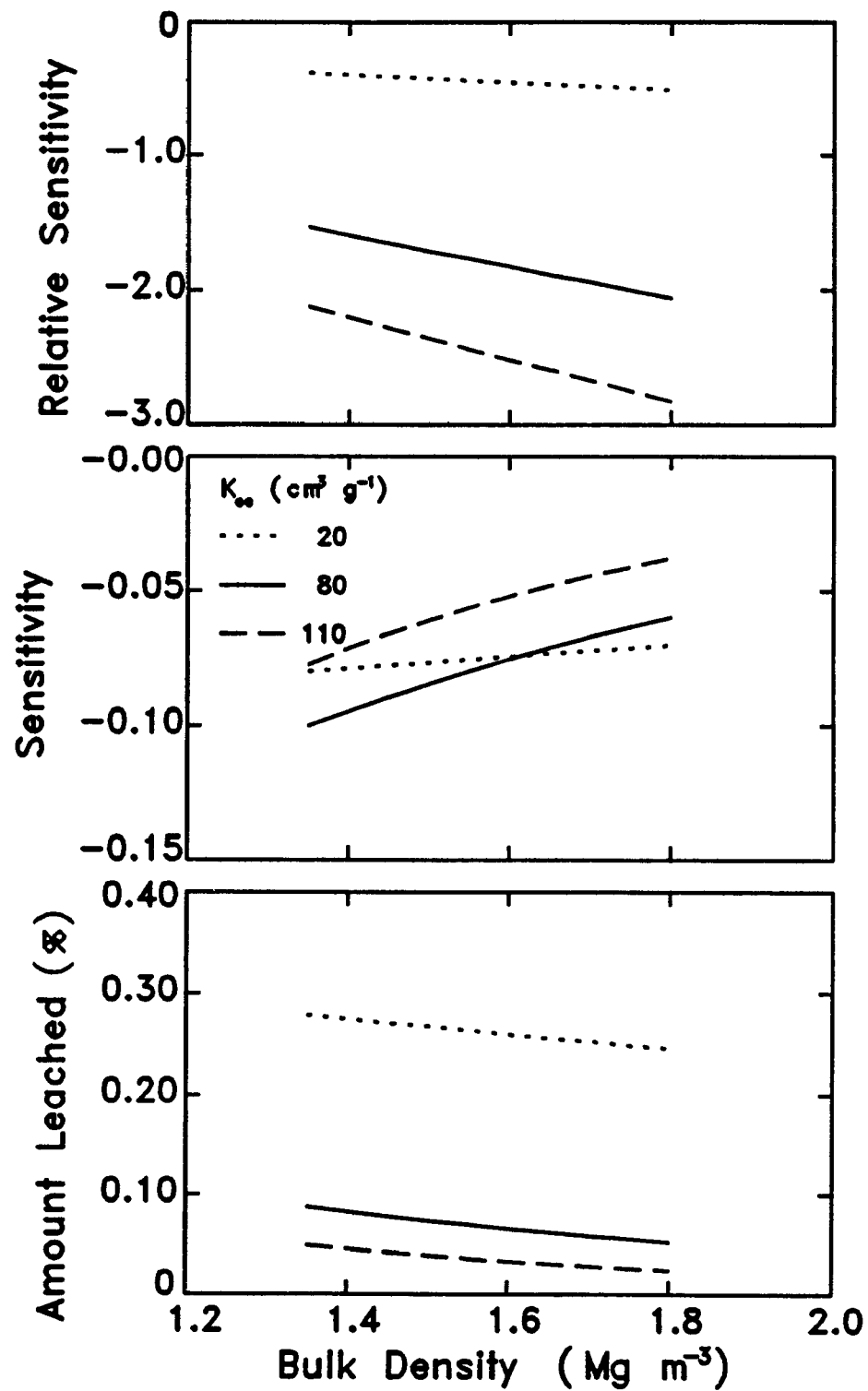
Figure 5.16. Sensitivity of travel time to soil bulk density for chemicals with different organic carbon partition coefficients.
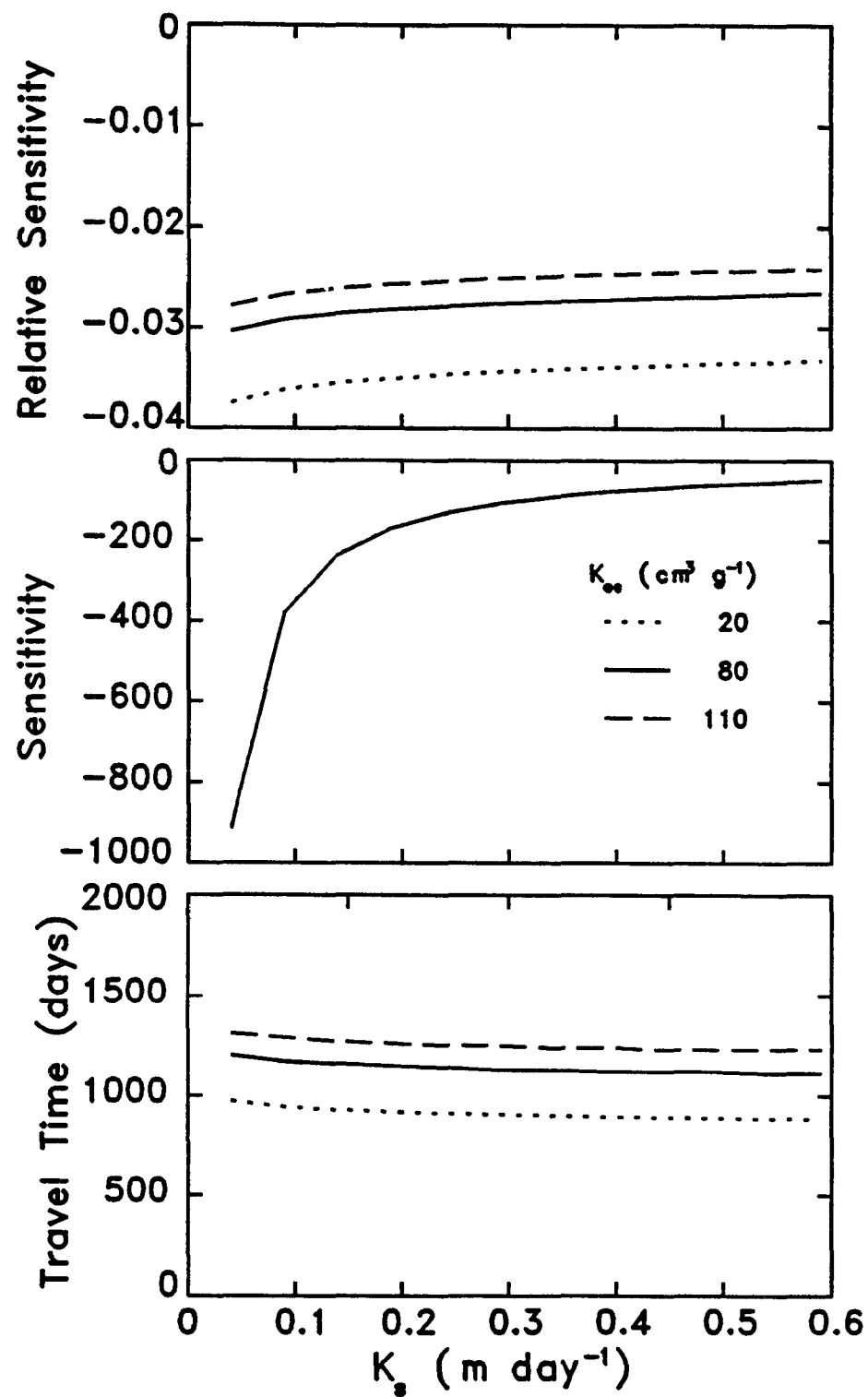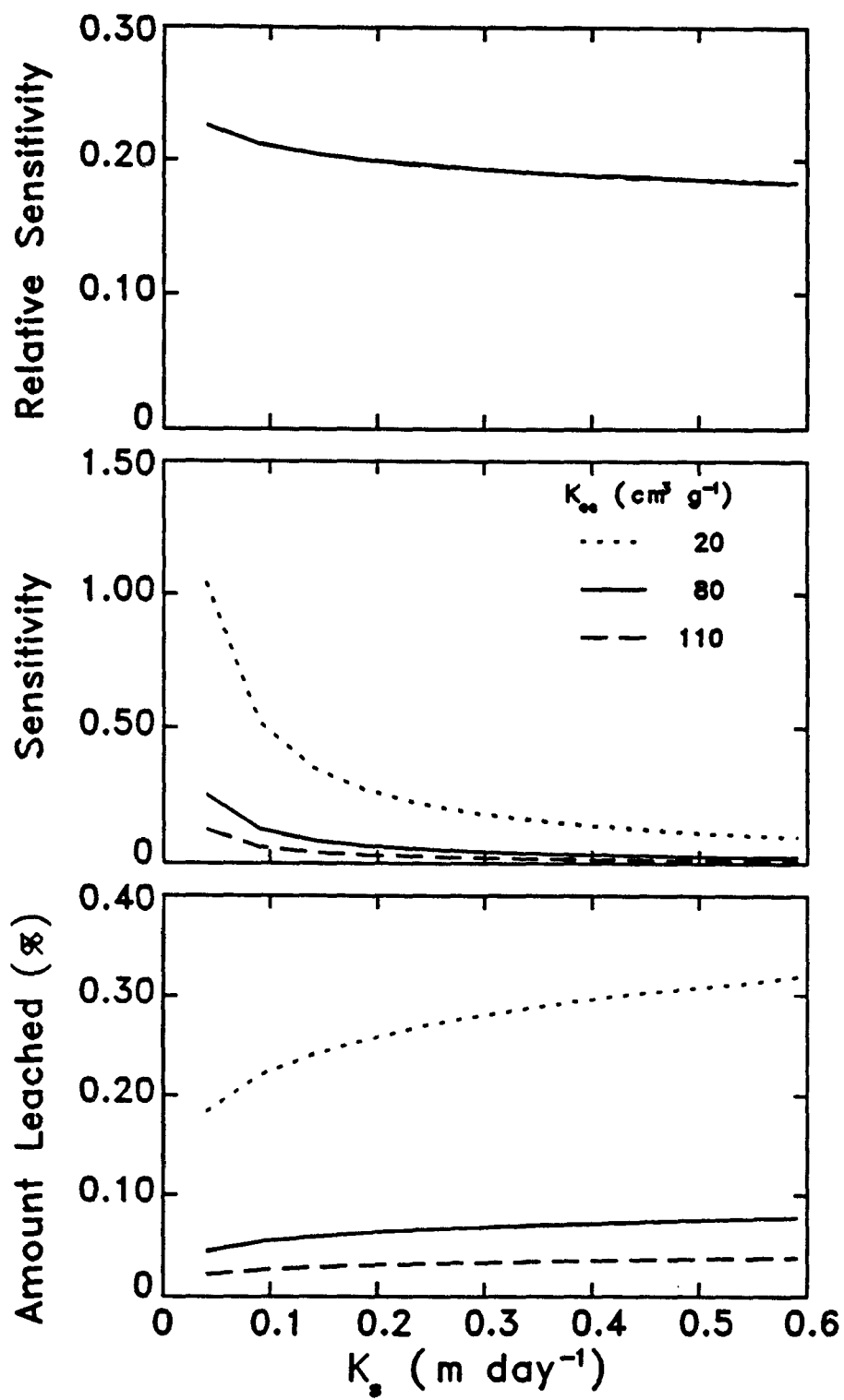
Figure 5.17. Sensitivity of travel time to soil saturated hydraulic conductivity for chemicals with different organic carbon partition coefficients.
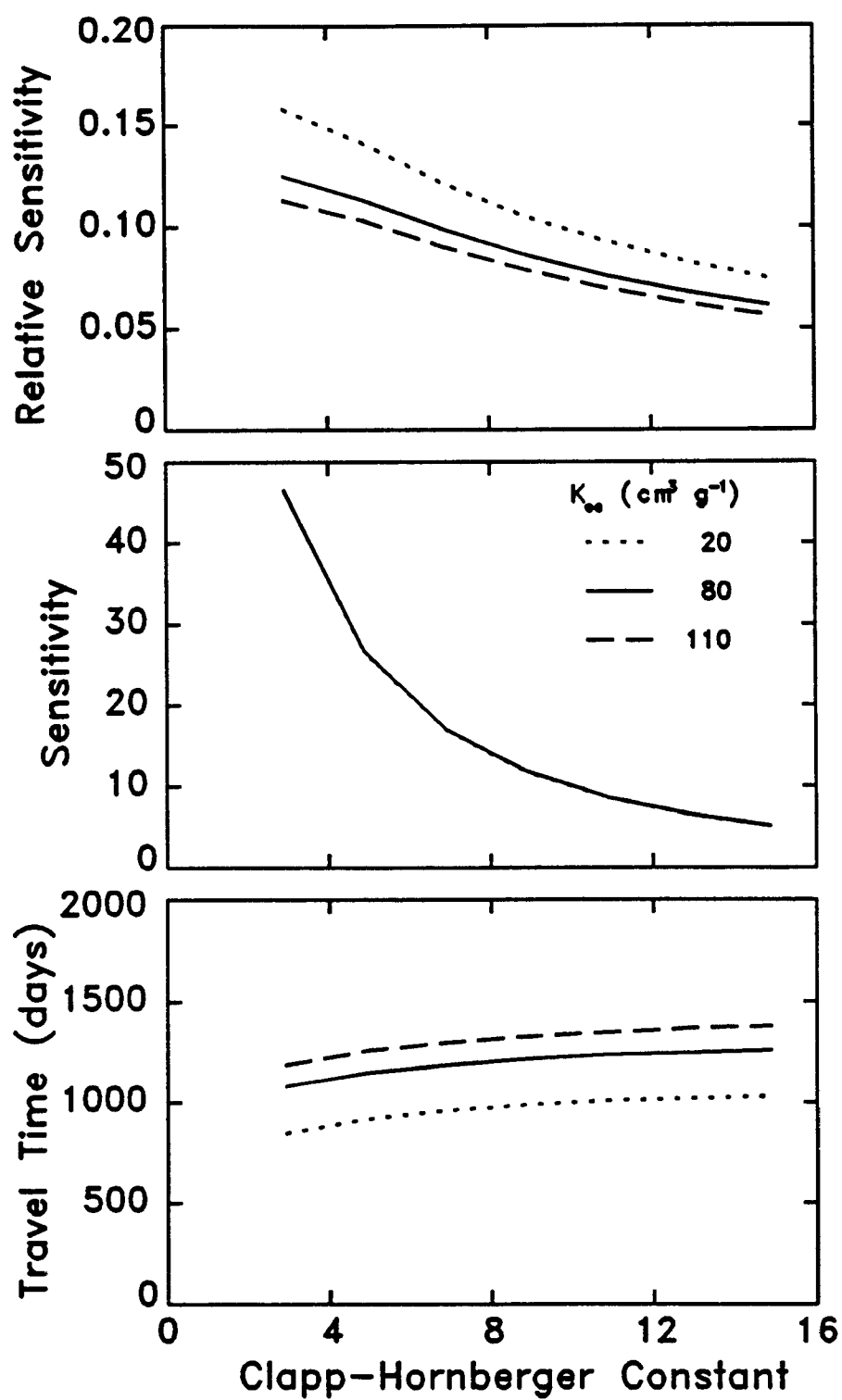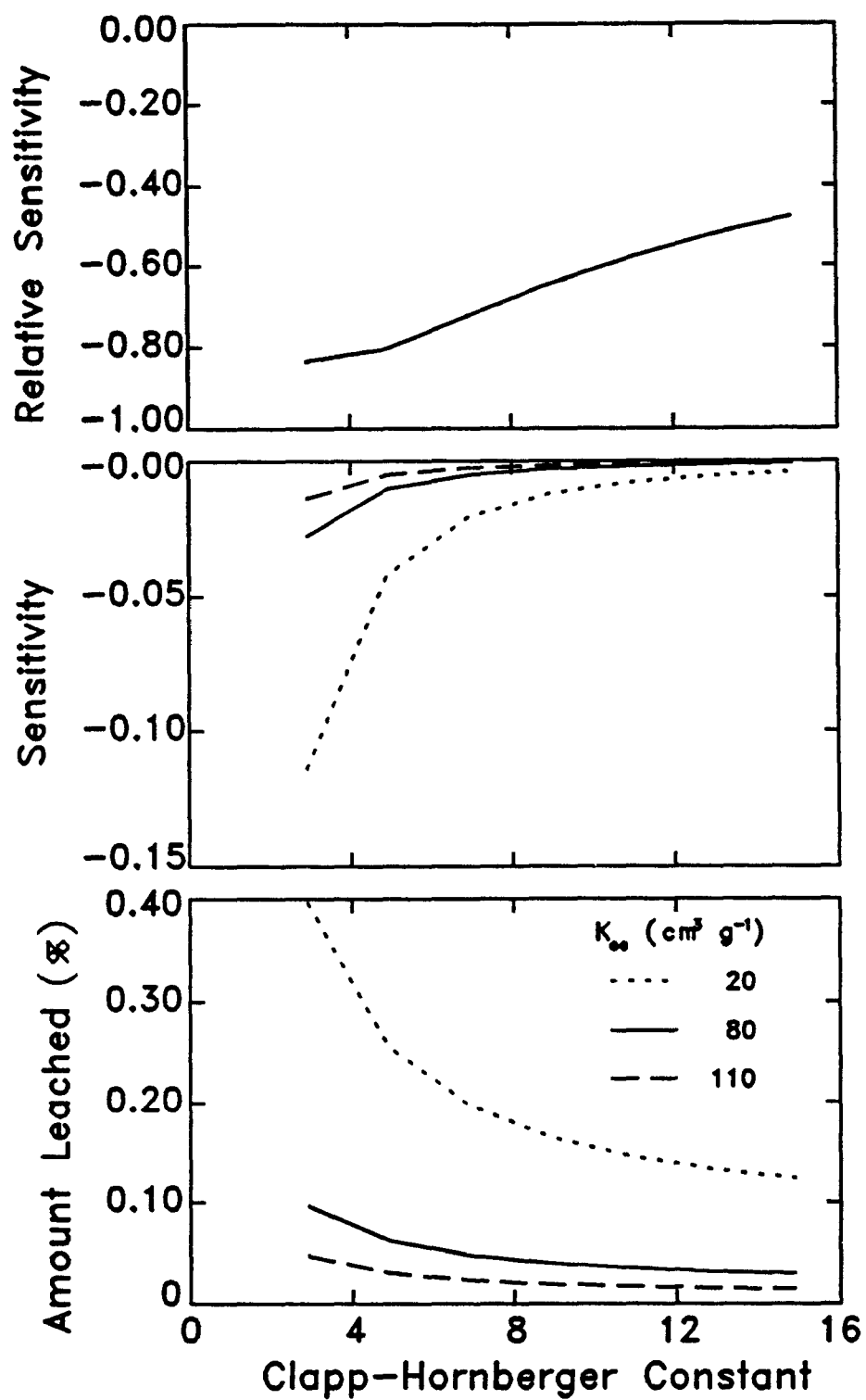
Figure 5.18. Sensitivity of travel time to Clapp-Hornberger constant for chemicals with different organic carbon partition coefficients.
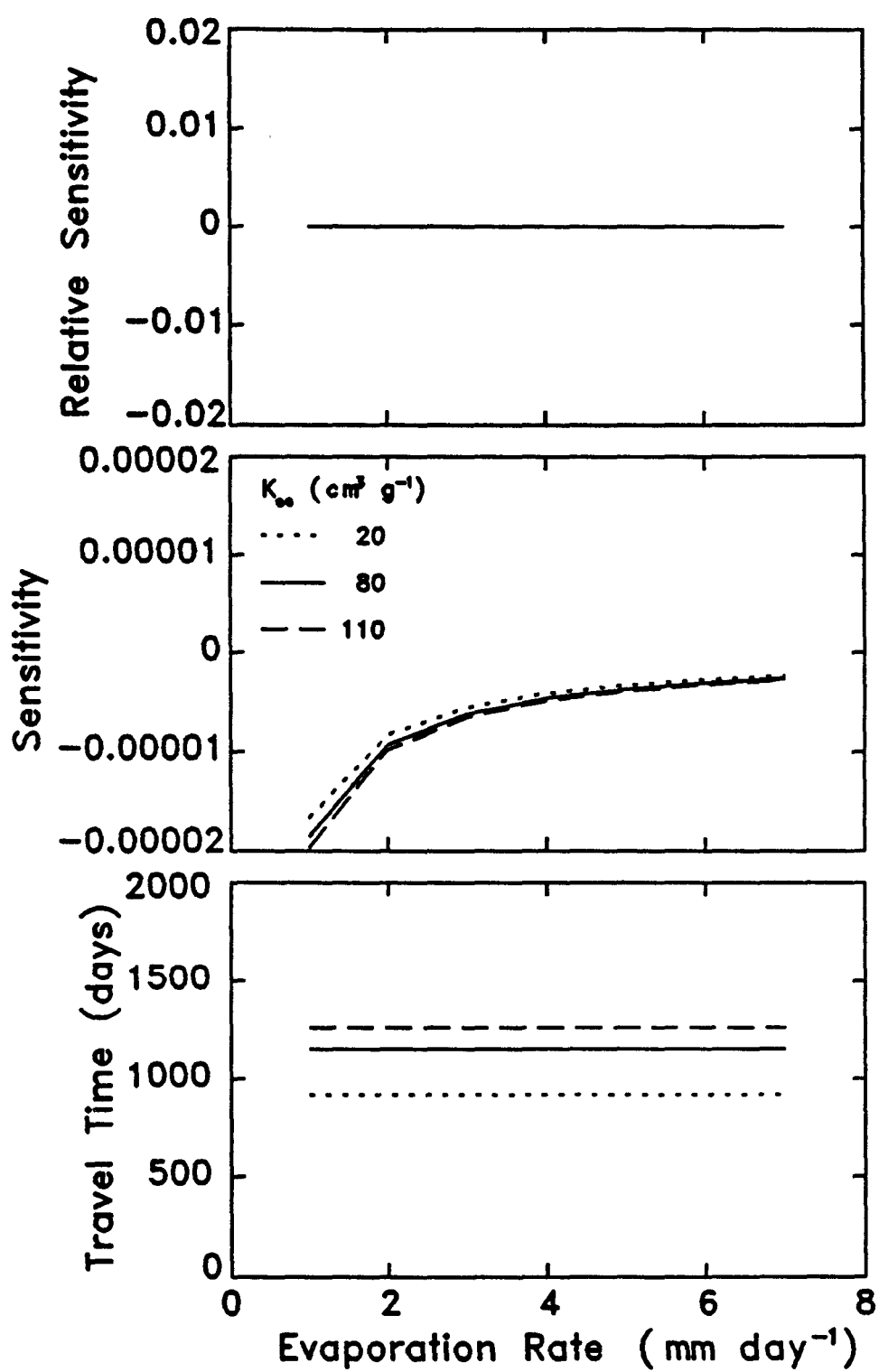
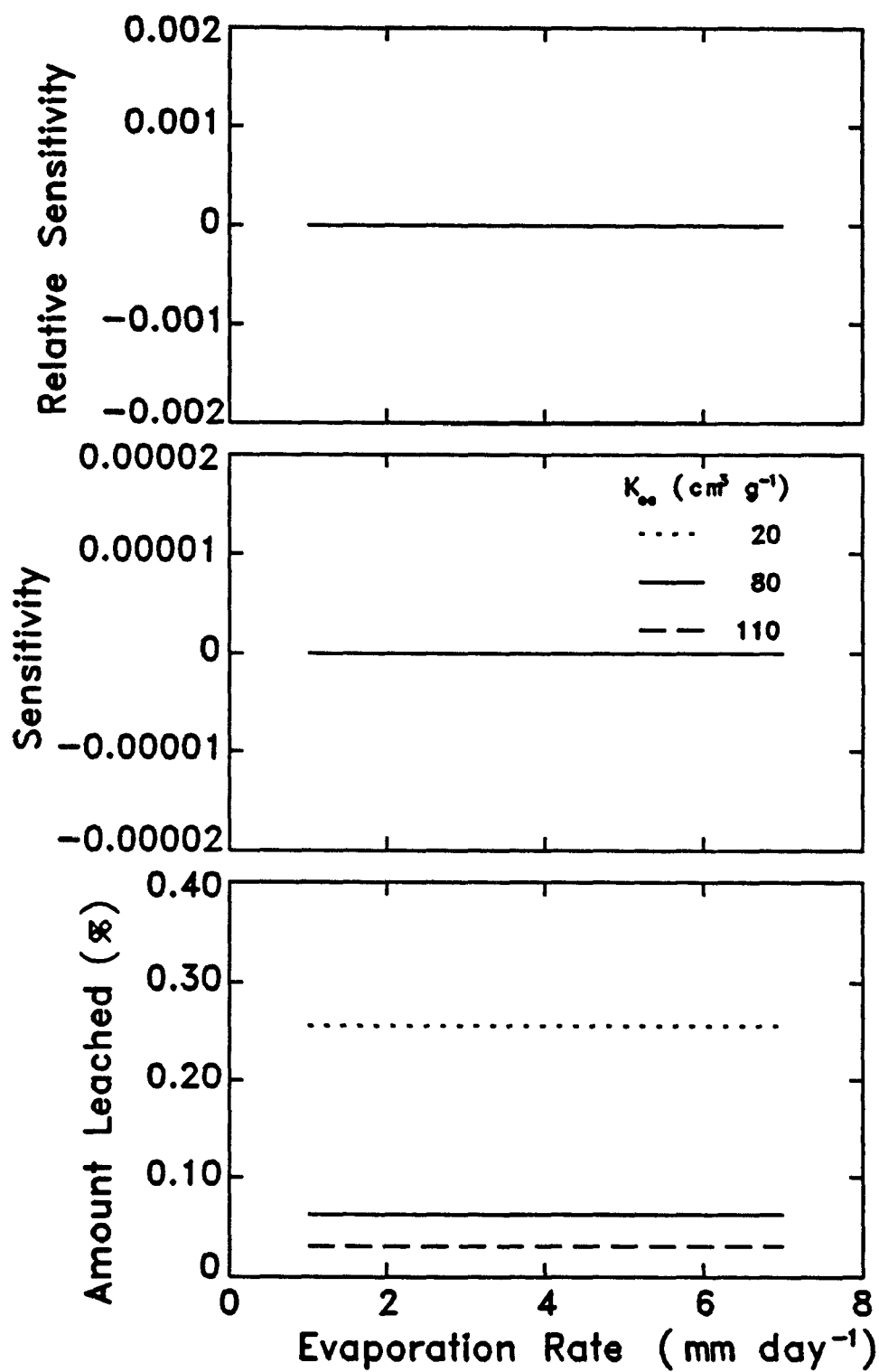Figure 5.19. Sensitivity of travel time to evaporation rate for chemicals with different carbon partition coefficients.
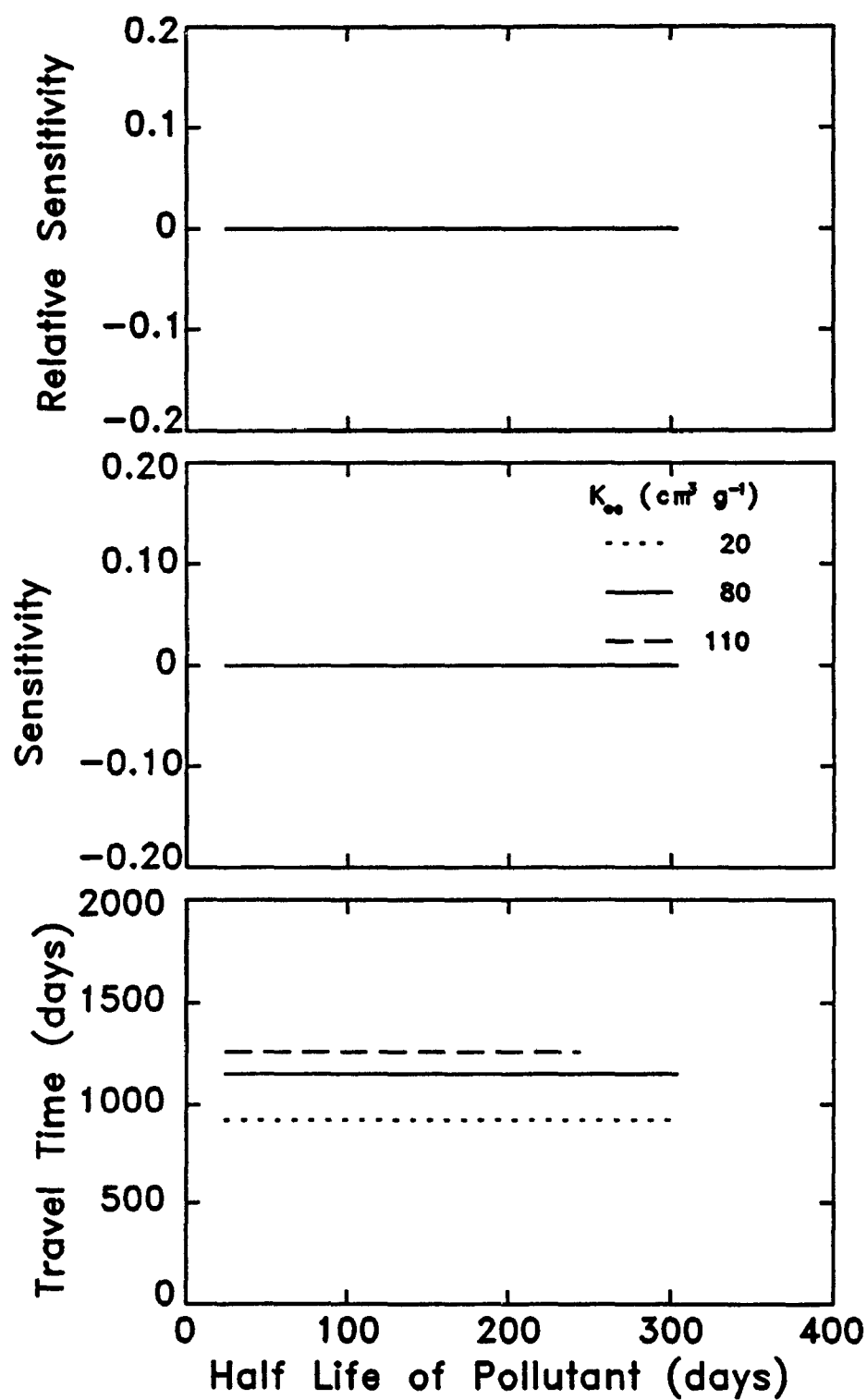
Figure 5.20. Sensitivity of travel time to degradation half-life of the pollutant for chemicals with different organic carbon partition coefficients.
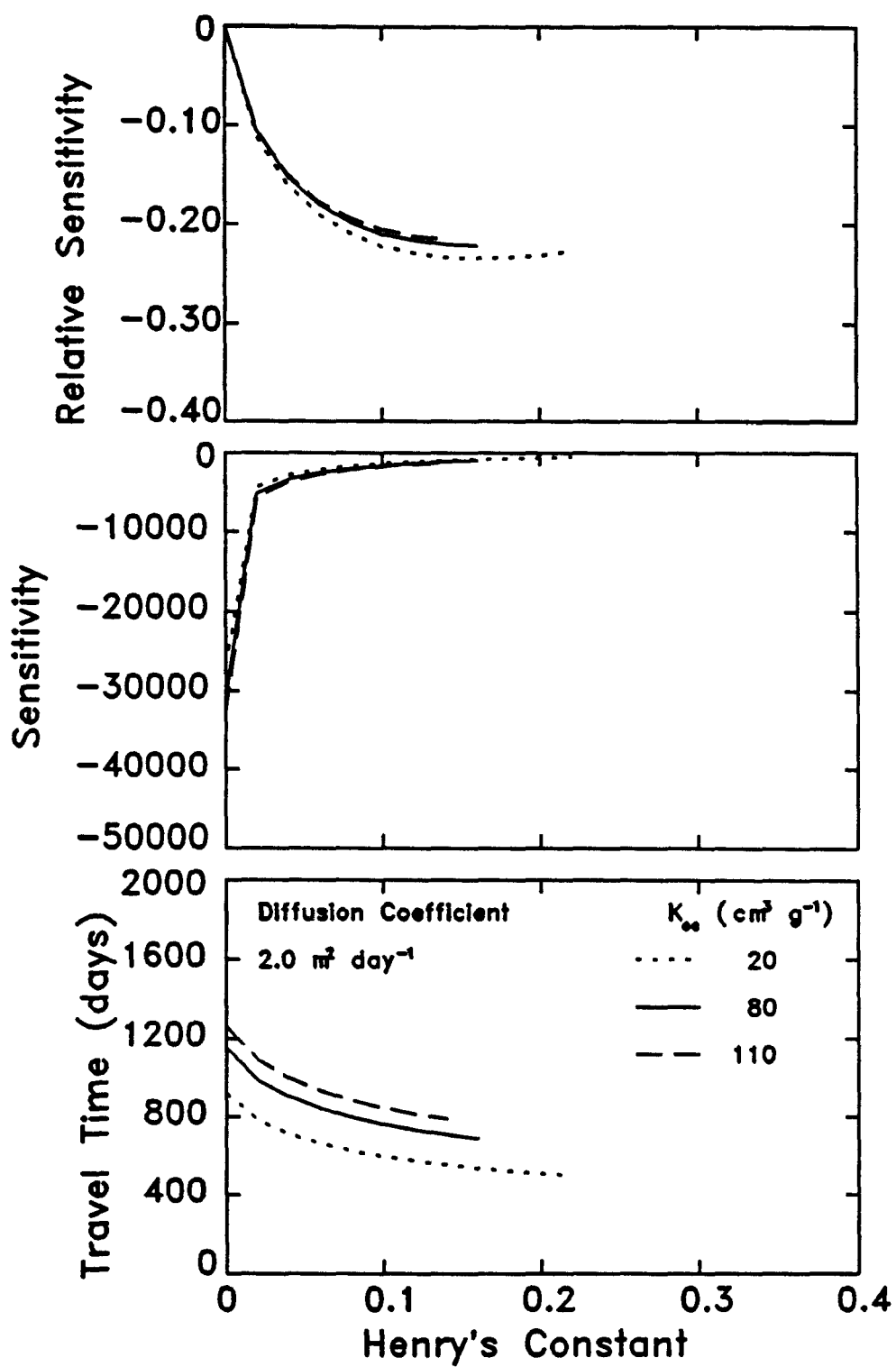
Figure 5.21. Sensitivity of travel time to Henry's constant for chemicals with different organic carbon partition coefficients.
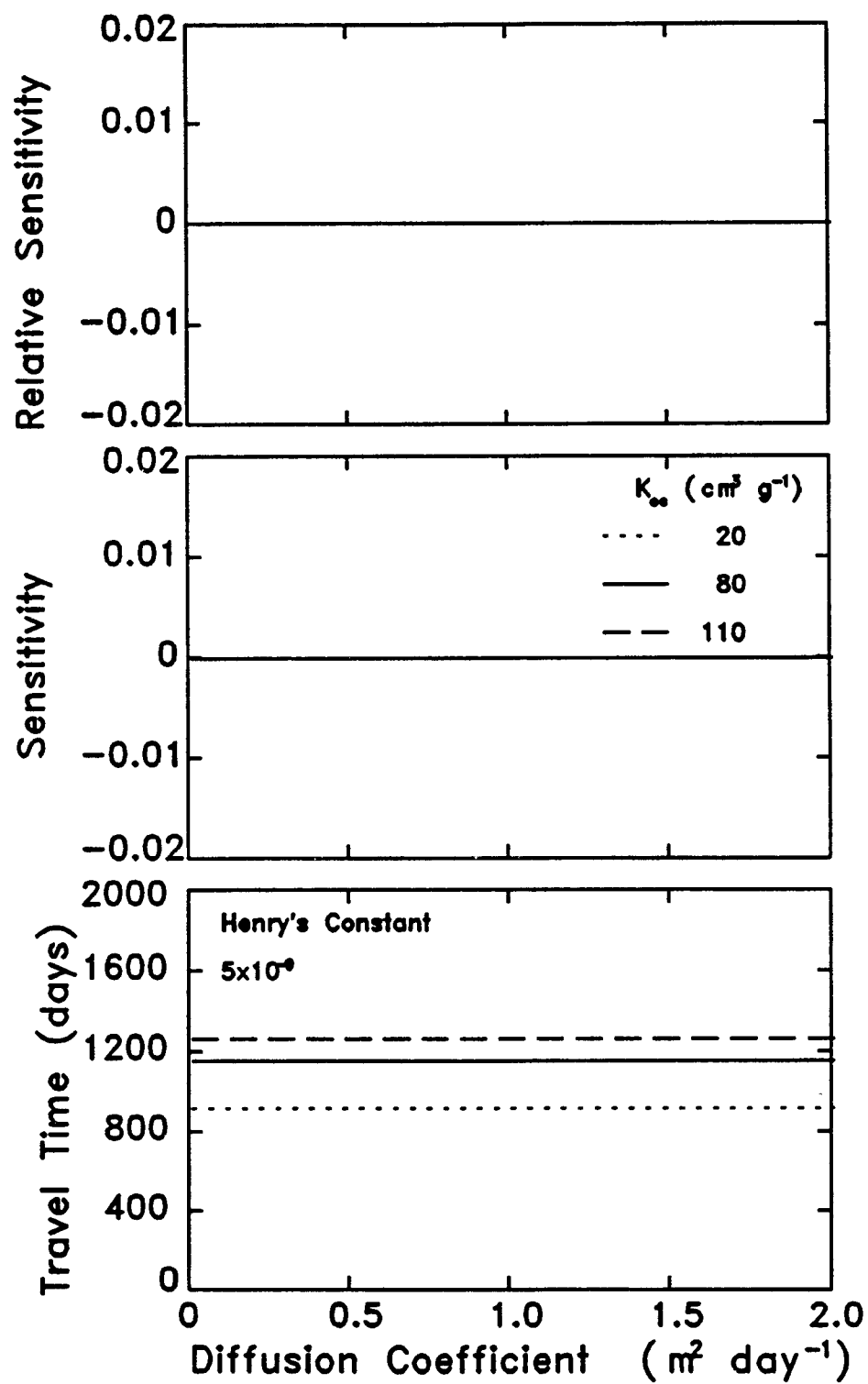
Figure 5.22. Sensitivity of travel time to the diffusion coefficient of the pollutant in air for chemicals with different organic carbon partition coefficients and very small Henry's constant.
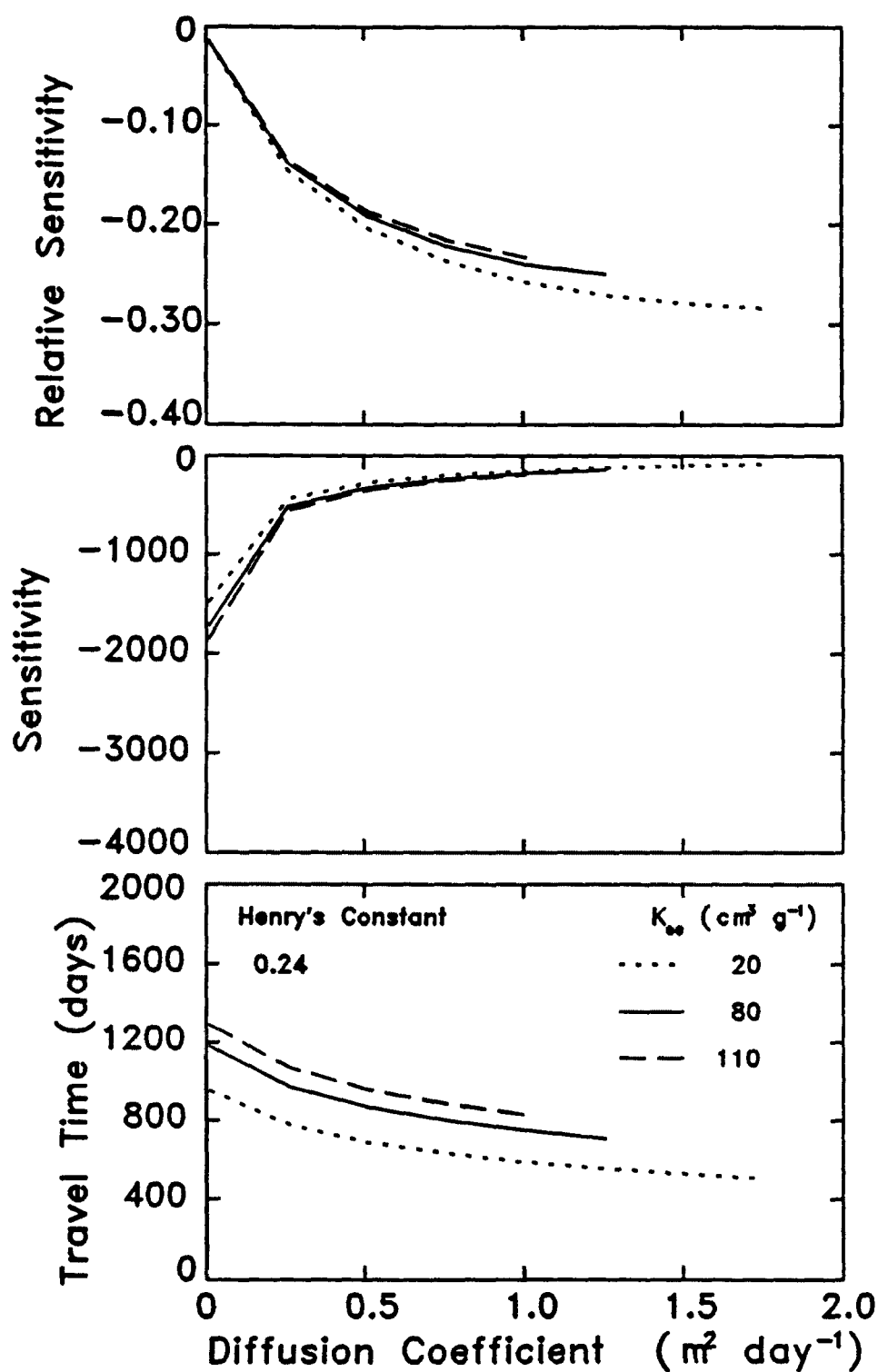
Figure 5.23. Sensitivity of travel time to the diffusion coefficient of the pollutant in air for chemicals with different organic carbon partition coefficients and Henry's constant of benzene.
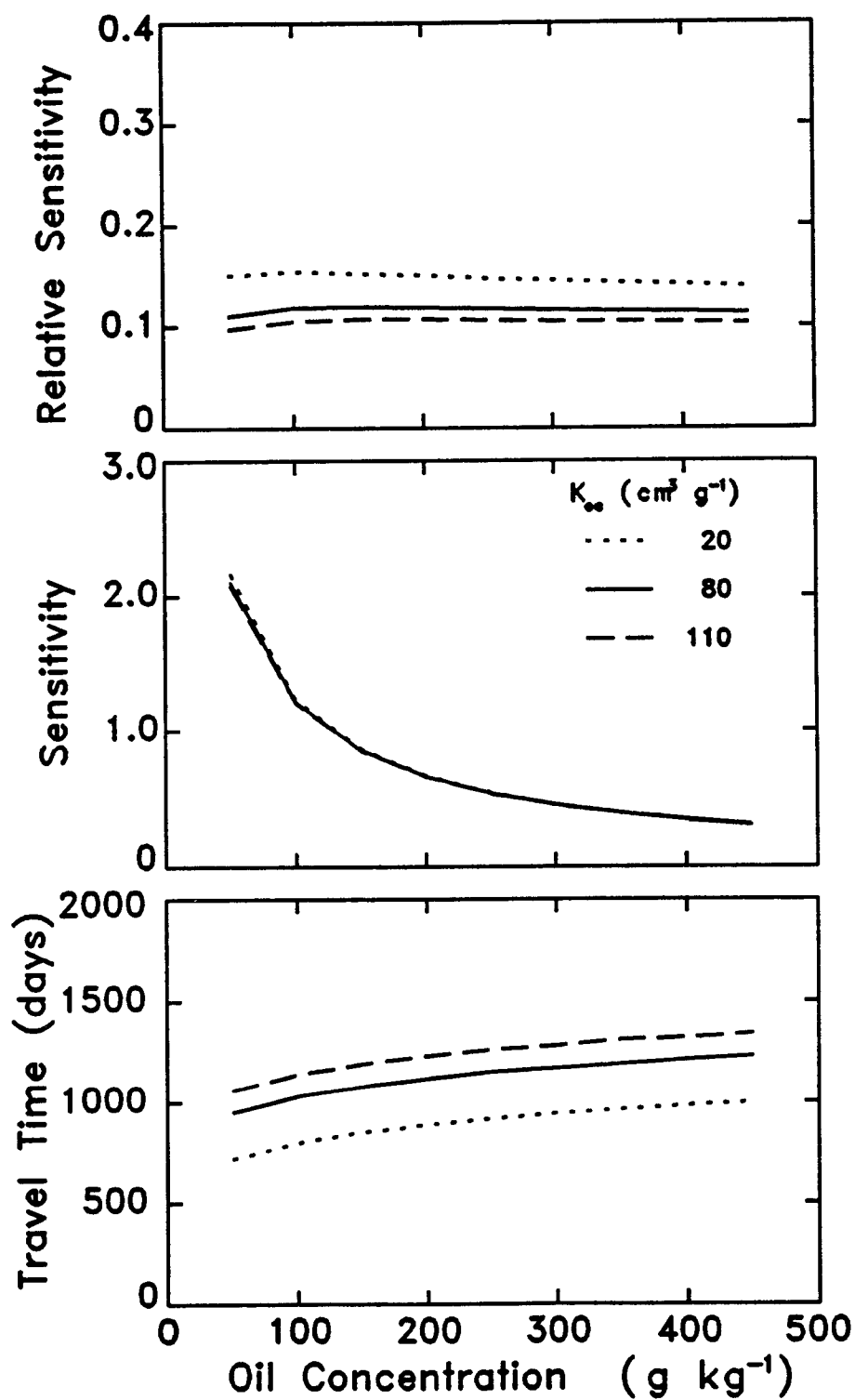
Figure 5.24. Sensitivity of travel time to concentration of oil in the sludge for chemicals with different organic carbon partition coefficients.
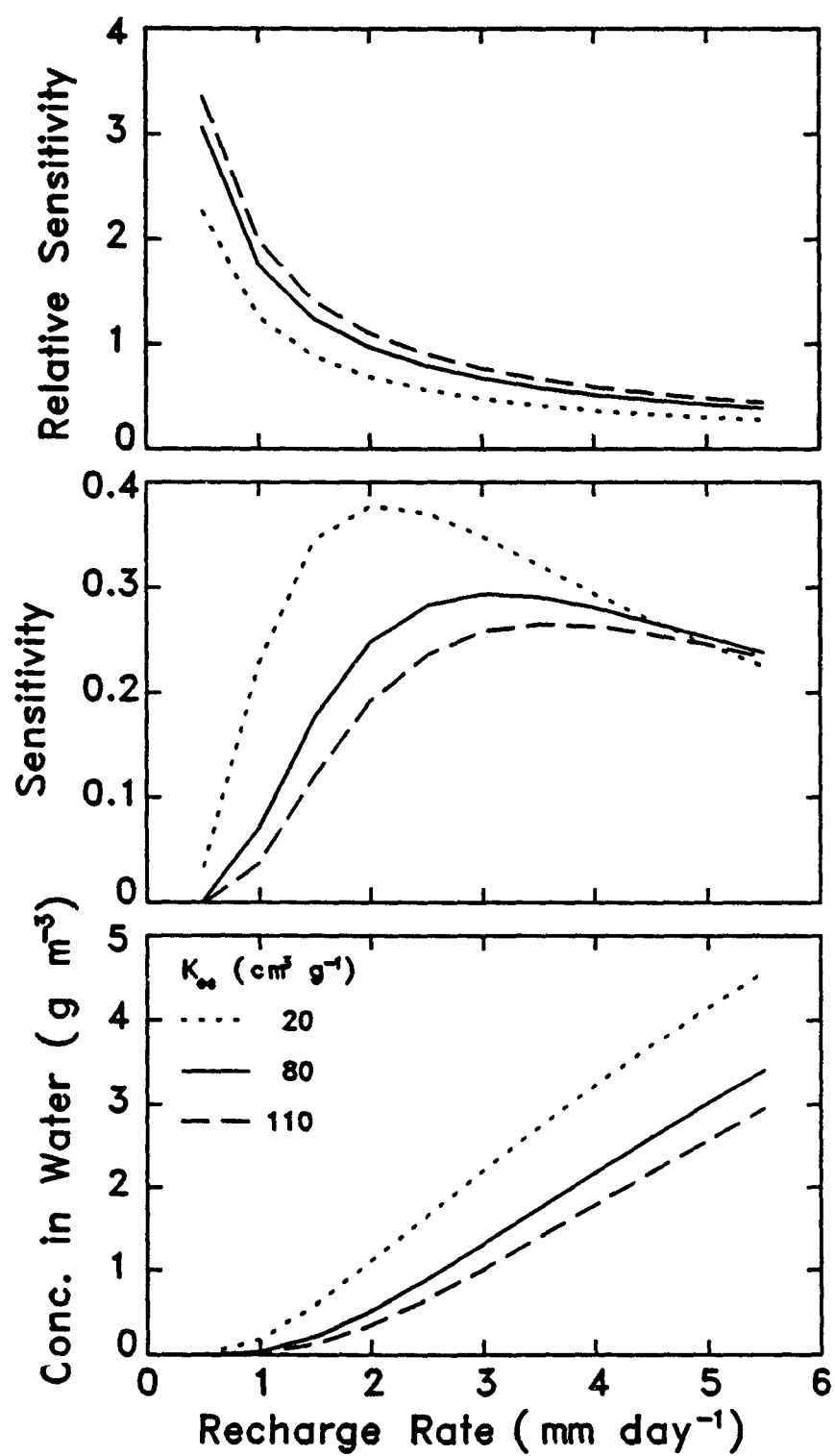
Figure 5.25. Sensitivity of concentration of pollutant in water to recharge rate for chemicals with different organic carbon partition coefficients.
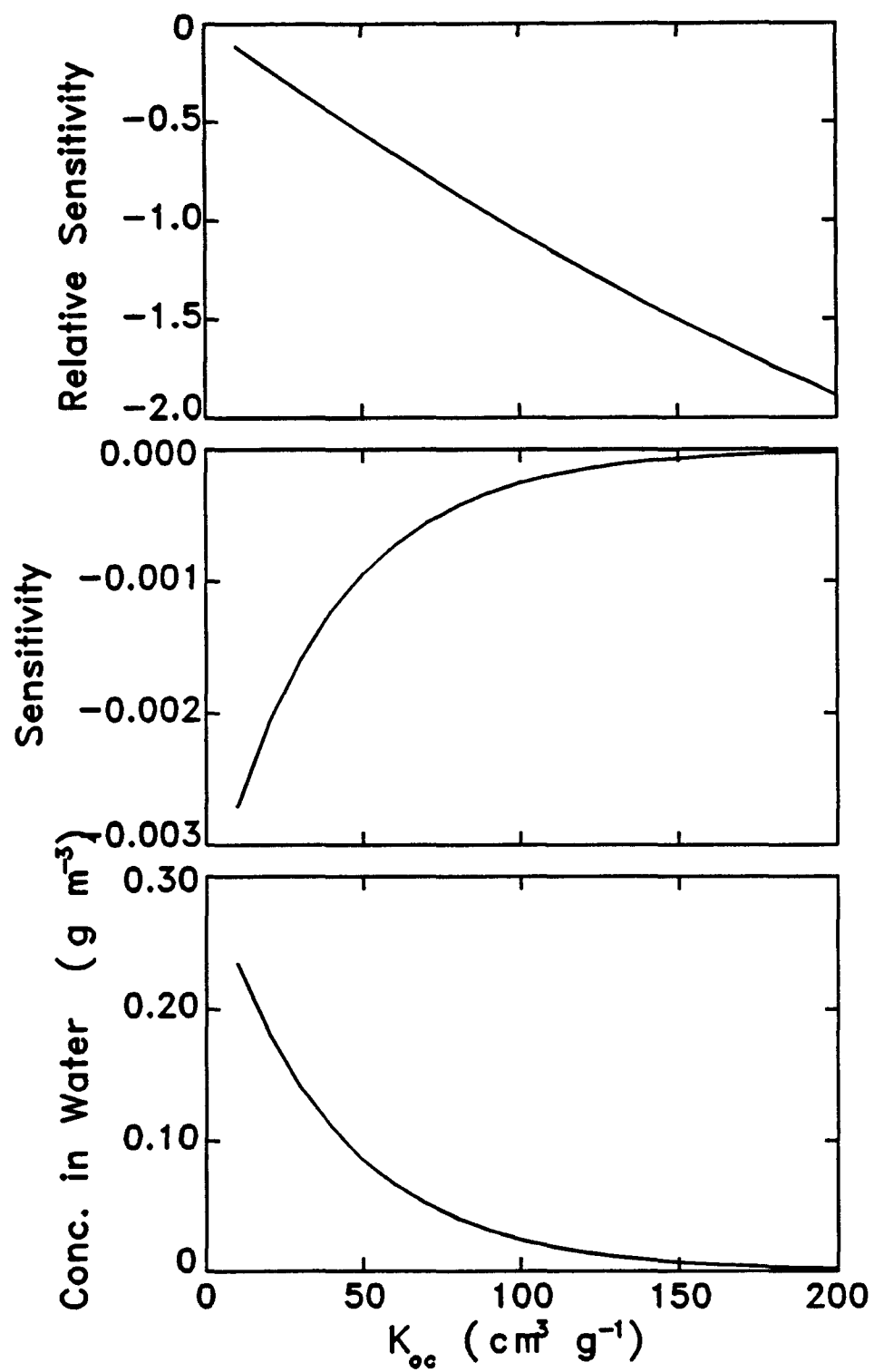
Figure 5.26. Sensitivity of concentration of pollutant in water to organic carbon partition coefficient.
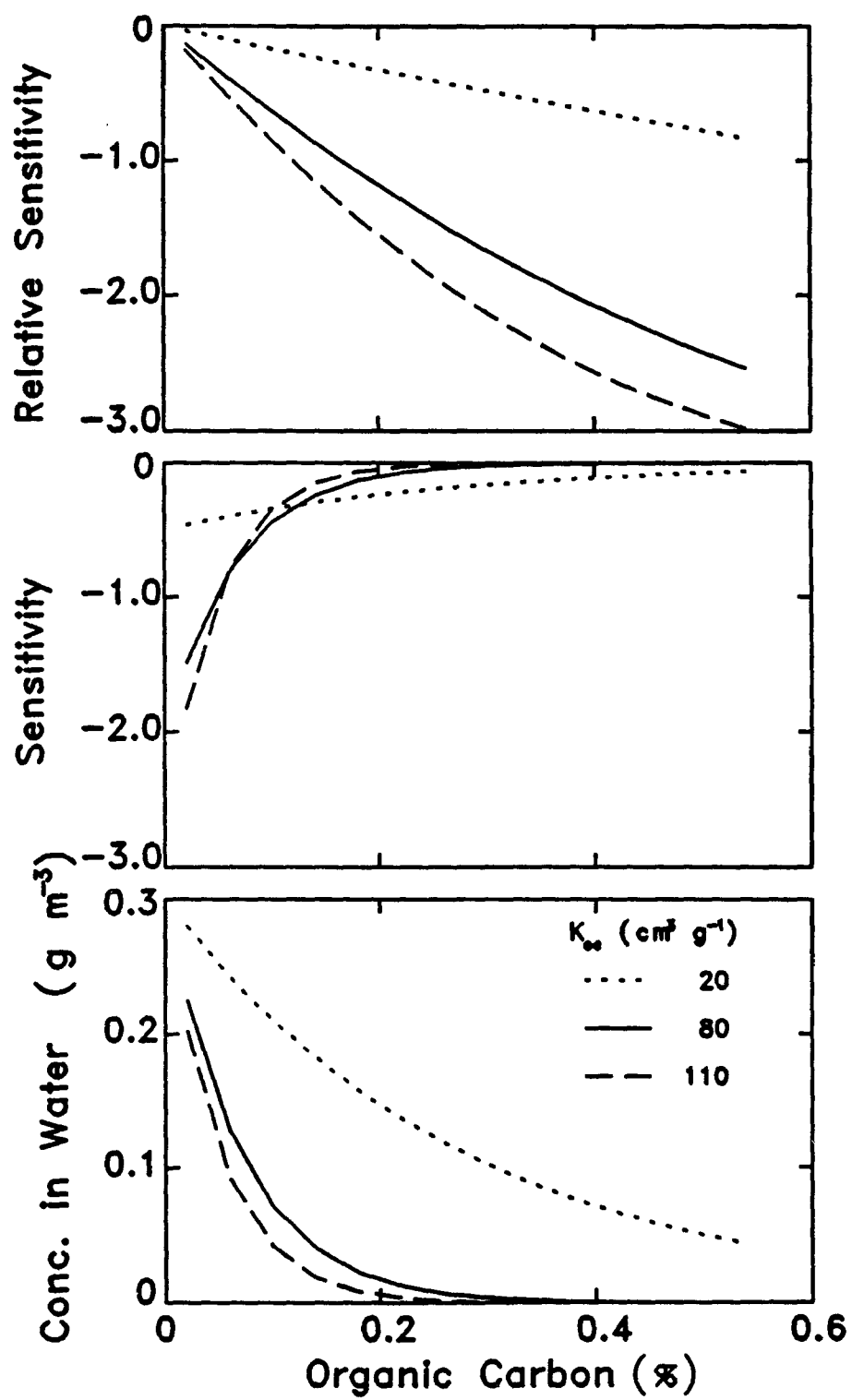
Figure 5.27. Sensitivity of concentration of pollutant in water to organic carbon content for chemicals with different organic carbon partition coefficients.
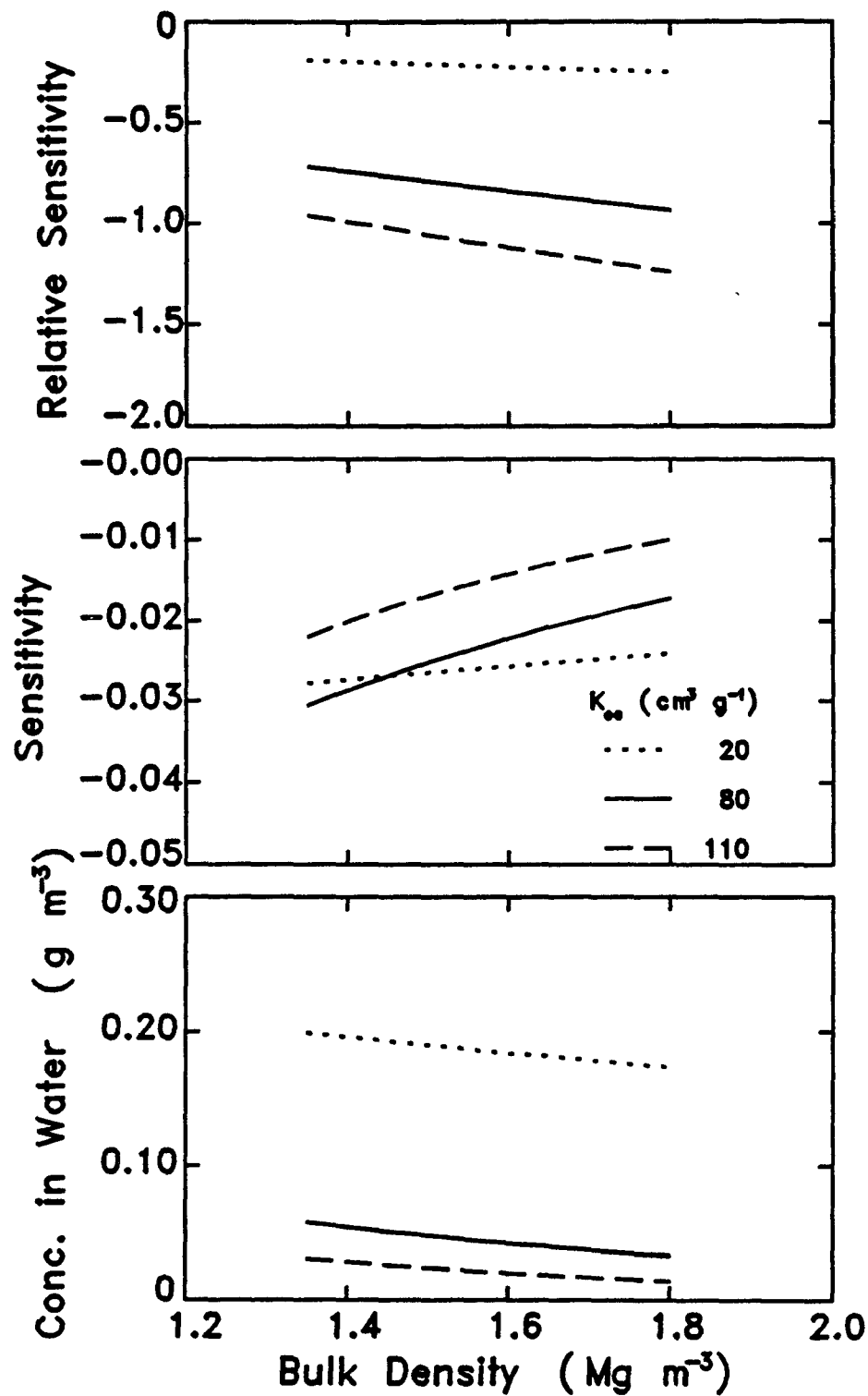
Figure 5.28. Sensitivity of concentration of pollutant in water to soil bulk density for chemicals with different organic carbon partition coefficients.
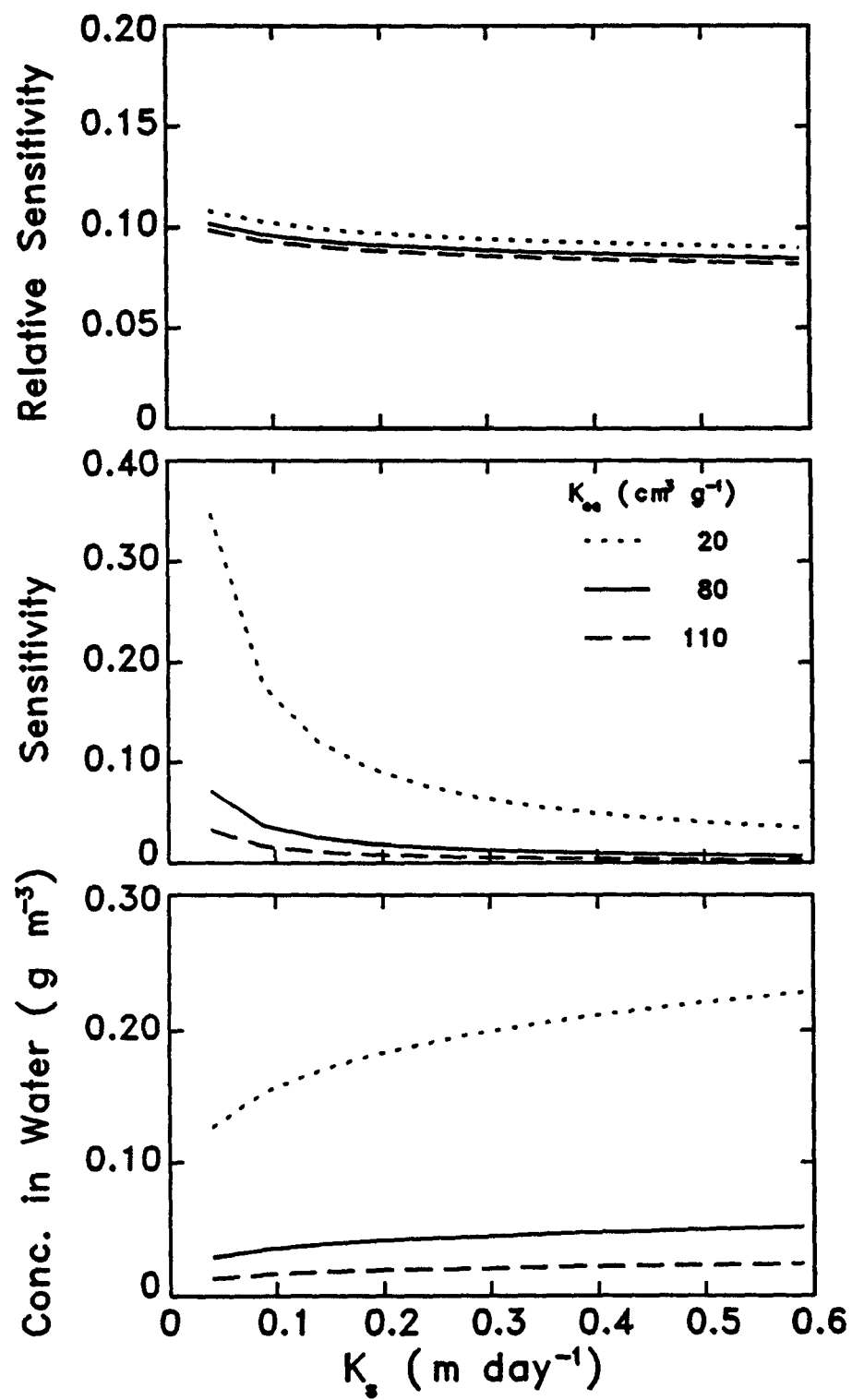
Figure 5.29. Sensitivity of concentration of pollutant in water to soil saturated hydraulic conductivity for chemicals with different organic carbon partition coefficients.
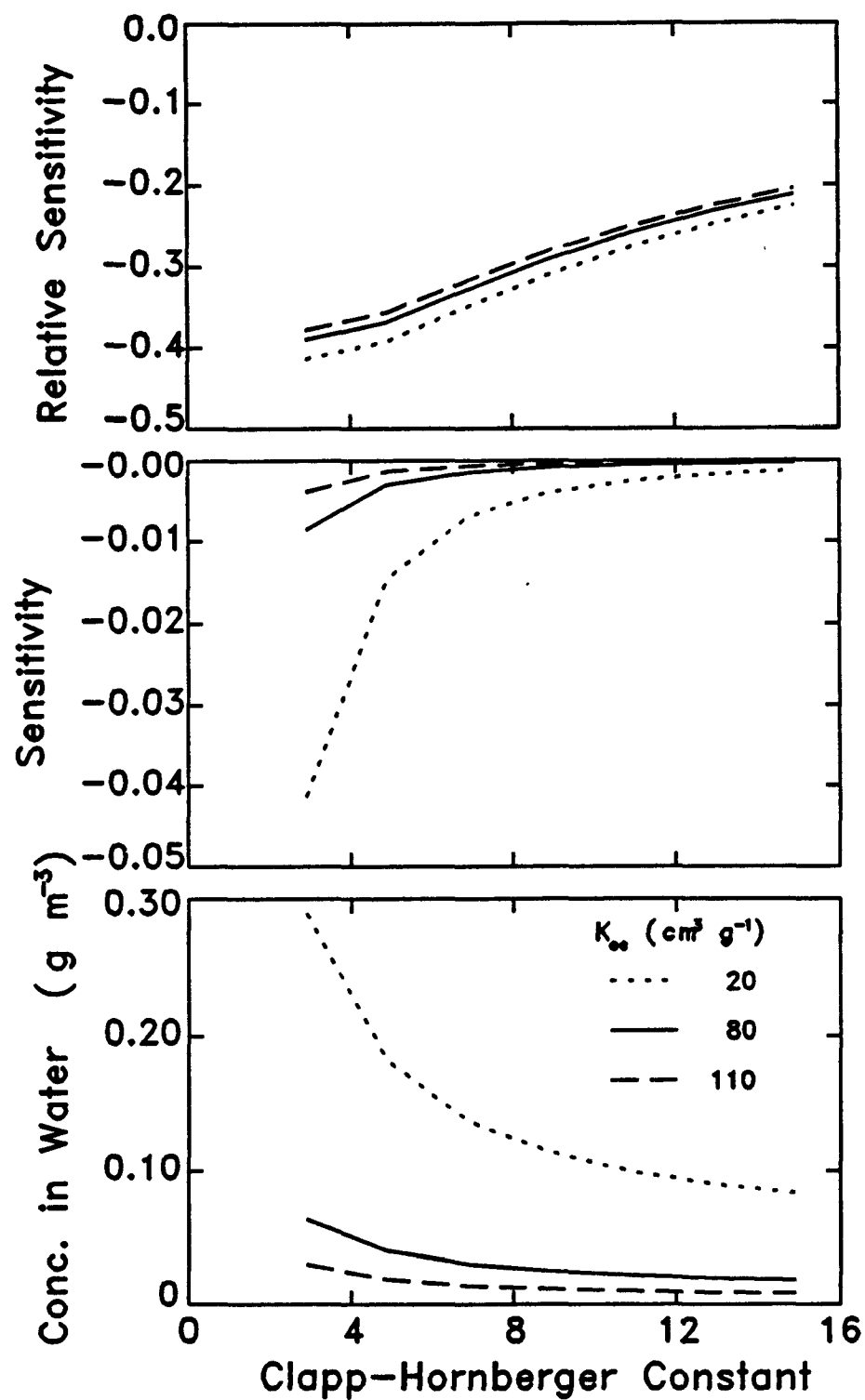
Figure 5.30. Sensitivity of concentration of pollutant in water to Clapp-Hornberger constant for chemicals with different organic carbon partition coefficients.
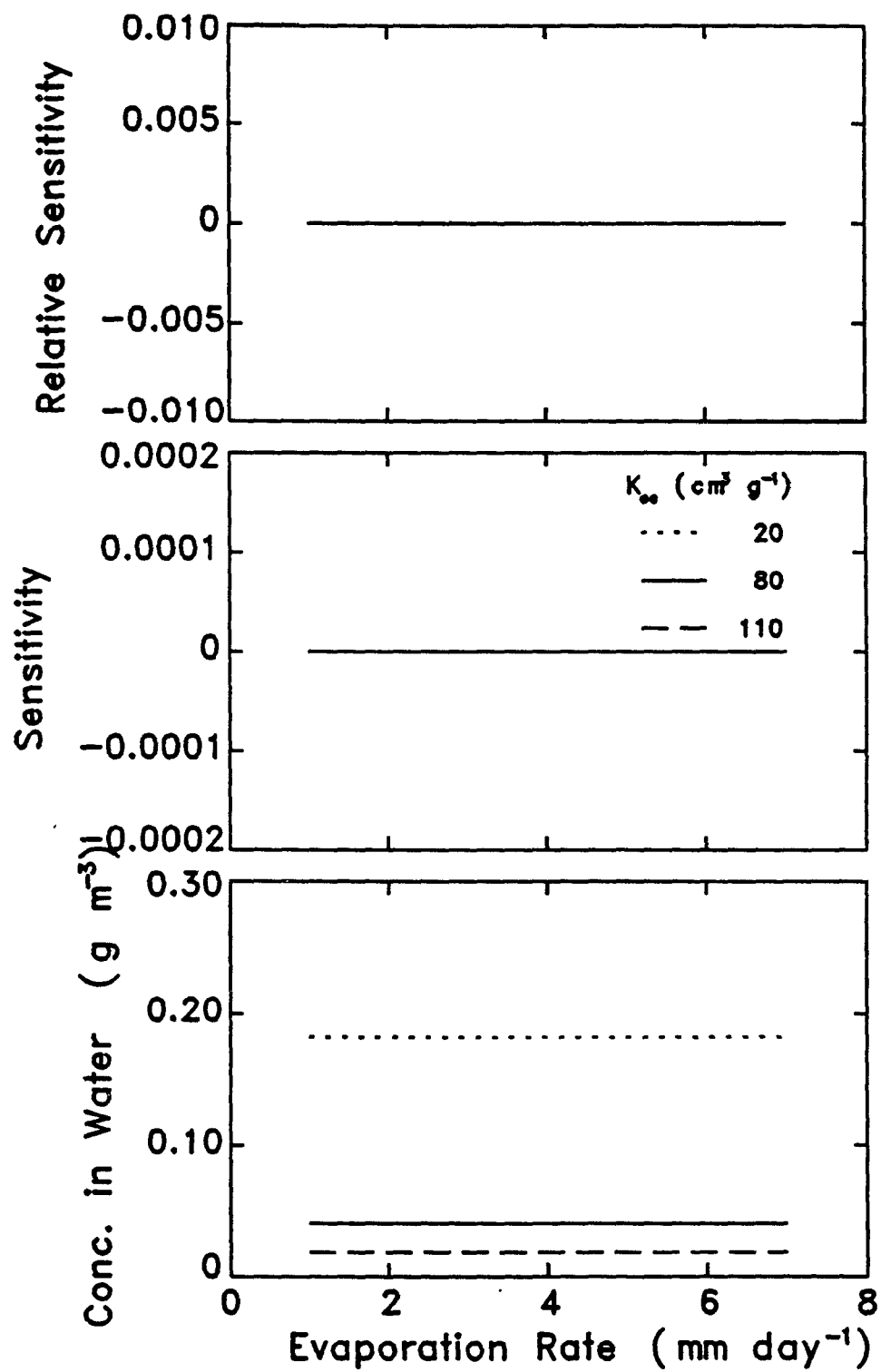
Figure 5.31. Sensitivity of concentration of pollutant in water to evaporation rate for chemicals with different organic carbon partition coefficients.
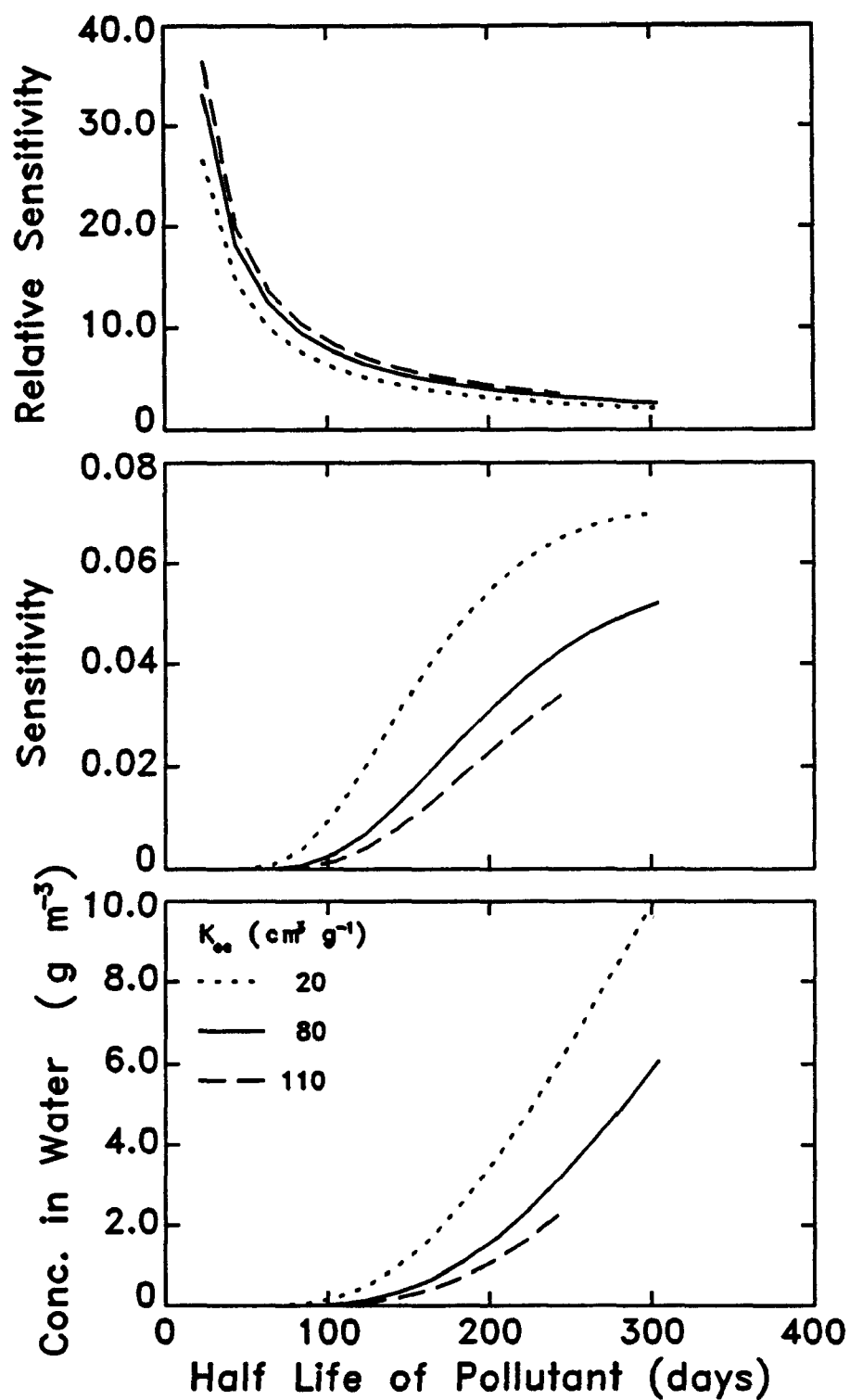
Figure 5.32. Sensitivity of concentration of pollutant in water to degradation half-life of the pollutant for chemicals with different organic carbon partition coefficients.

61
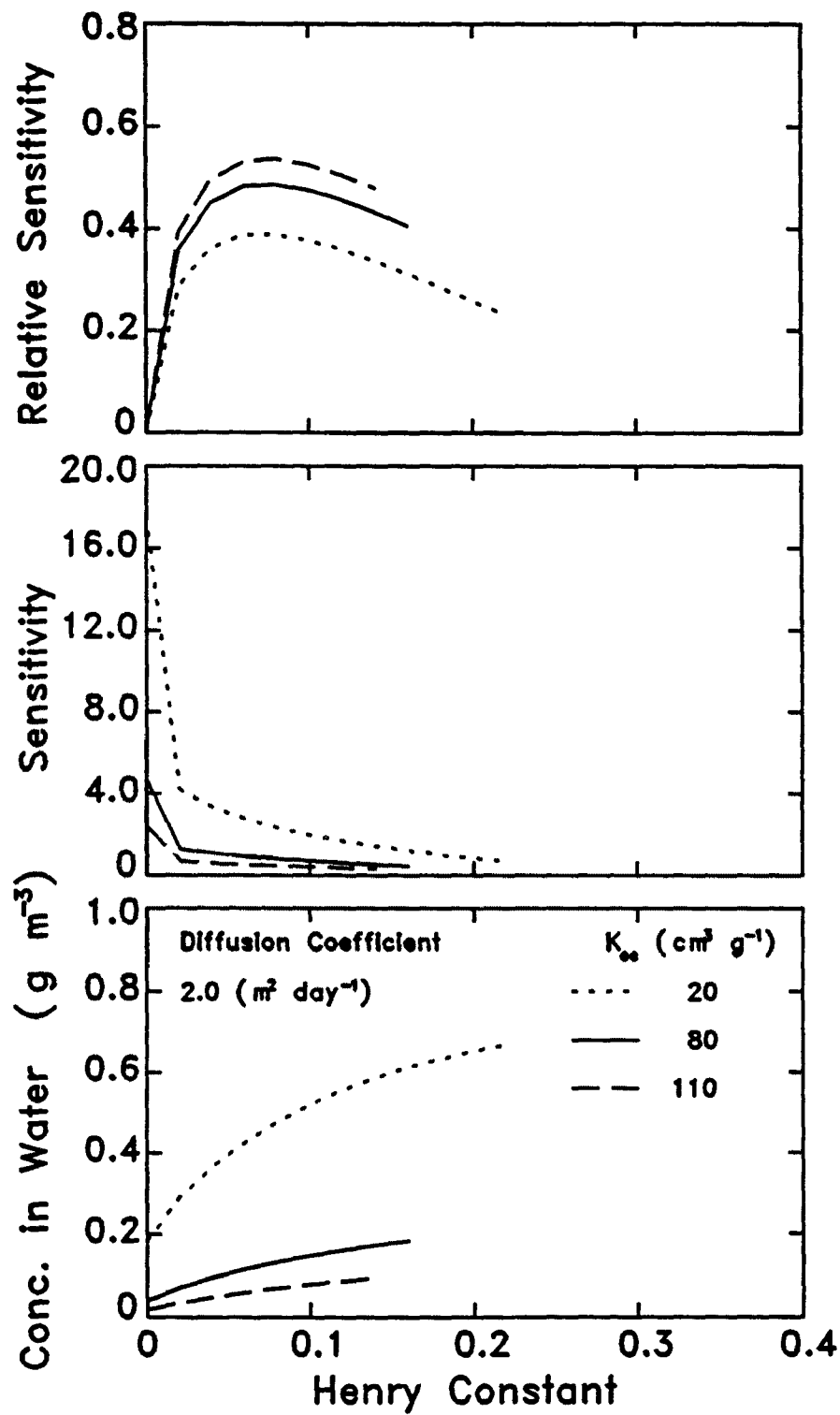
Figure 5.33. Sensitivity of concentration of pollutant in water to Henry's constant for chemicals with different organic carbon partition coefficients.
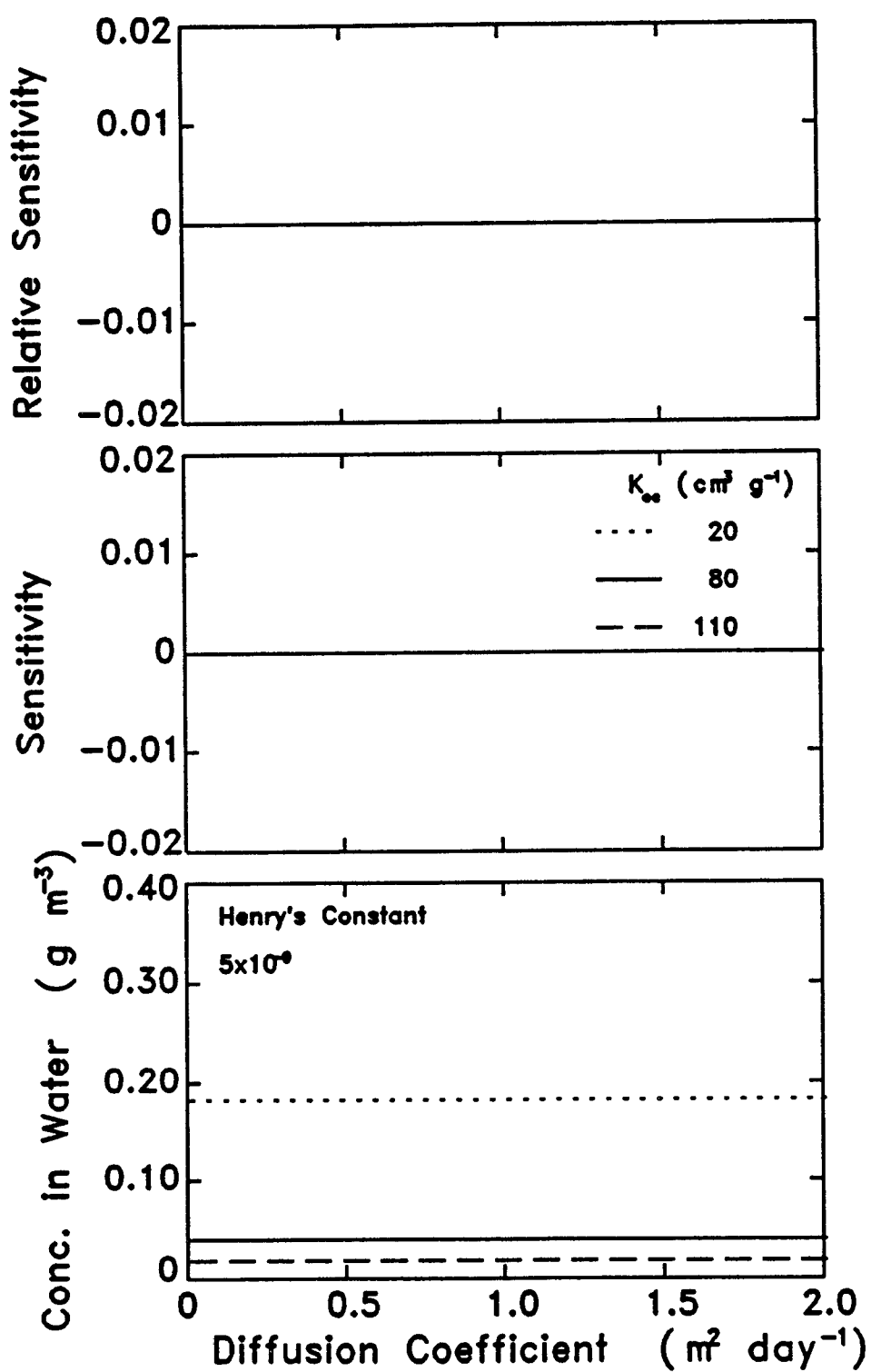
Figure 5.34. Sensitivity of concentration of pollutant in water to the diffusion coefficient of the pollutant in air for chemicals with different organic carbon partition coefficients and very small Henry's constant.
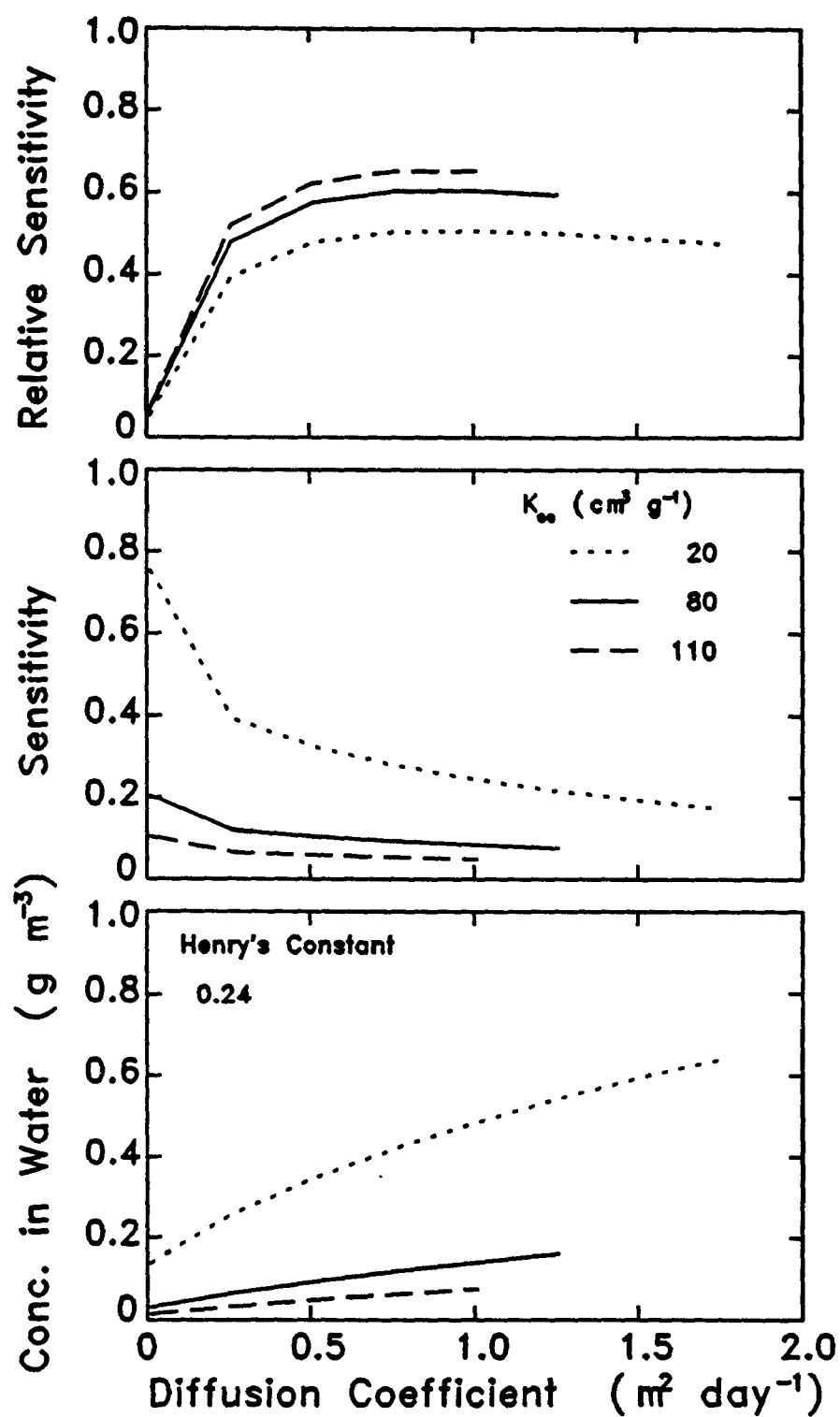
Figure 5.35. Sensitivity of concentration of pollutant in water to the diffusion coefficient of the pollutant in air for chemicals with different organic carbon partition coefficients and Henry's constant of benzene.
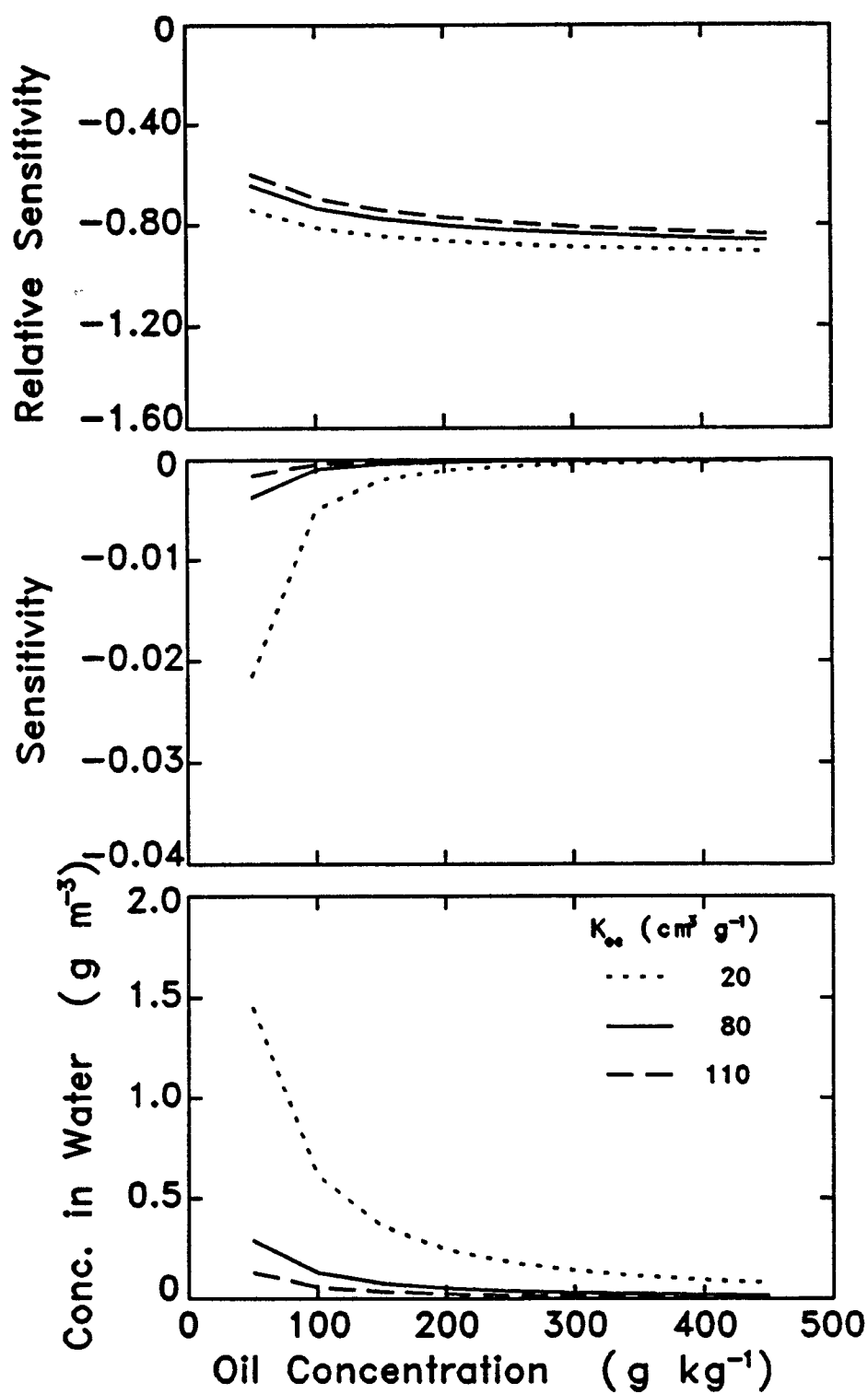
Figure 5.36. Sensitivity of concentration of pollutant in water to concentration of oil in the sludge for chemicals with different organic carbon partition coefficients.

Figure 5.37. Sensitivity of amount leached to recharge rate for chemicals with different organic carbon partition coefficients.

Figure 5.38. Sensitivity of amount leached to organic carbon partition coefficient.

Figure 5.39. Sensitivity of amount leached to organic carbon content for chemicals with different organic carbon partition coefficients.
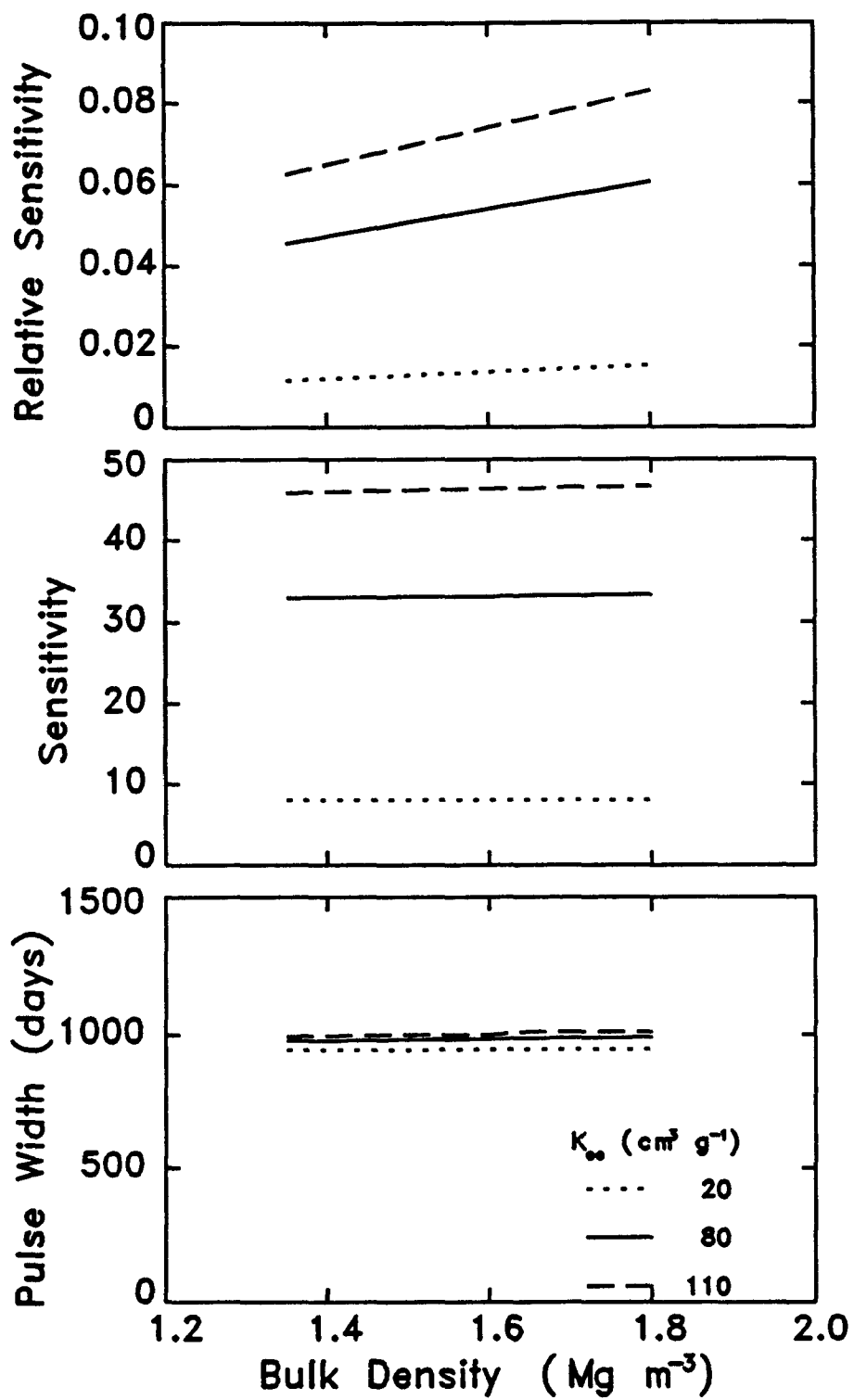
Figure 5.40. Sensitivity of amount leached to soil bulk density for chemicals with different organic carbon partition coefficients.
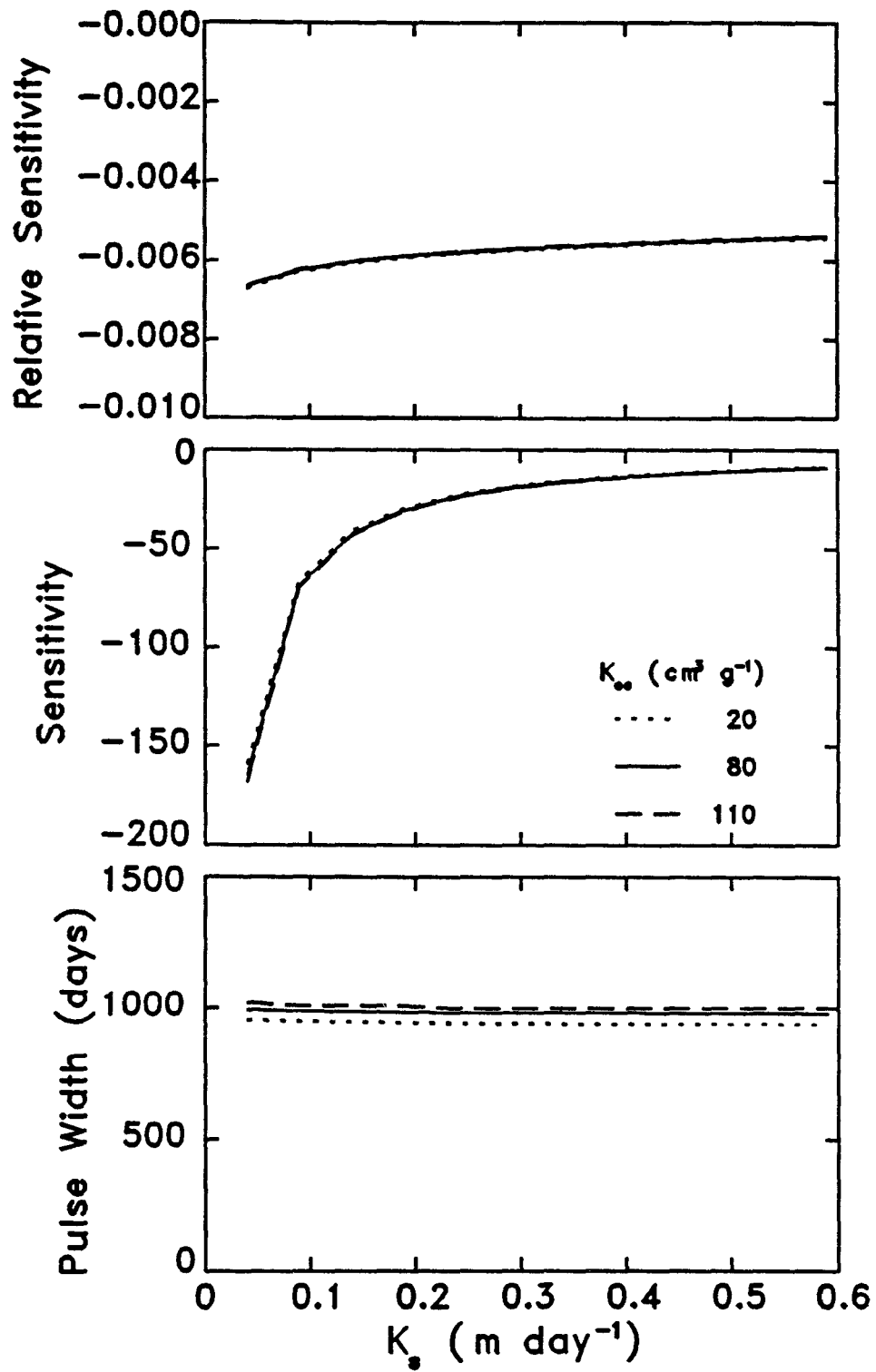
Figure 5.41. Sensitivity of amount leached to soil saturated hydraulic conductivity for chemicals with different carbon partition coefficients.
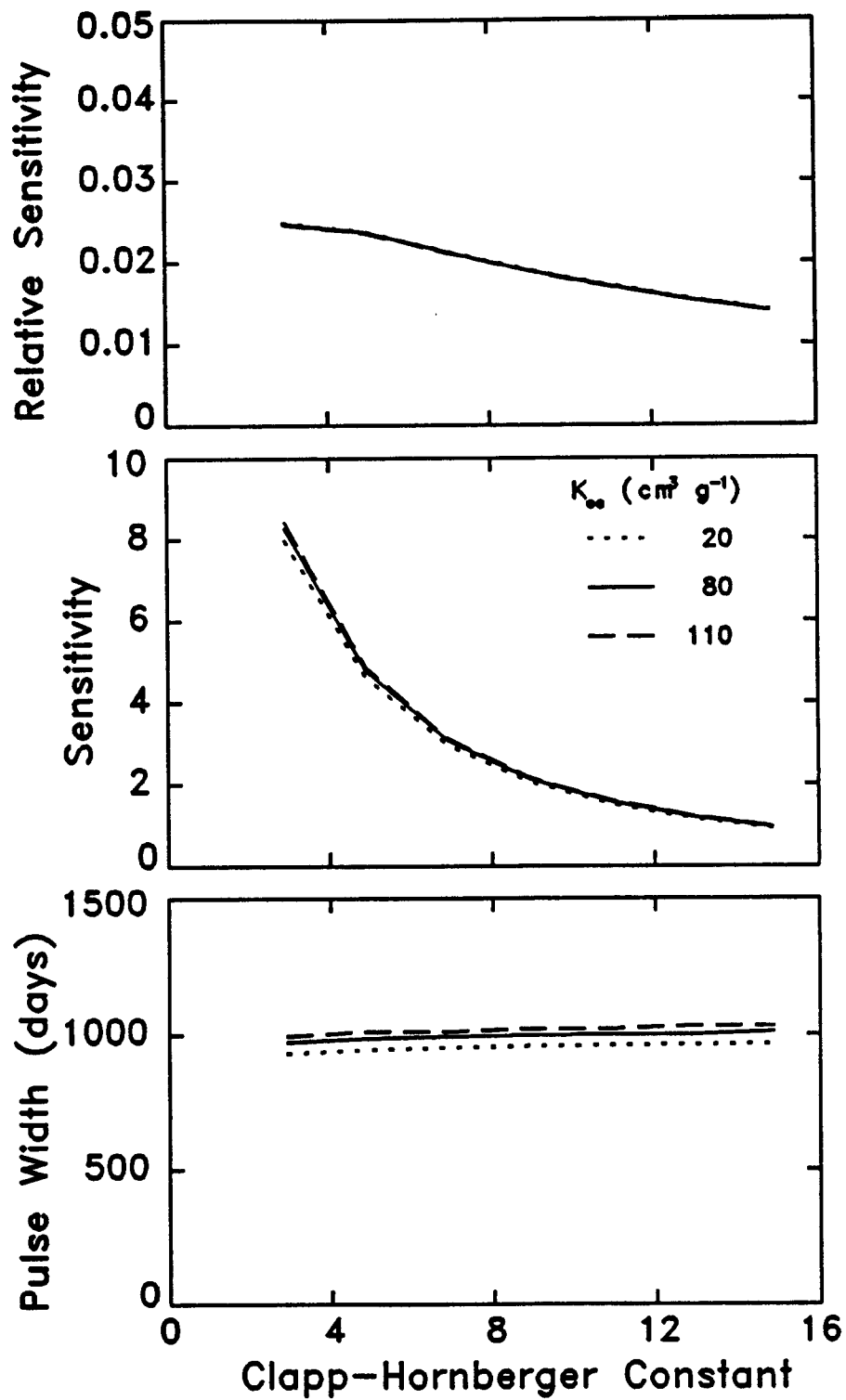
Figure 5.42. Sensitivity of amount leached to Clapp-Hornberger constant for chemicals with different carbon partition coefficients.
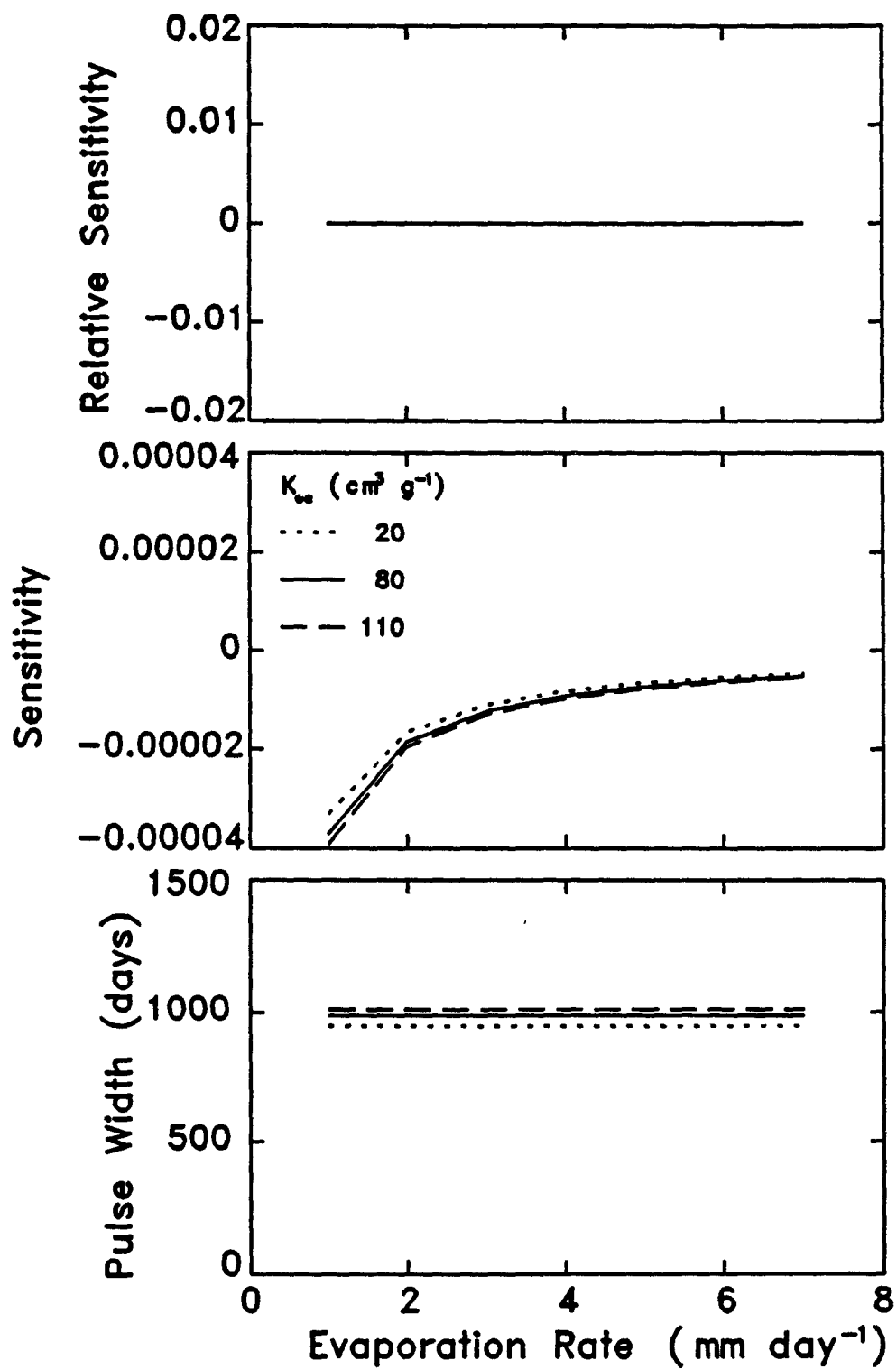
Figure 5.43. Sensitivity of amount leached to evaporation rate for chemicals with different carbon partition coefficients.
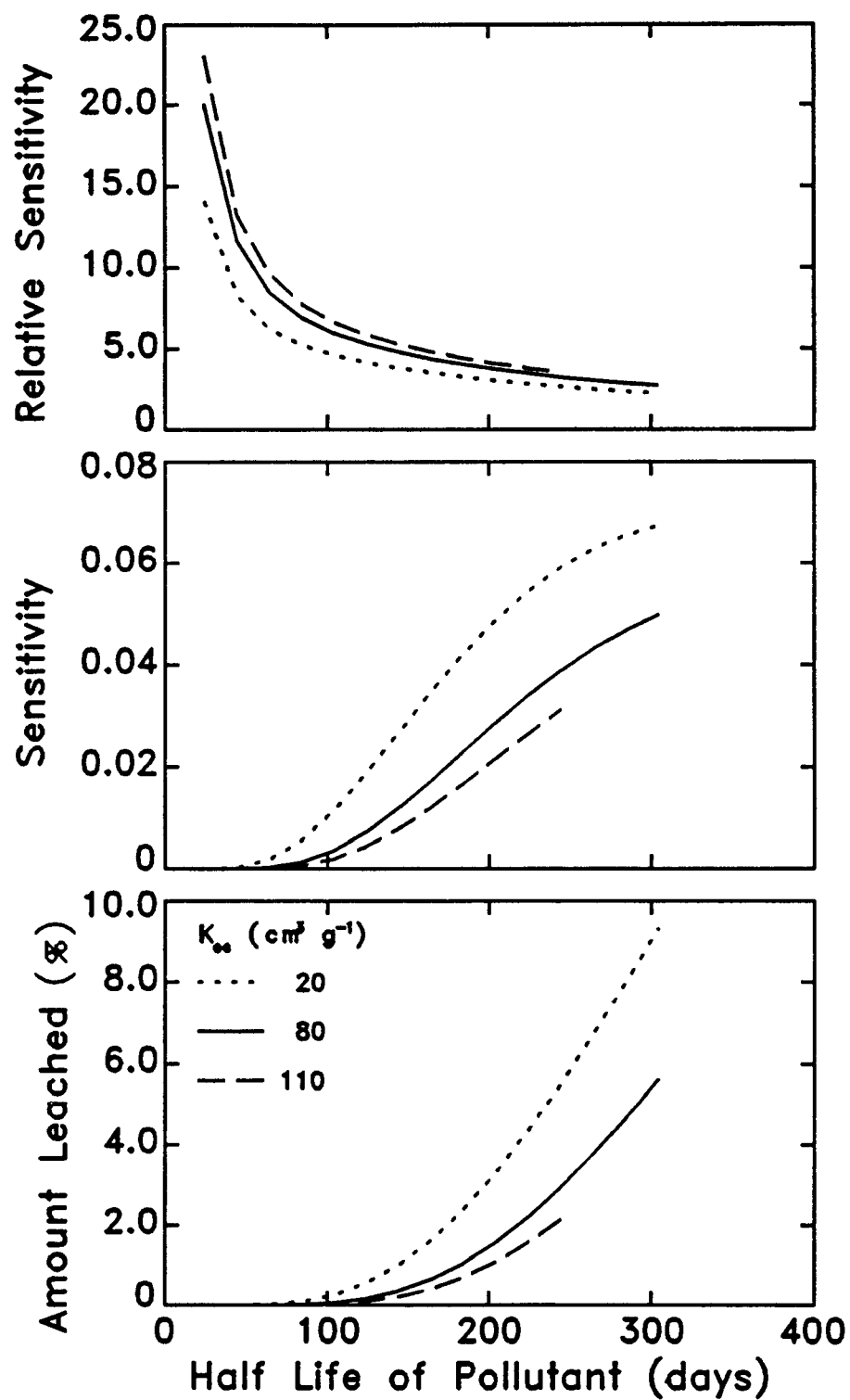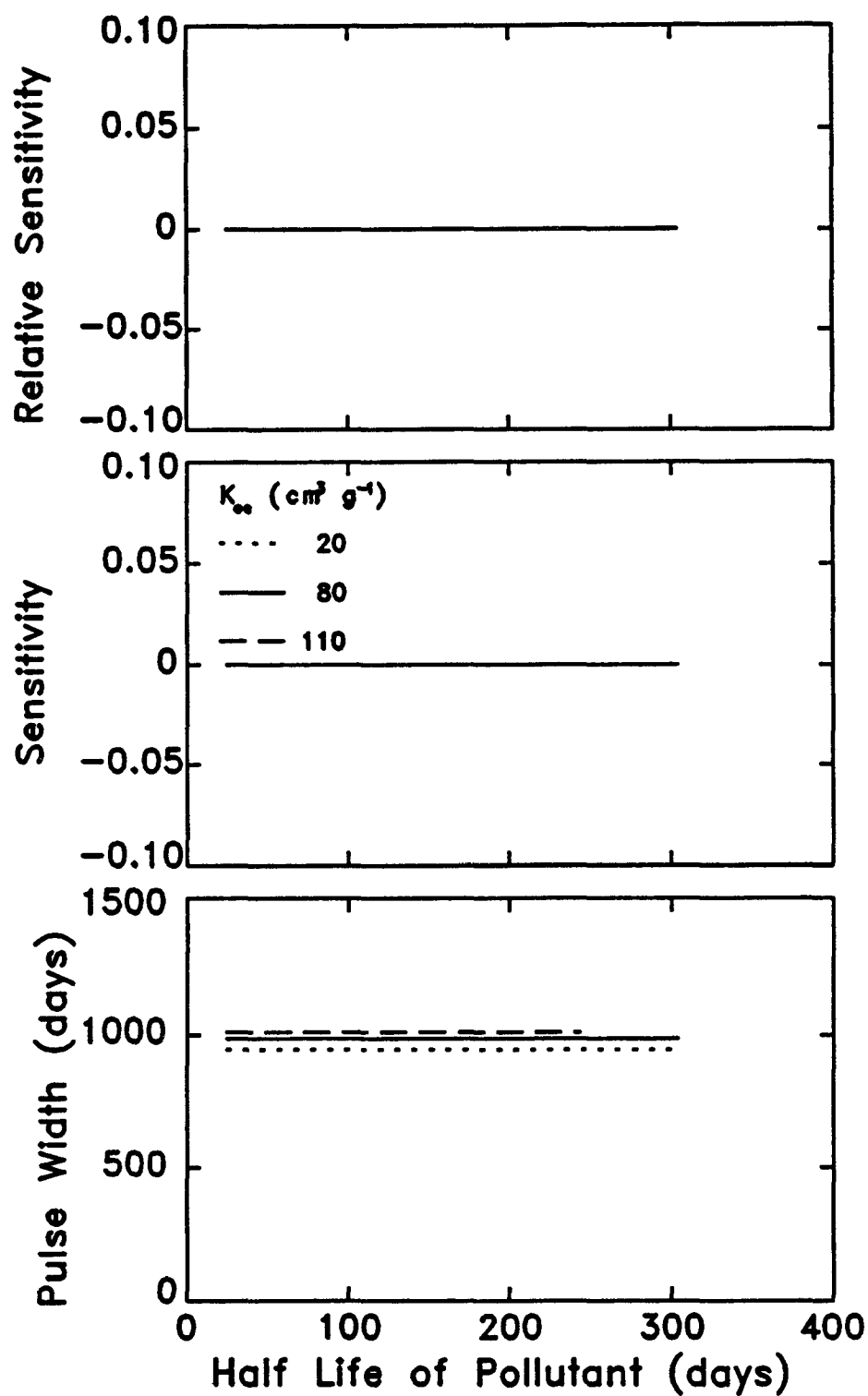
Figure 5.44. Sensitivity of amount leached to degradation half-life of the pollutant for chemicals with different carbon partition coefficients.
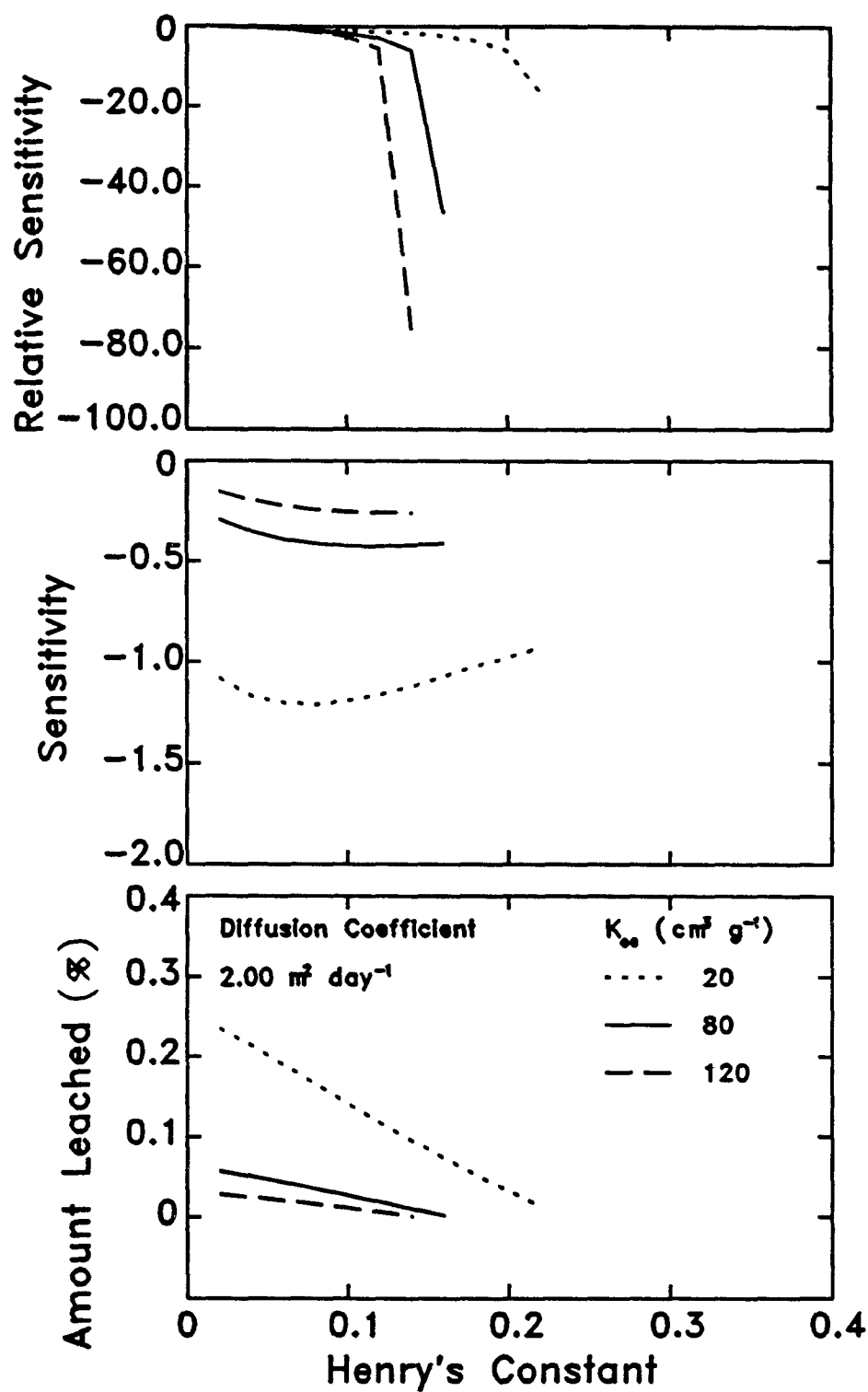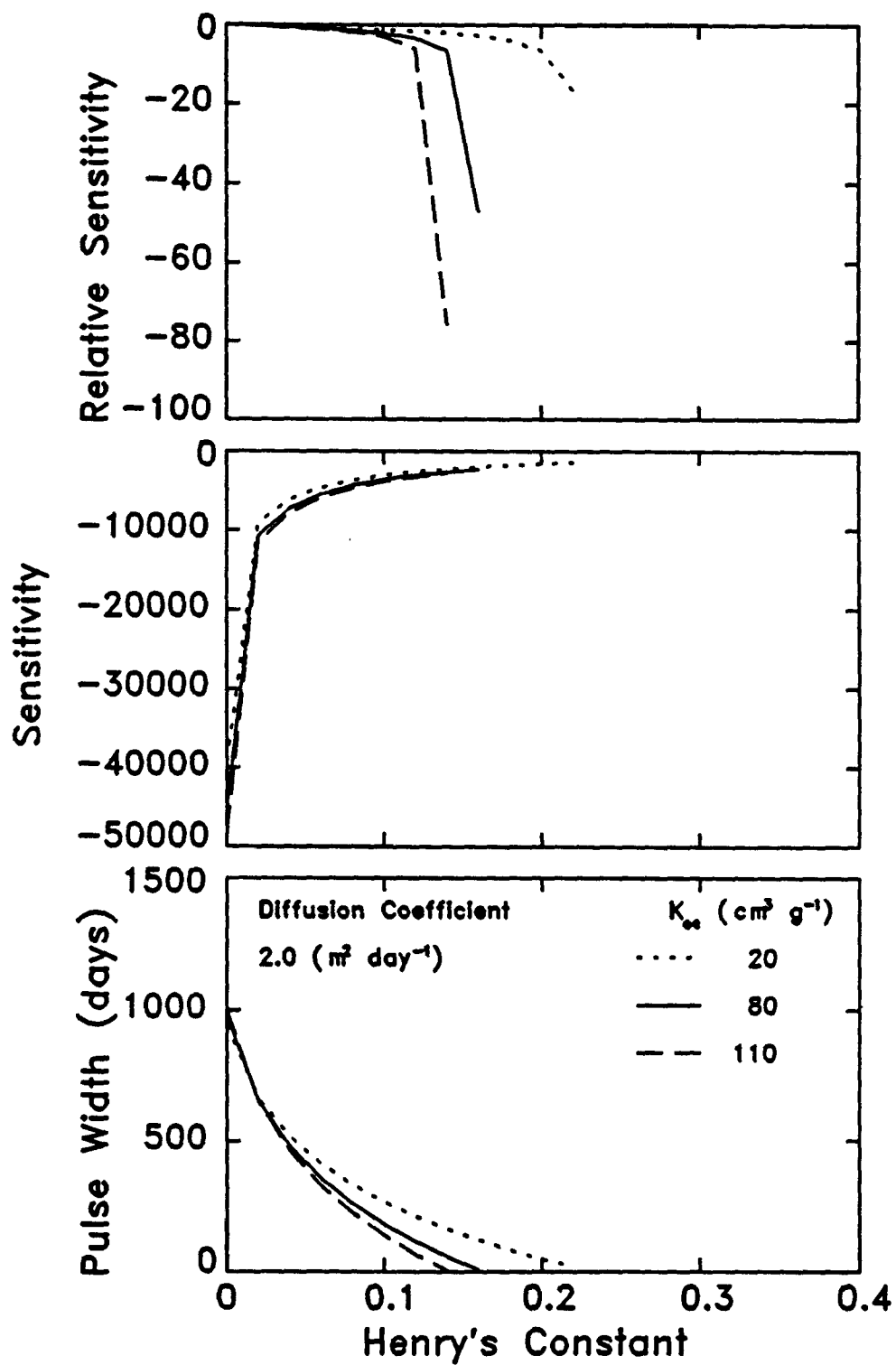
Figure 5.45. Sensitivity of amount leached to Henry's constant for chemicals with different carbon partition coefficients.
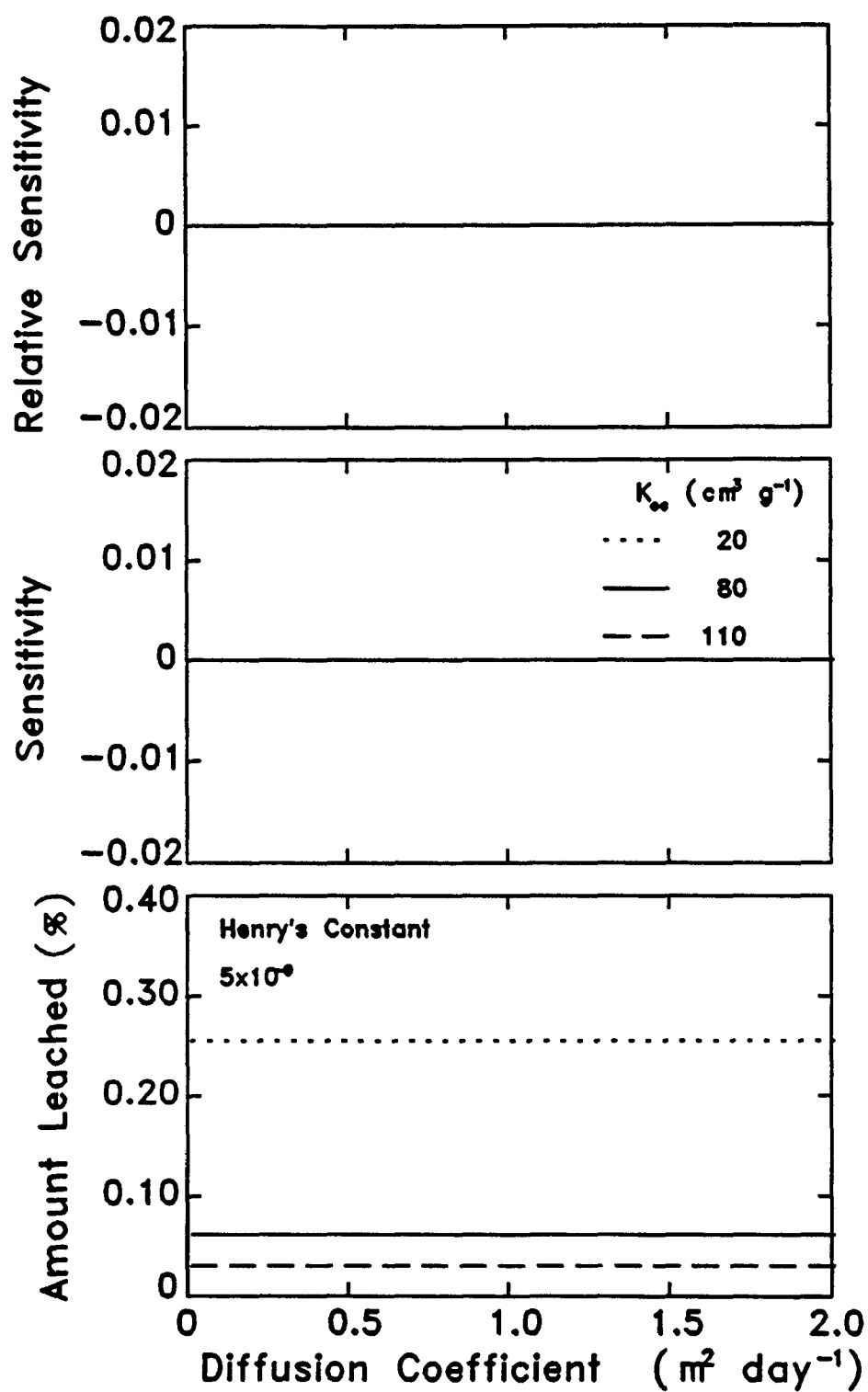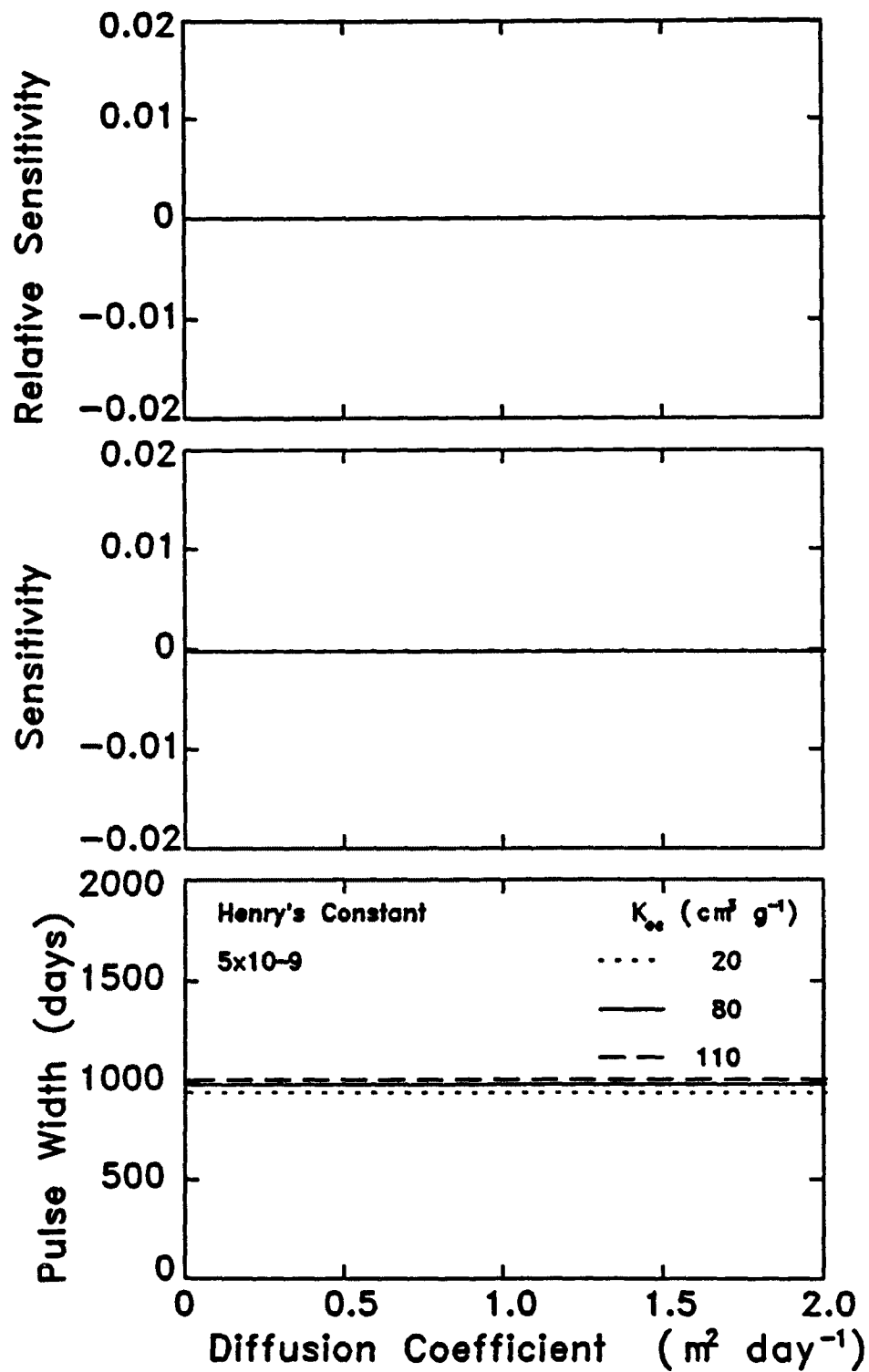
Figure 5.46. Sensitivity of amount leached to the diffusion coefficient of the pollutant in air for chemicals with different carbon partition coefficients and very small Henry's constant.
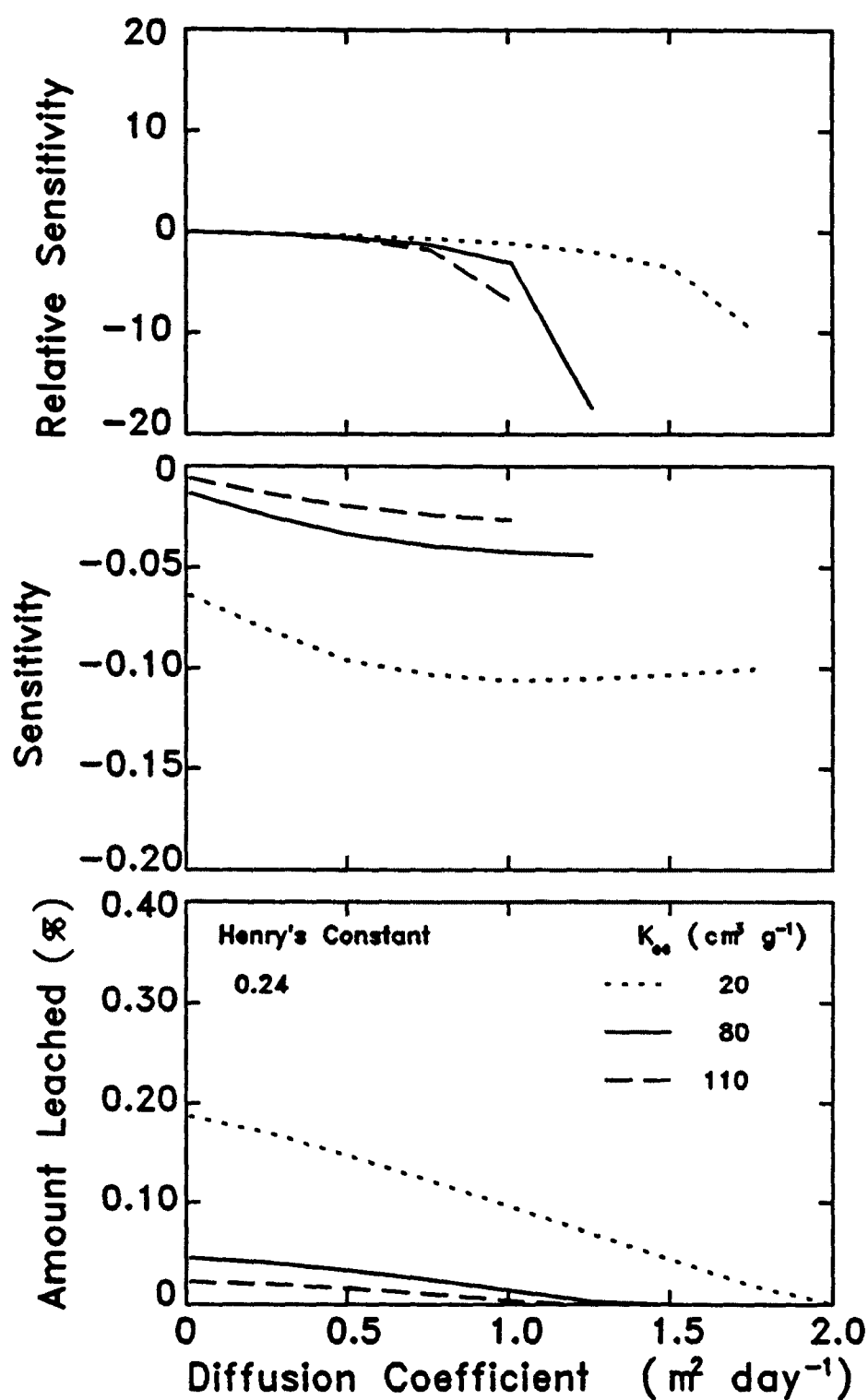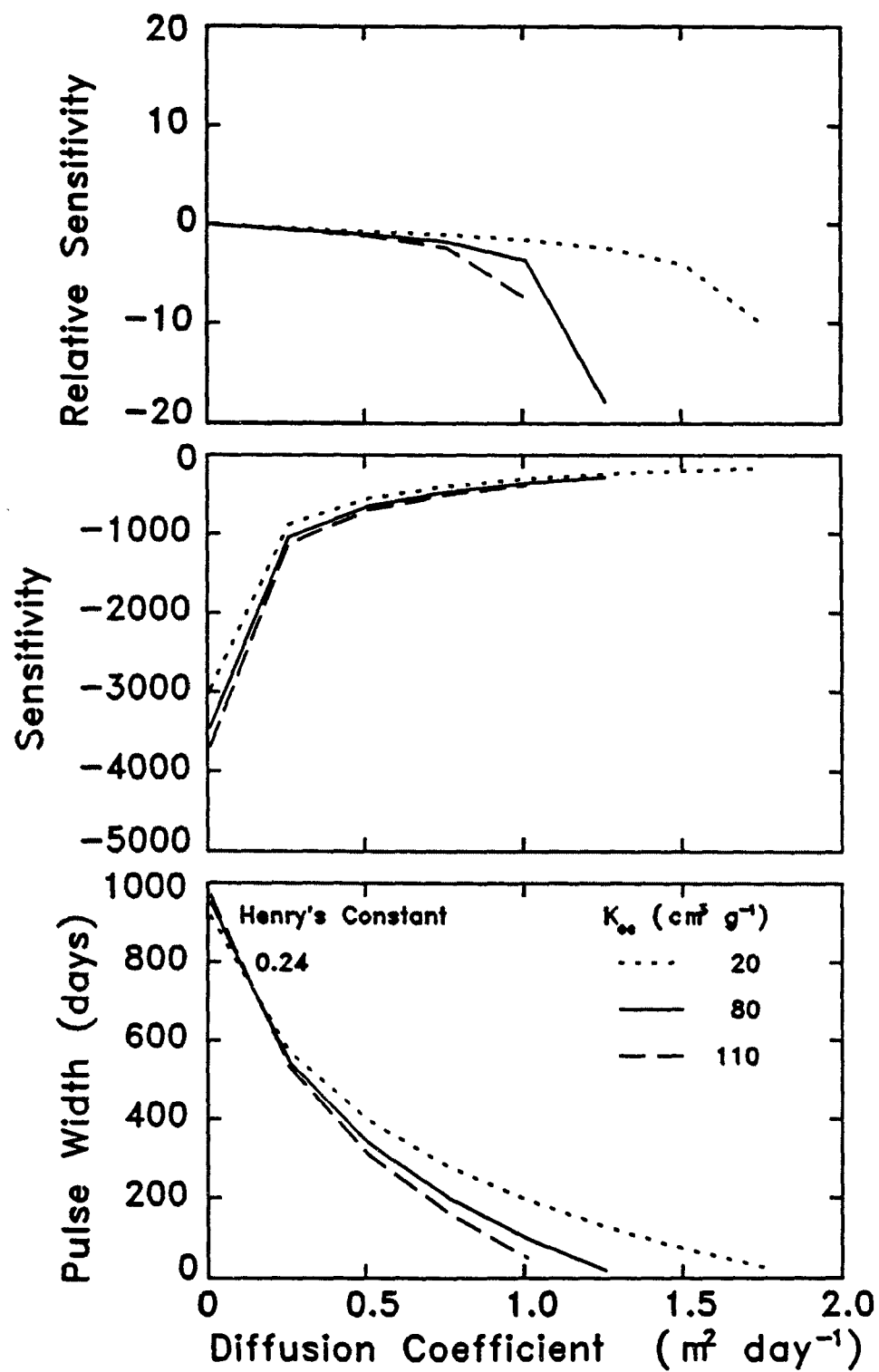
Figure 5.47. Sensitivity of amount leached to the diffusion coefficient of the pollutant in air for chemicals with different carbon partition coefficients and Henry's constant of benzene.
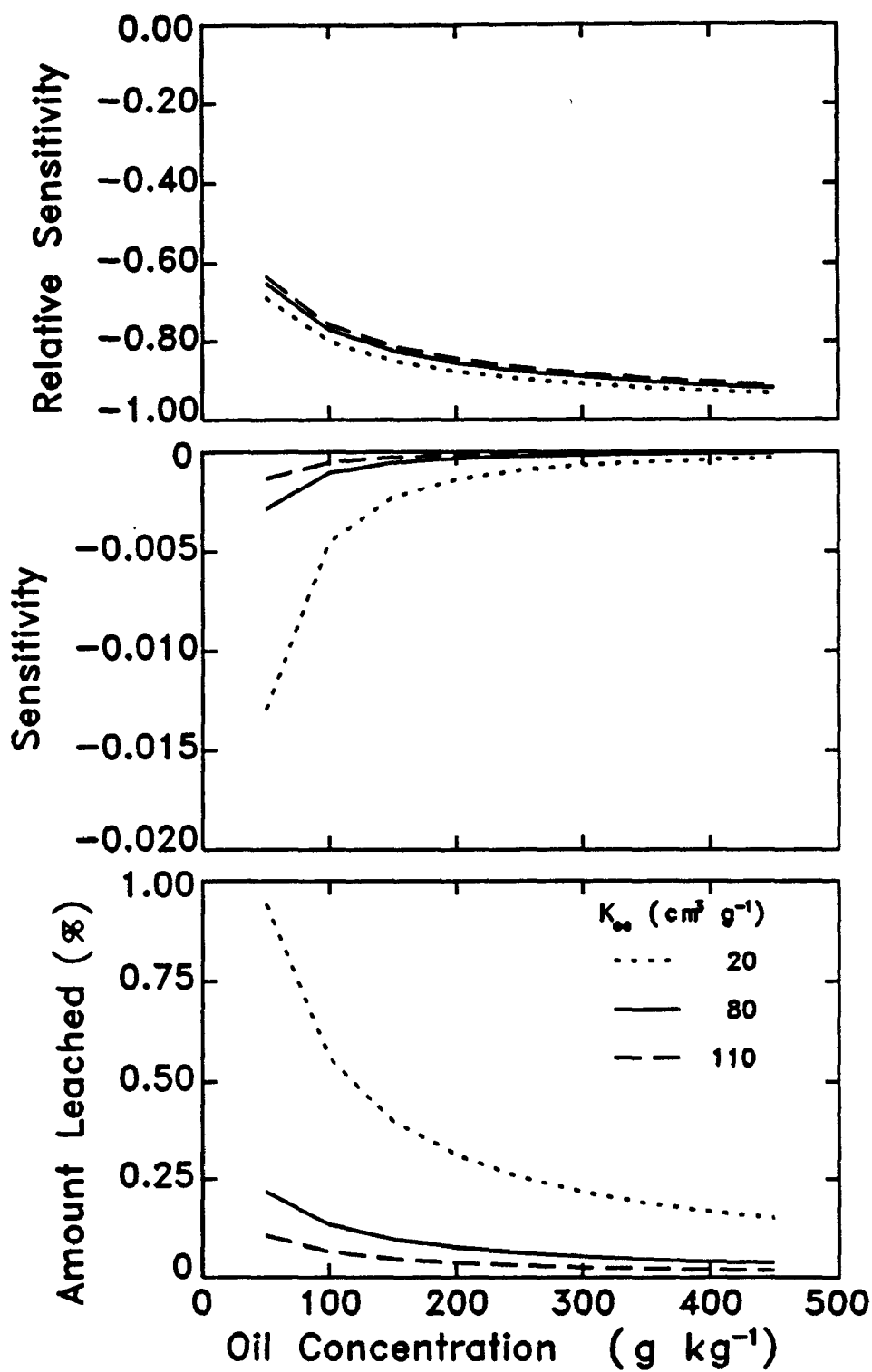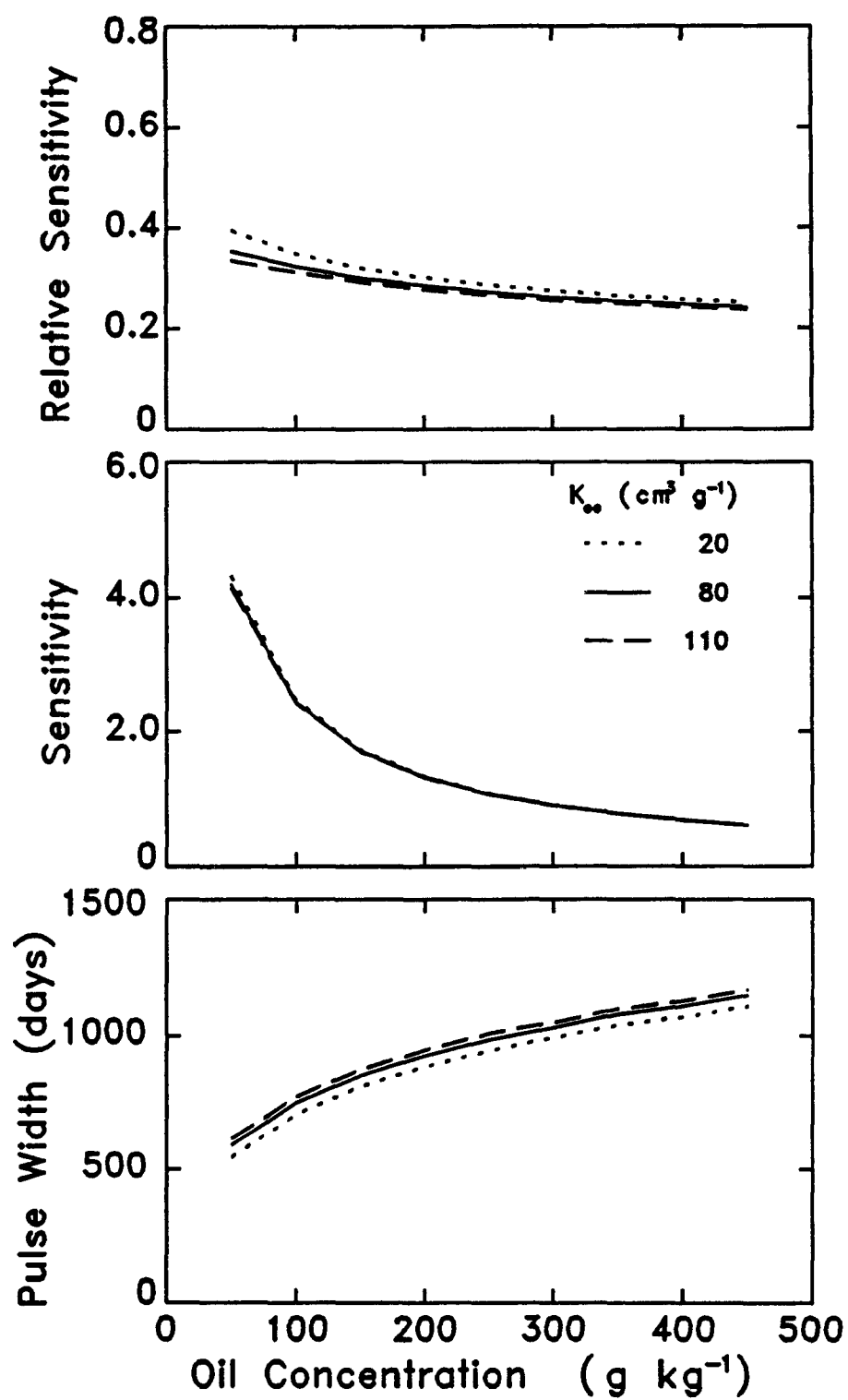
Figure 5.48. Sensitivity of amount leached to concentration of oil in the sludge for chemicals with different carbon partition coefficients.
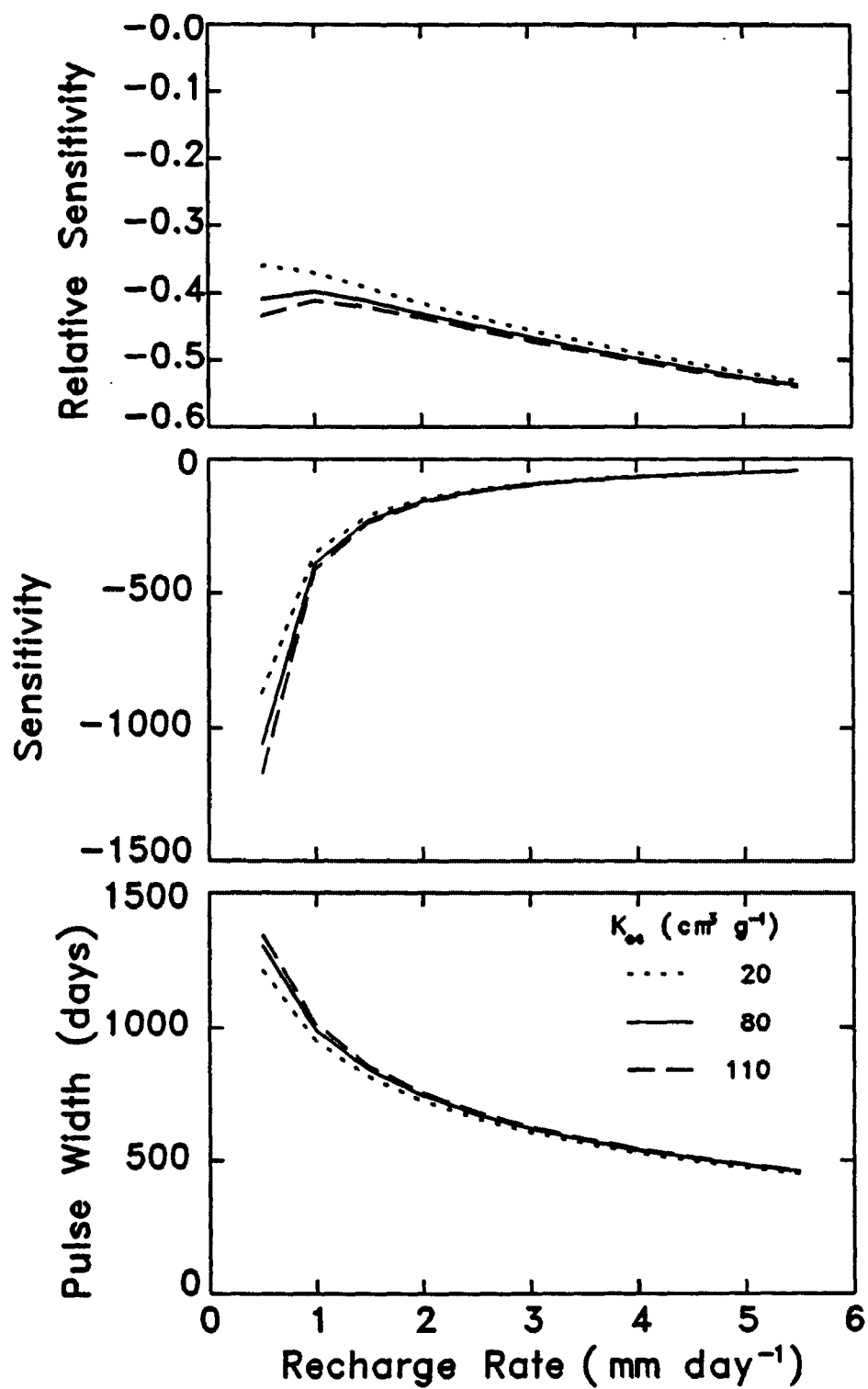
Figure 5.49. Sensitivity of pulse width to recharge rate for chemicals with different organic carbon partition coefficients.
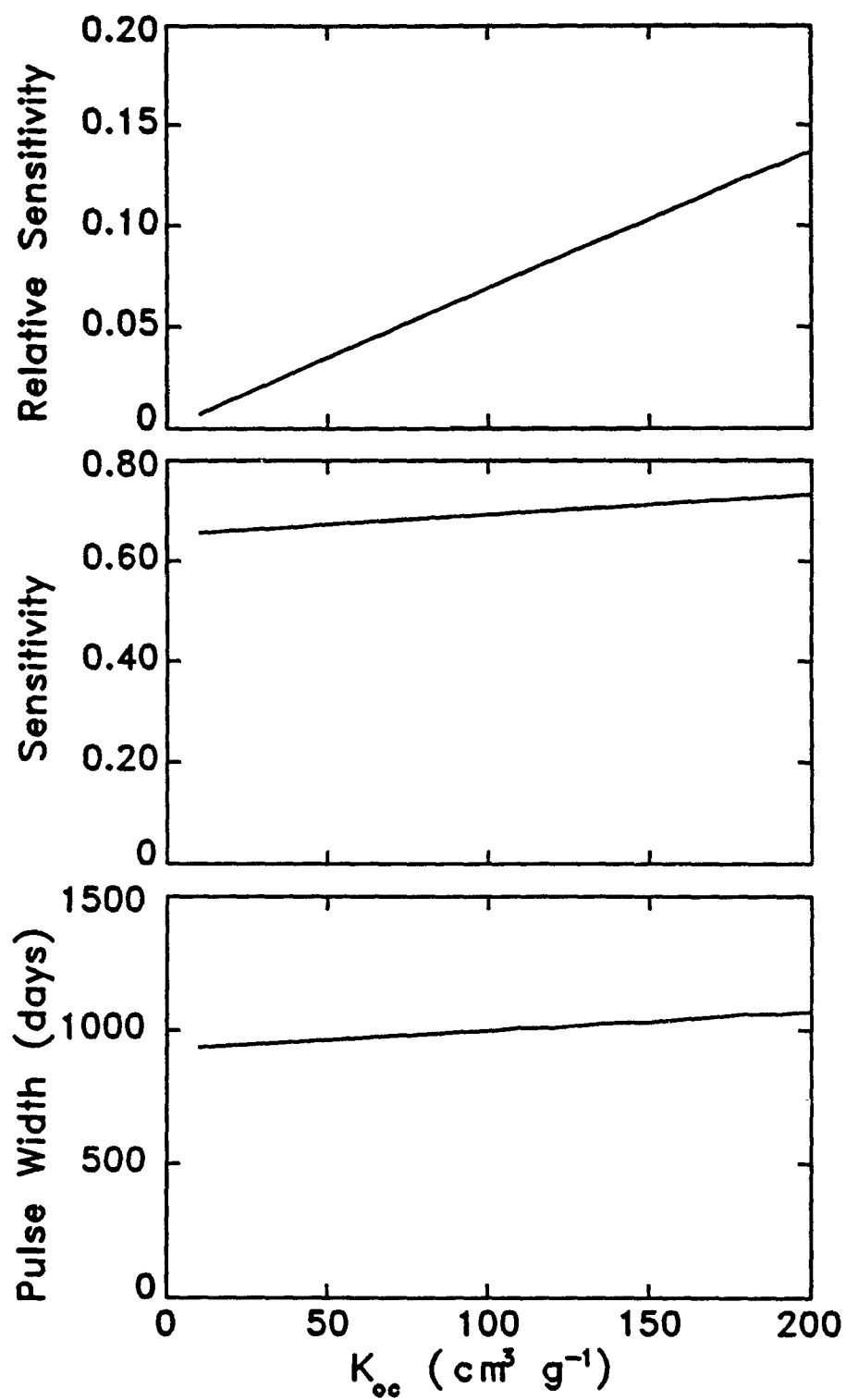
Figure 5.50. Sensitivity of pulse width to organic carbon partition coefficient.
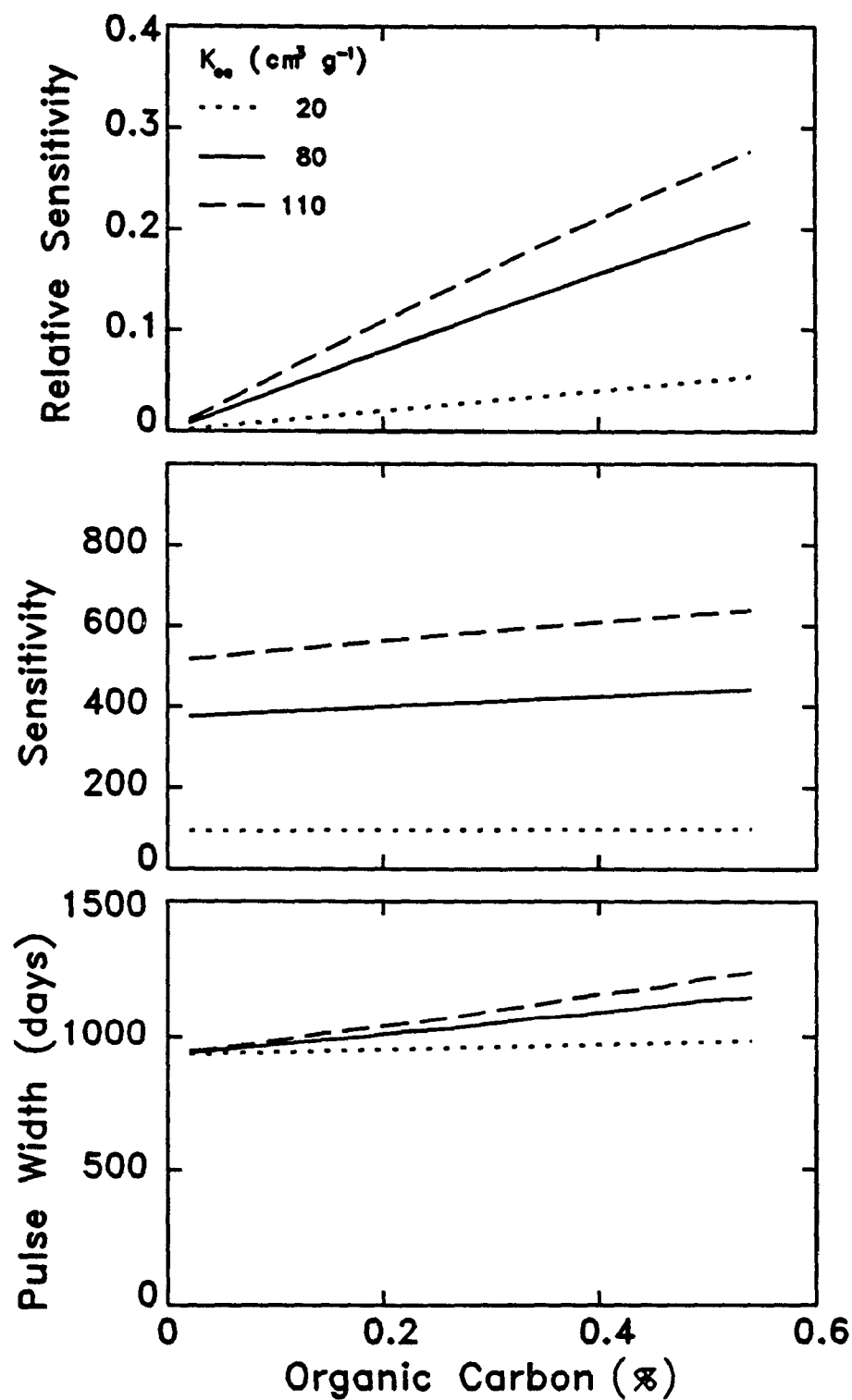
Figure 5.51. Sensitivity of pulse width to organic carbon content for chemicals with different organic carbon partition coefficients.

Figure 5.52. Sensitivity of pulse width to soil bulk density for chemicals with different carbon partition coefficients.

Figure 5.53. Sensitivity of pulse width to soil saturated hydraulic conductivity for chemicals with different carbon partition coefficients.

Figure 5.54. Sensitivity of pulse width to Clapp-Hornberger constant for chemicals with different carbon partition coefficients.

Figure 5.55. Sensitivity of pulse width to evaporation rate for chemicals with different carbon partition coefficients.

Figure 5.56. Sensitivity of pulse width to degradation half-life of the pollutant for chemicals with different carbon partition coefficients.

Figure 5.57. Sensitivity of pulse width to Henry's constant for chemicals with different carbon partition coefficients.

Figure 5.58. Sensitivity of pulse width to the diffusion coefficient of the pollutant in air for chemicals with different carbon partition coefficients and very small Henry's constant.

Figure 5.59. Sensitivity of pulse width to the diffusion coefficient of the pollutant in air for chemicals with different carbon partition coefficients and Henry's constant of benzene.

Figure 5.60. Sensitivity of pulse width to concentration of oil in the sludge for chemicals with different carbon partition coefficients.
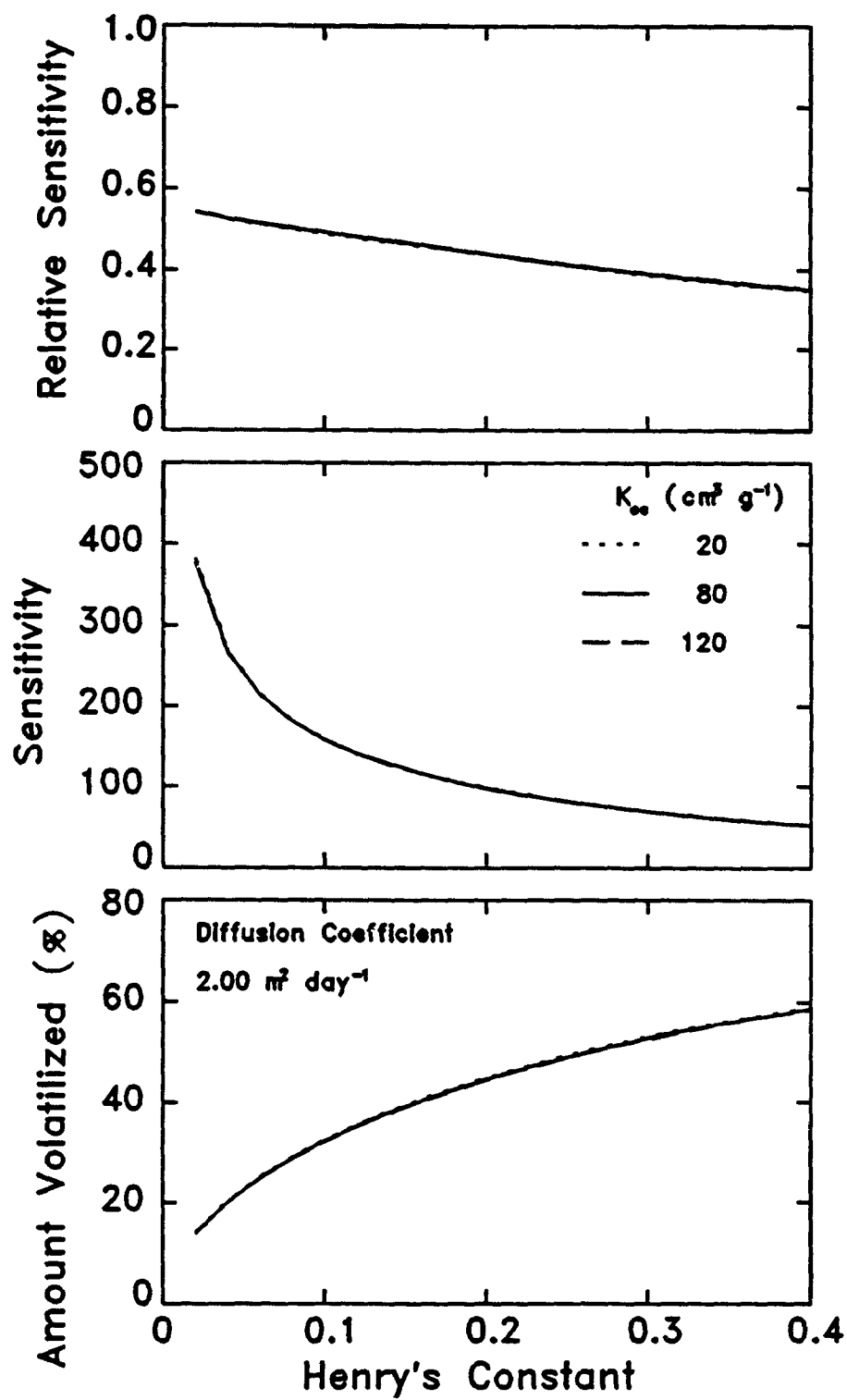
Figure 5.61. Sensitivity of the amount of pollutant lost in the vapor phase to Henry's constant for chemicals with different carbon partition coefficients.

90
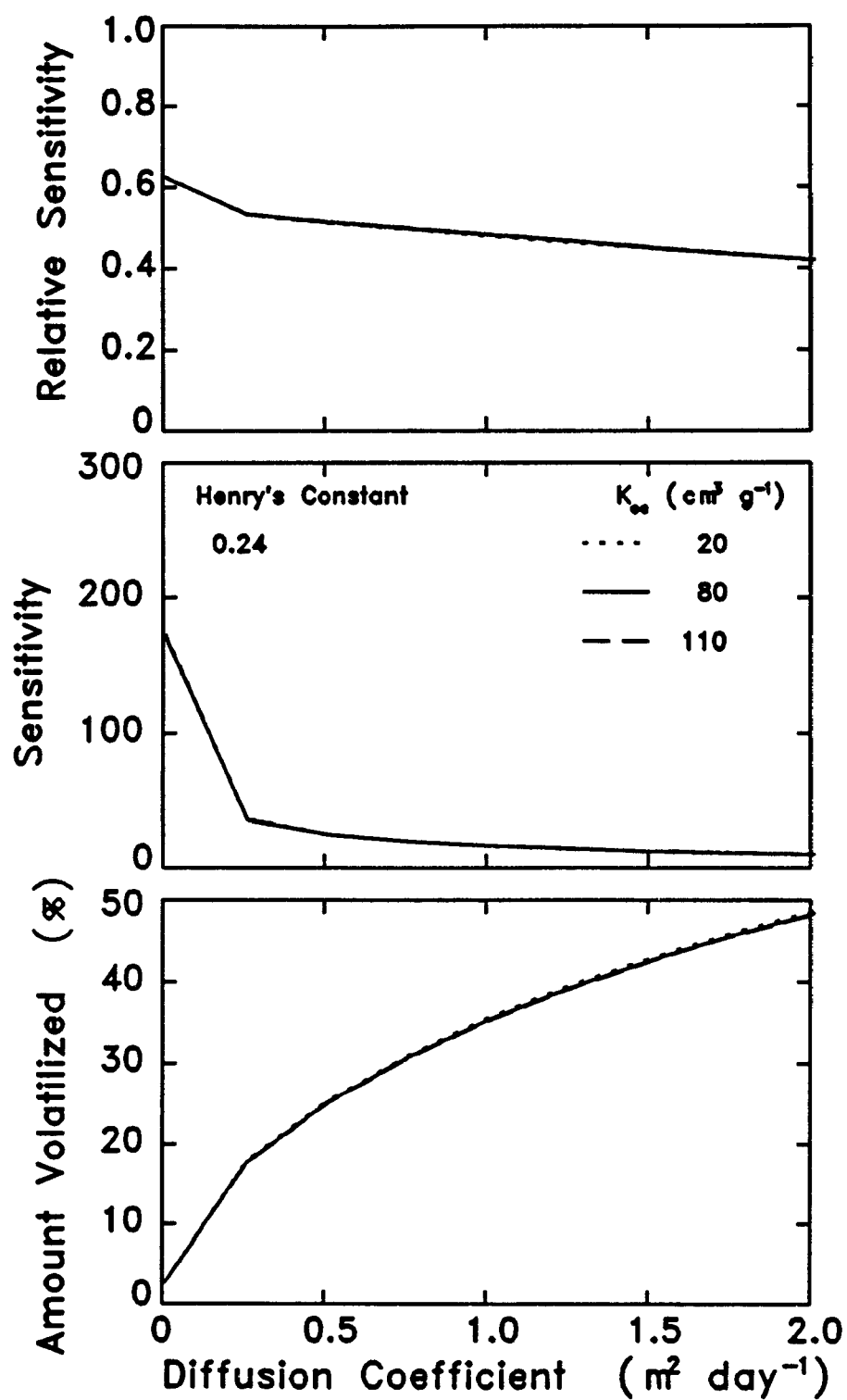
Figure 5.62. Sensitivity of the amount of pollutant lost in the vapor phase to diffusion coefficient for chemicals with different carbon partition coefficients.

# SECTION 6

## SENSITIVITY RESULTS FOR VIP MODEL

VIP was written to model movement of a chemical in a system similar to that used in RITZ. VIP includes oxygen transport, exchange, and loss which are not present in RITZ. It also incorporates chemical movement in the vapor phase for the pollutant. The resulting equations are solved numerically. Table 6.1 contains the input parameters used in this analysis of VIP.

Figure 6.1 shows the predicted concentration of pollutant at the 2-m depth as a function of time for both VIP and RITZ. The conditions modeled here represent conditions for which vapor movement is minimal and oxygen is not limited so the two models would be expected to agree. The time at which the pollutant reaches 2 m and the concentration in water at that time are in good agreement between the models. The end of the contaminant pulse is much more gradual for VIP than for RITZ. Also, the concentration of pollutant in water during the duration of the pulse decreases more rapidly in VIP than in RITZ. As the mesh size in depth decreases from 15.3 to 1.5 cm, the end of the pulse moves to earlier times and approaches the time predicted by RITZ. This suggests that the gradual decline at the end of the pulse may be due to the numerical techniques used in solving the problem. We were not able to test VIP for smaller mesh sizes since a maximum of 150 mesh points in depth can be used.

Figure 6.2 shows the concentration of pollutant in water at the 2-m depth as a function of time for 3 recharge rates. These results show that the travel time and pulse width increase as the recharge rate increases as was observed in the analysis of RITZ. Figures 6.3 to 6.12 show concentration of pollutant in water as functions of time for different values of partition coefficients, organic carbon contents, bulk density, saturated hydraulic conductivity, Clapp-Hornberger constant, half-life of pollutant, Henry's constant, diffusion coefficient, and oil content. The impact of these parameters upon concentration are nearly identical to those discussed for RITZ with the following exceptions:

1. The rate of decrease in concentration as a function of time during the duration of the pulse is greater than that predicted by RITZ. This is surprising since the two models predict the same concentration at the leading edge of the pulse.

2. The pulse width predicted by VIP is somewhat greater than that predicted by RITZ due to the gradual decline in concentration at the trailing edge of the pulse.

3. When model parameters are such that substantial movement takes place in the vapor phase, radically different concentration functions are predicted by VIP. Figure 6.9 shows this behavior for different values of Henry's constant with a large diffusion coefficient. VIP predicts low concentrations of pollutant at the 2-m depth at very small times for simulations with Henry's constants exceeding 0.005. RITZ does not predict this early arrival of the contaminant (see Figure 5.9). Also, although VIP predicts the end of the pulse will occur at an earlier time, the change is not as large as that predicted by RITZ. Figures 6.11 and 5.11 also illustrate substantial differences in predicted pollutant movement. While VIP shows a rapid increase in concentration at 2 m to a concentration of 0.01 g m$^{-3}$, RITZ predicts the pollutant never reaches that depth.

These results imply that sensitivity coefficients for VIP are approximately those of RITZ for conditions when vapor movement is of minor importance and oxygen-limiting conditions do not exist. A thorough examination of the sensitivities under oxygen-limiting conditions was not carried out.

Table 6.1. Values of input parameters used for sensitivity analysis in VIP model.

**Soil Properties**

| | |
|---|---|
| Soil porosity (--) | 0.378 |
| Bulk density (Mg m$^{-3}$) | 1.65 |
| Saturated hydraulic conductivity (m day$^{-1}$) | 0.19 |
| Clapp and Hornberger constant (--) | 4.9 |

**Site Characteristics**

| | |
|---|---|
| Plow zone depth (m) | 0.5 |
| Treatment zone depth (m) | 2.0 |
| Mean daily recharge rate during each month (mm day$^{-1}$) | 1.0 |
| Temperature during each month in plow zone (°C) | 25 |
| Temperature during each month in treatment zone (°C) | 25 |
| Temperature correction coefficient for each month (--) | 1 |
| Sludge application rate (g/100g soil) | 3.03 |
| Pollutant concentration in the sludge (g Mg$^{-1}$) | 4000 |
| Weight fraction of oil in waste (kg kg$^{-1}$) | 0.25 |
| Weight fraction of water in sludge (kg kg$^{-1}$) | 0.01 |
| Density of sludge (Mg m$^{-3}$) | 1.0 |
| Application period (days) | 100000 |
| Application frequency within application period (days) | 10000 |

**Pollutant Properties**

| | |
|---|---|
| Oil-water partition coefficient in plow zone (g m$^{-3}$) | 700 |
| Oil-water partition coefficient in lower treatment zone (g m$^{-3}$) | 700 |
| Air-water partition coefficient in plow zone (g m$^{-3}$) | 5.0E-9 |
| Air-water partition coefficient in lower treatment zone (g m$^{-3}$) | 5.0E-9 |
| Soil-water partition coefficient in plow zone (cm$^3$ g$^{-1}$) | 0.112 |
| Soil-water partition coefficient in lower treatment zone (cm$^3$ g$^{-1}$) | 0.112 |
| Degradation constant within oil in plow zone (day$^{-1}$) | 0.00667 |
| Degradation constant within oil in lower treatment zone (day$^{-1}$) | 0.00667 |
| Degradation constant within water in plow zone (day$^{-1}$) | 0.00667 |
| Degradation constant within water in lower treatment zone (day$^{-1}$) | 0.00667 |
| Dispersion coefficient for pollutant in unsat. pore space (m$^2$ day$^{-1}$) | 2.0 |
| Adsorption/desorption rate constant water/soil (day$^{-1}$) | 1000 |
| Adsorption/desorption rate constant water/oil (day$^{-1}$) | 1000 |
| Adsorption/desorption rate constant water/air (day$^{-1}$) | 1000 |

Table 6.1. Continued.

Oxygen Properties
    Oil-air partition coefficient in plow zone $(g \, g^{-1})$      1.0E-7
    Oil-air partition coefficient in lower treatment zone $(g \, g^{-1})$      1.0E-7
    Water-air partition coefficient in plow zone $(g \, g^{-1})$      1.0E-7
    Water-air partition coefficient in lower treatment zone $(g \, g^{-1})$      1.0E-7
    Oxygen half-saturation constant with respect to oil degradation $(g \, m^{-3})$      1.0E-9
    Oxygen half-saturation constant within air phase in plow zone $(g \, m^{-3})$      1.0E-7
    Oxygen half-saturation constant within air phase in treatment zone $(g \, m^{-3})$      1.0E-7
    Oxygen half-saturation constant within oil phase in plow zone $(g \, m^{-3})$      1.0E-7
    Oxygen half-saturation constant within oil phase in treatment zone $(g \, m^{-3})$      1.0E-7
    Oxygen half-saturation constant within water phase in plow zone $(g \, m^{-3})$      1.0E-7
    Oxygen half-saturation constant within water phase in treatment zone $(g \, m^{-3})$      1.0E-7
    Stoichiometric ratio of oxygen to pollutant consumed      3
    Stoichiometric ratio of oxygen to oil consumed      3
    Oxygen transfer rate coefficient between oil and air phases $(day^{-1})$      1000
    Oxygen transfer rate coefficient between water and air phases $(day^{-1})$      1000

Properties of Oil
    Density of oil $(Mg \, m^{-3})$      0.8
    Degradation rate constant of oil $(day^{-1})$      0.003467
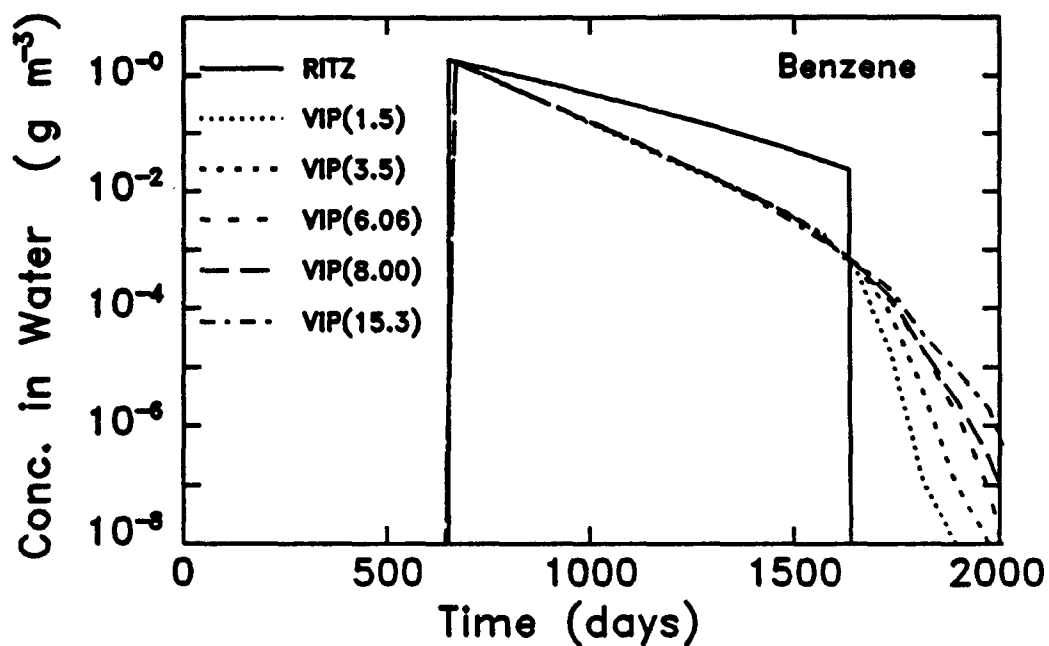
Figure 6.1. Predicted concentration of pollutant in water at the 2-m depth as a function of time using the RITZ model and using the VIP model with different mesh sizes. Numbers in parentheses are mesh sizes in centimeters.
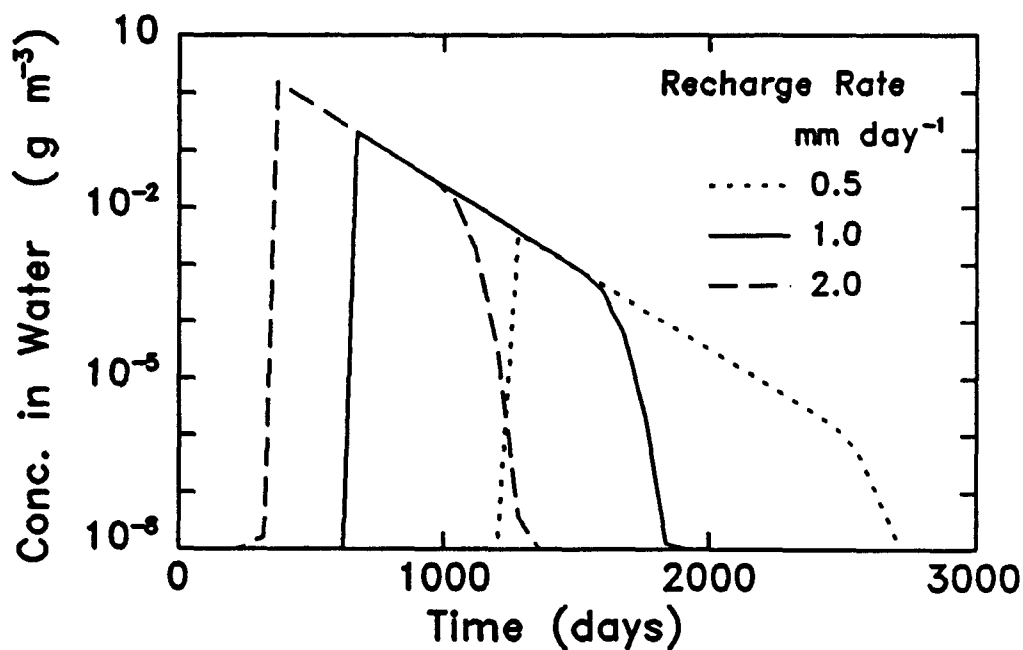


Figure 6.2. Concentration of pollutant in water at the 2-m depth as a function of time for three recharge rates.
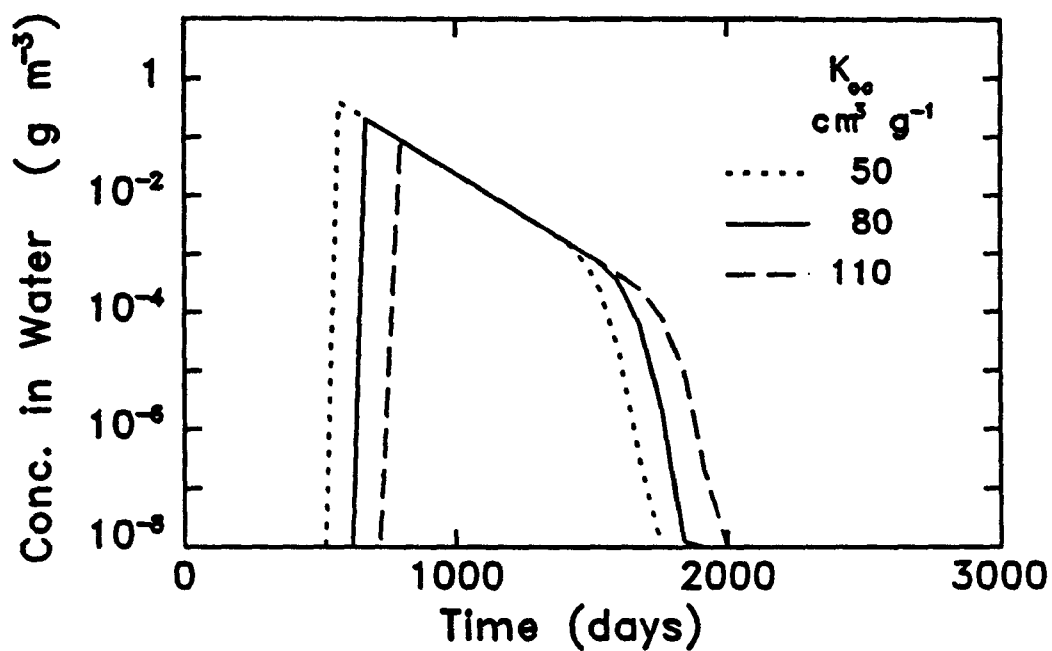
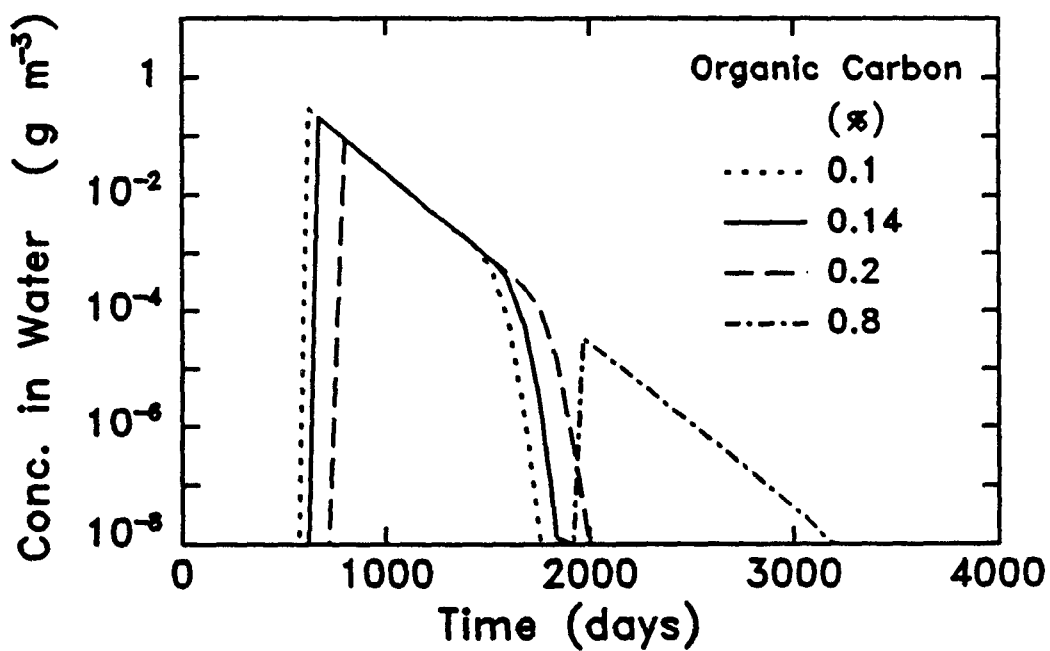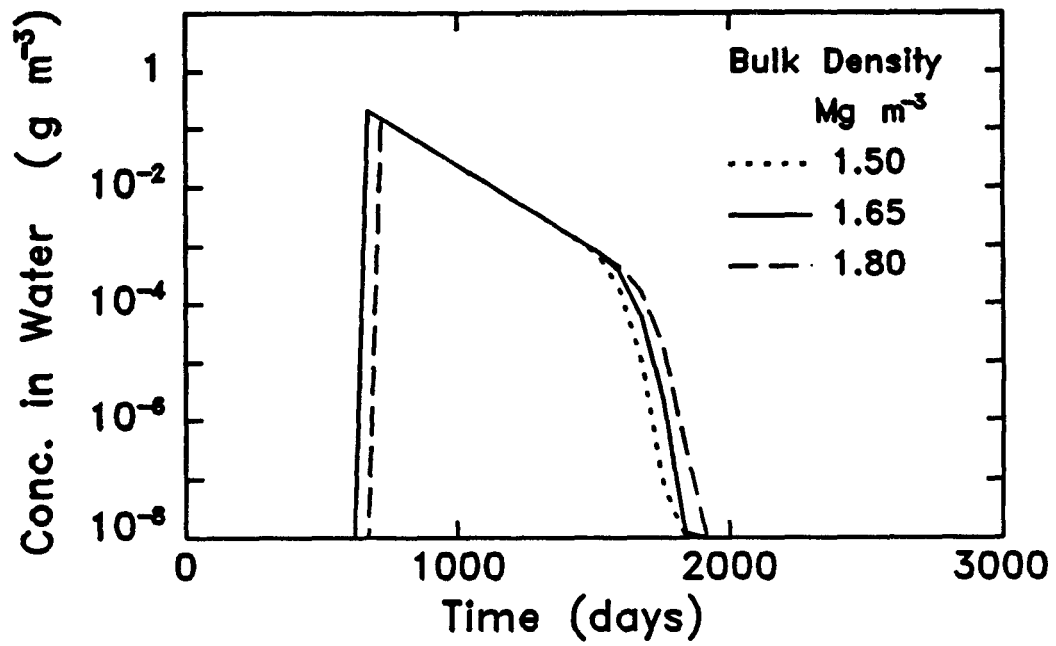Figure 6.3. Concentration of pollutant in water at the 2-m depth as a function of time for three organic carbon partition coefficients.
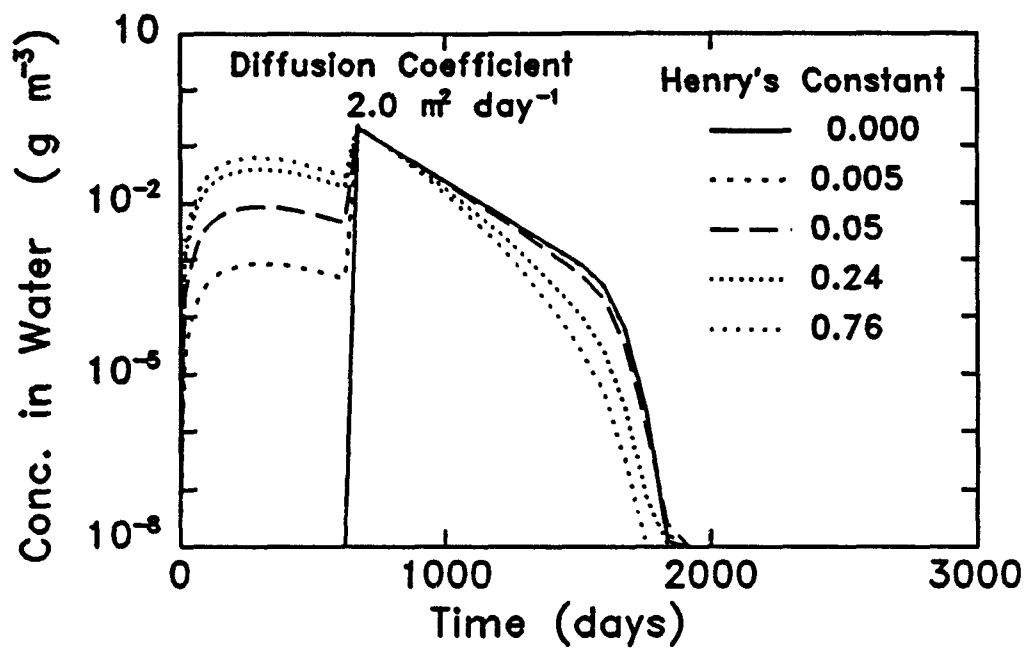


Figure 6.4. Concentration of pollutant in water at the 2-m depth as a function of time for different organic carbon contents.

Figure 6.5. Concentration of pollutant in water at the 2-m depth as a function of time for different bulk density values.
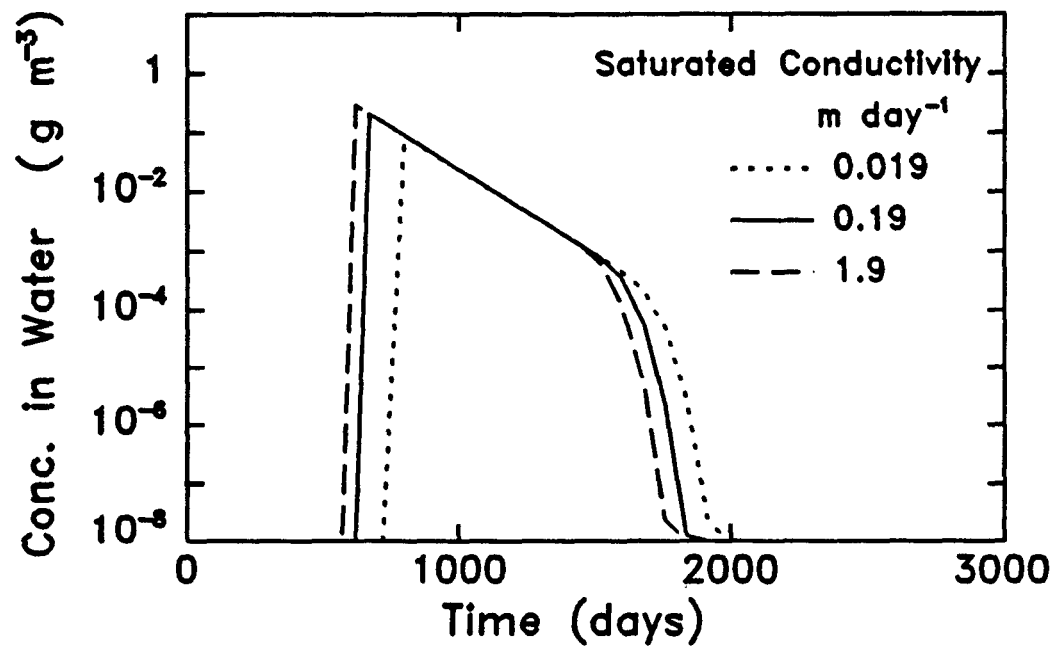


Figure 6.6. Concentration of pollutant in water at the 2-m depth as a function of time for different values of saturated hydraulic conductivity.
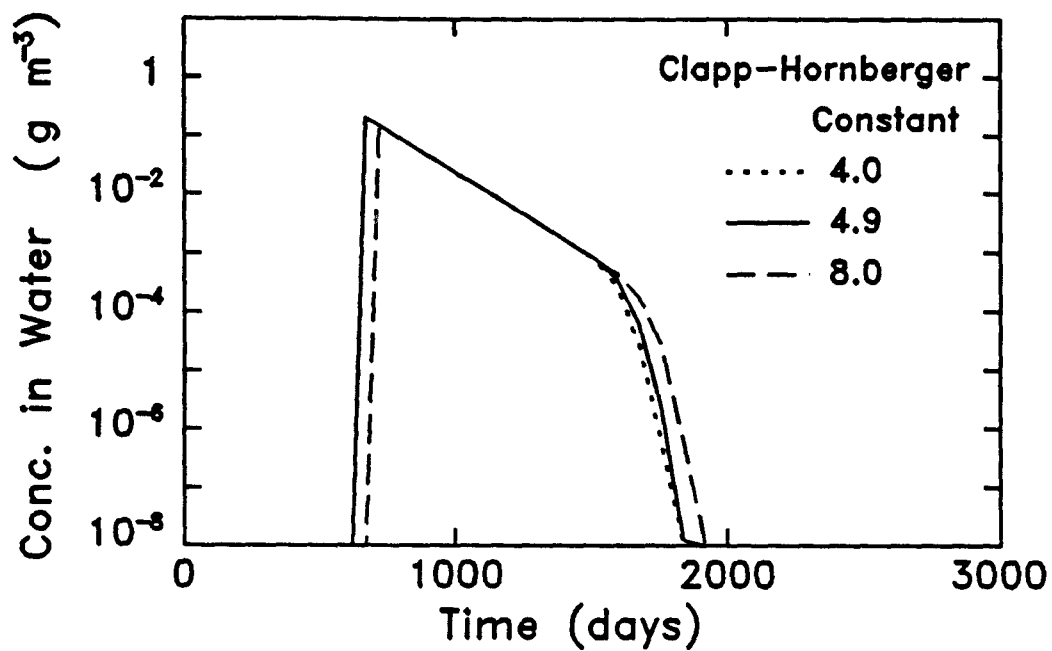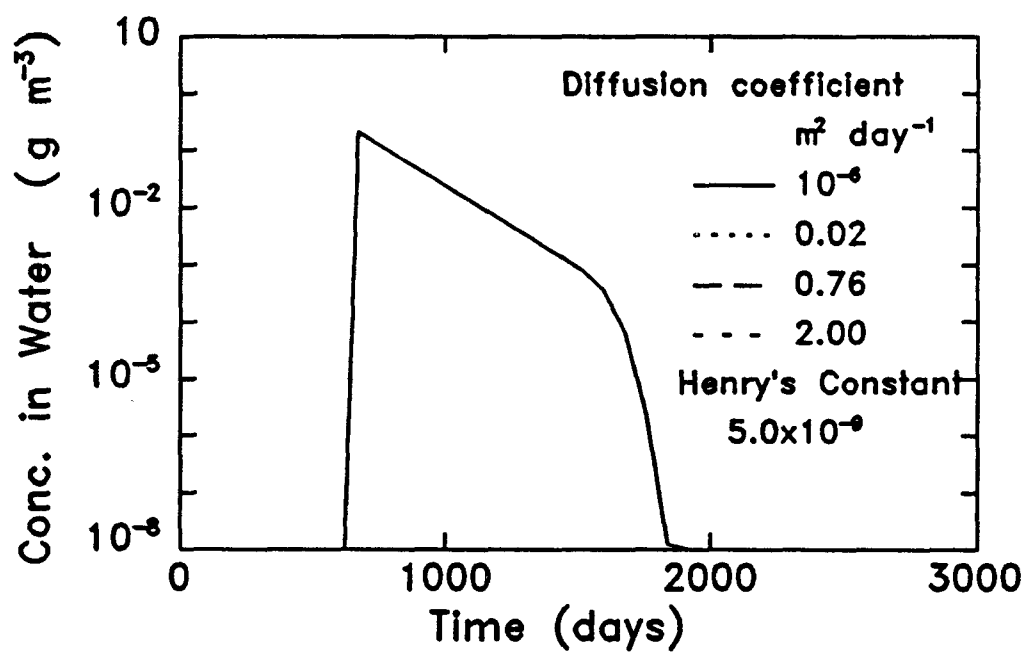
Figure 6.7. Concentration of pollutant in water at the 2-m depth as a function of time for different values of the Clapp-Hornberger constant.
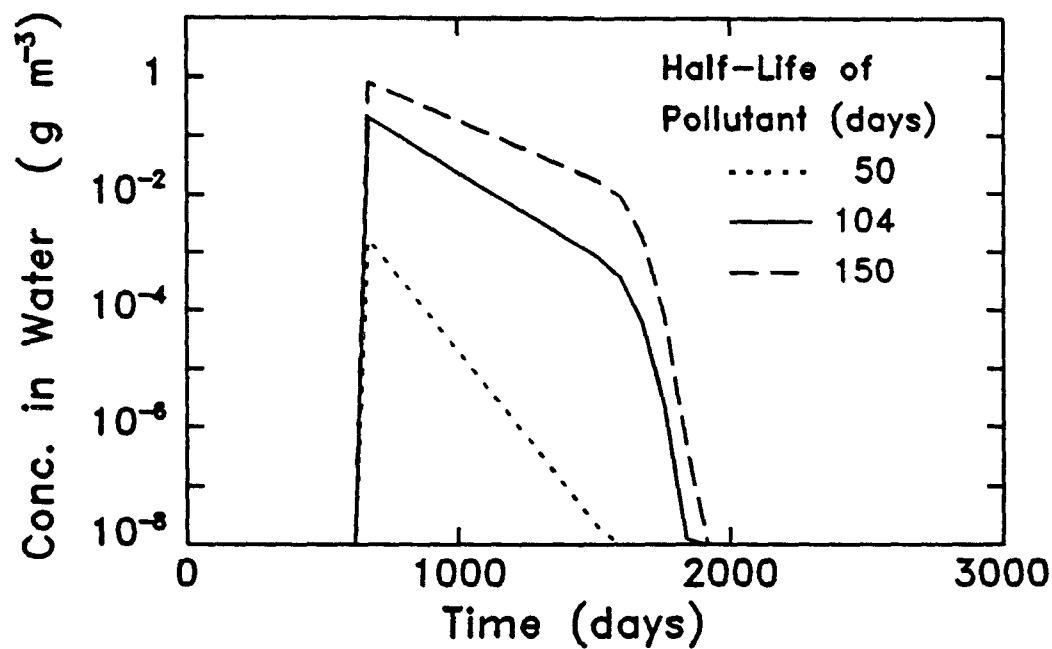


Figure 6.8. Concentration of pollutant in water at the 2-m depth as a function of time different values of degradation half-life.

Figure 6.9. Concentration of pollutant in water at the 2-m depth as a function of time for different values of Henry's constant.
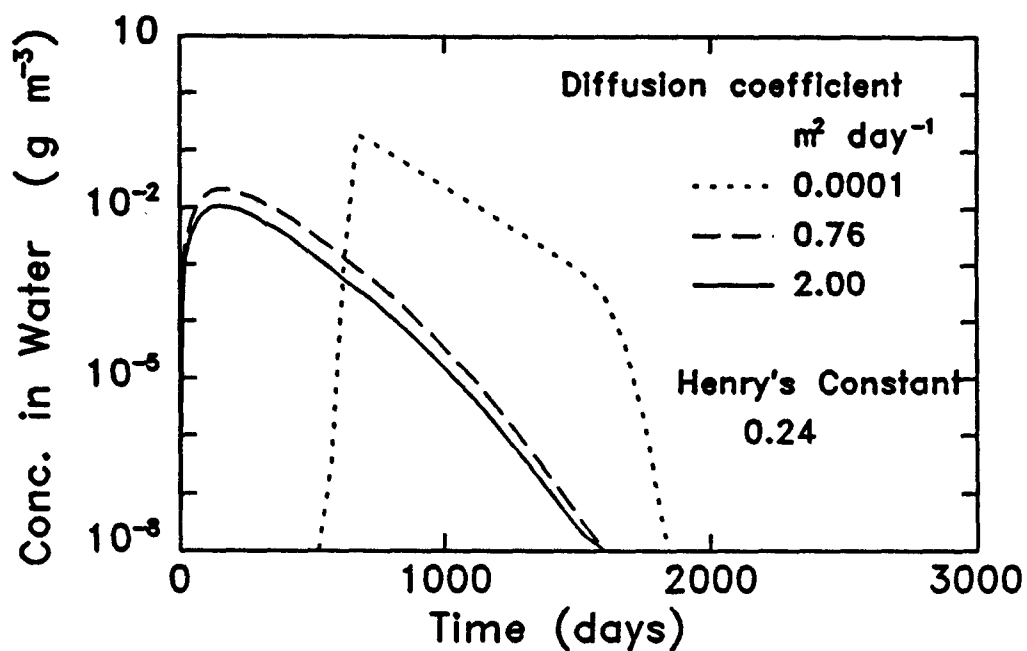


Figure 6.10. Concentration of pollutant in water at the 2-m depth as a function of time for different diffusion coefficients and a small Henry's constant.

Figure 6.11. Concentration of pollutant in water at the 2-m depth as a function of time for different diffusion coefficients and a large Henry's constant for benzene.
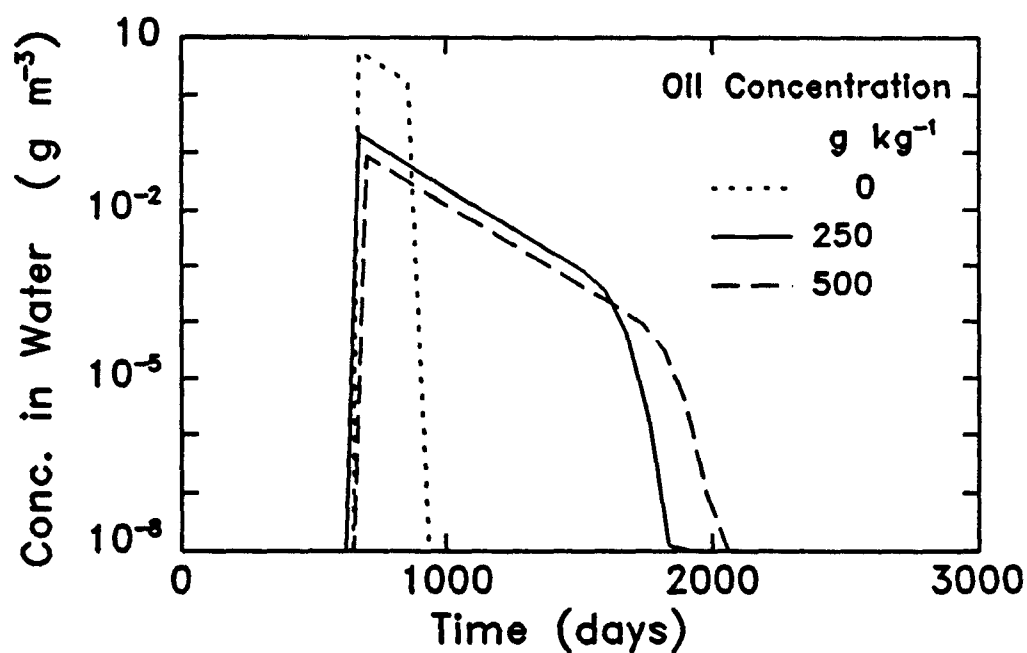


Figure 6.12. Concentration of pollutant in water at the 2-m depth as a function of time for different concentrations of oil in the sludge.

100

# SECTION 7

## SENSITIVITY RESULTS FOR CMLS MODEL

### Impact of Model Simplifications

The predicted position of the chemical in the soil profile as a function of time is shown in Figure 7.1 for three simulations. (Input parameters for soil properties are given in Table 4.2). The first case is predicted by RITZ when no oil is present in the plow zone so the soil and chemical properties are uniform with depth. The second case is predicted by CMLS using the same uniform soil properties used in RITZ and using average daily infiltration and evapotranspiration values as used in RITZ. The third case is predicted by CMLS using layered soil properties of Norfolk but still using average daily infiltration and evapotranspiration. A root depth of 0.5 m was used in the CMLS simulations. When totally uniform systems are simulated, the predicted positions of the bottom of the chemical pulse are in good agreement between RITZ and CMLS. CMLS predicts that the top of the chemical moves more rapidly through the shallow soil layers than does RITZ. Hence the duration of the pulse entering the water table is less for CMLS than for RITZ. This difference is because RITZ assumes that the flux of water at every depth in the soil is the same. Therefore the top and bottom of the chemical move at the same velocity (when no oil is present). In CMLS the flux of water passing any depth on a particular day is the difference between the flux entering the soil surface and the amount of water stored in the soil profile above that depth. Therefore, the flux of water in the root zone decreases with depth so chemicals near the soil surface move more rapidly than chemicals below the root zone. (CMLS predicts that the top and bottom of the chemical pulse move at the same speed when the root zone depth is zero and the soil properties are uniform with depth.)

CMLS allows the user to model movement through layered soils where soil-water and chemical properties change with depth. The third set of lines in Figure 7.1 shows the predicted movement of benzene when the soil is considered a layered system rather than a uniform one. In this case, the chemical reaches the 2-m depth approximately 150 days earlier than when average soil properties are used. The duration of the chemical pulse entering the water table is greater for the layered soil than for the uniform soil. This is primarily due to a lower velocity of chemical in the shallow soil layers where the sorption coefficient is greater than in the uniform case. For this soil, the use of uniform soil properties causes CMLS to overestimate the travel time and to underestimate the amount leached.

The simulations above using CMLS and RITZ assume the daily infiltration and evapotranspiration are equal to their long term average values for 1983 to 1991. CMLS was used to estimate benzene movement using daily water fluxes for starting dates of January 1 of 1983 to 1990. Results are shown in Table 7.1. Using layered soils with uniform fluxes results in a 23% lower travel time than the totally uniform system. Using layered soils and daily fluxes gives a mean travel time which is 47% less than the uniform soil - uniform flux case. The amounts leached for the layered soil with uniform flux and the layered soil with daily flux are 4 and 18 times greater than the uniform case, respectively. These leaching amounts are based on a half-life of 100 days. If the half-life were less than 100 days these factors would be larger. When average infiltration and evapotranspiration rates are used in CMLS, solute leaching is underestimated since the impact of large rainfall events and the resulting large water fluxes are essentially ignored.

### General Impact of Input Parameters

Figure 7.2 shows the positions of the top and bottom of the chemical pulse as functions of time. The different lines represent predicted depths for infiltration and evapotranspiration data beginning January 1 of 1983, 1985, and 1987. Rainfall distributions for three year periods beginning on these dates are shown in Figure 7.3. Clearly the water fluxes or the weather sequences used to drive the model have a large impact

Table 7.1. Comparison of predicted travel time, duration of loading, and amount leached for benzene the Norfolk soil with different levels of simplification. Weather for Fairhope, Alabama. Model used was CMLS.

| | Travel Time (days) | Duration (Days) | Amount Leached (%) |
|---|---|---|---|
| Uniform Soil/Uniform Water Fluxes | 699 | 70 | 1.0 |
| Layered Soil/Uniform Water Fluxes | 541 | 115 | 3.8 |
| Layered Soil/Daily Water Fluxes | | | |
| Beginning Year | | | |
| 1983 | 327 | 242 | 32.9 |
| 1984 | 573 | 152 | 3.6 |
| 1985 | 374 | 72 | 9.9 |
| 1986 | 423 | 5 | 5.4 |
| 1987 | 224 | 87 | 29.9 |
| 1988 | 276 | 28 | 16.3 |
| 1989 | 370 | 58 | 9.6 |
| 1990 | 395 | 320 | 33.0 |
| Mean | 370.2 | 120.5 | 17.6 |

upon the predictions. Therefore, weather will have a large impact upon the sensitivity coefficients. Since it is desired to get an understanding of the sensitivity for any weather sequence, the model was run many times for different weather sequences characteristic of a site. Results from all of the different simulations were summarized and used in the sensitivity analysis. The site chosen is near Fort Cobb, Oklahoma. Annual rainfall there varied from 398 to 1034 mm during the 1948 to 1975 time period. Average annual rainfall was 709 mm during that time period. Weather sequences were generated using the weather generator developed by Richardson and Wright (1984) which is incorporated into the current version of CMLS. Probability distributions of travel time and amount leached to ground water were obtained and used in subsequent analyses.

Figure 7.4 shows a histogram of travel time for the top of the chemical to reach a depth of 2 meters and a second histogram of the relative amount of chemical originating at the soil surface which passes the 2.0 meter depth. The different values shown are due only to different weather sequences, each of which is equally likely at the Fort Cobb site. Each histogram is based on 100 simulations. Predicted travel times vary from 707 days to 5056 days. The corresponding values for the amount of chemical leached below 2 m range from more than $10^{-2}$ to less than $10^{-15}$ percent of that applied. Figure 7.5 shows the distribution of travel times expressed as cumulative probability distributions. Lines are shown for both the top and the bottom of the chemical pulse.

Since the weather has such a large impact upon travel time and amount leached, the results in this section are presented as cumulative probability plots each based on 100 simulations with different lines

102

representing results for different input parameters of interest. For example, Figure 7.6 shows probability distributions for travel time for 4 partition coefficients. The travel times increase as the partition coefficient, $K_{oc}$, increases as expected from equations 9 and 23. At a probability level of 0.50, travel times increase from 1375 days to 2250 days as $K_{oc}$ increases from 0 to 160 $cm^3/g$. That corresponds to a 400-fold decrease in amount leached for the 100-day half-life that was used.

Figure 7.7 shows the dependence of travel time upon organic carbon content. Here the solid line represents the distribution of travel times for the Norfolk soil. Other lines on the graph represent results when the organic carbon content of each soil layer is increased by 0.1%, 0.5% and 1%. The travel time at a particular probability level increases greatly as organic carbon content increases (see Eqn 23). The increase appears to be greater at the probability level of 0.90 than it does at the 0.10 level. That is, the increase in travel time per unit increase in organic carbon content is larger for weather sequences producing lower leaching rates than in weather producing larger leaching rates.

The travel time is shown to increase as the field capacity of the soil increases in Figure 7.8. This is expected since increasing the field capacity increases the soils capacity to store water and reduces the flux of water moving below the root zone. The travel time was found to decrease with an increase in water content at wilting point (Figure 7.9). This is true since a decrease in the wilting point value will increase water storage capacity. The impact of both of these parameters is greater at high probability levels which correspond to greater travel times and generally lower infiltration.

Figure 7.10 contains curves for three different bulk densities. Differences between the curves are small indicating the travel time depends only slightly upon soil bulk density. This is consistent with results observed for RITZ (Figure 5.4) and those observed for the steady state model (Figure 3.3).

CMLS computes the flux of water moving past the chemical each day after performing a water balance for infiltration and evapotranspiration. This water balance depends upon the depth to which water is extracted from the soil (or the root depth), the evapotranspiration and the infiltration. Potential evapotranspiration is estimated from weather data using the Blaney-Criddle technique (Blaney and Criddle, 1962). Actual evapotranspiration is related to potential evapotranspiration with a proportional constant, called crop coefficient. Infiltration in CMLS is estimated from daily rainfall using the SCS curve number method (USDA-SCS, 1972). As the curve number increases, the amount of runoff increases and infiltration decreases. Figures 7.11, 7.12, and 7.13 show the cumulative probability distributions of travel time for different root depths, crop coefficients, and curve numbers, respectively. Travel times increase as root depth increases since the soil is capable of storing more water in the root zone leaving less to percolate deeply into the profile and leach the chemical. Travel times increase as crop coefficients increase since added evapotranspiration results in dryer root zones which can store a larger portion of infiltrating water. Travel times increase as the curve number increases since daily infiltration decreases as curve numbers increase (especially for curve numbers above 70). The impact of each of these parameters increases as the probability level increases.

Sensitivity Coefficients

Figures 7.6 to 7.13 provide an overview of the dependence of travel time upon different input parameters and upon weather. This section presents sensitivity coefficients computed for the travel time, pulse width, and amount leached. Figure 7.14 shows the median travel time, pulse width, and amount leached as functions of the organic carbon partition coefficient, $K_{oc}$. Results are shown for three soils. (Points plotted for travel time in the Norfolk soil correspond to the 4 travel times shown on Figure 7.6 at a probability level of 0.50). Results could also be shown for other probability levels of interest. Figure 7.15 shows the travel time and its sensitivity coefficients for three levels of probability and a $K_{oc} = 80$ $cm^3$ $g^{-1}$ in the Norfolk soil. In the lower graph of Figure 7.15 the line labeled 10% shows the travel time which is not exceeded in 10% of the simulations at each value of $K_{oc}$. The line labeled 50% shows the travel time which is not exceeded in

103

50% of the simulations. That line represents the median travel time for each value of $K_{oc}$. The line labeled 90% shows the time which is not exceeded in 90% of the simulations. The middle graph of Figure 7.15 shows the sensitivity for each line in the lower graph. Since travel time increases approximately linearly with $K_{oc}$, the sensitivity coefficient, S, for travel time is nearly constant. The upper graph shows the relative sensitivity for each line. Table 7.2 summarizes these sensitivities for travel times. In a similar manner, Tables 7.3 and 7.4 summarize the sensitivities for pulse width and amount leached, respectively.

Figures 7.16 to 7.19 show median travel time, pulse width, and amount leached (as a percent of the initial amount) as functions of organic carbon content, bulk density, water content at field capacity, and water content at wilting point, respectively. The median travel time, pulse width, and amount leached are shown as functions of root depth, crop coefficient, and curve number in Figures 7.20 to 7.22. The sensitivity coefficients for these input parameters are also shown in Tables 7.2, 7.3, and 7.4.

Travel time and pulse width appear to be linear functions of the parameters shown in Tables 7.2 and 7.3 except for the curve number. Thus the sensitivity coefficient, S, is constant for the range of data used. Figure 7.22 shows that the travel time and pulse width are approximately linear for curve numbers in the range of 0 to 80 and in the range from 80 to 90. Therefore the coefficients in Tables 14 and 15 contain values for each of these ranges.

The logarithm of the amount of chemical leached past 2 meters changes linearly with the parameters analyzed (except for curve number). That means the S is proportional to the amount leached or S divided by the amount leached is a constant. This fact can be used to estimate S for any amount from the values shown in Table 7.4. Two sets of coefficients are present in Table 7.4 for curve numbers at each $K_{oc}$ since the range is broken up into two parts as discussed above.

From Table 7.2 we can see that the sensitivity coefficients are positive for all parameters except water content at wilting point. Relative sensitivities generally increase in absolute value in the order of curve number (for values less than 80), $K_{oc}$, bulk density, water content at wilting point, organic carbon content, root depth, crop coefficient, water content at field capacity, and curve number for values above 80. Within a particular input parameter, the sensitivity coefficient, S, tends to increase as the probability level increases. A 3-fold increase is not uncommon for several parameters. Relative sensitivities are generally constant or decrease somewhat as probability levels increase. For many of the parameters shown, the difference in travel times between the 10% and 90% probability lines is greater than the difference due to the parameter being analyzed. This illustrates again that uncertainty in water fluxes due to unknown daily weather in the future is a major component of the total uncertainty in a predicted value.

Results shown in Table 7.3 indicate that the pulse width increases greatly as the probability level increases. Those increases are 50-fold or more in many cases. Sensitivity coefficients generally increase with probability as well, although relative sensitivities remain approximately unchanged.

Table 7.4 shows that relative sensitivities for amount leached are generally negative since the amount leached decreases as the parameter value increases. The magnitudes of these relative sensitivities are much greater than those for travel time or pulse width. The magnitudes of these relative sensitivities are greater than 1 which means the relative change in predicted amount leached will be greater than the relative change in the parameter itself. A partial explanation for these large values of relative sensitivity is that the amount leached is a small number so small absolute changes in the amount leached represent large relative changes.

It is noteworthy that all of the relative sensitivity coefficients shown in Tables 7.2-7.4 are larger than 0.54 in absolute value for some range of the parameters and some probability level. This indicates that all of the CMLS parameters are important.

104

Table 7.2. Sensitivity coefficients for travel time (days) which are not exceeded in 10%, 50%, and 90% of the simulations performed. Weather is for Caddo County, Oklahoma. Model used was CMLS.

| Parameter | Parameter Value | Probability 10% | | | Probability 50% | | | Probability 90% | | |
|---|---|---|---|---|---|---|---|---|---|---|
| | | Time | S | $S_r$ | Time | S | $S_r$ | Time | S | $S_r$ |
| Partition Coefficient | | | | | | | | | | |
| - Norfolk soil | 80.0 | 1040 | 4.8 | 0.37 | 1820 | 5.6 | 0.25 · | 2830 | 4.8 | 0.14 |
| - Mclain soil | 80.0 | 2880 | 25.0 | 0.70 | 3630 | 28.5 | 0.63 | 4360 | 29.6 | 0.54 |
| - Cobb soil | 80.0 | 2300 | 16.2 | 0.56 | 3710 | 21.3 | 0.46 | 5240 | 22.9 | 0.35 |
| Organic Carbon | | | | | | | | | | |
| - Koc= 80 ml/g OC | 0.64 | 4310 | 6180 | 0.92 | 5520 | 7160 | 0.83 | 7020 | 8420 | 0.77 |
| - Koc= 40 ml/g OC | 0.64 | 2480 | 3010 | 0.78 | 3490 | 3750 | 0.69 | 4783 | 3970 | 0.53 |
| Bulk Density | | | | | | | | | | |
| - Koc= 80 ml/g OC | 1.60 | 1130 | 627 | 0.89 | 1870 | 573 | 0.49 | 2860 | 467 | 0.26 |
| - Koc= 40 ml/g OC | 1.60 | 972 | 0.0 | 0.0 | 1610 | 767 | 0.76 | 2620 | 3.3 | 0.00 |
| Field Capacity | | | | | | | | | | |
| - Koc= 80 ml/g OC | 0.242 | 1130 | 9800 | 2.10 | 1920 | 19900 | 2.51 | 2770 | 26700 | 2.33 |
| - Koc= 40 ml/g OC | 0.242 | 935 | 7100 | 1.84 | 1590 | 17500 | 2.68 | 2630 | 22900 | 2.10 |
| Wilting Point | | | | | | | | | | |
| - Koc= 80 ml/g OC | 0.068 | 722 | -4570 | 0.43 | 1410 | -11300 | -0.54 | 2280 | -11700 | -0.35 |
| - Koc= 40 ml/g OC | 0.068 | 638 | -1530 | 0.16 | 1330 | -6700 | -0.34 | 2140 | -11800 | -0.37 |
| Root Depth | | | | | | | | | | |
| - Koc=160 ml/g OC | 0.600 | 1490 | 1260 | 0.51 | 2300 | 2890 | 0.75 | 3280 | 5190 | 0.95 |
| - Koc= 80 ml/g OC | 0.600 | 1220 | 1630 | 0.80 | 1900 | 3050 | 0.96 | 2780 | 5520 | 1.19 |
| - Koc= 40 ml/g OC | 0.600 | 943 | 1420 | 0.90 | 1670 | 3170 | 1.14 | 2550 | 5200 | 1.23 |
| Crop Coefficient | | | | | | | | | | |
| - Koc= 80 ml/g OC | 1.00 | 1100 | 1270 | 1.16 | 1820 | 1970 | 1.08 | 2800 | 3130 | 1.12 |
| - Koc= 40 ml/g OC | 1.00 | 822 | 907 | 1.10 | 1560 | 1730 | 1.10 | 2400 | 3220 | 1.34 |
| Curve Number | | | | | | | | | | |
| - Koc=160 ml/g OC | 40 | 1660 | 4.9 | 0.12 | 2510 | 7.8 | 0.12 | 3520 | 8.8 | 0.10 |
| - Koc= 80 ml/g OC | 40 | 1150 | 5.3 | 0.18 | 1940 | 6.8 | 0.14 | 3010 | 8.6 | 0.12 |
| - Koc= 40 ml/g OC | 40 | 957 | 3.7 | 0.15 | 1750 | 5.5 | 0.13 | 2710 | 7.3 | 0.11 |
| - Koc=160 ml/g OC | 85 | 3420 | 268 | 6.65 | 5010 | 366 | 6.21 | 6540 | 446 | 5.80 |
| - Koc= 80 ml/g OC | 85 | 2740 | 237 | 7.35 | 4090 | 317 | 6.59 | 5870 | 426 | 6.16 |
| - Koc= 40 ml/g OC | 85 | 2220 | 195 | 7.48 | 3740 | 304 | 6.91 | 5490 | 425 | 6.58 |

Table 7.3. Sensitivity coefficients for pulse width (days) which are not exceeded in 10%, 50%, and 90% of the simulations performed. Weather is for Caddo County, Oklahoma. Model used was CMLS.

| Parameter | Parameter Value | Probability | | | | | | | | |
|---|---|---|---|---|---|---|---|---|---|---|
| | | 10% | | | 50% | | | 90% | | |
| | | Width | S | $S_r$ | Width | S | $S_r$ | Width | S | $S_r$ |
| Partition Coefficient | | | | | | | | | | |
| - Norfolk soil | 80.0 | 37 | 0.46 | 1.00 | 292 | 3.63 | 0.99 | 707 | 6.42 | 0.73 |
| - Mclain soil | 80.0 | 546 | 6.62 | 0.97 | 885 | 9.44 | 0.85 | 1460 | 13.2 | 0.72 |
| - Cobb soil | 80.0 | 42 | 0.52 | 1.00 | 359 | 4.17 | 0.93 | 1130 | 8.53 | 0.60 |
| Organic Carbon | | | | | | | | | | |
| - Koc = 80 ml/g OC | 0.64 | 122 | 215 | 1.13 | 659 | 747 | 0.72 | 1500 | 1040 | 0.45 |
| - Koc = 40 ml/g OC | 0.64 | 58 | 117 | 1.28 | 382 | 374 | 0.63 | 846 | 501 | 0.38 |
| Bulk Density | | | | | | | | | | |
| - Koc = 80 ml/g OC | 1.60 | 14 | -37 | -4.3 | 329 | 247 | 1.20 | 1040 | 357 | 0.55 |
| - Koc = 40 ml/g OC | 1.60 | 1 | 0 | 0.0 | 138 | 93 | 1.08 | 567 | -130 | -0.37 |
| Field Capacity | | | | | | | | | | |
| - Koc = 80 ml/g OC | 0.242 | 14 | -250 | -4.2 | 330 | -1100 | -0.81 | 968 | 1160 | 2.89 |
| - Koc = 40 ml/g OC | 0.272 | 1 | 0 | 0.0 | 137 | 1300 | 2.30 | 704 | 1240 | 4.25 |
| Wilting Point | | | | | | | | | | |
| - Koc = 80 ml/g OC | 0.068 | 17 | 800 | 3.2 | 267 | -1100 | -0.28 | 779 | -6800 | -0.59 |
| - Koc = 40 ml/g OC | 0.068 | 0.5 | 33.3 | 4.5 | 154 | -1170 | -0.51 | 603 | -3730 | -0.42 |
| Root Depth | | | | | | | | | | |
| - Koc = 160 ml/g OC | 0.600 | 237 | -1170 | -2.95 | 578 | -1180 | -1.22 | 1420 | 1150 | 0.49 |
| - Koc = 80 ml/g OC | 0.600 | 85 | -425 | -3.00 | 307 | -550 | -1.07 | 893 | 888 | 0.60 |
| - Koc = 40 ml/g OC | 0.600 | 31 | -155 | -3.00 | 140 | -570 | -2.44 | 492 | 385 | 0.47 |
| Crop Coefficient | | | | | | | | | | |
| - Koc = 80 ml/g OC | 1.00 | 14 | -35 | -2.50 | 281 | 392 | 1.40 | 838 | 1450 | 1.72 |
| - Koc = 40 ml/g OC | 1.00 | 1 | -7.5 | -5.00 | 136 | 60 | 0.44 | 610 | 1160 | 1.90 |
| Curve Number | | | | | | | | | | |
| - Koc = 160 ml/g OC | 40 | 84 | 1.01 | 0.48 | 594 | 1.72 | 0.12 | 1440 | 3.37 | 0.09 |
| - Koc = 80 ml/g OC | 40 | 12 | 0.20 | 0.68 | 247 | 1.47 | 0.24 | 893 | 1.90 | 0.08 |
| - Koc = 40 ml/g OC | 40 | 1 | 0.29 | 1.63 | 82 | 0.45 | 0.22 | 564 | 3.14 | 0.22 |
| - Koc = 160 ml/g OC | 85 | 82 | -9.70 | -10.1 | 791 | 14.6 | 1.57 | 2090 | 99.2 | 4.03 |
| - Koc = 80 ml/g OC | 85 | 14 | -1.90 | -11.1 | 345 | 3.60 | 0.89 | 1240 | 37.4 | 2.57 |
| - Koc = 40 ml/g OC | 85 | 2 | -0.30 | -17.0 | 126 | 0.40 | 0.27 | 952 | 31.5 | 2.81 |

Table 7.4. Sensitivity coefficients for amount leached (% of initial amount) which was exceeded in 10%, 50%, and 90% of the simulations. Weather is for Caddo County, Oklahoma. Model used was CMLS.
(Note: S/Amount is nearly constant for the range of parameters tested.)

| Parameter | Parameter Value | Probability 10% | | | Probability 50% | | | Probability 90% | | |
|---|---|---|---|---|---|---|---|---|---|---|
| | | Amount | S | $S_r$ | Amount | S | $S_r$ | Amount | S | $S_r$ |
| **Partition Coefficient** | | | | | | | | | | |
| -Norfolk soil | 80.0 | 3.0E-1 | -4.7E-3 | -1.24 | 2.7E-03 | -4.2E-05 | -1.24 | 1.0E-06 | -2.0E-08 | -15.9 |
| -Mclain soil | 80.0 | 9.2E-5 | -1.0E-5 | -9.17 | 7.4E-07 | -9.4E-08 | -1.02 | 2.4E-09 | -3.4E-10 | -11.3 |
| -Cobb soil | 80.0 | 2.3E-4 | -2.1E-5 | -7.14 | 1.9E-08 | -2.2E-09 | -9.07 | 1.7E-13 | -2.0E-14 | -9.5 |
| **Organic Carbon** | | | | | | | | | | |
| -Koc= 80 ml/g OC | 0.64 | 2.0E-9 | -7.7E-8 | -24.5 | 2.6E-13 | -1.2E-12 | -29.2 | 4.7E-19 | -2.8E-17 | -38.6 |
| -Koc= 40 ml/g OC | 0.64 | 7.1E-5 | -1.3E-3 | -11.4 | 3.3E-08 | -7.9E-07 | -15.2 | 4.0E-12 | -1.0E-10 | -16.9 |
| **Bulk Density** | | | | | | | | | | |
| -Koc= 80 ml/g OC | 1.60 | 1.6E-1 | -9.0E-2 | -0.88 | 3.0E-03 | -1.6E-03 | -0.87 | 2.1E-06 | -1.1E-06 | -0.83 |
| -Koc= 40 ml/g OC | 1.60 | 2.5E-1 | -1.5E-2 | -0.10 | 4.1E-0E | -1.7E-03 | -0.65 | 3.8E-06 | 0.0E+00 | 0.00 |
| **Field Capacity** | | | | | | | | | | |
| -Koc= 80 ml/g OC | 0.242 | 2.0E+1 | -1.3E+3 | -15.3 | 2.5E-01 | -2.4E+01 | -23.6 | 1.8E-04 | -3.7E-02 | -49.6 |
| -Koc= 40 ml/g OC | 0.242 | 4.0E+1 | -3.7E+3 | -22.6 | 4.5E-01 | -4.4E+01 | -23.6 | 4.1E-04 | -8.5E-02 | -50.1 |
| **Wilting Point** | | | | | | | | | | |
| -Koc= 80 ml/g OC | 0.068 | 4.2E+1 | 1.1E+3 | 1.80 | 3.8E-01 | 2.8E+01 | 5.1 | 8.2E-04 | 7.4E-02 | 6.2 |
| -Koc= 40 ml/g OC | 0.068 | 5.8E+2 | 5.7E+4 | 6.67 | 1.3E+01 | 2.2E+03 | 11.4 | 1.1E-01 | 2.8E+01 | 16.7 |
| **Root Depth** | | | | | | | | | | |
| -Koc=160 ml/g OC | 0.60 | 4.5E-1 | -2.2E+0 | -2.97 | 5.0E-02 | -2.5E-01 | -3.00 | 2.4E-03 | -1.2E-02 | -3.00 |
| -Koc= 80 ml/g OC | 0.60 | 6.9E-1 | -3.4E+0 | -2.93 | 8.2E-02 | -4.1E-01 | -3.00 | 4.6E-03 | -2.3E-02 | -3.00 |
| -Koc= 40 ml/g OC | 0.60 | 9.5E-1 | -4.5E+0 | -2.85 | 1.1E-01 | -5.6E-01 | -3.00 | 6.2E-03 | -3.1E-02 | -3.00 |
| **Crop Coefficient** | | | | | | | | | | |
| -Koc= 80 ml/g OC | 1.00 | 3.4E-1 | -2.5E+0 | -7.45 | 3.4E-03 | -3.1E-02 | -8.96 | 1.9E-06 | -3.5E-05 | -18.3 |
| -Koc= 40 ml/g OC | 1.00 | 5.9E-1 | -3.5E+0 | -5.90 | 8.8E-03 | -7.3E-02 | -8.38 | 8.8E-06 | -1.9E-04 | -2.11 |
| **Curve Number** | | | | | | | | | | |
| -Koc=160 ml/g OC | 40 | 5.9E-2 | -1.8E-3 | -1.24 | 2.9E-04 | -1.2E-05 | -1.70 | 1.2E-07 | -5.9E-09 | -1.89 |
| -Koc= 80 ml/g OC | 40 | 1.2E-1 | -2.0E-3 | -0.65 | 8.6E-04 | -3.3E-05 | -1.53 | 4.8E-07 | -2.1E-08 | -1.80 |
| -Koc= 40 ml/g OC | 40 | 2.6E-1 | -6.9E-3 | -1.07 | 1.5E-03 | -4.8E-05 | -1.28 | 1.0E-06 | -4.4E-08 | -1.76 |
| -Koc=160 ml/g OC | 85 | 3.7E-6 | -5.3E-6 | -121 | 5.9E-11 | -1.4E-10 | -196 | 1.4E-16 | -4.7E-16 | -277 |
| -Koc= 80 ml/g OC | 85 | 6.2E-5 | -7.8E-5 | -108 | 1.4E-09 | -2.8E-09 | -172 | 2.5E-15 | -7.5E-15 | -257 |
| -Koc= 40 ml/g OC | 85 | 1.9E-4 | -2.0E-4 | - 92 | 4.9E-09 | -9.7E-09 | -169 | 8.4E-15 | -2.5E-14 | -249 |
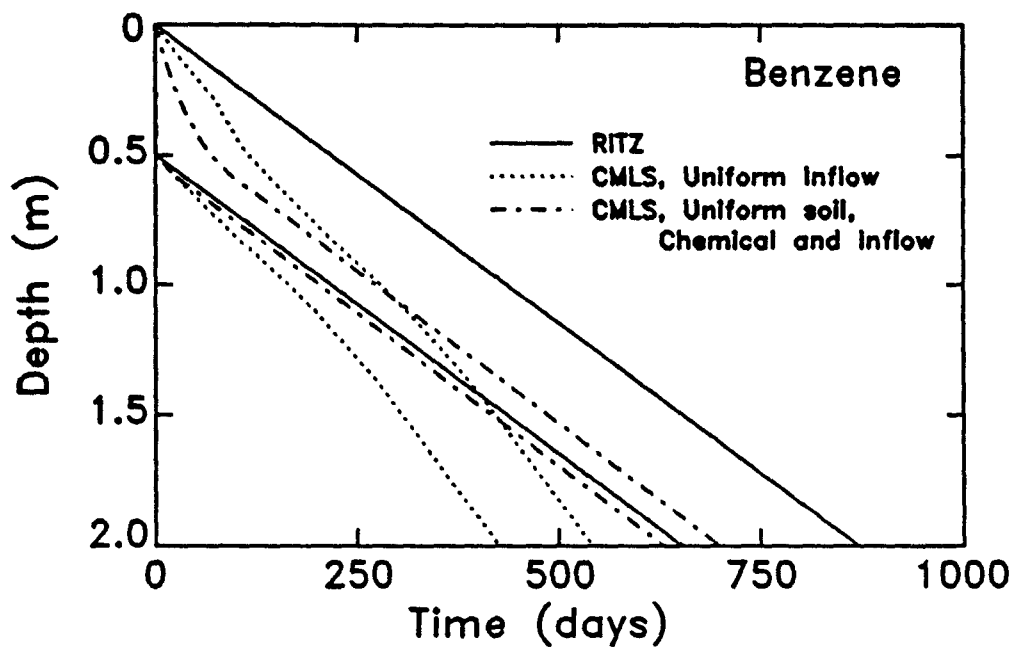
Figure 7.1 Predicted position of benzene as a function of time using RITZ and CMLS with uniform water flux at the soil surface as well as uniform soil and chemical properties. Predictions from CMLS are also shown for uniform water flux but depth dependent and chemical properties.
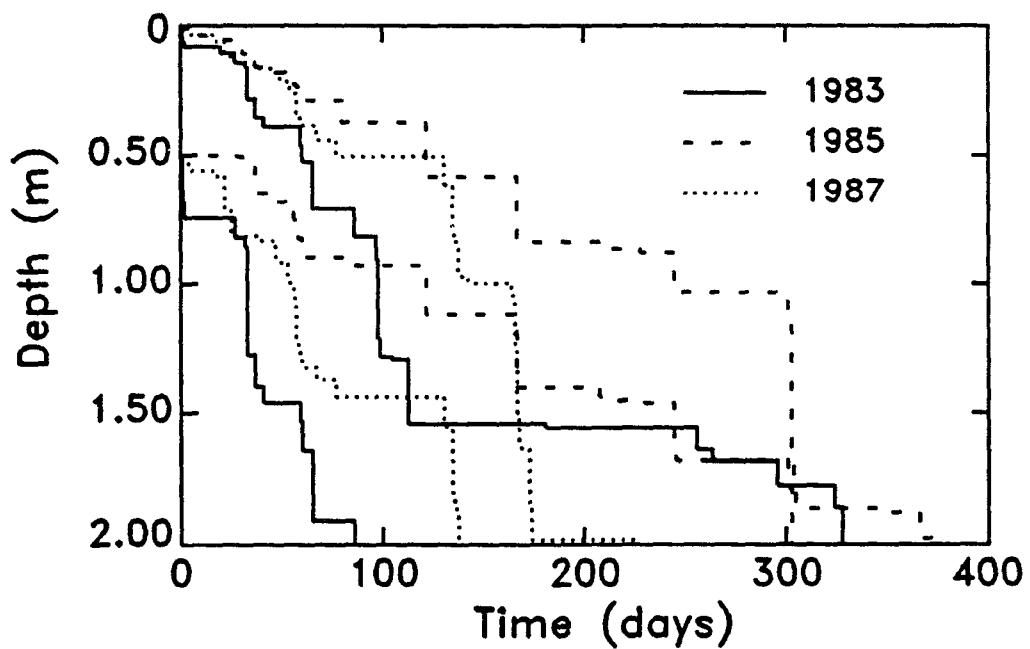


Figure 7.2. Predicted position of the top and bottom of the pollutant as functions of time for daily infiltration and evapotranspiration values and three different dates for the simulation.
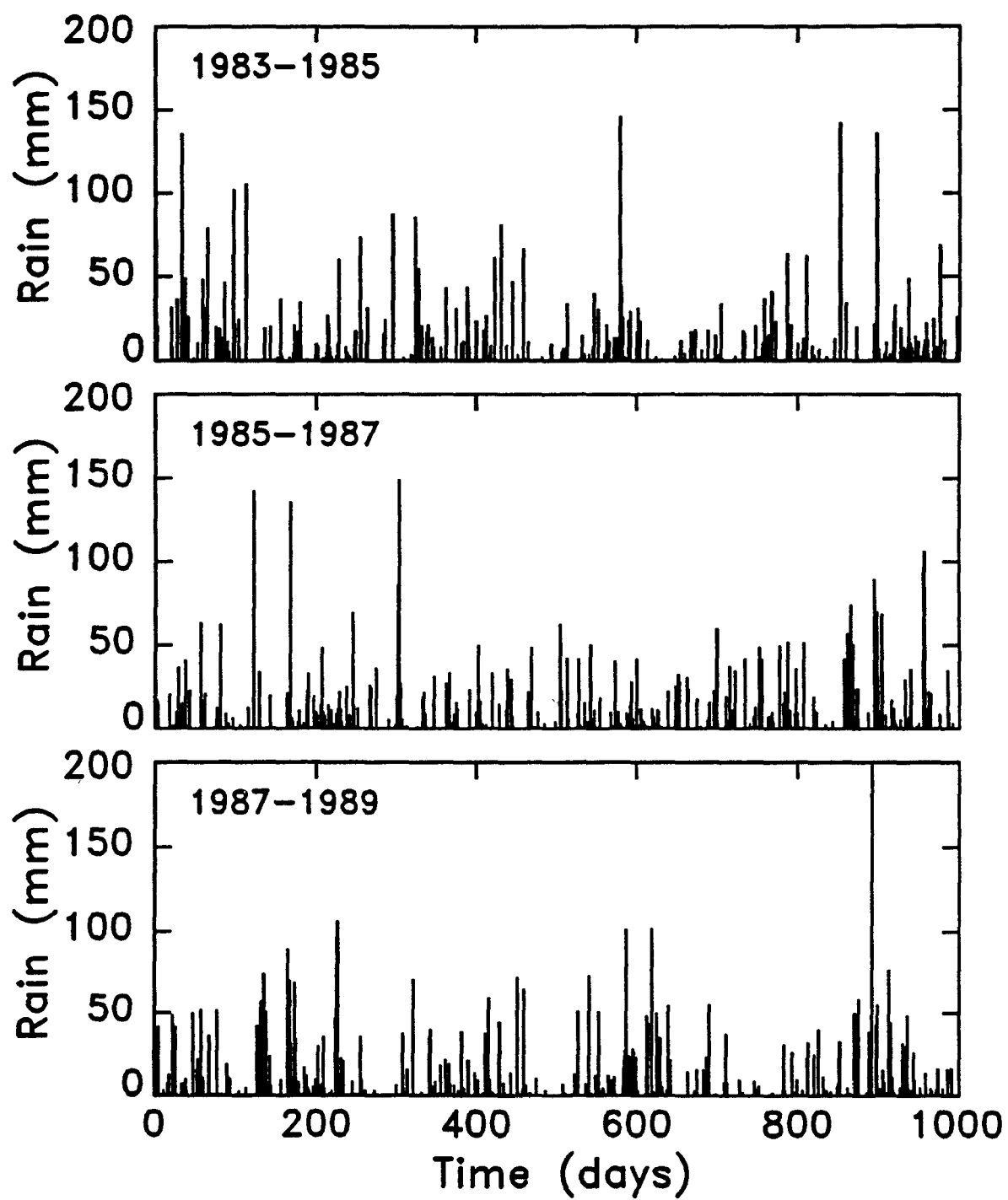
Figure 7.3. Daily rainfall distributions for three-year periods starting January 1 at the Fairhope site in Alabama.
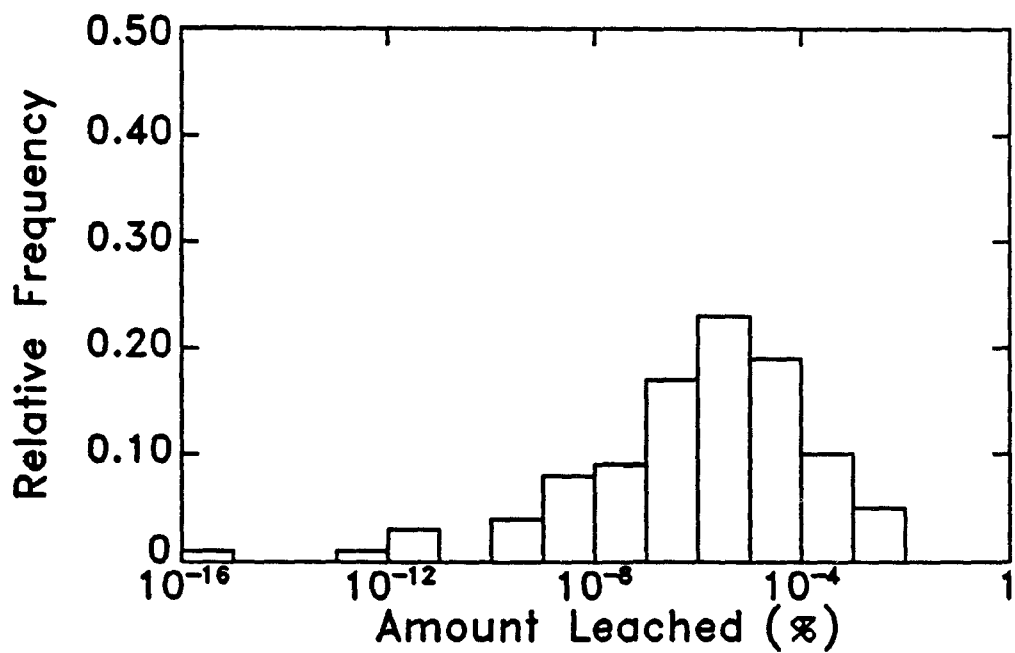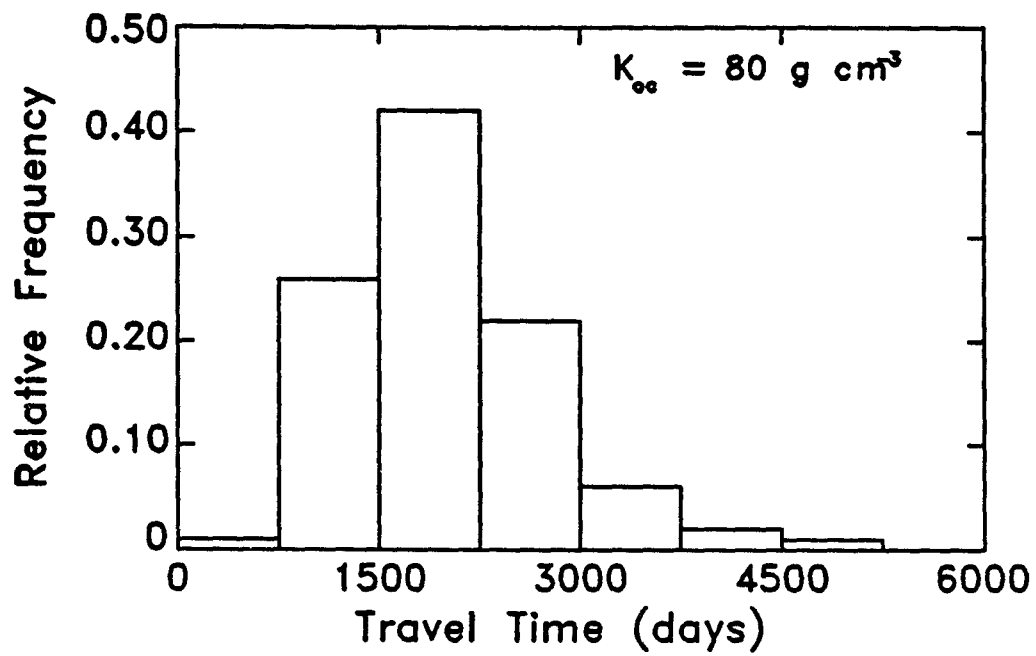
Figure 7.4. Upper graph is a histogram of the travel time for a chemical to move from the soil surface to a depth of 2 m. for different weather sequences equally likely to occur in Caddo County, Oklahoma. Lower graph is a histogram of the amount leached as a percent of the amount applied.

110
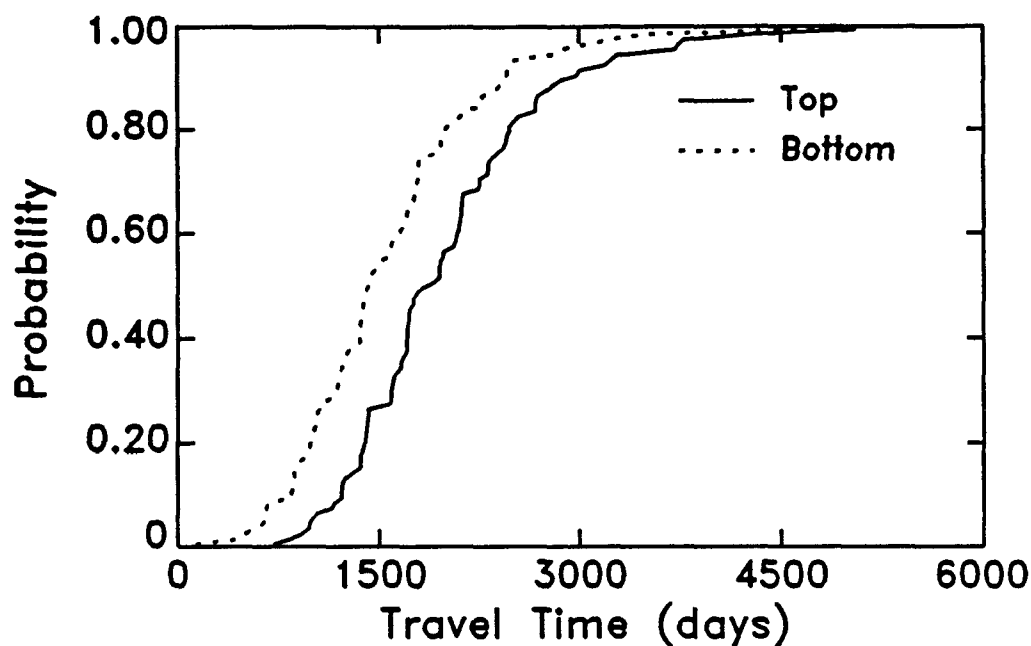
Figure 7.5. The probability that different travel times for the top and bottom of the pollutant to reach a depth of 2m. will not be exceeded.
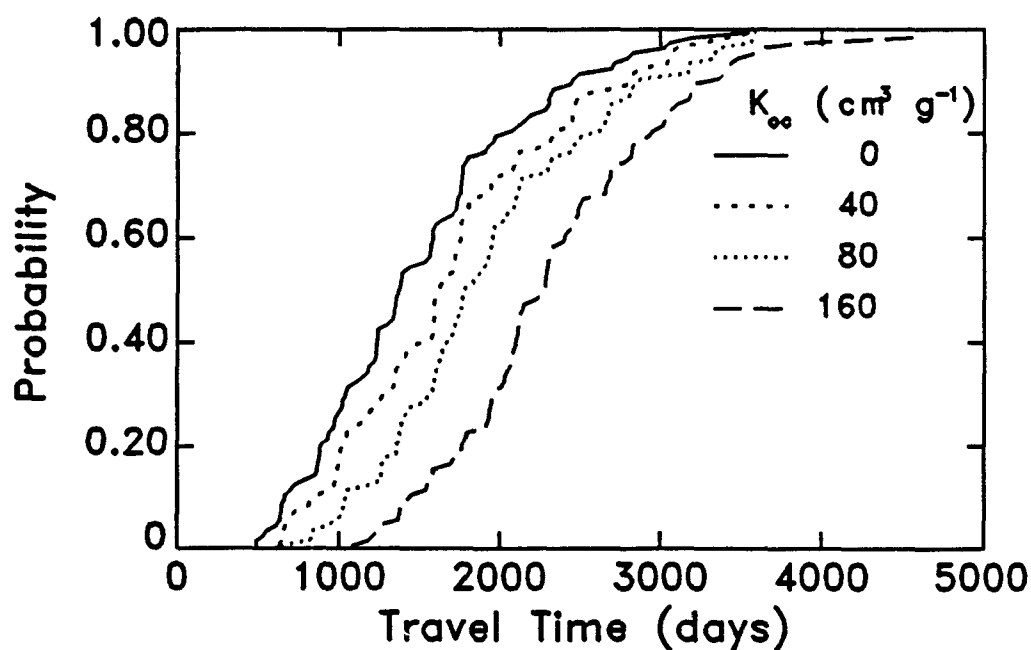


Figure 7.6. The probability that different travel times for the top of the pollutant to reach a depth of 2m. will not be exceeded for organic carbon partition coefficients of 0, 40, 80, and 160 $cm^3$ $g^{-1}$.

111
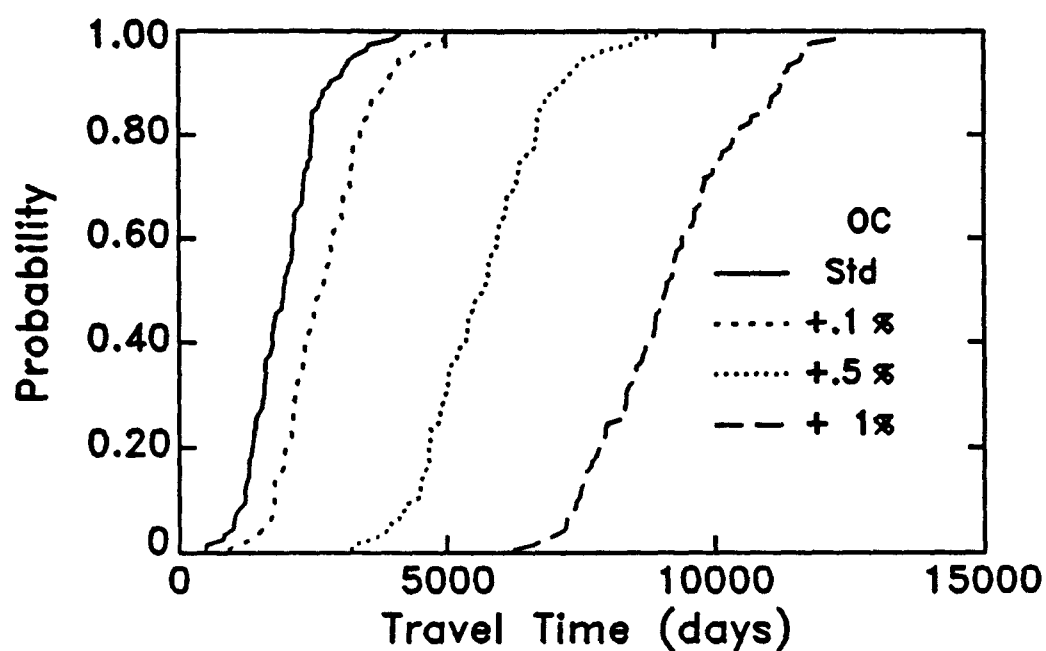
Figure 7.7. The probability that different travel times for the top of the pollutant to reach a depth of 2m. will not be exceeded for organic carbon contents which are 0%, 0.1%, 0.5%, and 1% greater than the standard Norfolk soil.
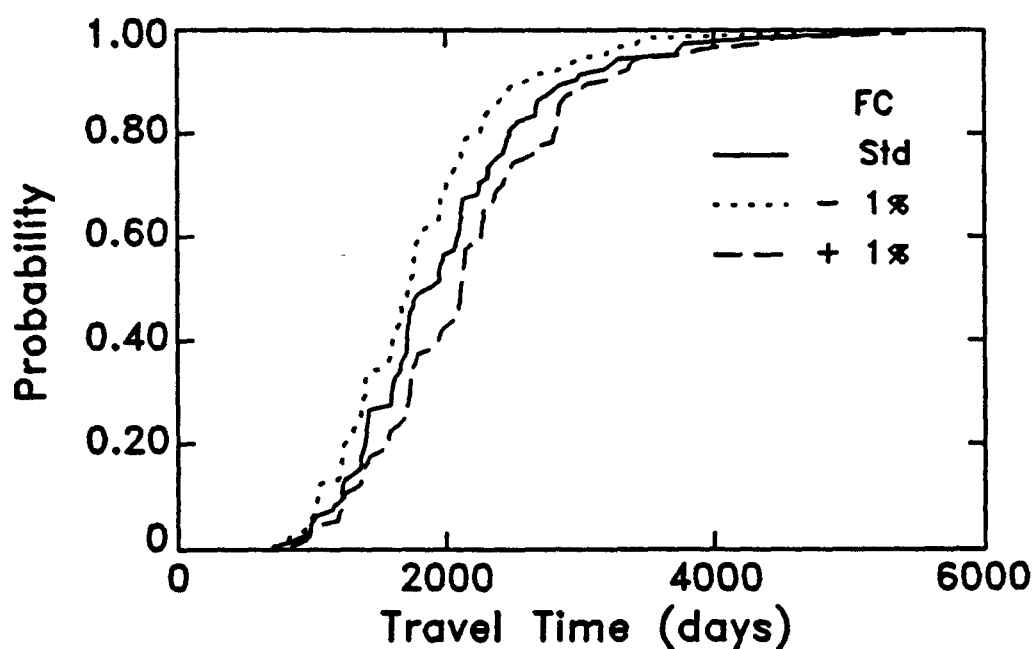


Figure 7.8. The probability that different travel times for the top of the pollutant to reach a depth of 2m. will not be exceeded for field capacity values which are 0, -0.01, and 0.01 $m^3$ $m^{-3}$ greater than the standard Norfolk soil.
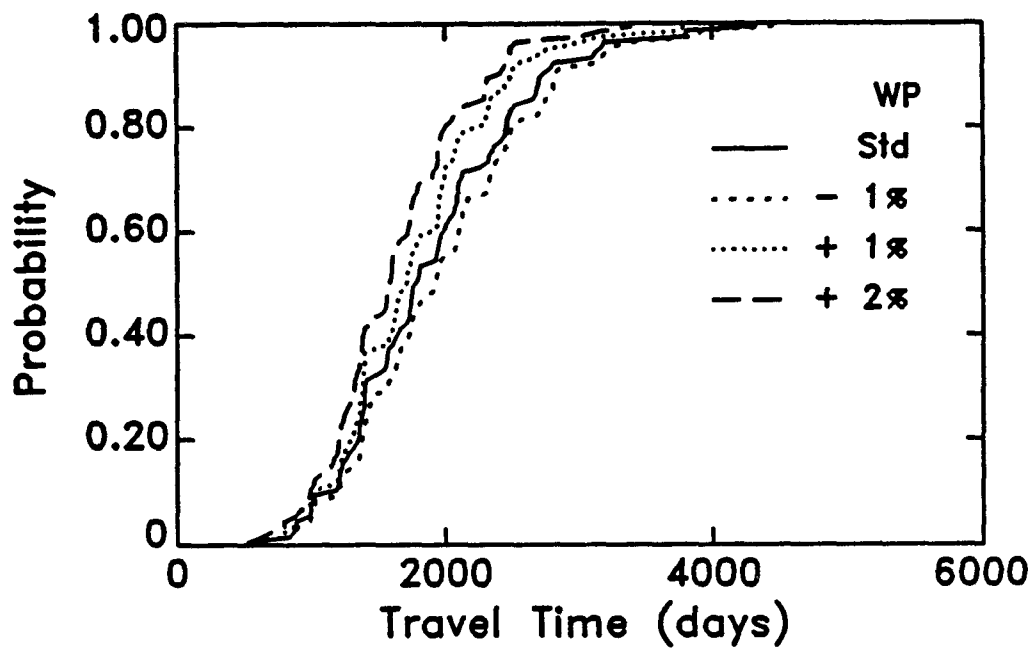
Figure 7.9. The probability that different travel times for the top of the pollutant to reach a depth of 2m. will not be exceeded for wilting point values which are 0, -0.01, 0.01, and 0.02 $m^3$ $m^{-3}$ greater than the standard Norfolk soil.
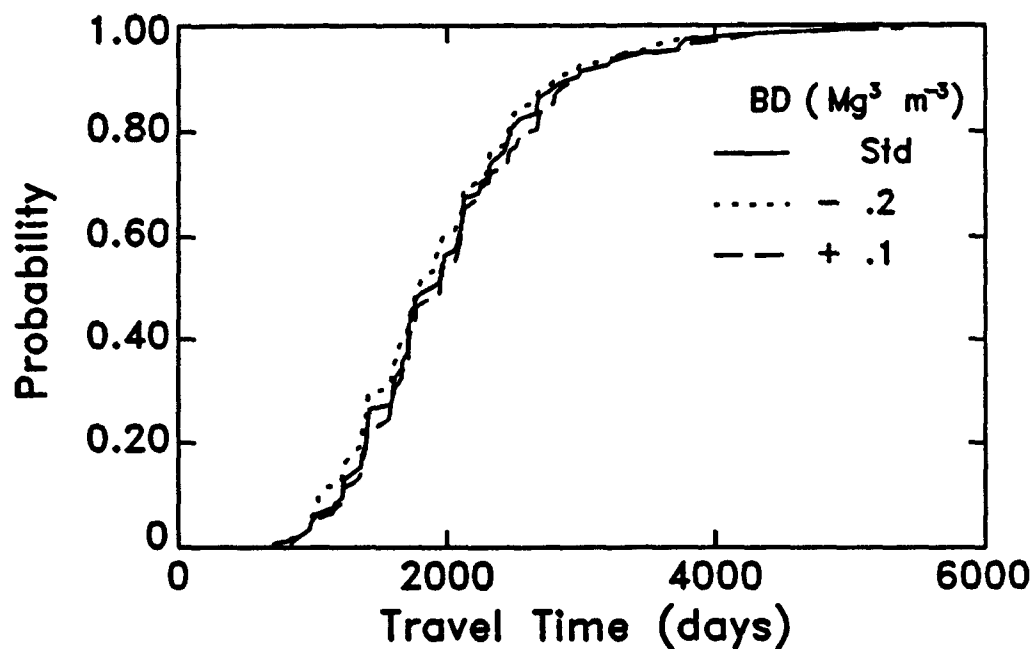


Figure 7.10. The probability that different travel times for the top of the pollutant to reach a depth of 2m. will not be exceeded for bulk density values which are 0, -0.2, and 0.1 Mg $m^{-3}$ greater than the standard Norfolk soil.
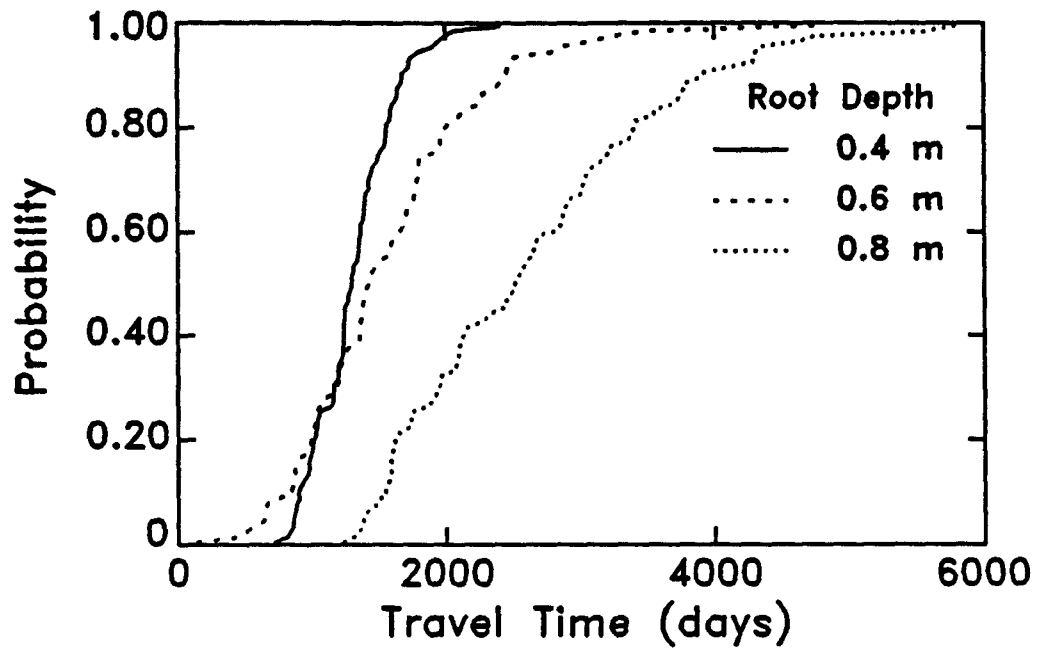
Figure 7.11. The probability that different travel times for the top of the pollutant to reach a depth of 2m. will not be exceeded for root depths of 0.4, 0.6 and 0.8 m.
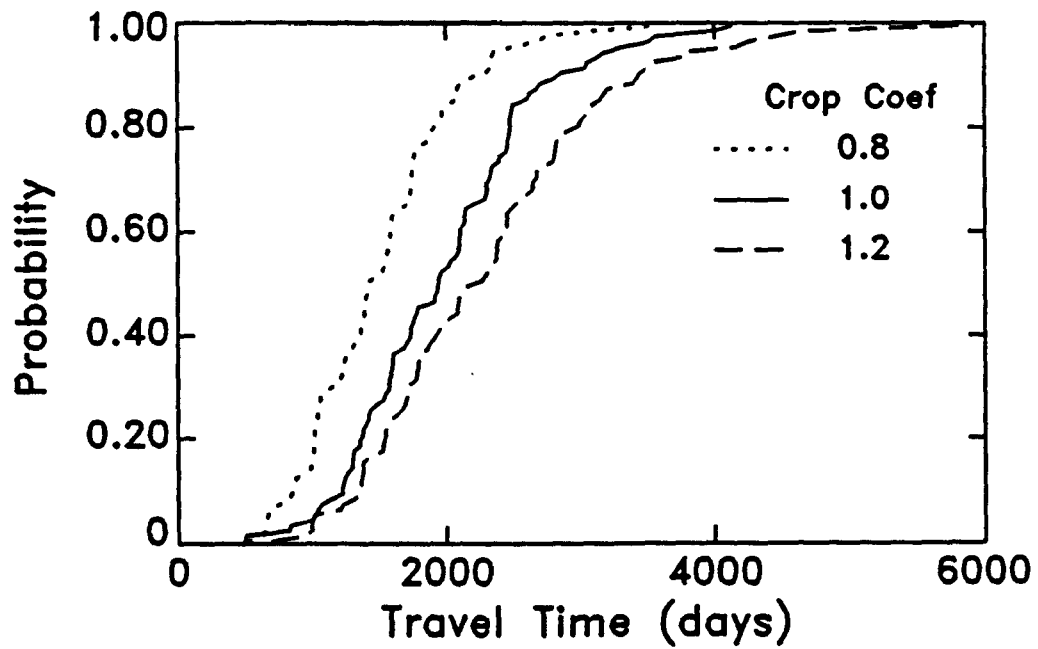


Figure 7.12. The probability that different travel times for the top of the pollutant to reach a depth of 2m. will not be exceeded for crop coefficients of 0.8, 1.0 and 1.2.
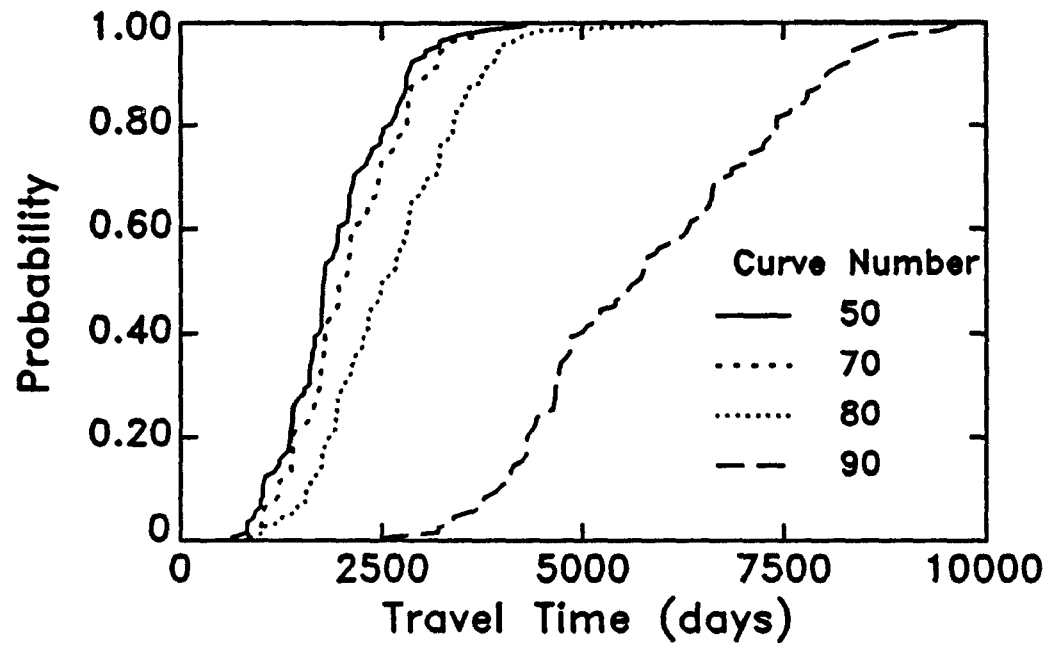
Figure 7.13. The probability that different travel times for the top of the pollutant to reach a depth of 2m. will not be exceeded for curve numbers of 50, 70, 80, and 90.
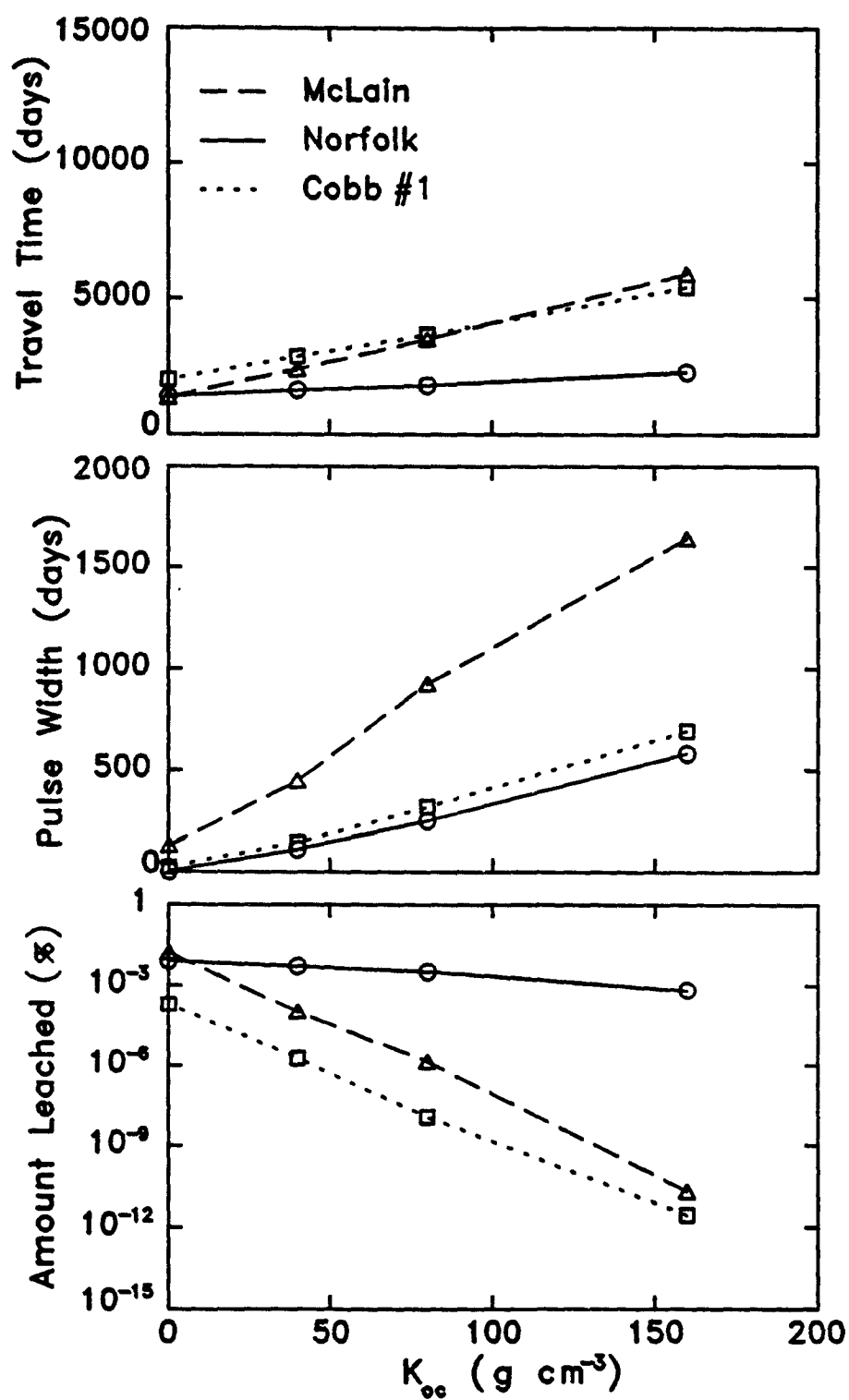
Figure 7.14. Median travel time, pulse width, and amount leached as functions of organic carbon partition coefficient for three soils.
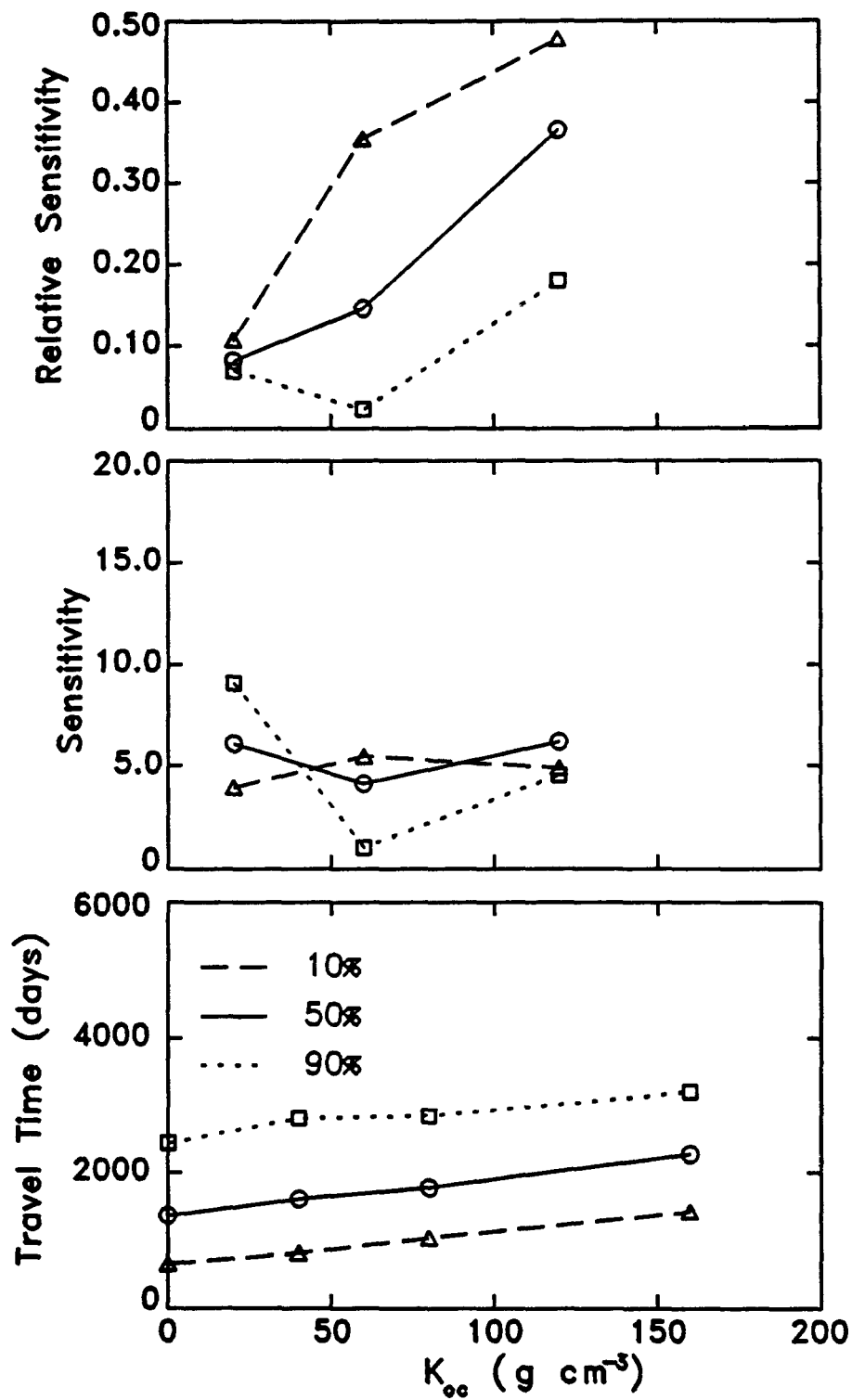
Figure 7.15. Travel time which is not exceeded in 10%, 50%, and 90% of the simulations as functions of organic carbon partition coefficient. Middle and upper figures show the sensitivity and relative sensitivity for each function.
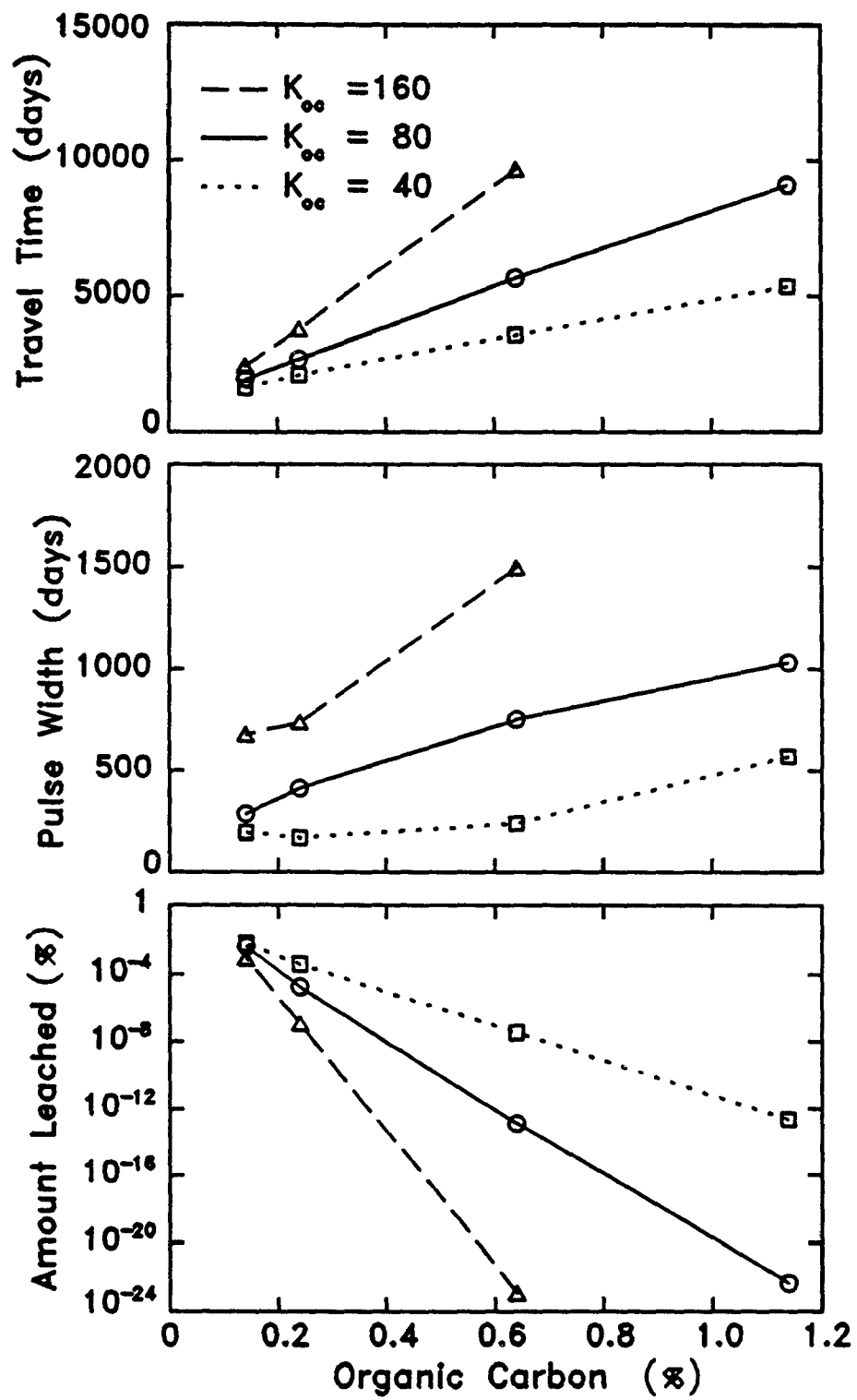
Figure 7.16. Median travel time, pulse width, and amount leached as functions of organic carbon content for three $K_{oc}$ values.

118
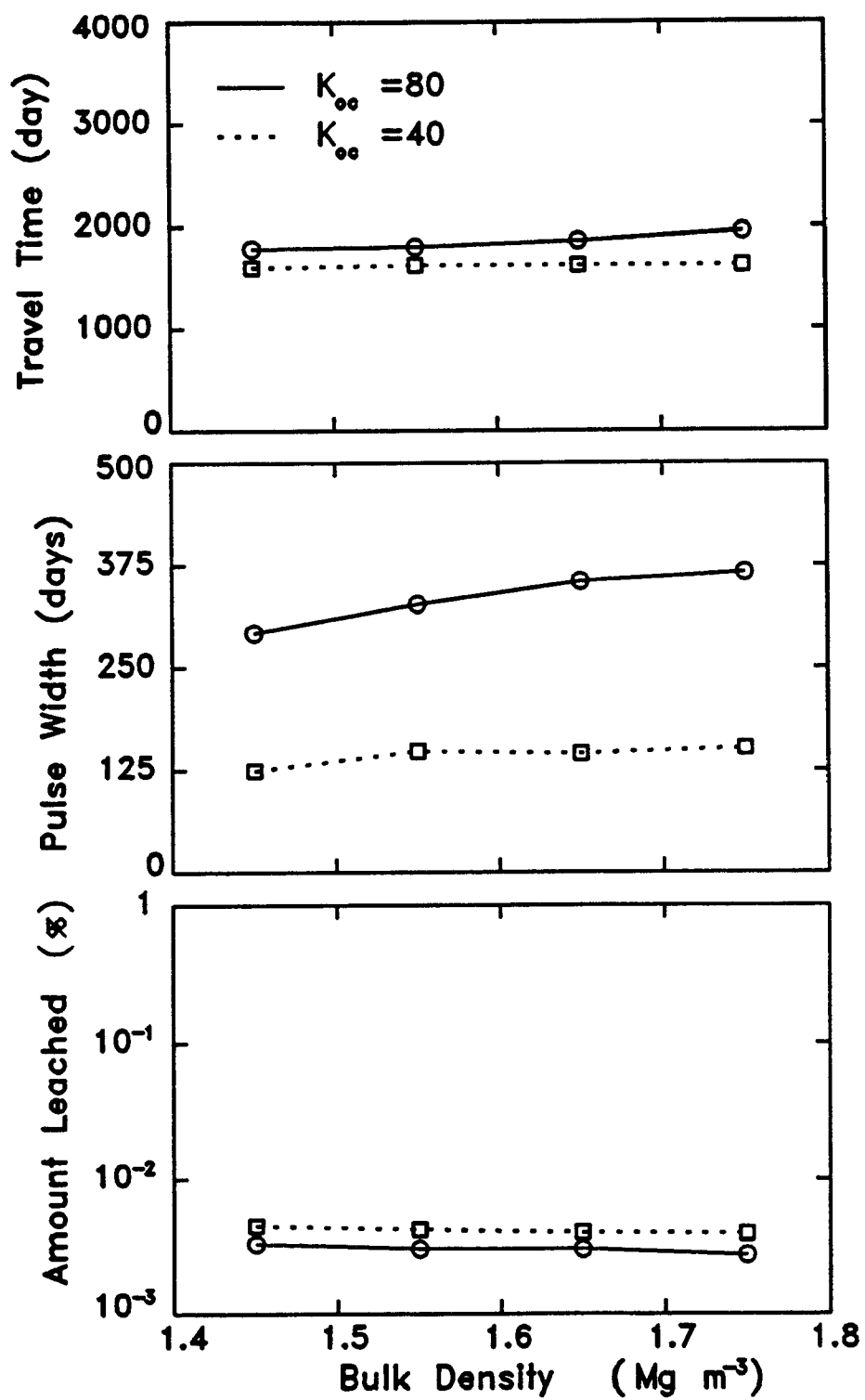
Figure 7.17. Median travel time, pulse width, and amount leached as functions of bulk density for two $K_{oc}$ values.
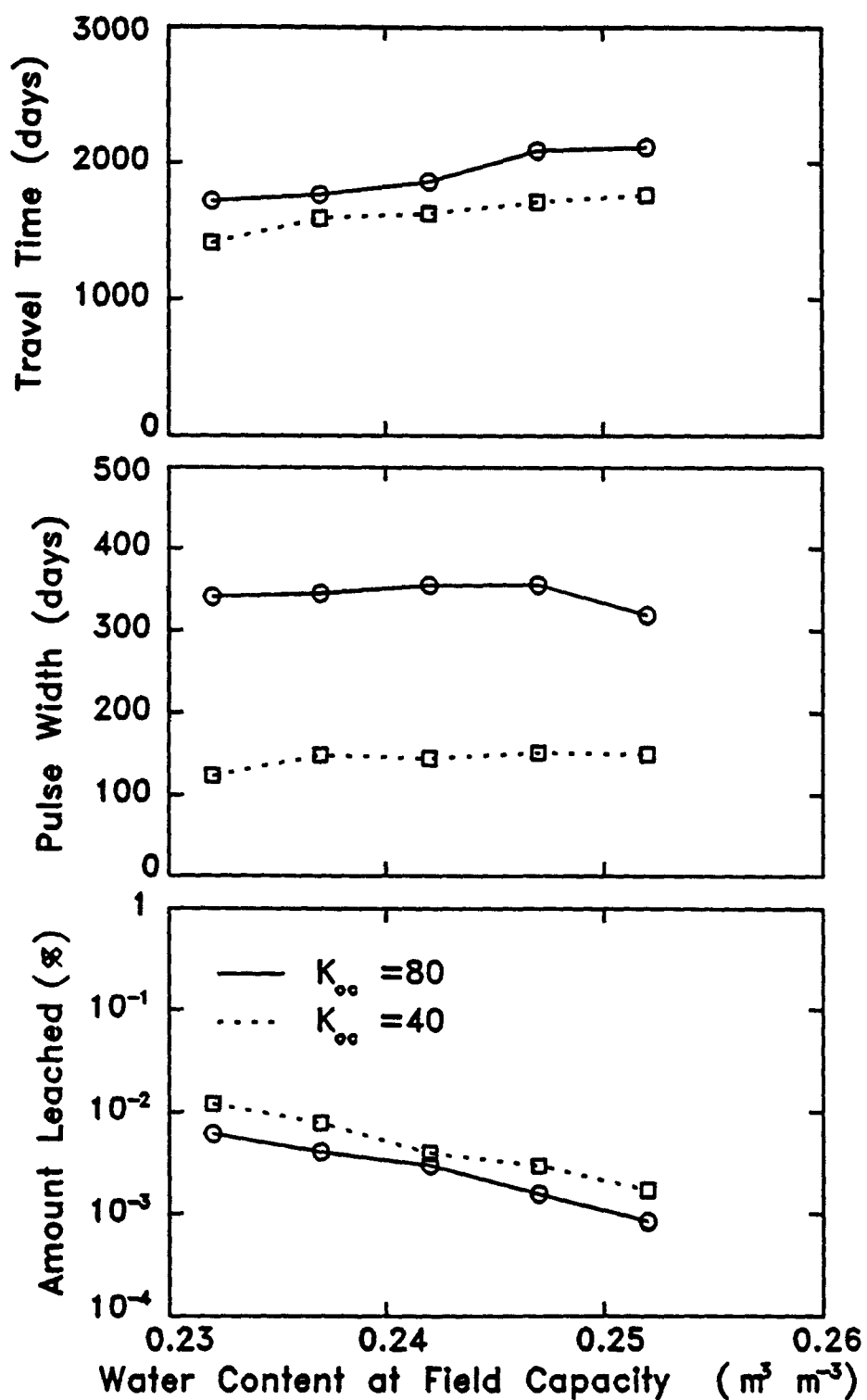
Figure 7.18. Median travel time, pulse width, and amount leached as functions of water content at field capacity for two $K_{oc}$ values.
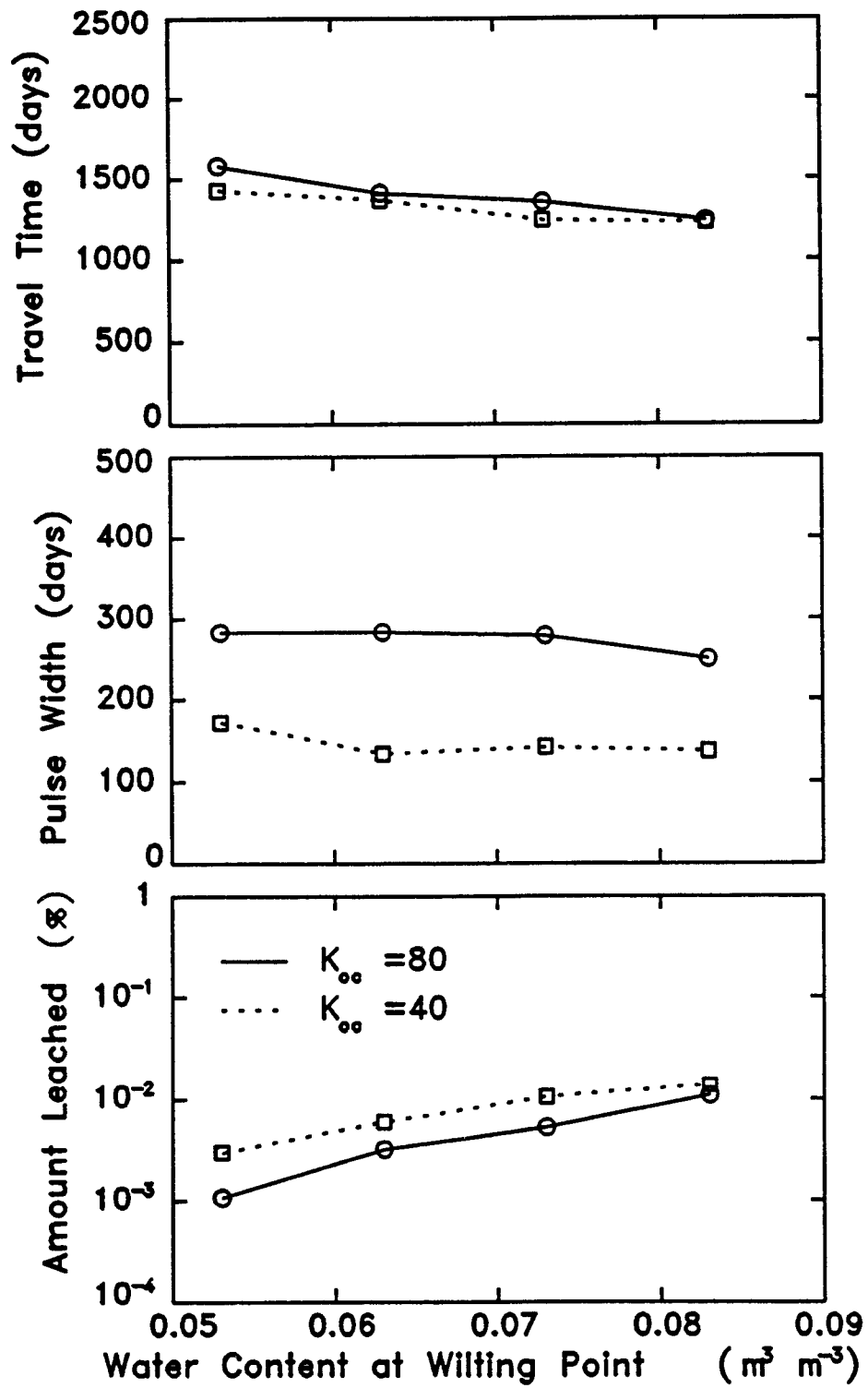
Figure 7.19. Median travel time, pulse width, and amount leached as functions of water content at permanent wilting point for two $K_{oc}$ values.
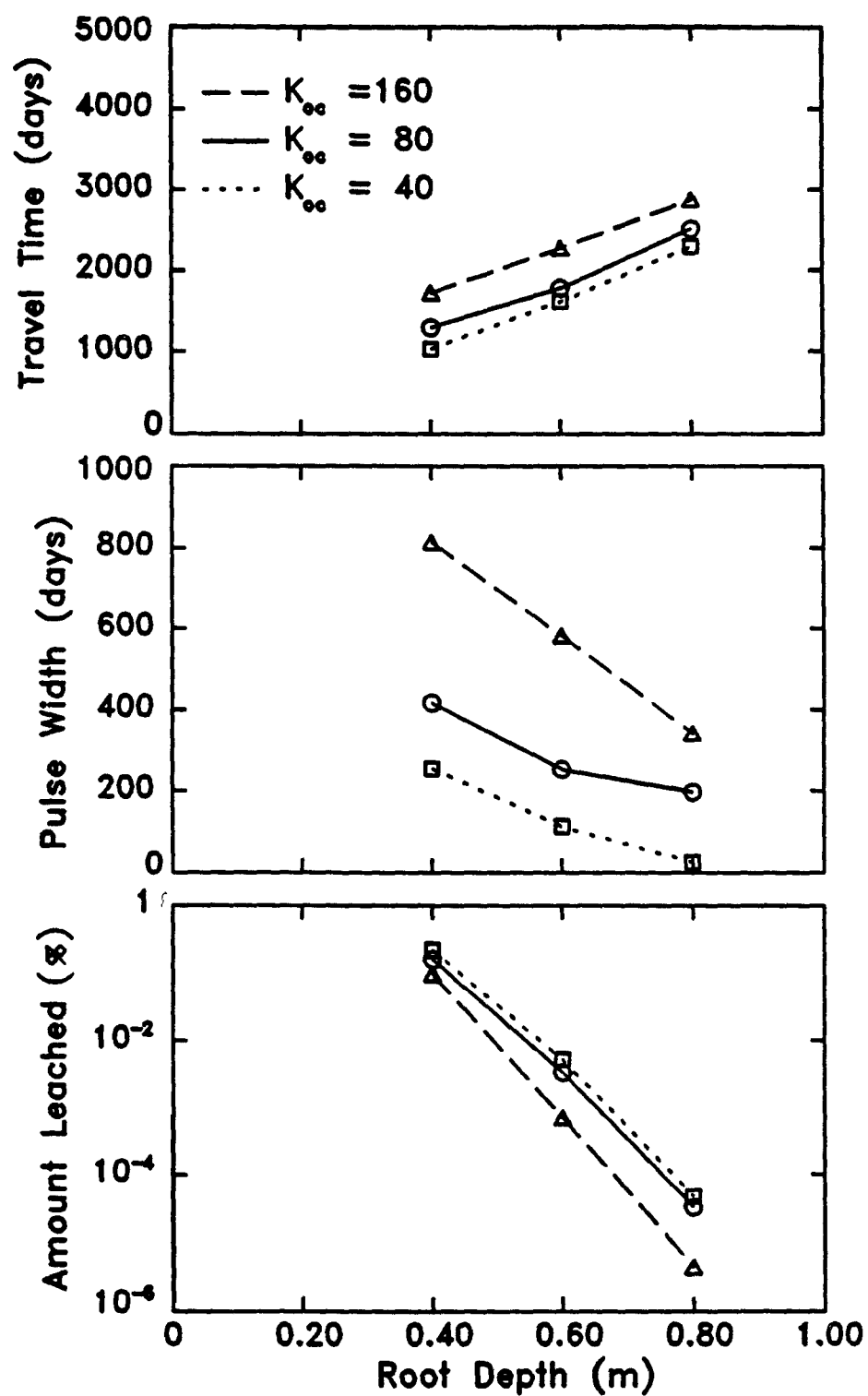
Figure 7.20. Median travel time, pulse width, and amount leached as functions of root depth for three $K_{oc}$ values.
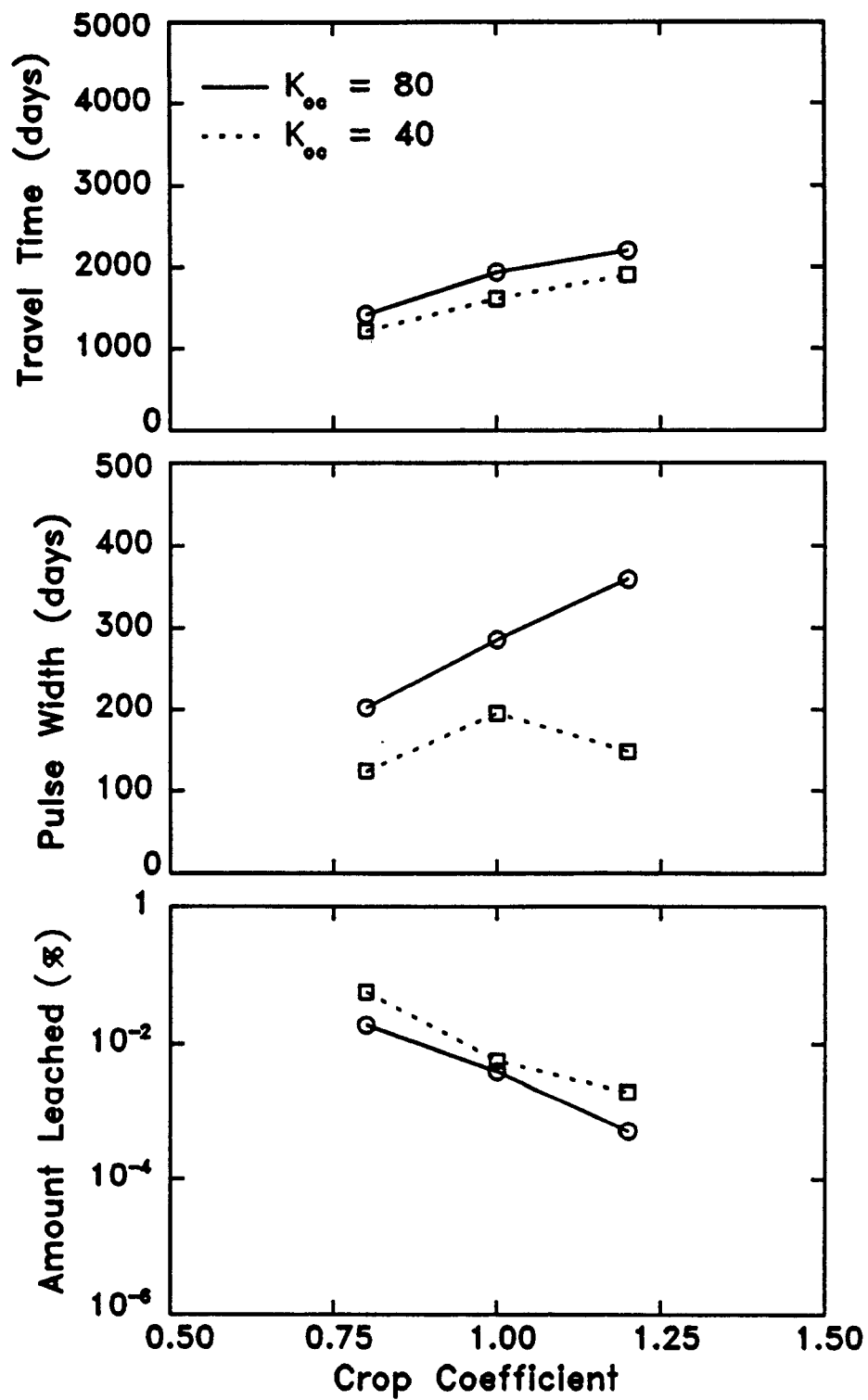
Figure 7.21. Median travel time, pulse width, and amount leached as functions of crop coefficient for two $K_{oc}$ values.
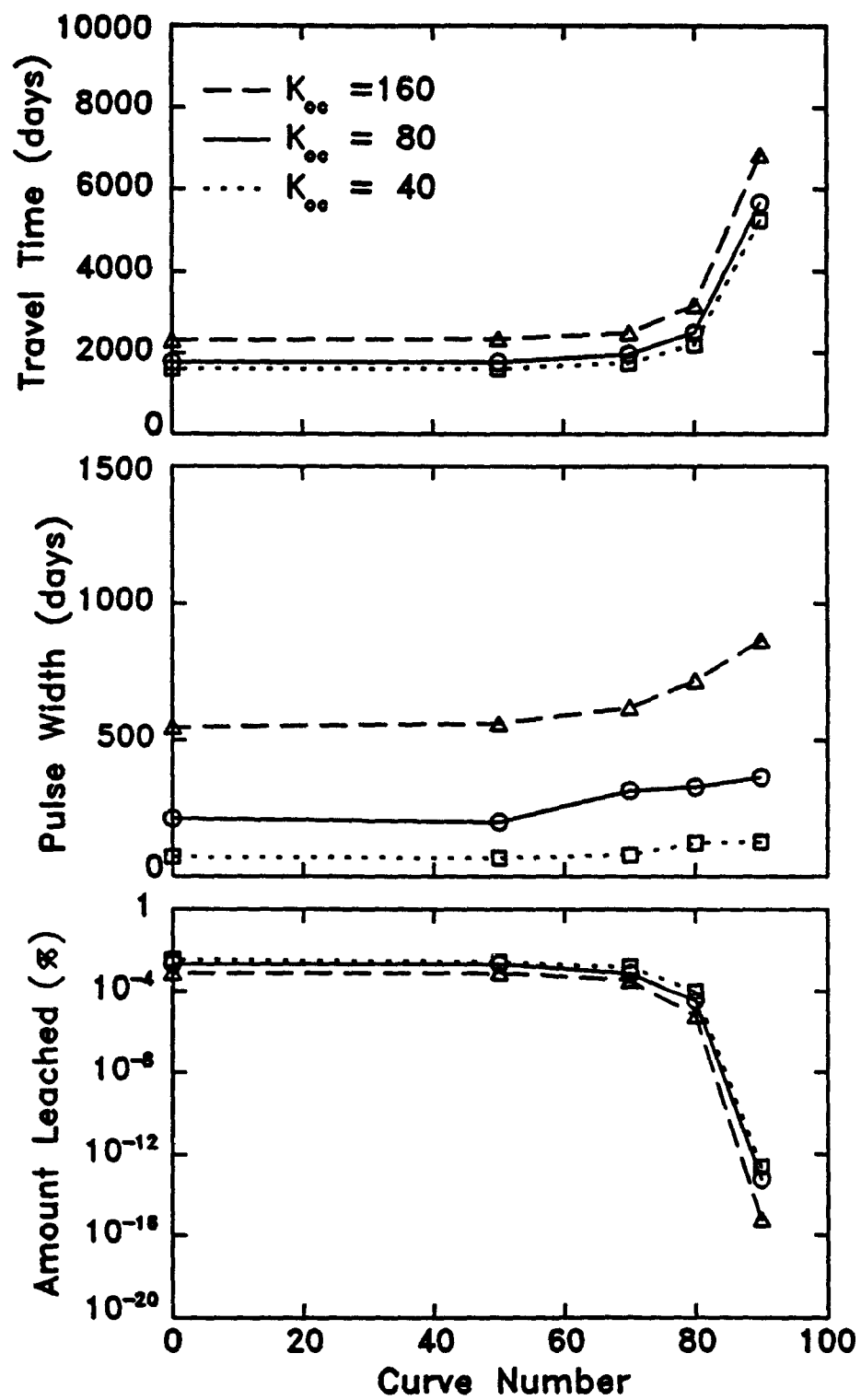
Figure 7.22. Median travel time, pulse width, and amount leached as functions of curve number for three $K_{oc}$ values.

124

# SECTION 8

## SENSITIVITY RESULTS FOR HYDRUS MODEL

### General Impact of Model Parameters

Figure 8.1 shows the predicted concentration of pollutant in water at a depth of 2 m for simulations with daily water fluxes. Results are shown for simulations beginning January 1, 1983, 1985, and 1987. Rainfall distributions following those dates are shown in Figure 7.3. As was observed in the case of CMLS, travel time, pulse width, and amount leached vary greatly with the different starting dates. The concentration curves are not smooth bell-shaped curves but have greatly different shapes due to different rainfall distributions. Pulse widths for these simulations are approximately 400 days. The predicted amounts of pollutant leached below the 2-m depth were 27%, 3%, and 10% for 1983, 1985, and 1987, respectively. The results for 1983 are in good agreement with those from CMLS (Figure 7.2 and Table 7.1). For 1985 and 1987, CMLS predicts more rapid movement to the 2-m depth and greater amounts leached.

The results presented in Figure 8.1 again indicate the large impact of weather variability upon predicted pollutant leaching. As a result, model sensitivity is dependent upon weather used. Ideally, we could run HYDRUS many times for different weather and incorporate probabilities into the analysis as was done with CMLS. That approach was not feasible in the time frame and funding of this project because of the computational time required. It would be worthwhile for future work. Instead, we chose to calculate model sensitivity using uniform soil properties and uniform water fluxes. This is a serious compromise since these assumptions simplify the flow and transport problem to the degree that many of the sophisticated features of HYDRUS do not enter into the solution. Table 8.1 contains the basic input parameters used in the sensitivity analysis which follows.

Figures 8.2 shows the concentration of pollutant at the 2-m depth as a function of time for different values of half-life. The concentration decreases substantially as the half-life decreases. The peak of the pulse in Figure 8.2 appears to move slightly to the left as half-life decreases. By comparing the curve in Figure 8.2 for a half-life of 104 days to those in Figure 8.1 we see that simulations using uniform soil and uniform flux results in a larger travel time and a lower concentration than predicted with daily fluxes and non-uniform soil properties.

Figure 8.3 shows the impact of different partition coefficients of chemicals in soil upon the concentration of pollutant at the 2-m depth as a function of time. This result is very similar to that obtained for organic carbon partition coefficient and organic carbon content in the previous models. This is reasonable since the partition coefficient is often approximated as the product of the organic carbon content and the organic carbon partition coefficient.

Figures 8.4 to 8.14 illustrate the dependence of concentration upon other model parameters. Note that the concentration scale shown on Figures 8.2, 8.3, 8.12, and 8.13 extends to 0.50 g m$^{-3}$ while its limit is 0.25 g m$^{-3}$ for the remaining figures. Figures 8.4 shows that the time at which the maximum concentration reaches a depth of 2 m decreases as the saturated hydraulic conductivity increases. The maximum concentration increases with increasing saturated hydraulic conductivity. The travel time increases and maximum concentration decreases as the bulk density of the soil increases as shown in Figure 8.5. The residual water content (see footnote in Table 4.2) has only a slight impact upon the concentration function (Figure 8.6). Figure 8.7 shows that the travel time increases somewhat as the saturated water content increases from 0.32 to 0.44 m$^3$ m$^{-3}$. The maximum concentration decreases by a factor of 2 over this range of water contents. Pollutant concentration changes substantially as the van Genuchten hydraulic parameter $\beta$ changes (Figure 8.8). A change from 0.02 to 0.04 cm$^{-1}$ in the van Genuchten parameter $\alpha$ produces a large change in travel time but an additional increase to 0.04 cm$^{-1}$ has little effect on the prediction (Figure 8.9). The impact of

Table 8.1. Values of input parameters used for sensitivity analysis in HYDRUS models.

Soil Properties (assumed uniform for each soil layer)

| | |
|---|---|
| Depth of soil layers (m) | 2.0 |
| Saturated water content ($m^3$ $m^{-3}$) | 0.38 |
| Saturated hydraulic conductivity (m $day^{-1}$) | 0.19 |
| Bulk density (Mg $m^{-3}$) | 1.637 |
| van Genuchten's $\alpha$ | 0.04 |
| van Genuchten's $\beta$ | 1.637 |
| Residual water content ($m^3$ $m^{-3}$) | 0.04 |

Site Characteristics

| | |
|---|---|
| Uniform rainfall intensity (mm $day^{-1}$) | 5.12 |
| Uniform potential evapotranspiration (mm $day^{-1}$) | 4.09 |

Pollutant Properties (assumed uniform for each soil layer)

| | |
|---|---|
| Molecular diffusion coefficient ($m^2$ $day^{-1}$) | 0.00004 |
| Dispersivity (m) | 0.027 |
| Decay coefficient for dissolved phase ($day^{-1}$) | 0.0067 |
| Decay coefficient for adsorbed phase ($day^{-1}$) | 0.0067 |
| Leading Freundlich isotherm coefficient ($cm^3$ $g^{-1}$) | 0.1136 |
| Freundlich isotherm exponent | 1.0 |

Root Water Uptake Parameters:

| | |
|---|---|
| Power constant in stress-response function | 3.0 |
| Pressure head at which transpiration is reduced by 50% (cm) | -200 |
| Root density/effectiveness value | 0.333 |

different values of dispersivity upon the concentration is shown in Figure 8.10. The width of the pulse increases and the maximum concentration decreases as the dispersivity increases. Recall that dispersion is one process which is ignored in RITZ, VIP and CMLS. No effect of diffusion coefficient was observed for the parameters used in this simulation (Figure 8.11).

The dependence of pollutant concentration upon water uptake parameters of the roots is shown in Figures 8.12 and 8.13. The travel time and concentration change appreciably as these parameters change. That is expected since these parameters determine the amount of infiltrating water lost to the atmosphere and therefore they have a direct impact upon the leaching of the pollutant below the root depth. Figure 8.14 shows that the travel time decreases and amount leached increases as the root depth increases. This behavior is unexpected and it does not persist to a depth of zero since the travel time is only 135 days for a root depth of zero.

Sensitivity Coefficients

Figures 8.15 to 8.26 show the travel time as a function of different input parameters. The figures also show the sensitivity coefficients calculated using equation 15 and relative sensitivities from equation 18. The relative sensitivities are summarized in Table 8.2. Figures 8.27 - 8.50 show the curves for pulse width and amount leached. Recall that positive relative sensitivities imply that the relative change in output is positive when the relative change in input parameter is positive. These results indicate the travel time is quite sensitive to the vanGenuchten $\beta$, the saturated water content, the partition coefficient, the root uptake potential, and the bulk density. Relative sensitivities for pulse width are quite high for saturated water

Table 8.2. Summary of relative sensitivities for travel time, pulse width, and amount leached for the HYDRUS model.

| Input Parameter | Travel Time | Pulse Width | Amount Leached |
|---|---|---|---|
| Partition coefficient | 0.12 to 0.42 | 0.3 to -0.25 | -0.4 to -3.5 |
| Saturated conductivity | -0.06 to -0.10 | -0.05 to -0.08 | 0.25 to -0.41 |
| Bulk density | 0.32 to 0.36 | 0.32 to 0.36 | -1.3 to -1.6 |
| Residual water content | 0.01 to 0.04 | 0.03 to 0.045 | -0.07 to -0.17 |
| Saturated water content | 0.45 to 0.55 | 0.42 to 0.45 | -2.0 to -2.6 |
| vanGenuchten $\beta$ | -0.52 to -0.25 | -0.45 to -0.18 | 2.2 to 1.0 |
| vanGenuchten $\alpha$ | 0.19 to 0 | 0.18 to -0.01 | -0.8 to 0.1 |
| Dispersivity | -0.05 to -0.12 | 0.25 to 0.24 | 0.06 to 0.16 |
| Diffusion coefficient | -0.001 to -0.015 | 0.004 to 0.03 | 0.003 to 0.035 |
| Root uptake pot. $h_{50}$ | 0.02 to -0.42 | 0.01 to 0.43 | -0.01 to -1.1 |
| Root uptake exponent | 0.25 to -0.15 | 0.26 to 0.15 | -1.0 to -0.6 |
| Root depth | -0.04 to -0.2 | -0.04 to -0.25 | 0.3 to 0.8 |

content, bulk density, dispersivity, and the vanGenuchten $\beta$ coefficient. Relative sensitivities to the partition coefficient vary continuously for relatively large positive values to large negative values. Relative sensitivities for amount leached are generally larger in magnitude than those for travel time and pulse width. Sensitivities for amount leached are opposite in sign to those for travel time. All three output parameters are quite insensitive to residual water content and diffusion coefficient.
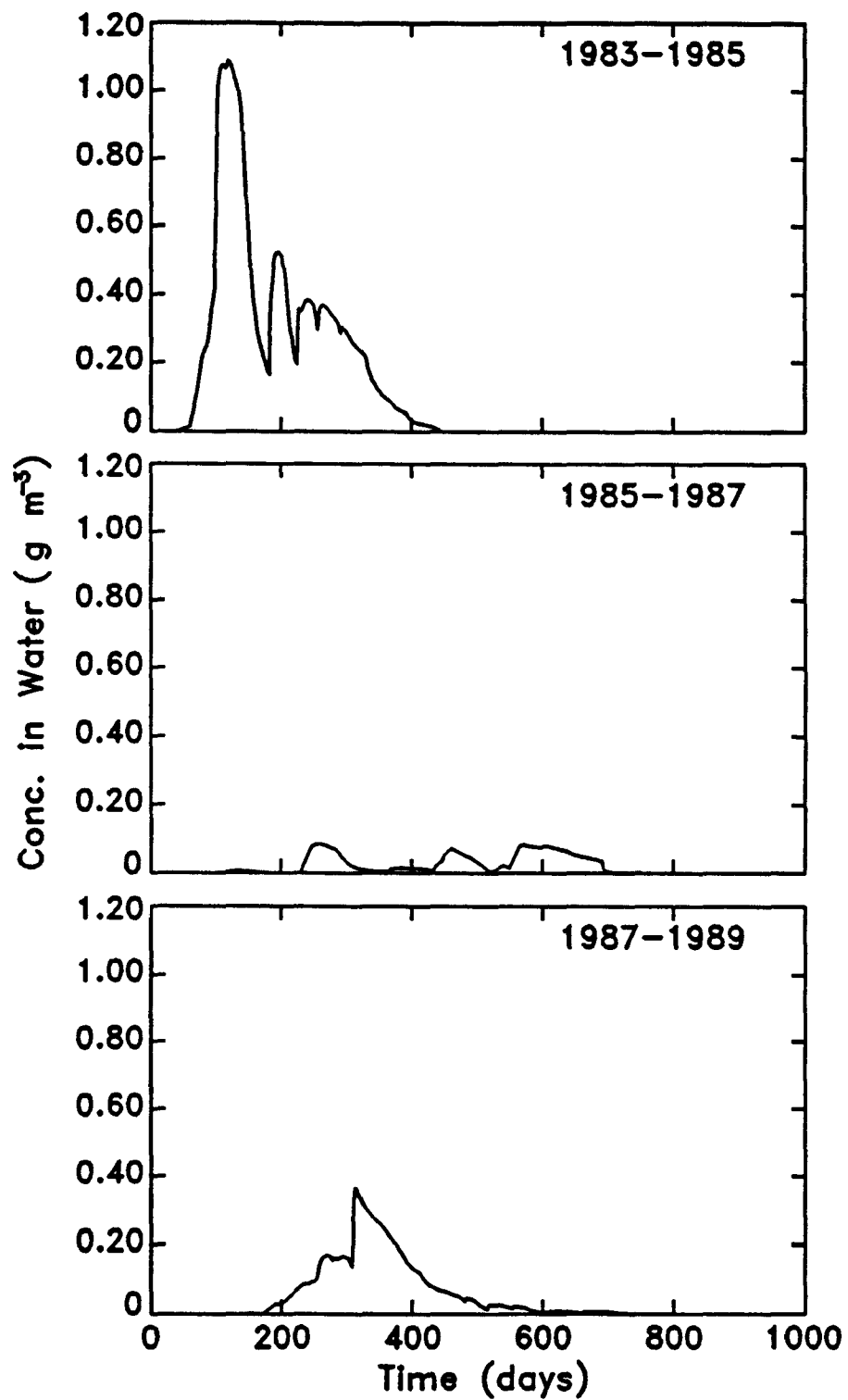
Figure 8.1. Concentration of pollutant in water at the 2-m depth as a function of time using HYDRUS with daily rainfall and daily evaporation. Different graphs show predictions for different starting dates.
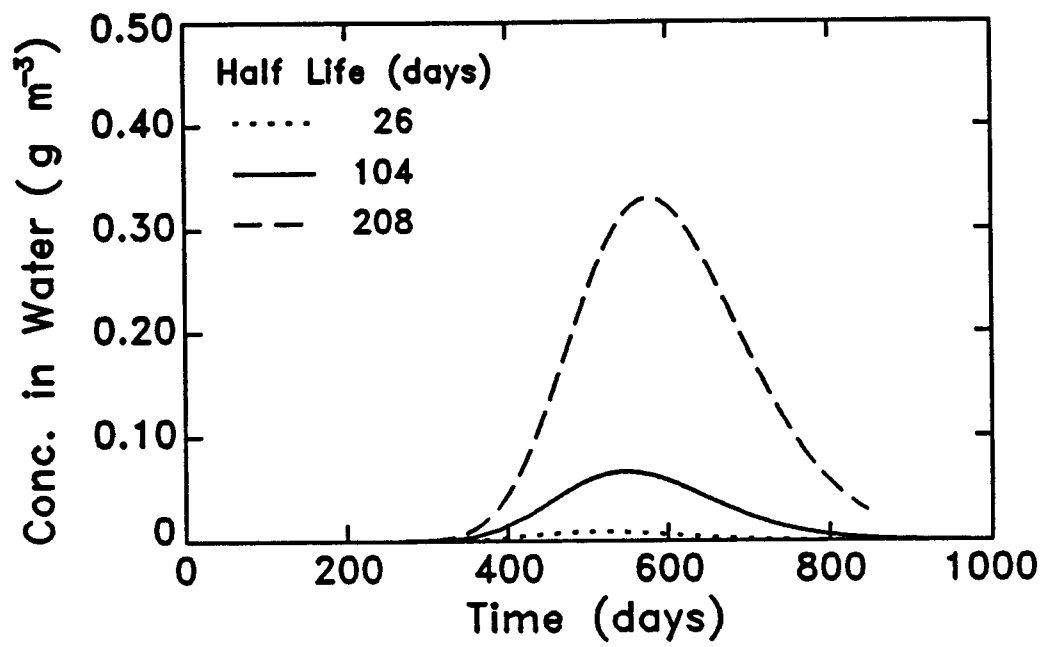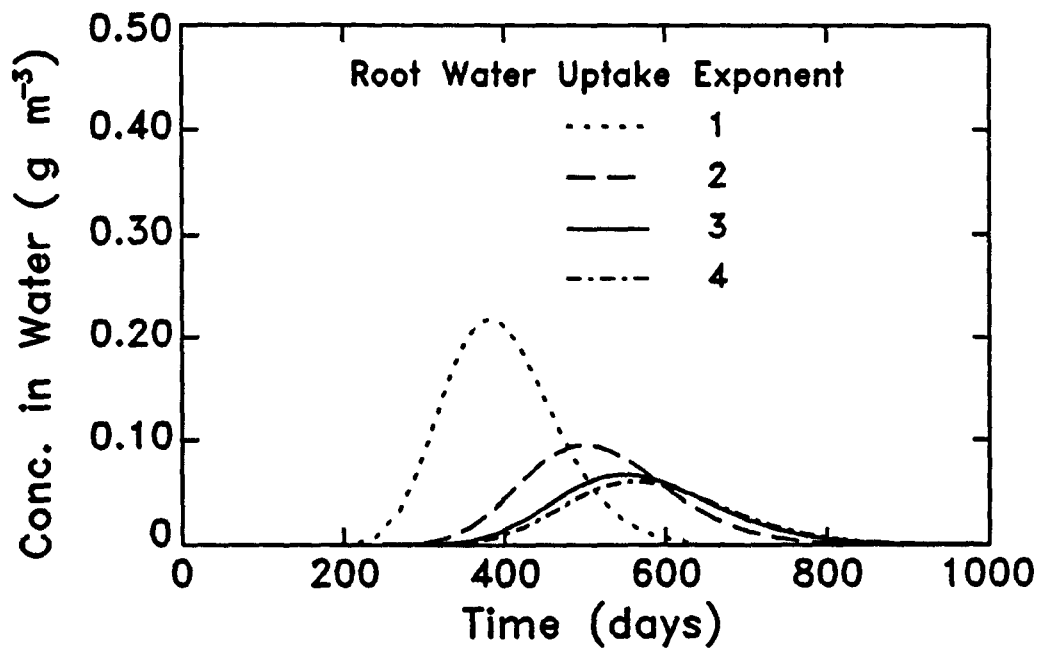
Figure 8.2. Concentration of pollutant in water at a depth of 2 meters for different values of half-life.
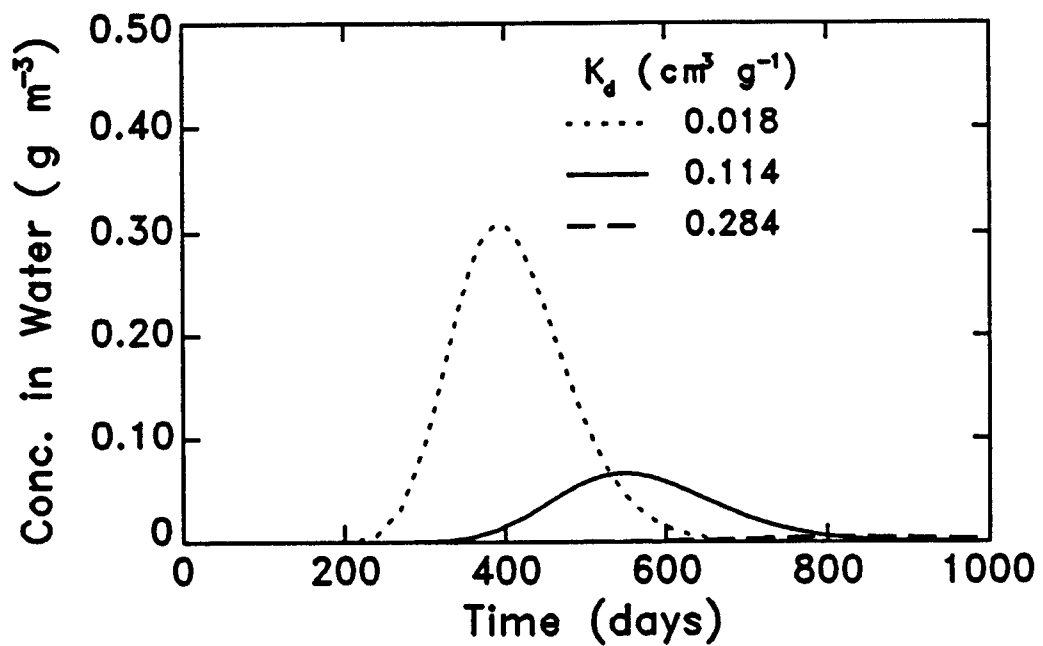


Figure 8.3. Concentration of pollutant in water at a depth of 2 meters for different values of partition coefficient.
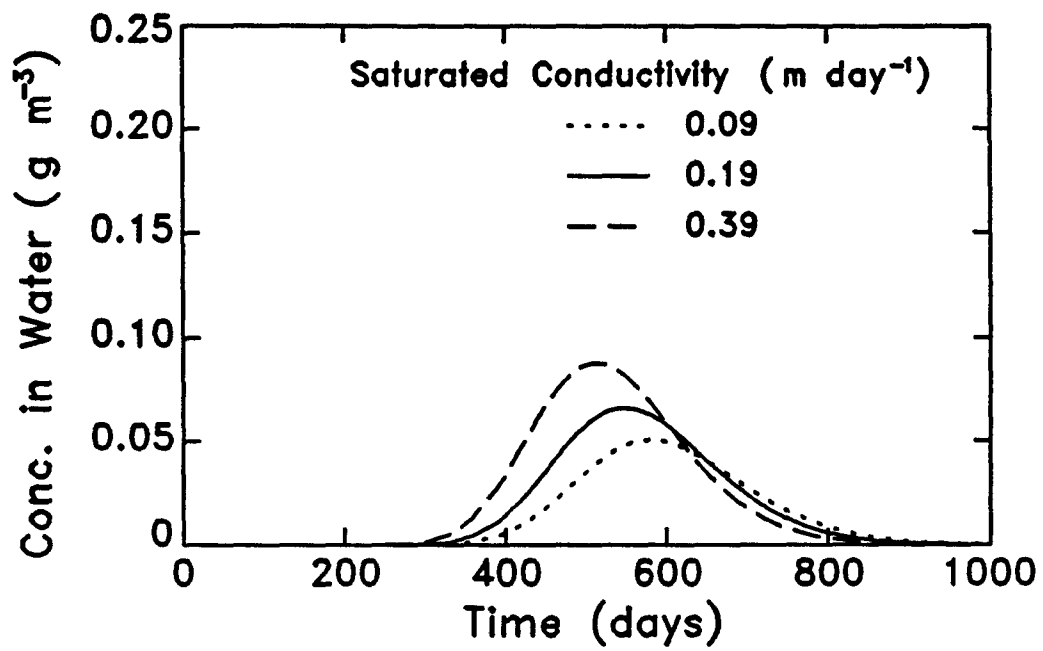
Figure 8.4. Concentration of pollutant in water at a depth of 2 meters for different values of saturated hydraulic conductivity.
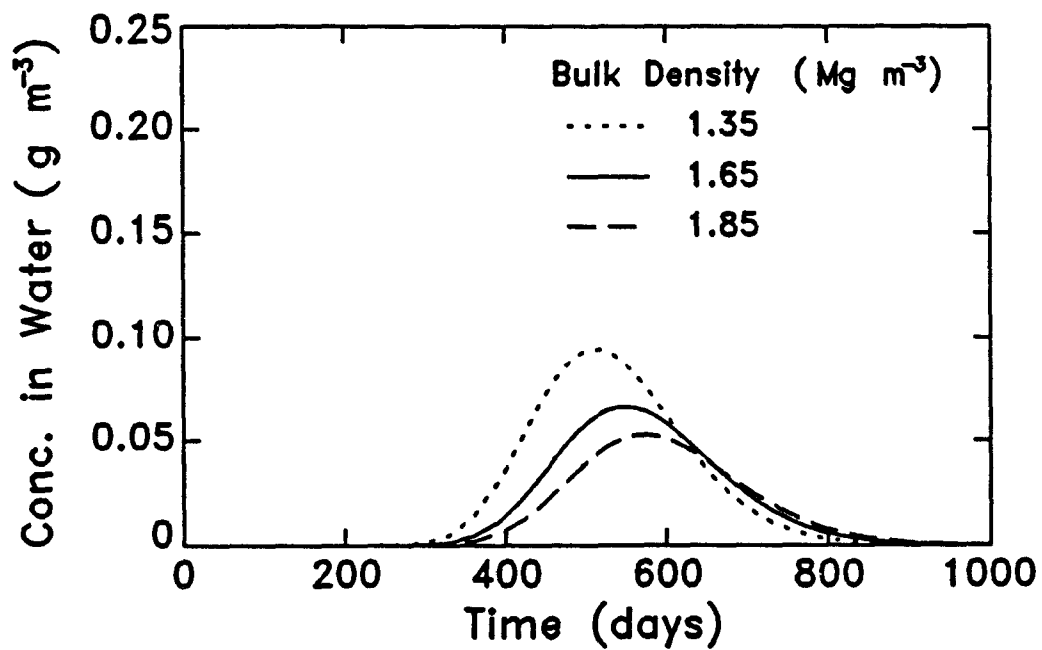


Figure 8.5. Concentration of pollutant in water at a depth of 2 meters for different values of bulk density.
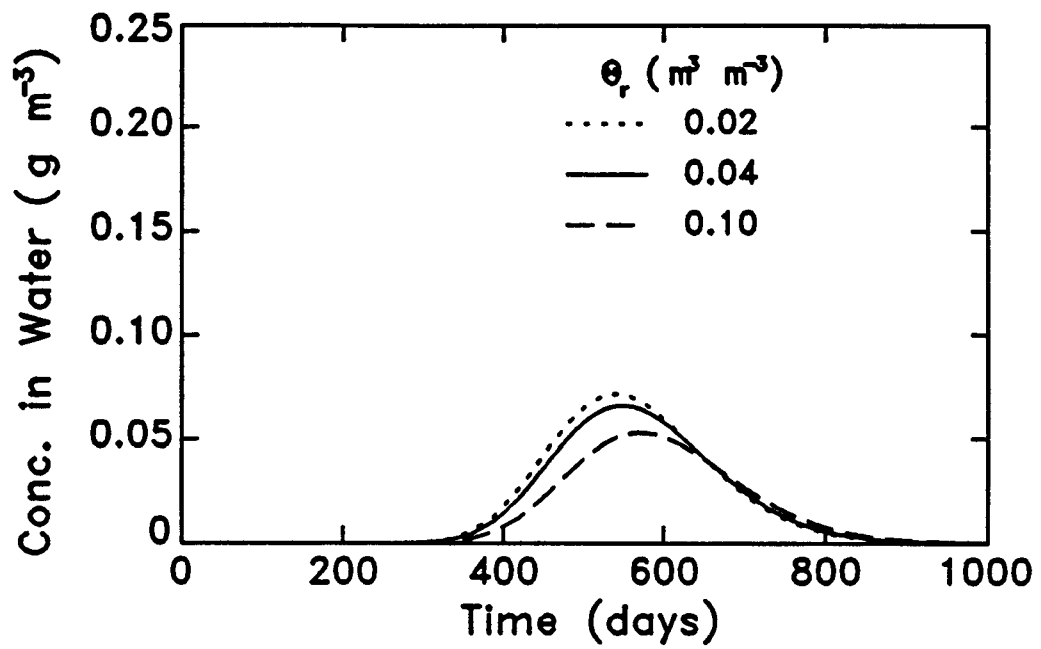
Figure 8.6. Concentration of pollutant in water at a depth of 2 meters for different values of residual water content.
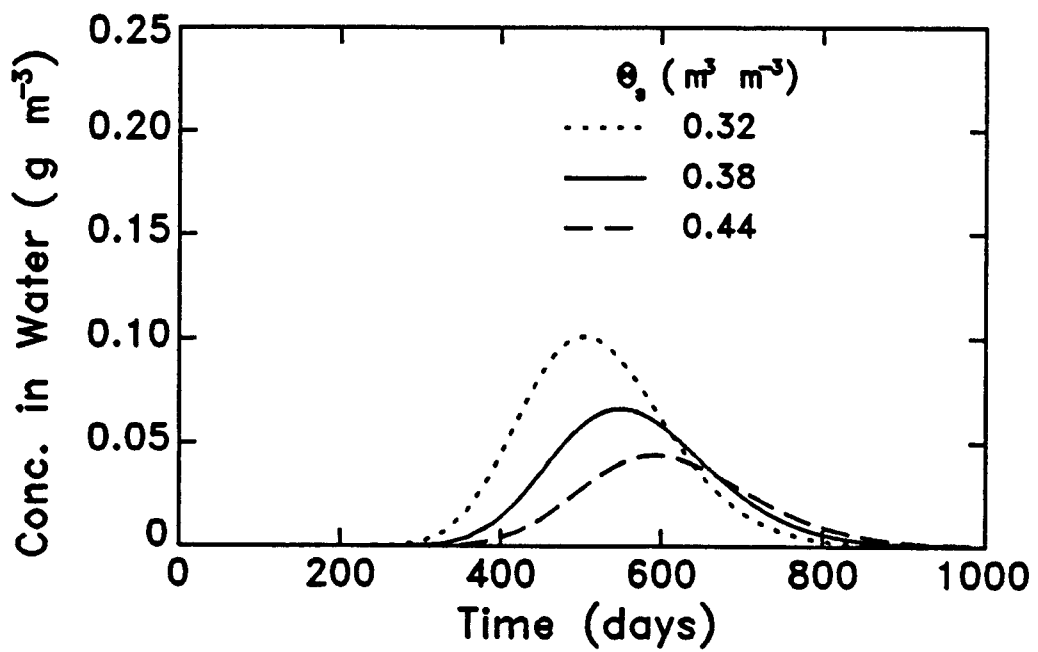


Figure 8.7. Concentration of pollutant in water at a depth of 2 meters for different values of saturated water content.
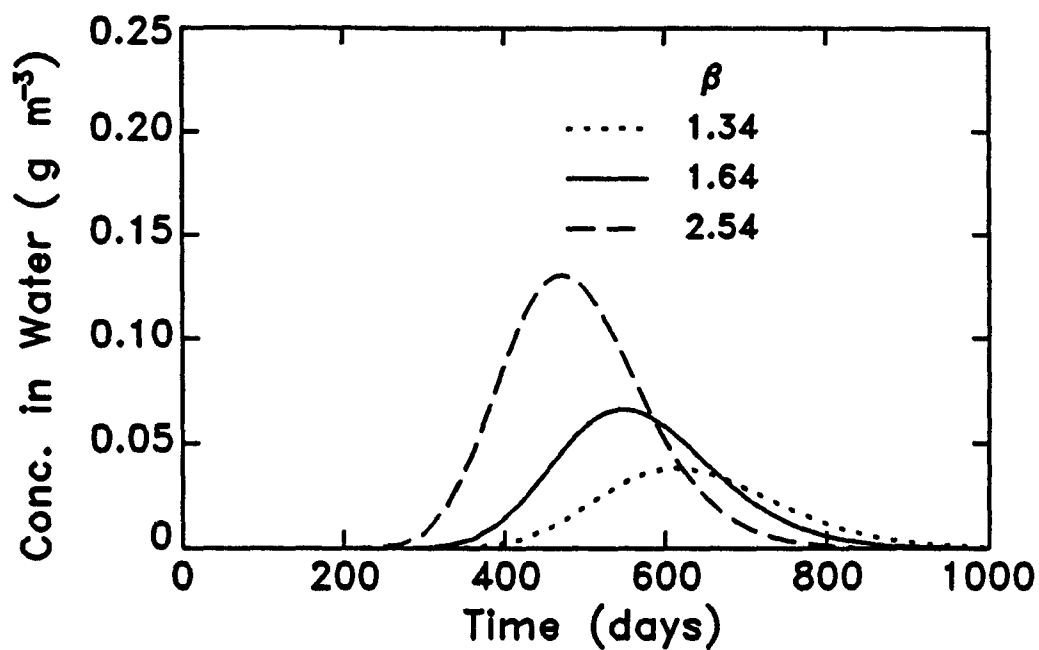
Figure 8.8. Concentration of pollutant in water at a depth of 2 meters for different values of van Genuchten β parameter.
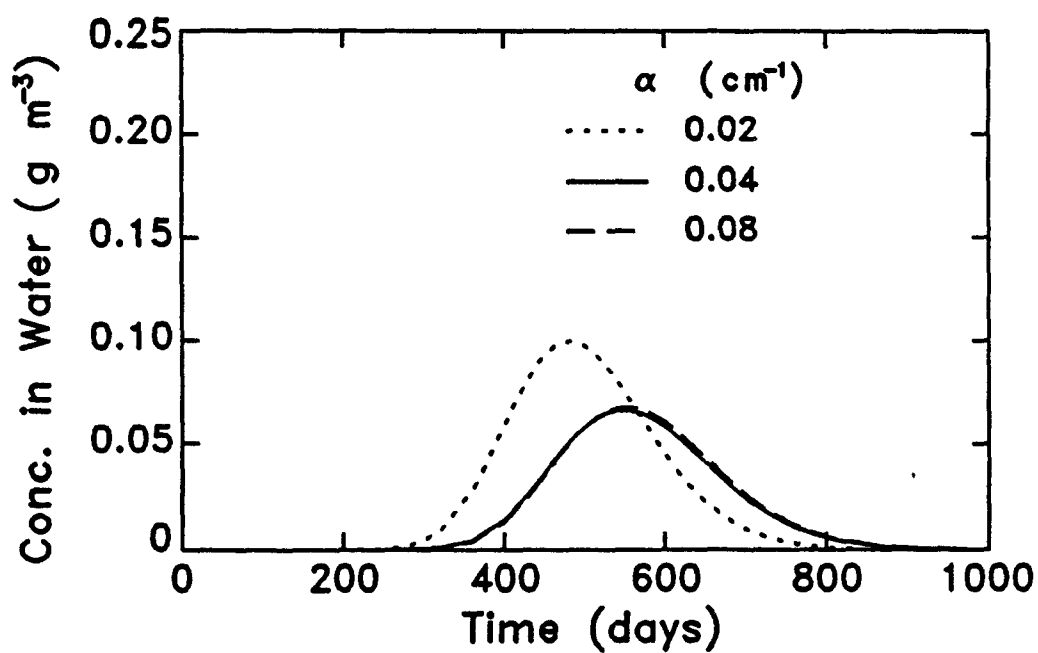


Figure 8.10. Concentration of pollutant in water at a depth of 2 meters for different values of van Genuchten α parameter.
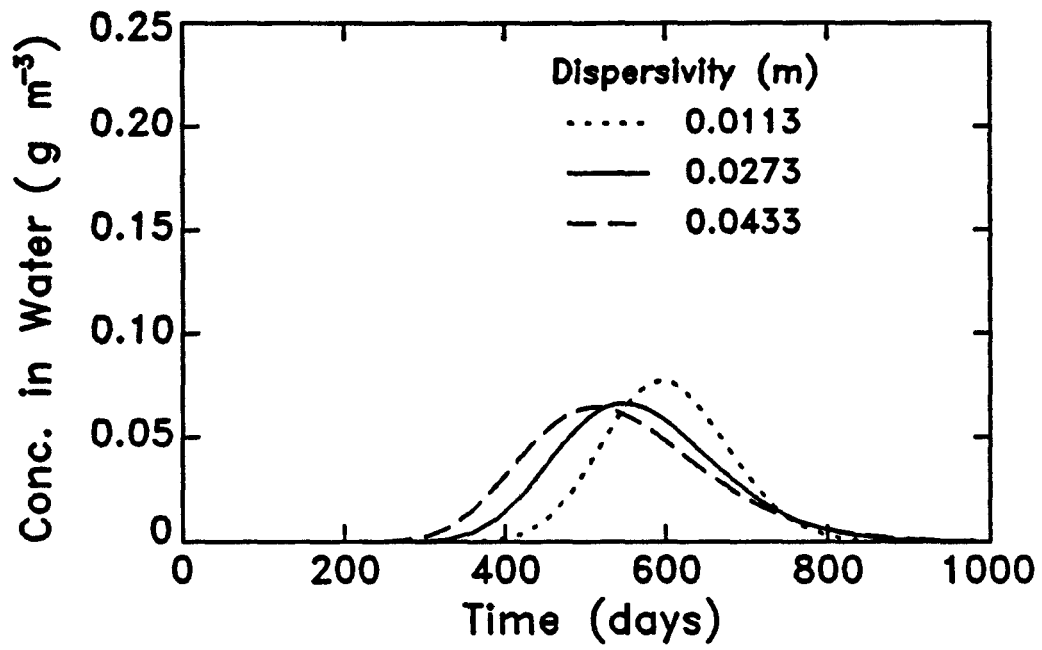
Figure 8.10. Concentration of pollutant in water at a depth of 2 meters for different values of dispersivity.
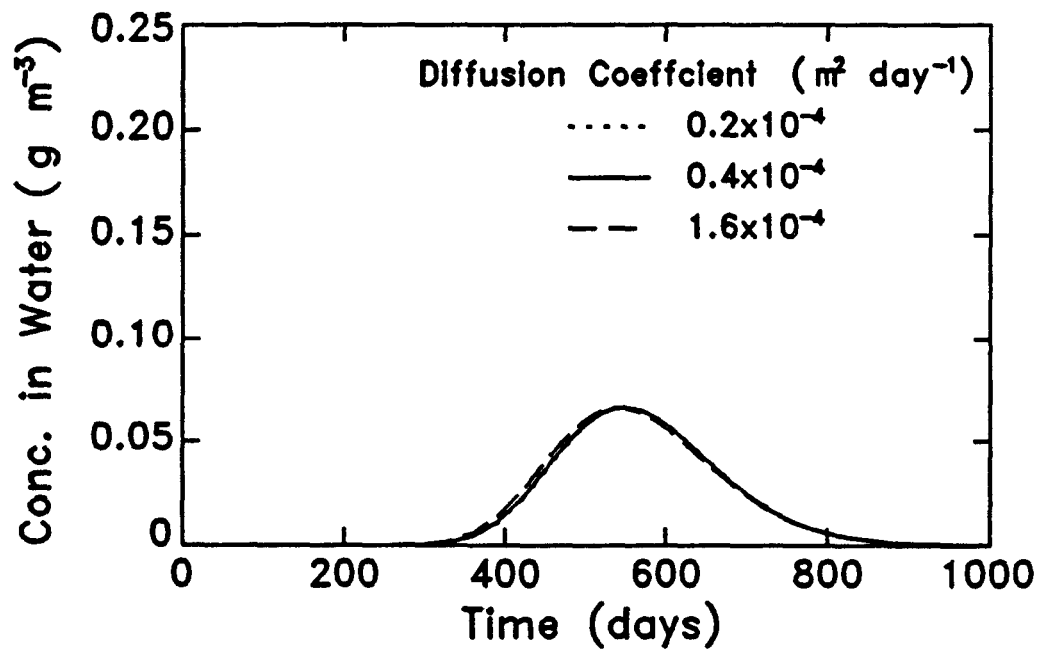


Figure 8.11. Concentration of pollutant in water at a depth of 2 meters for different values of diffusion coefficient.
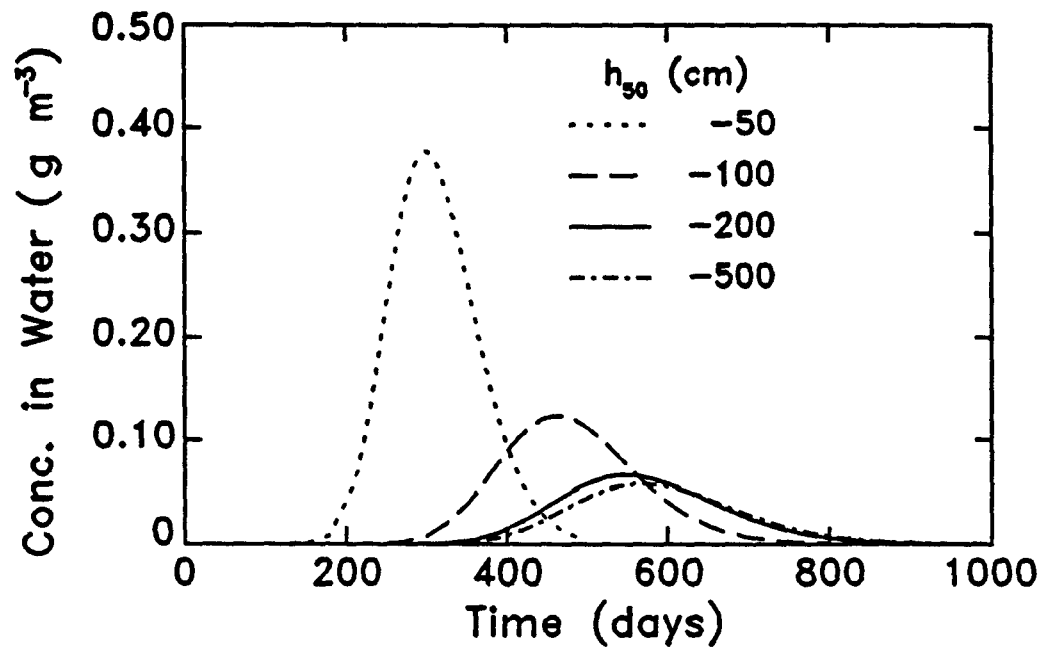
Figure 8.12. Concentration of pollutant in water at a depth of 2 meters for different values of root uptake potential $h_{50}$.



Figure 8.13. Concentration of pollutant in water at a depth of 2 meters for different values of root uptake exponents.
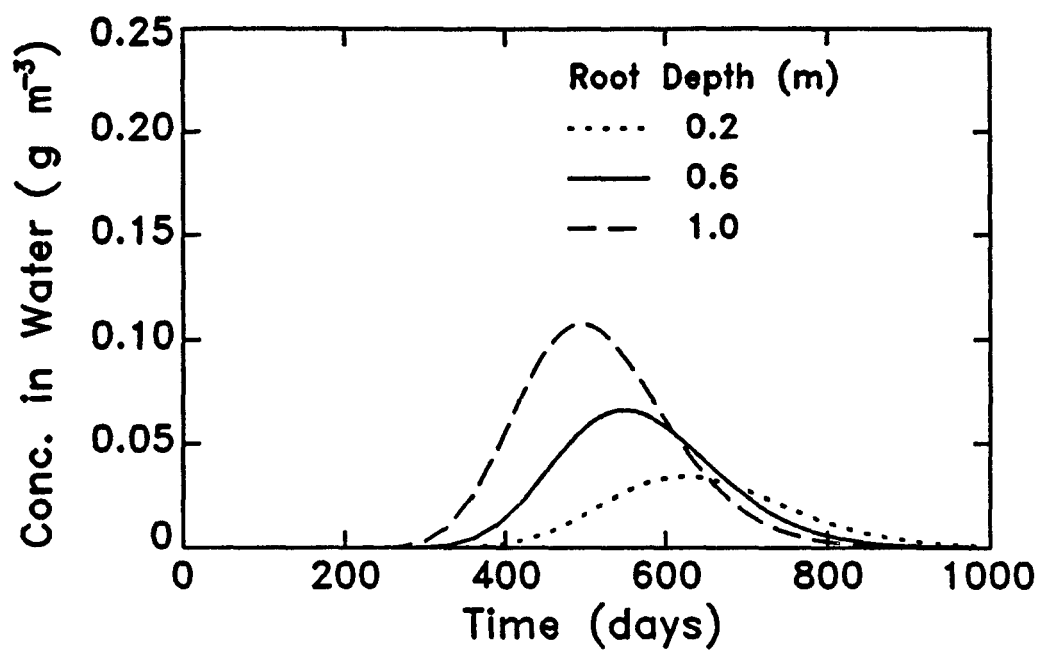
Figure 8.14. Concentration of pollutant in water at a depth of 2 meters for different values to root depth.

135
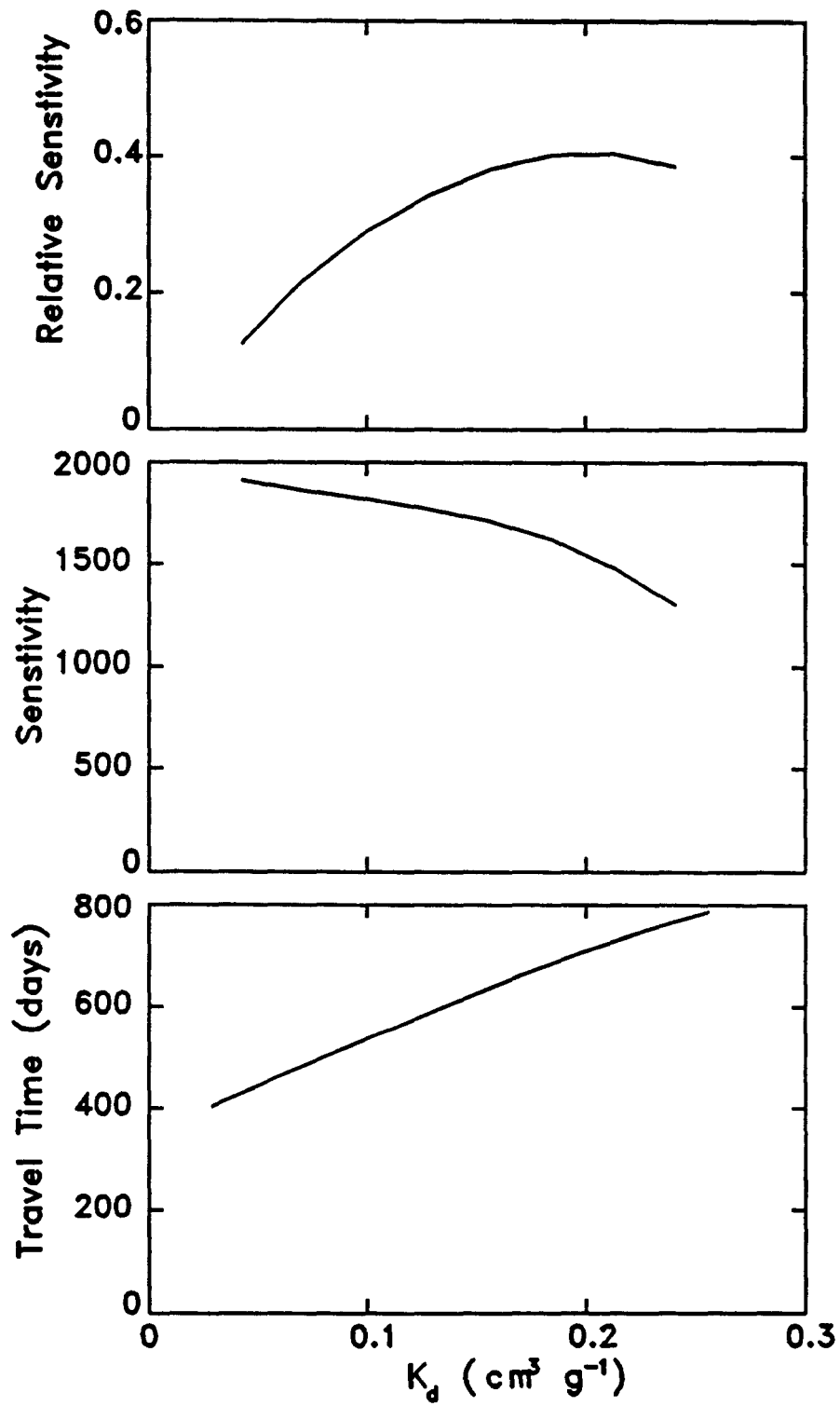
Figure 8.15. Sensitivity of travel time to partition coefficient.
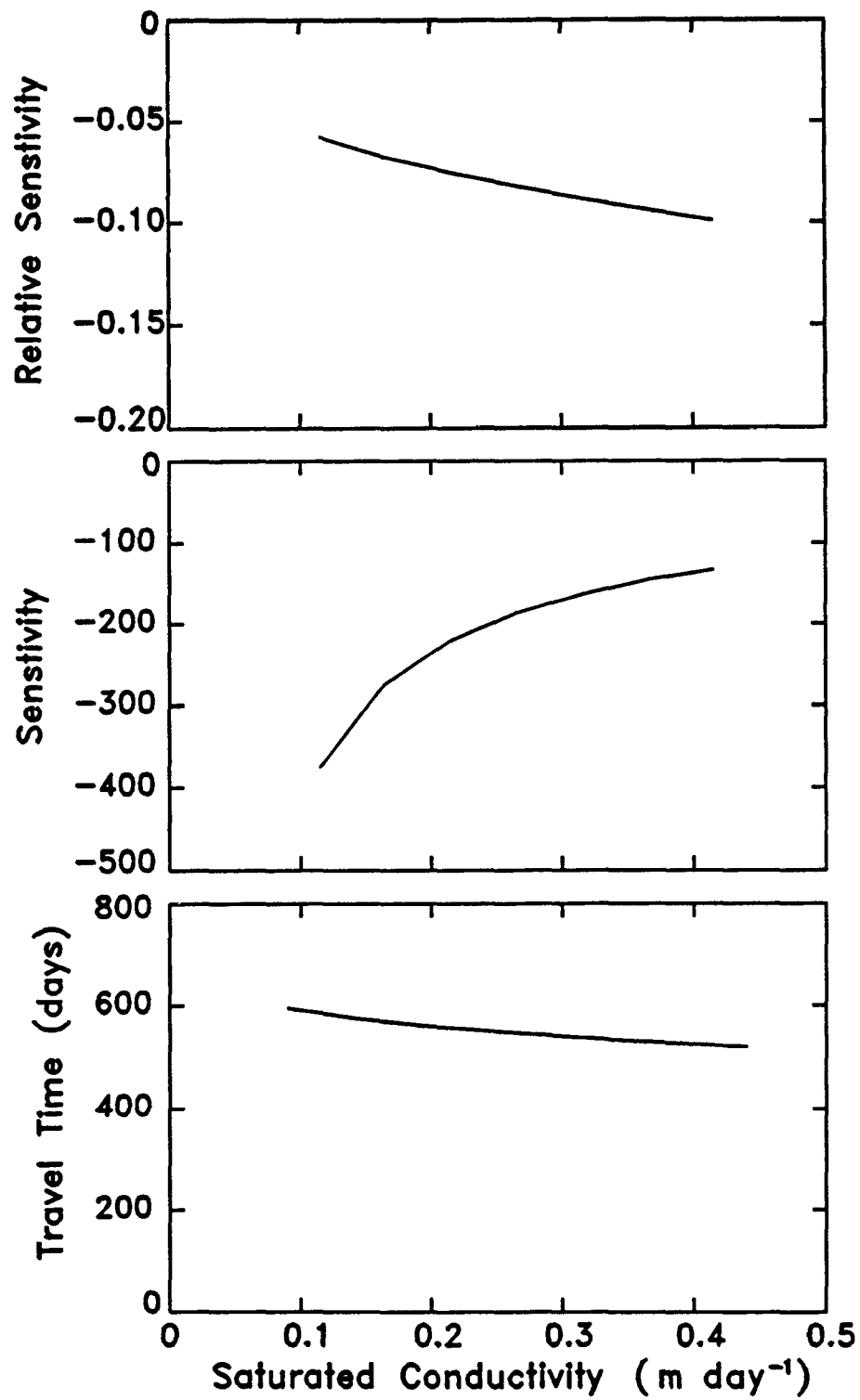
Figure 8.16. Sensitivity of travel time to saturated hydraulic conductivity.
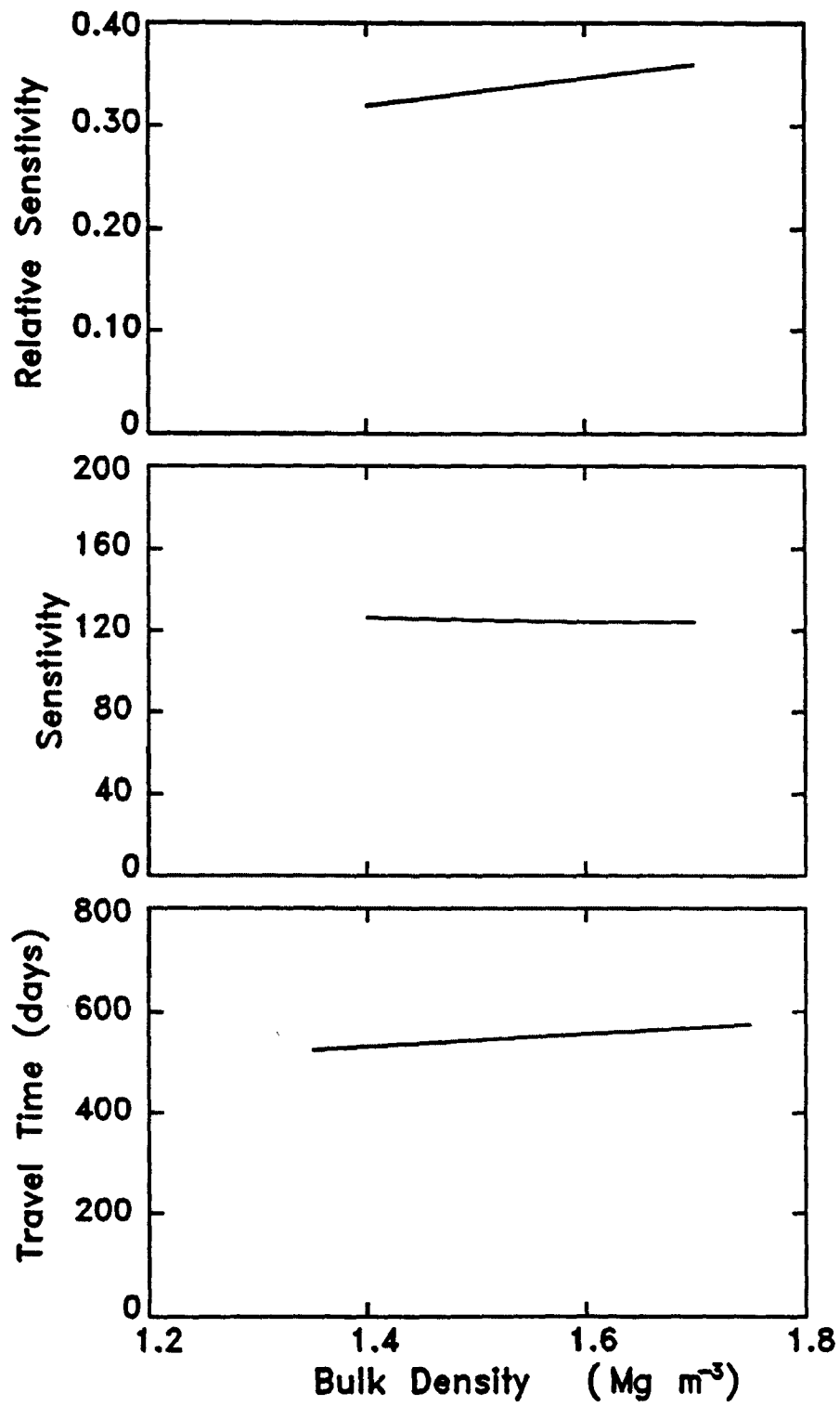
Figure 8.17. Sensitivity of travel time to bulk density.
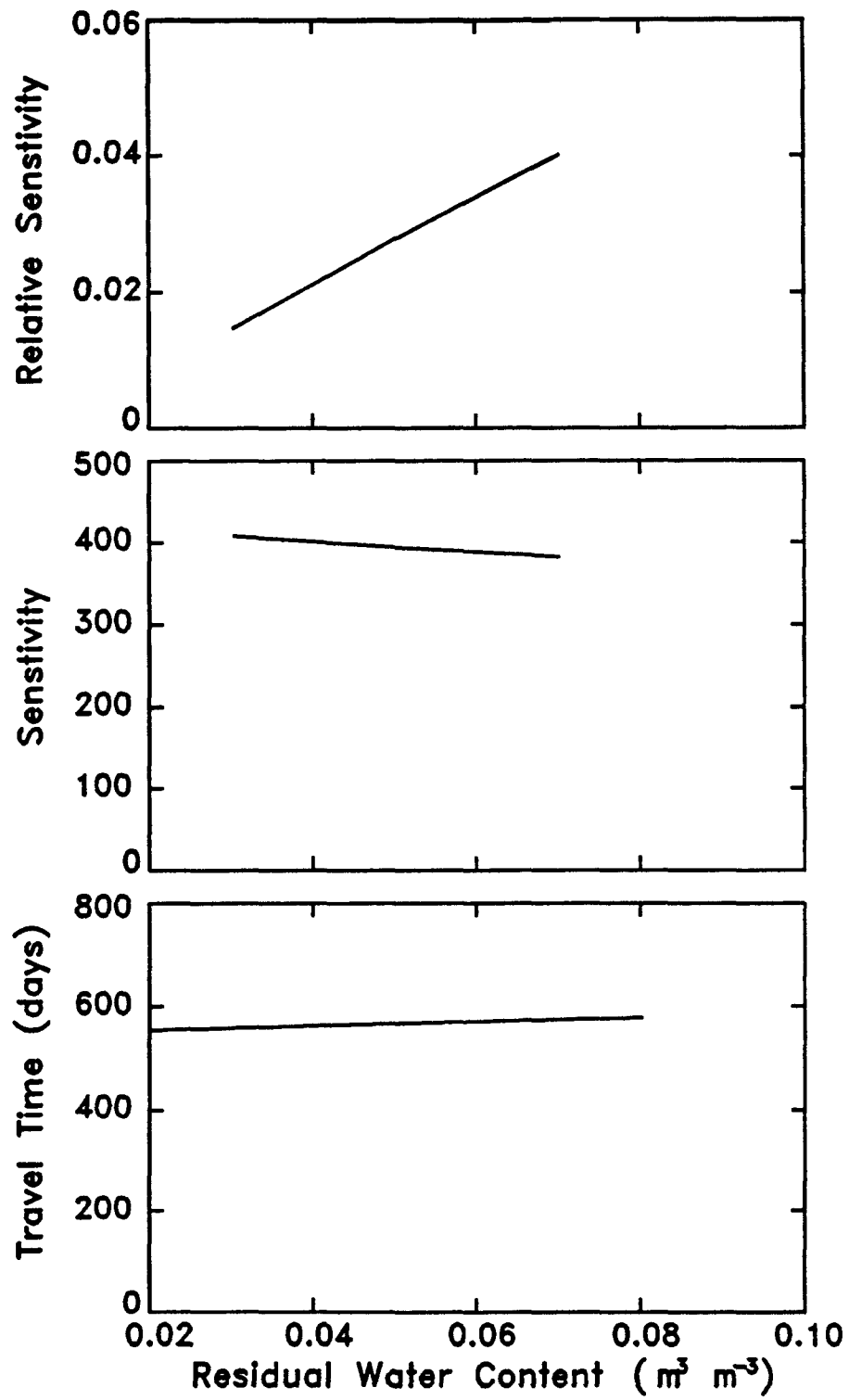
Figure 8.18. Sensitivity of travel time to residual water content.
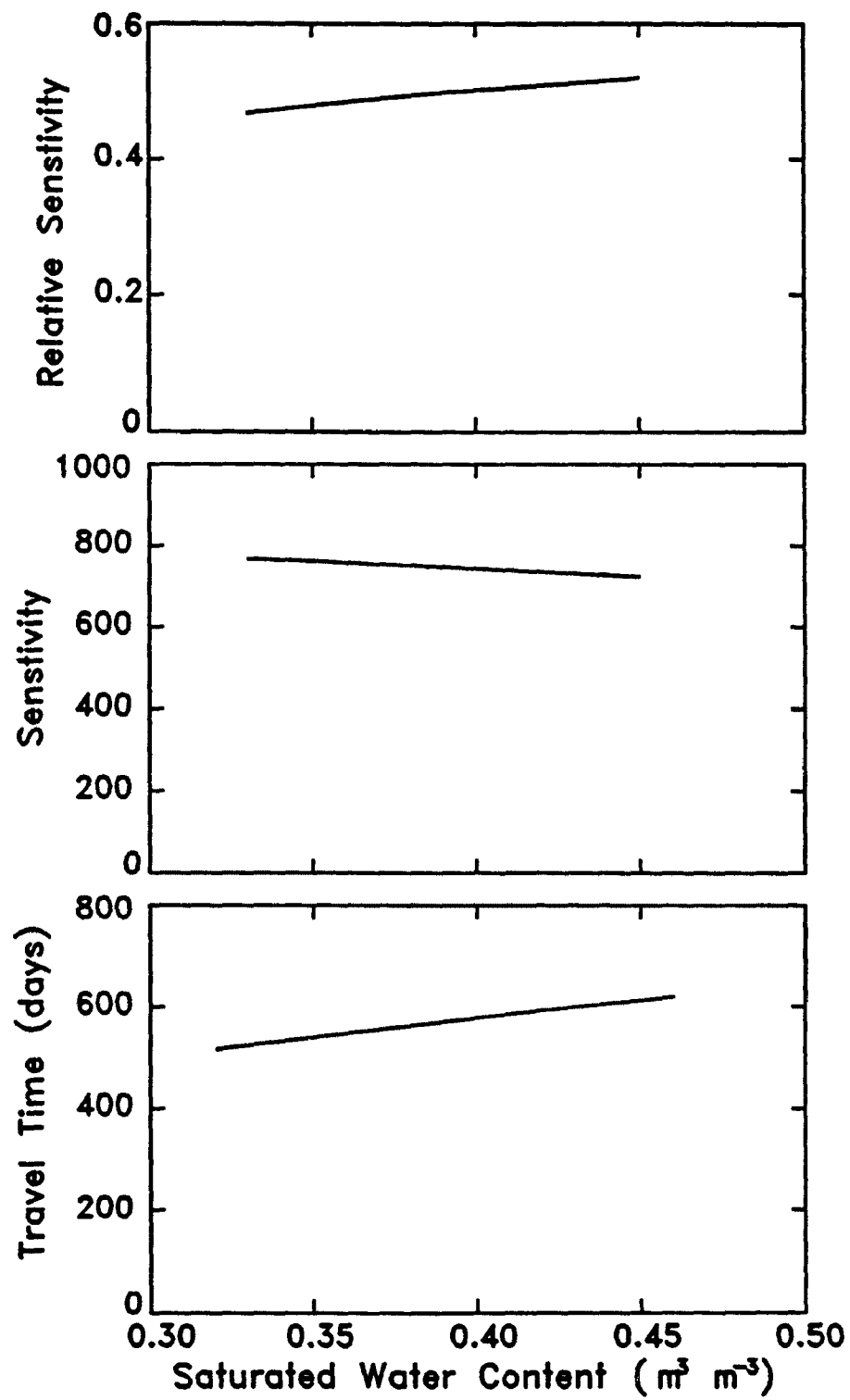
Figure 8.19. Sensitivity of travel time to saturated water content.
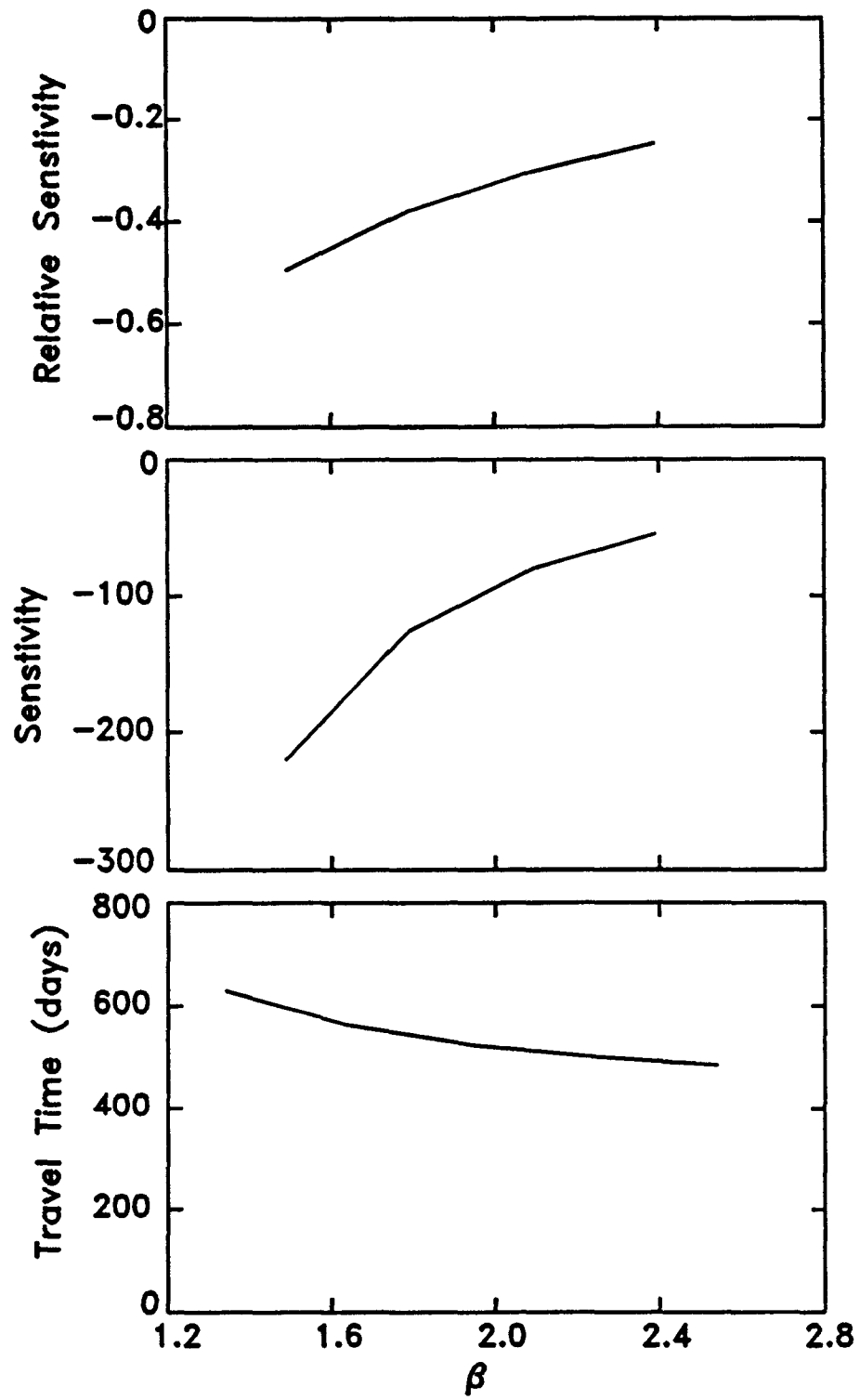
Figure 8.20. Sensitivity of travel time to the van Genuchten $\beta$ parameter.
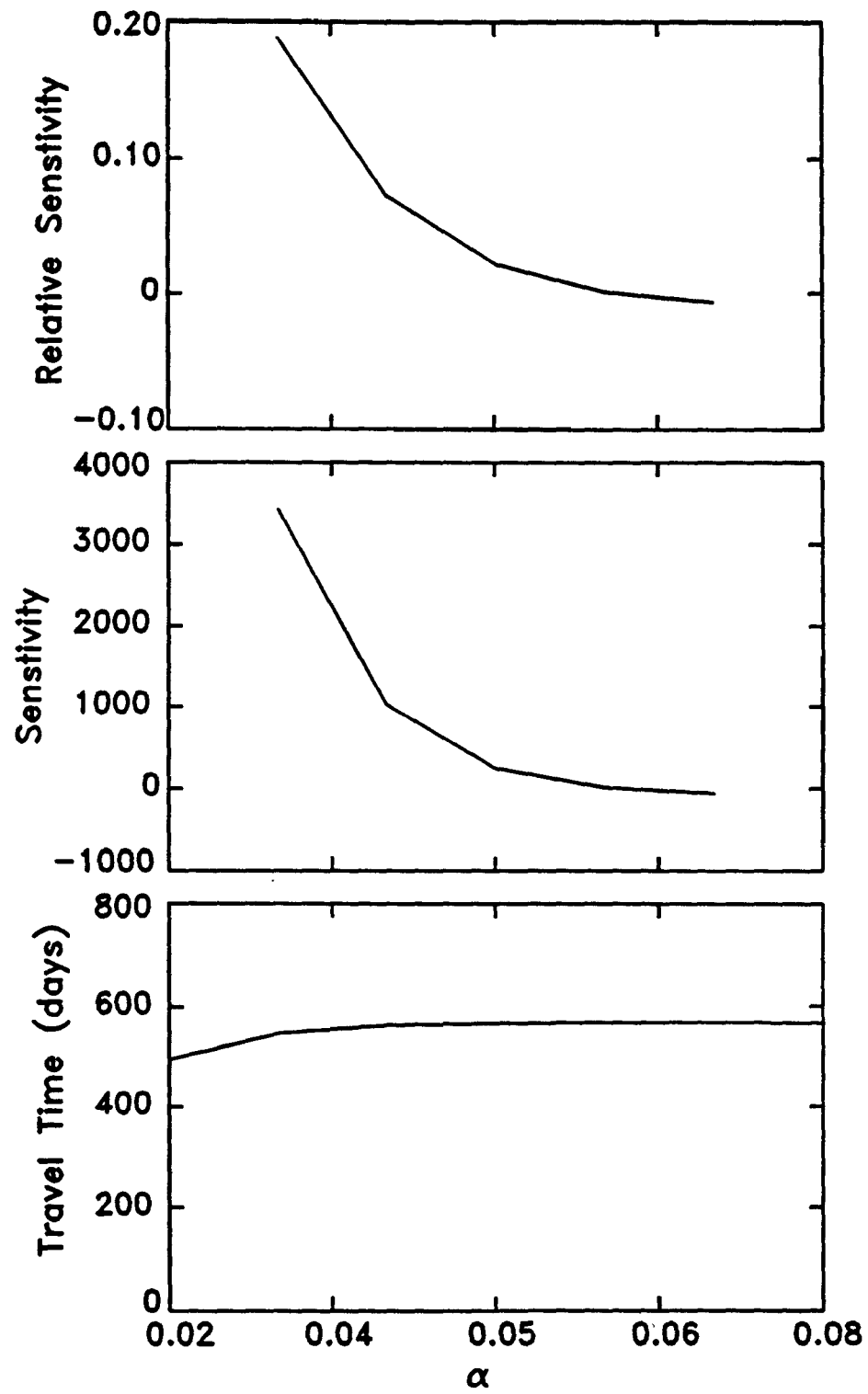
Figure 8.21. Sensitivity of travel time to the van Genuchten α parameter.
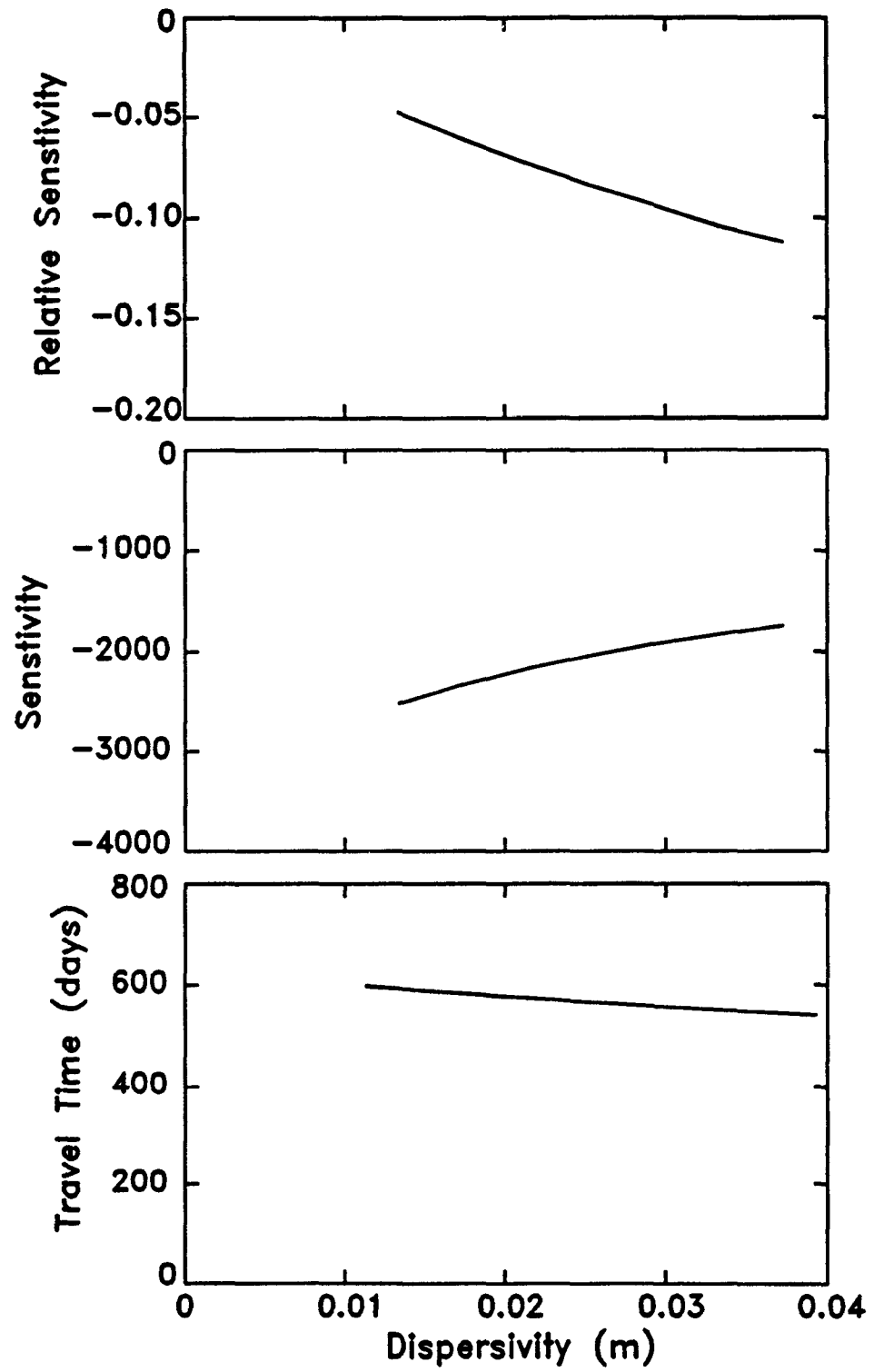
Figure 8.22. Sensitivity of travel time to dispersivity.
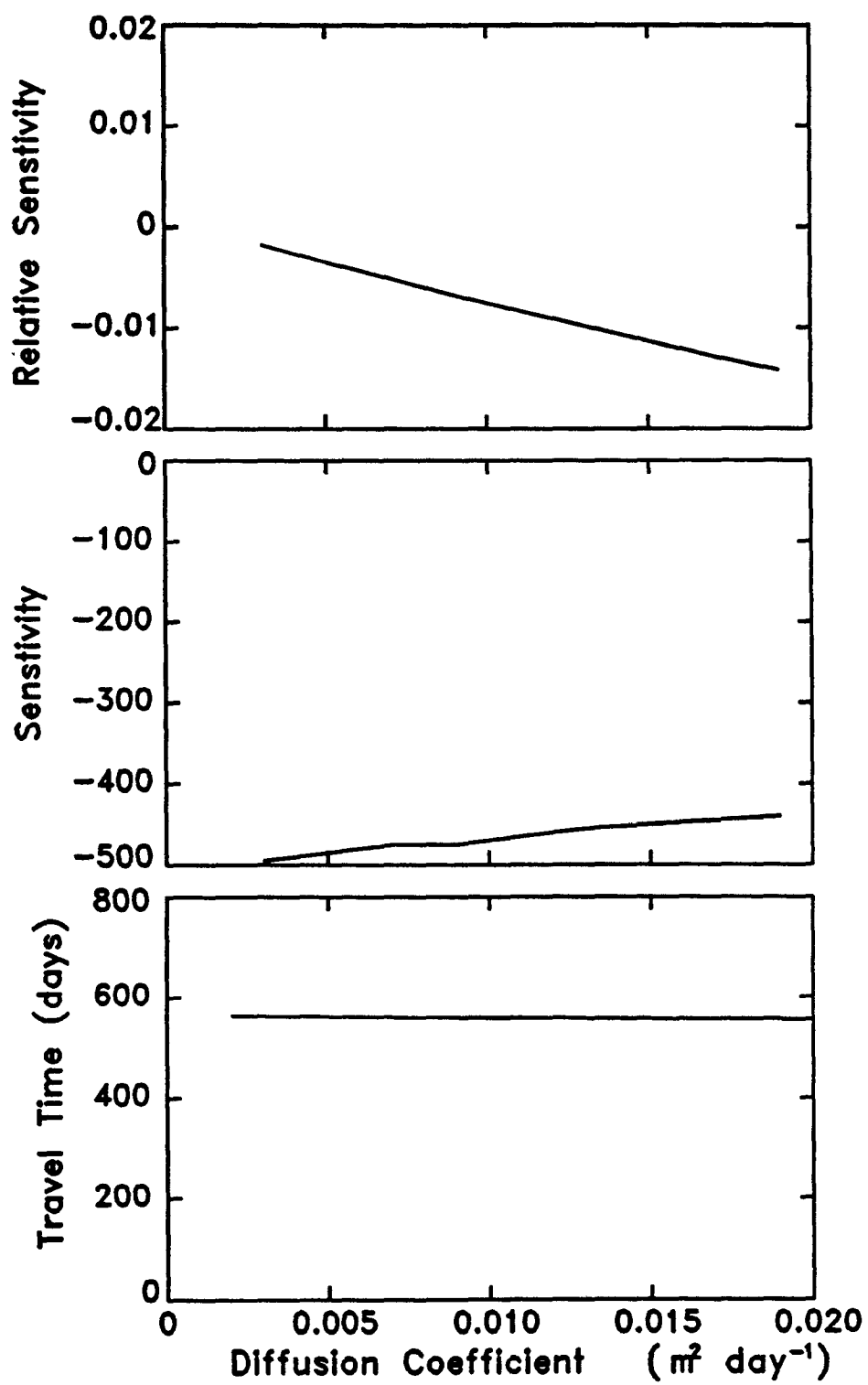
Figure 8.23. Sensitivity of travel time to diffusion coefficient.
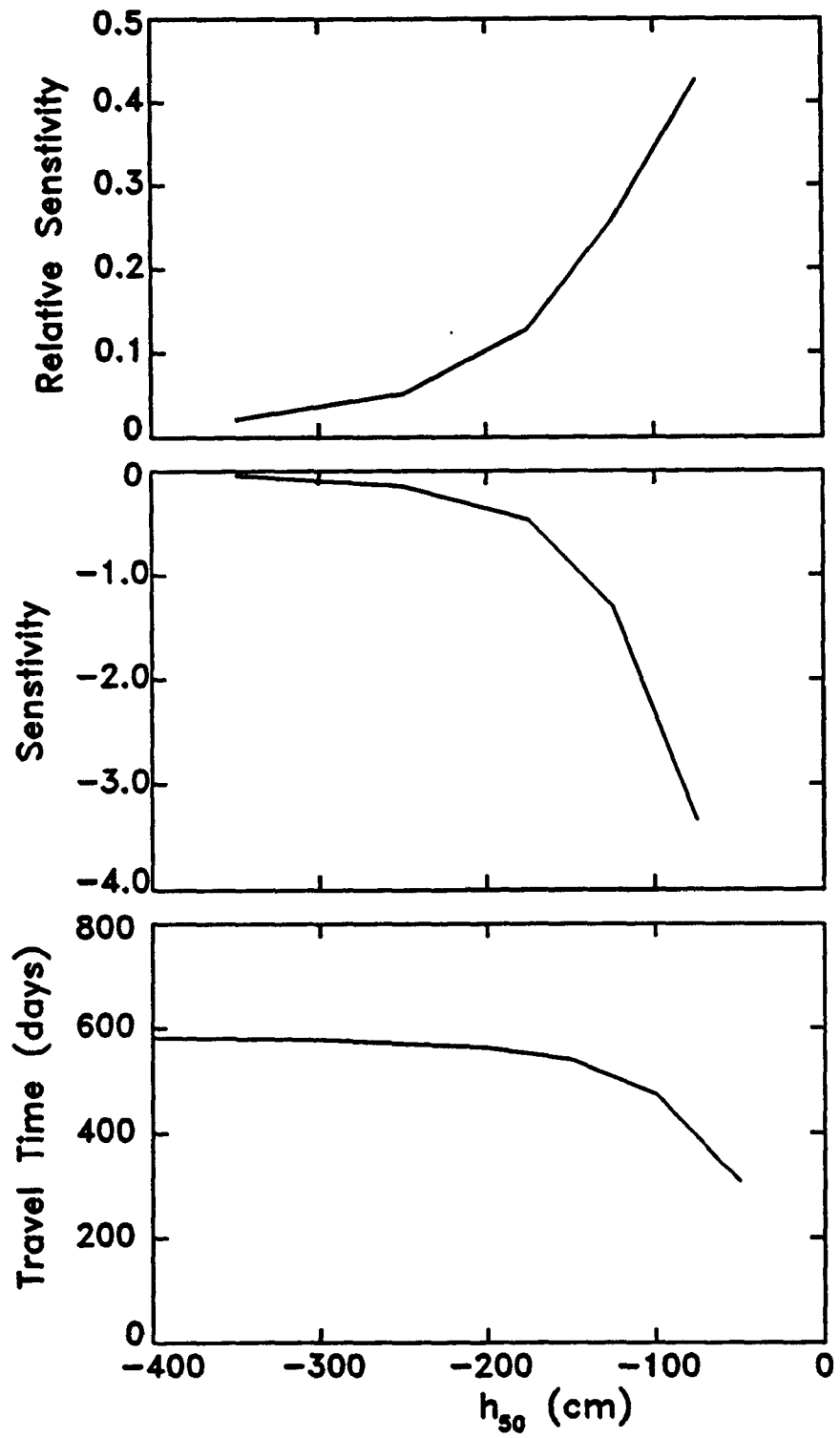
Figure 8.24. Sensitivity of travel time to root uptake potential, $h_{50}$.

145
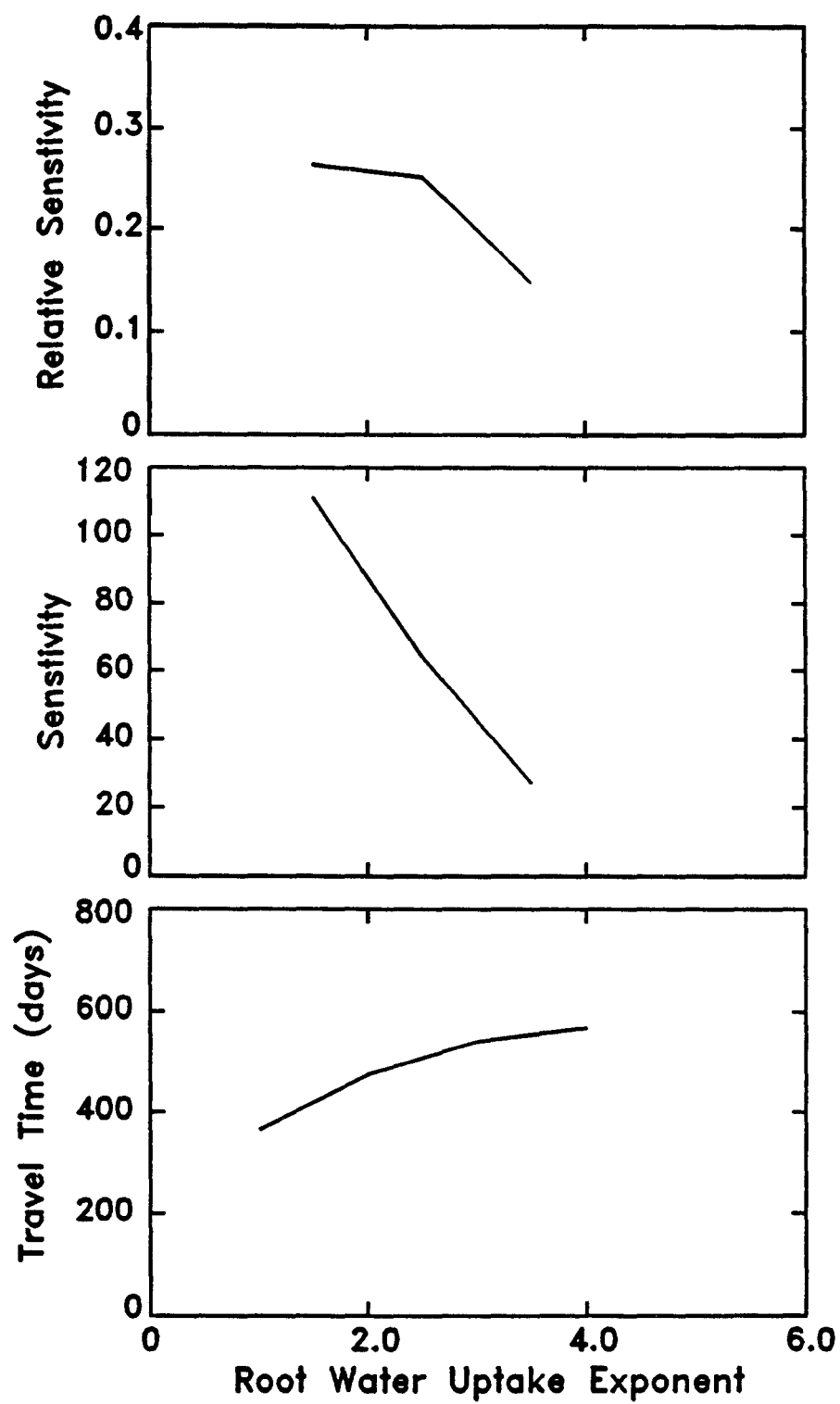
Figure 8.25. Sensitivity of travel time to root uptake exponent.
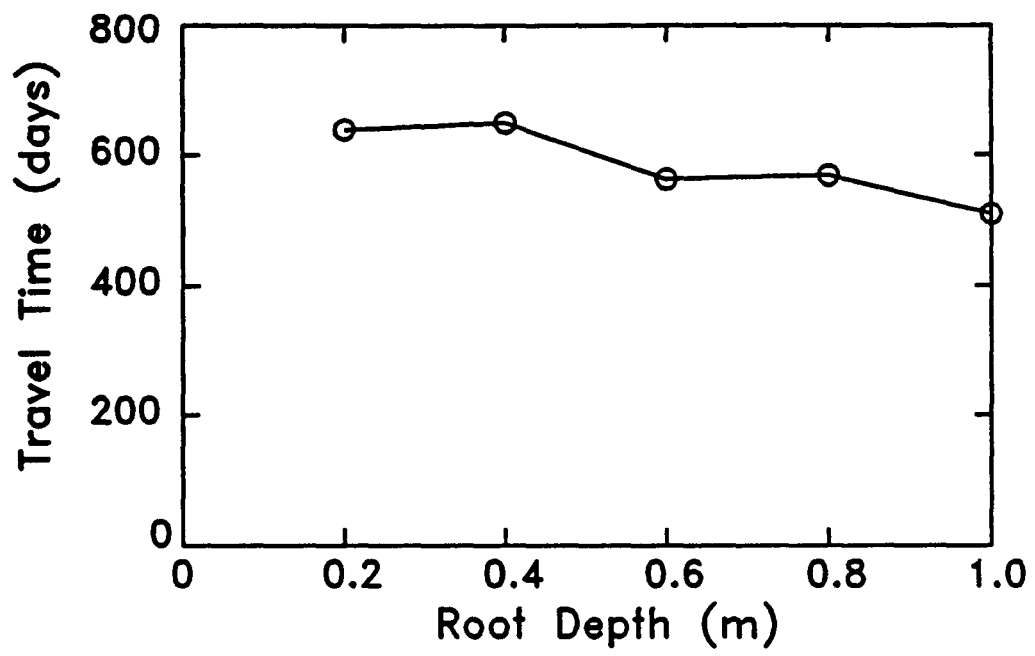
Figure 8.26. Travel time to 2-m depth as a function of root depth.
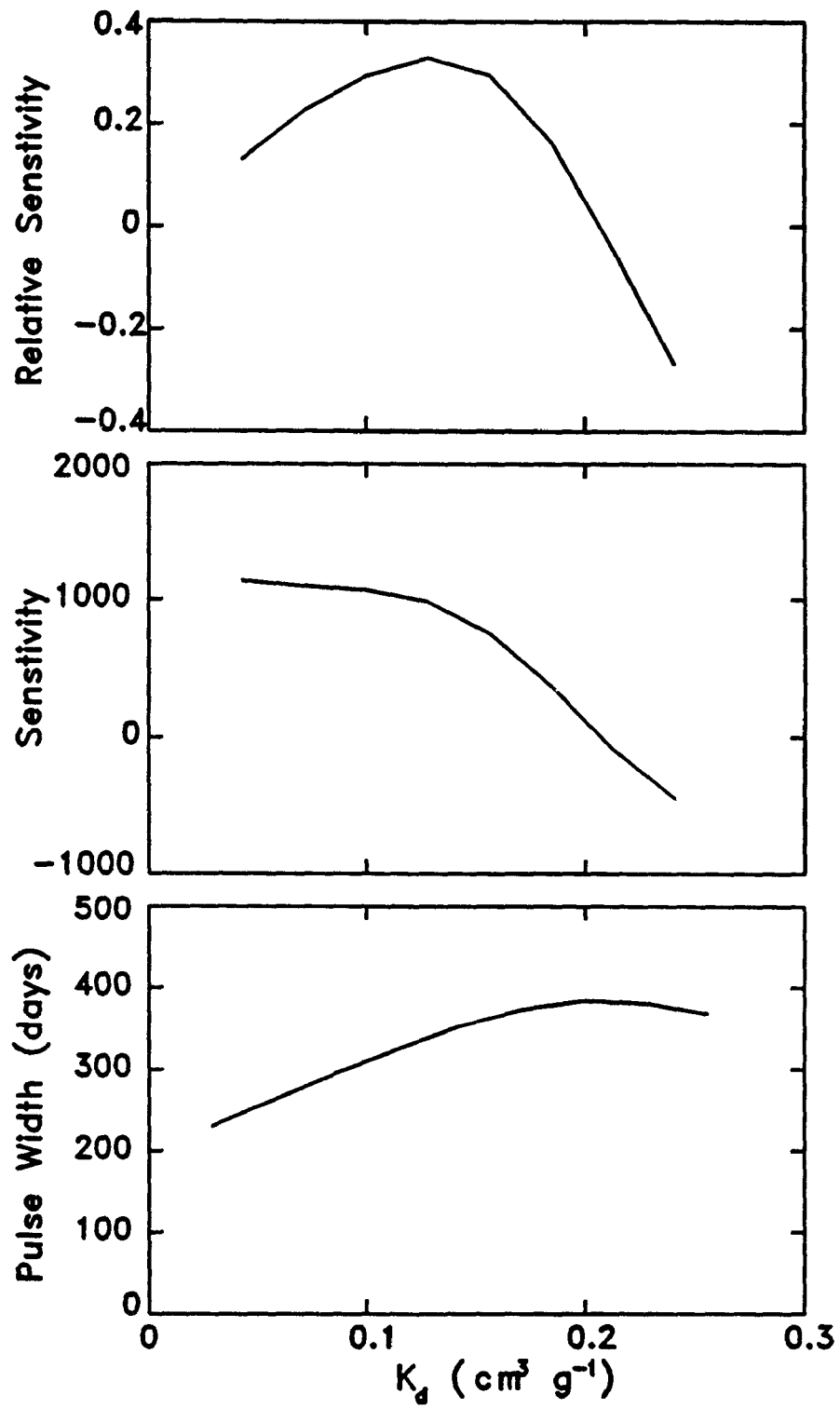
Figure 8.27. Sensitivity of pulse width to partition coefficient.
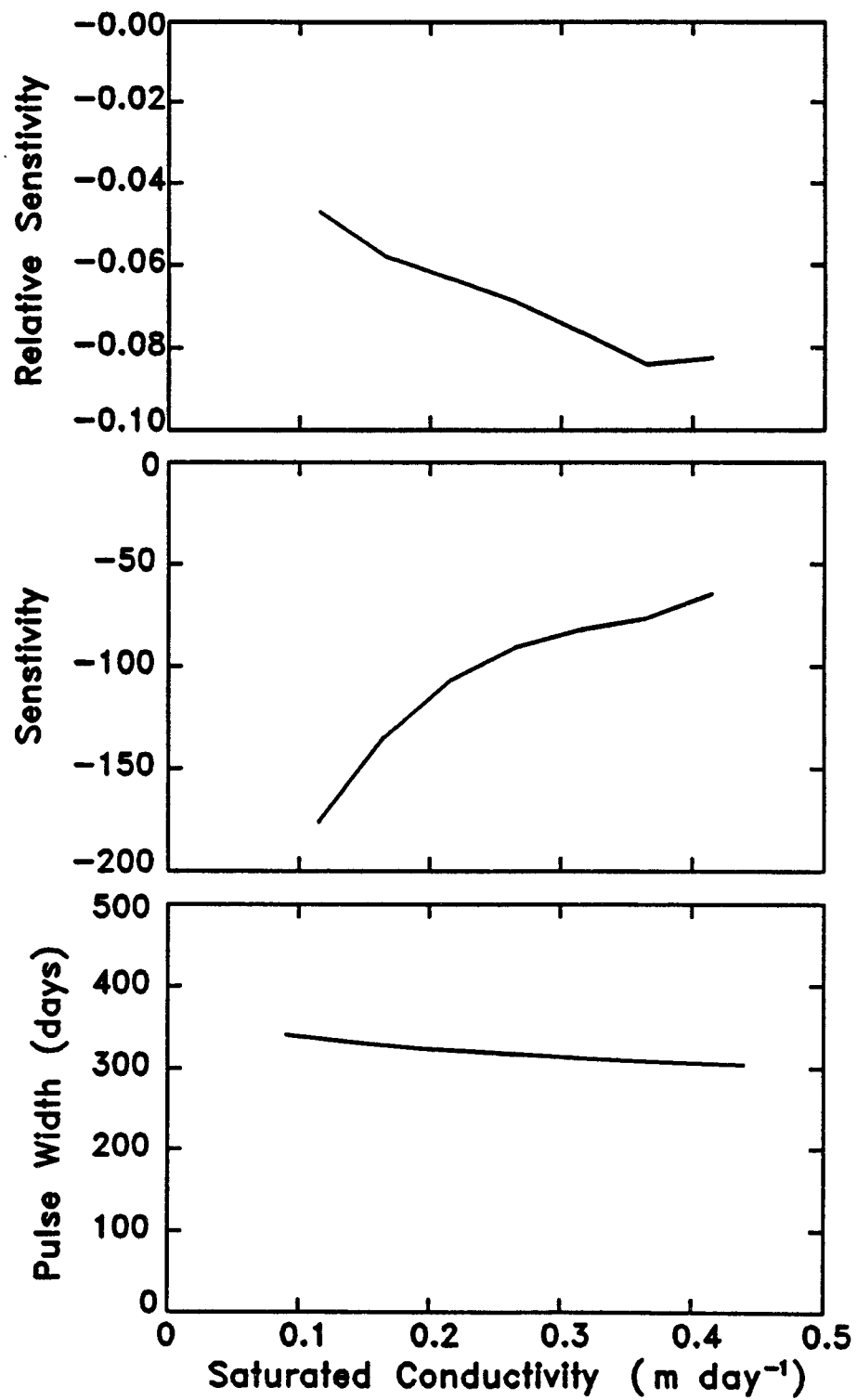
Figure 8.28. Sensitivity of pulse width to hydraulic conductivity.
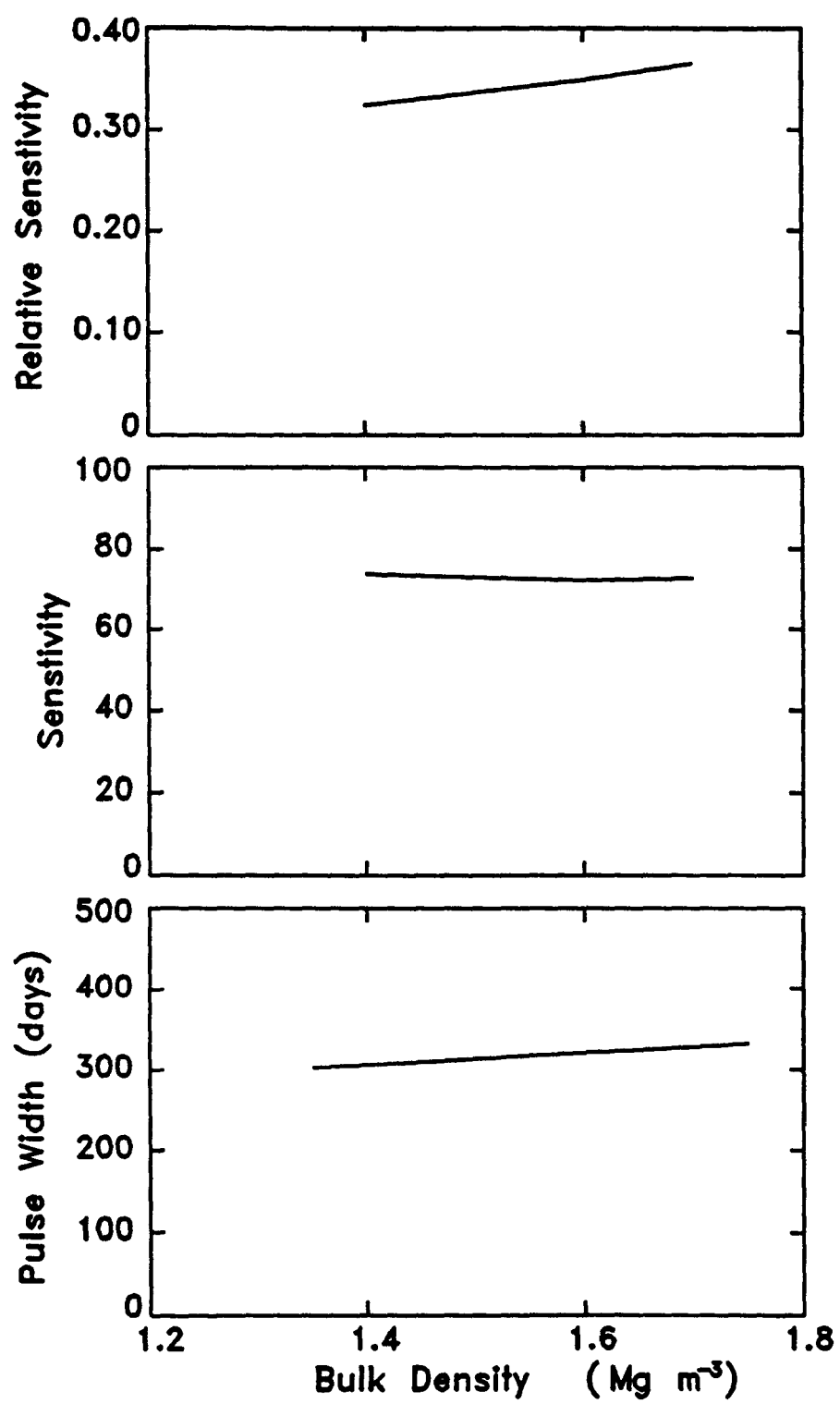
Figure 8.29. Sensitivity of pulse width to bulk density.
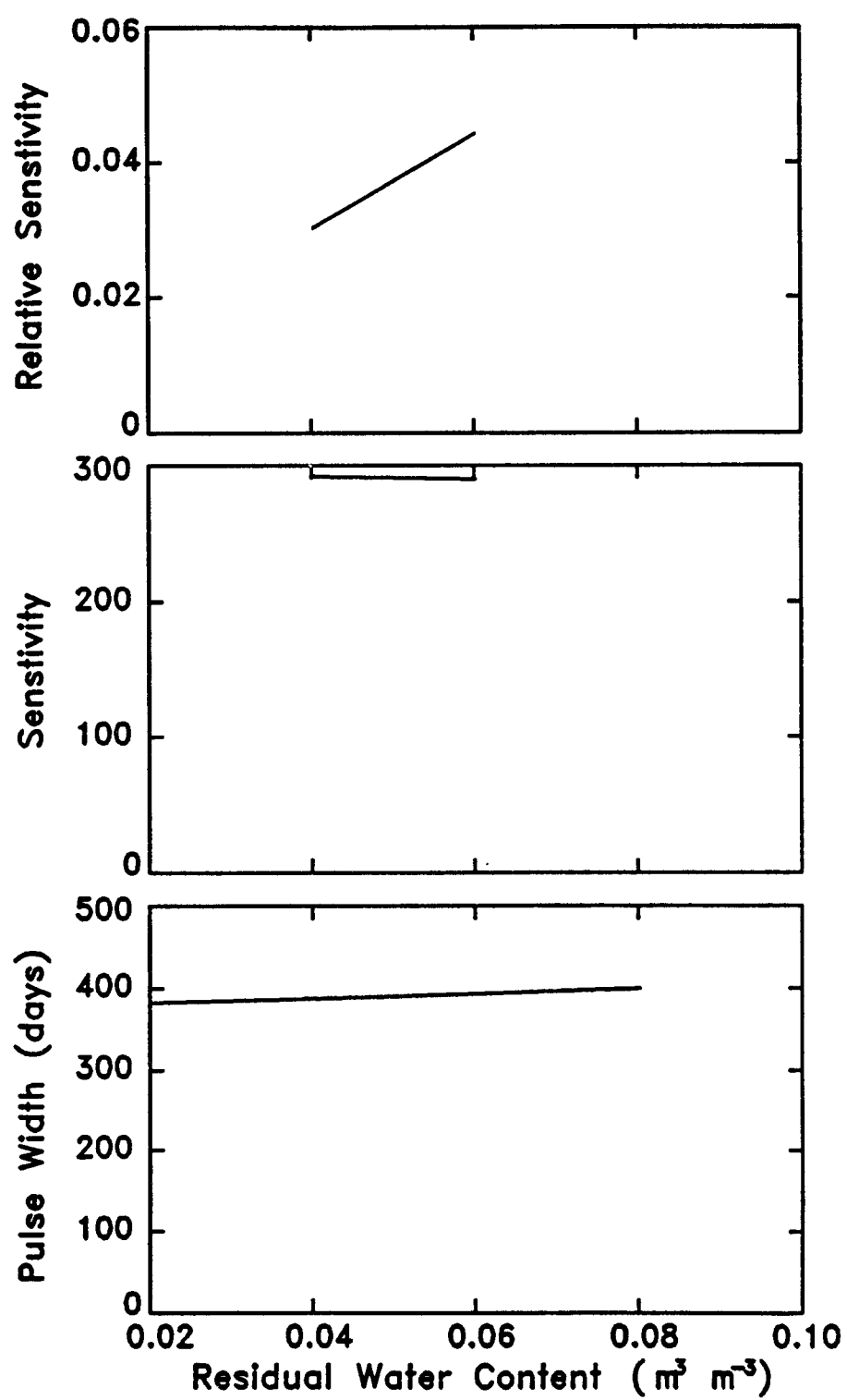
Figure 8.30. Sensitivity of pulse width to residual water content.
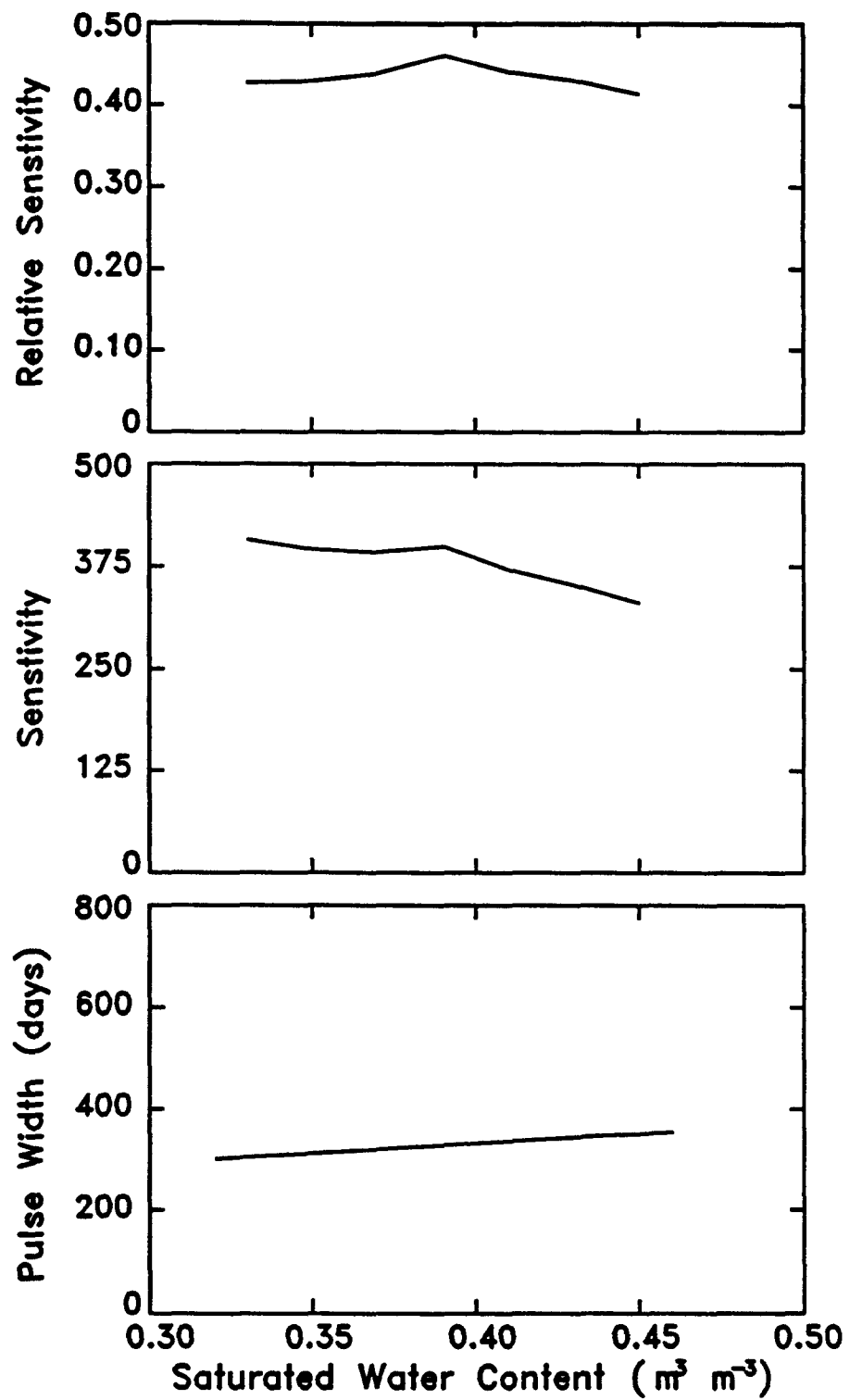
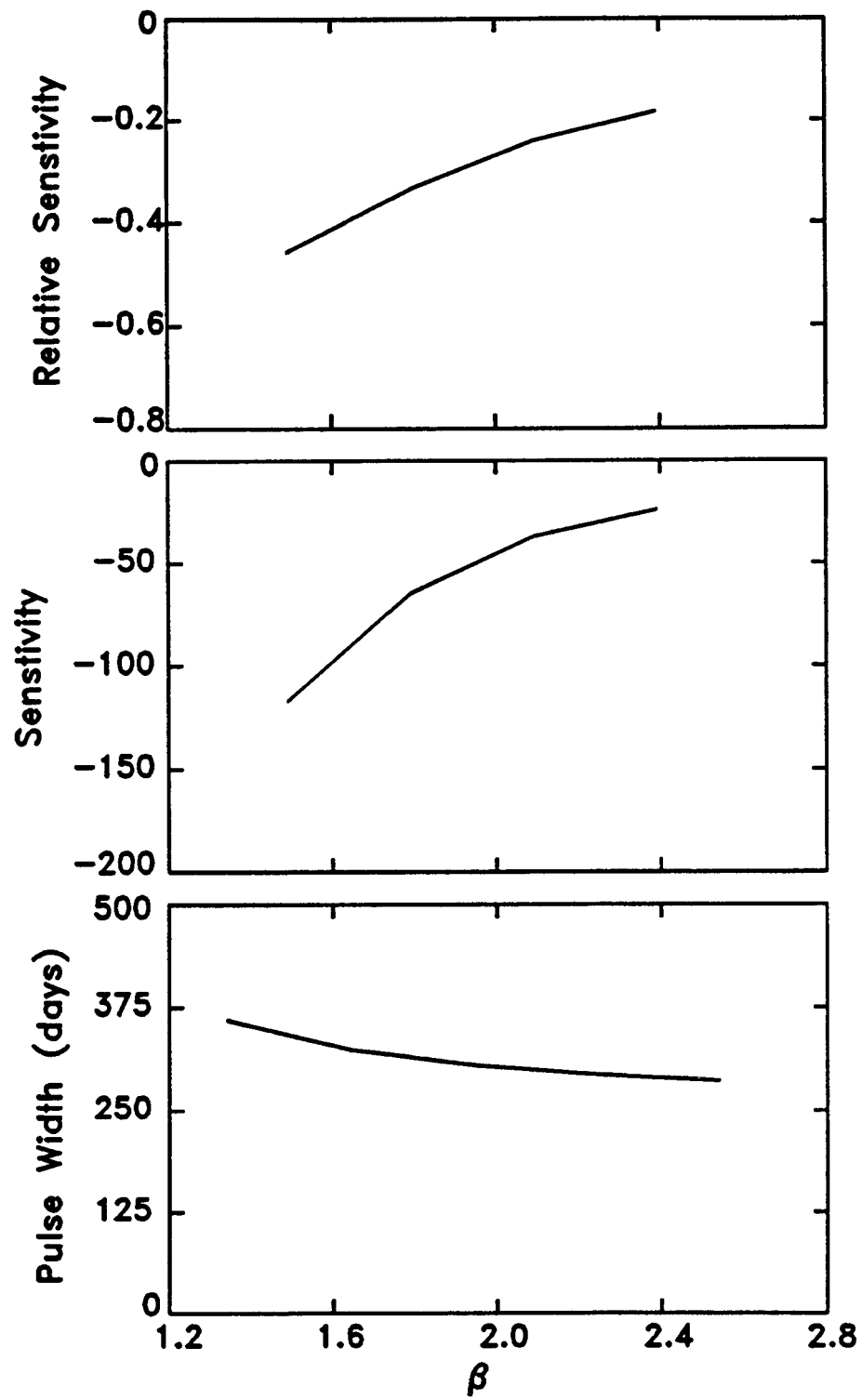Figure 8.31. Sensitivity of pulse width to saturated water content.

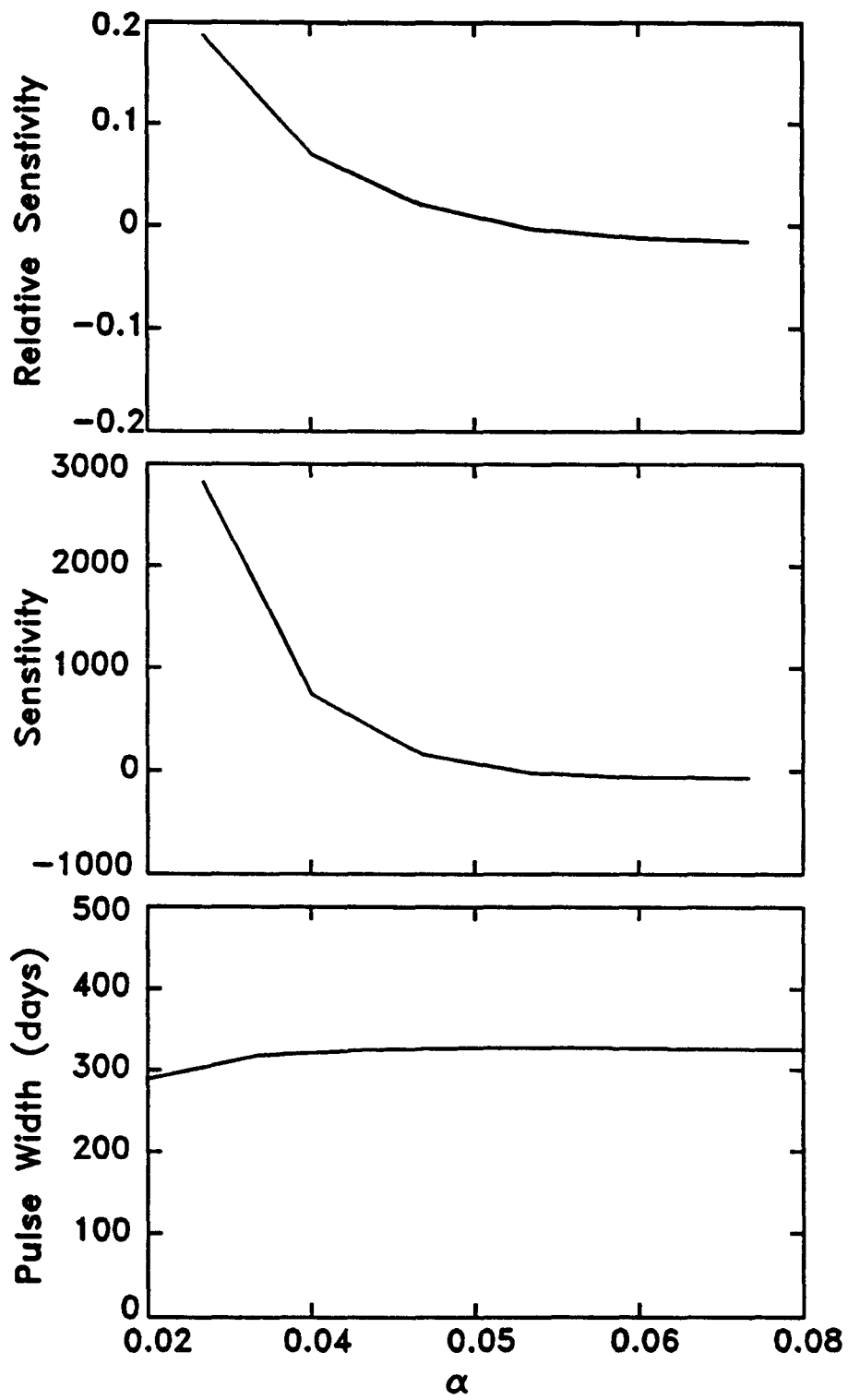Figure 8.32. Sensitivity of pulse width to the van Genuchten $\beta$ parameter.

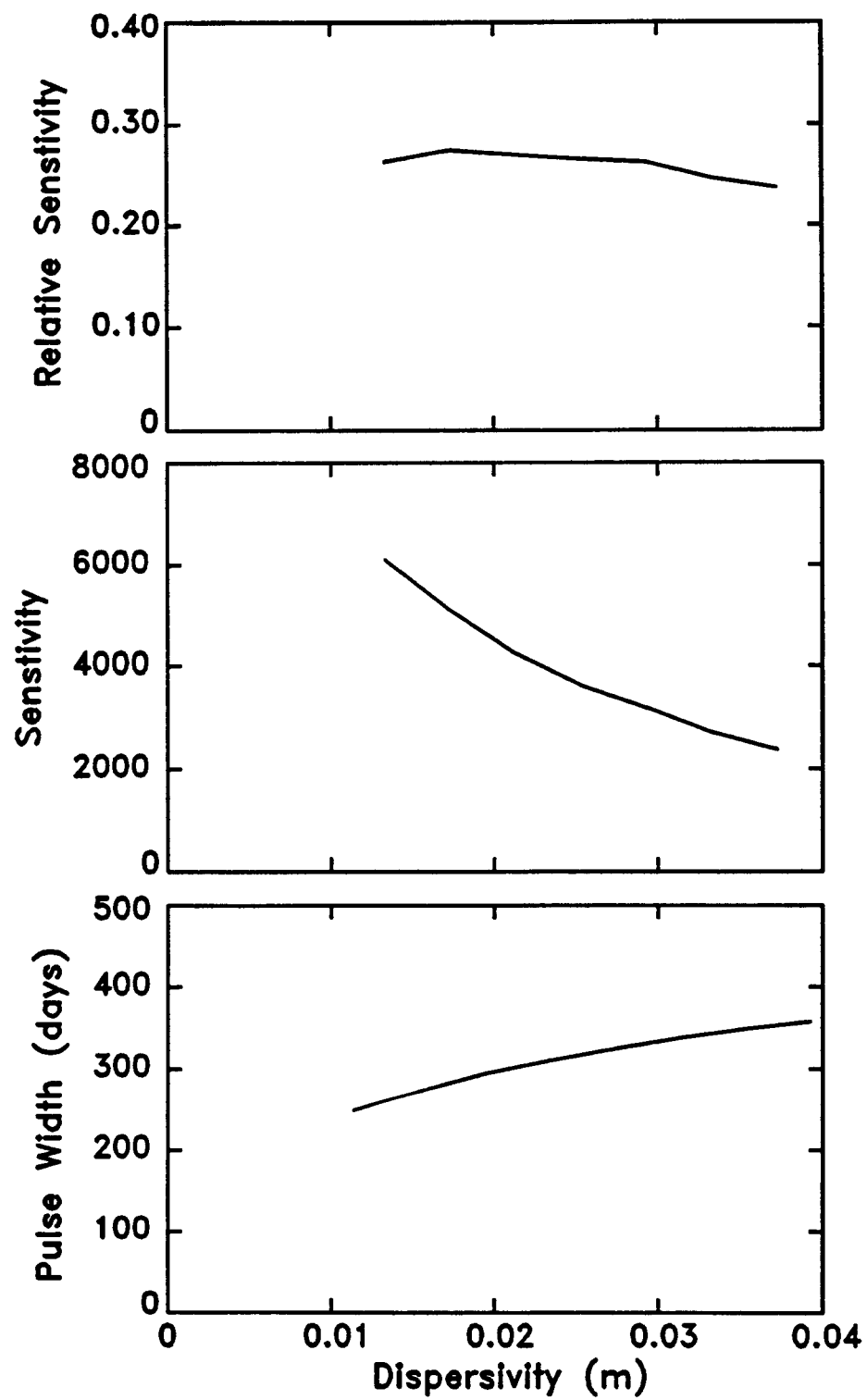Figure 8.33. Sensitivity of pulse width to the van Genuchten α parameter.

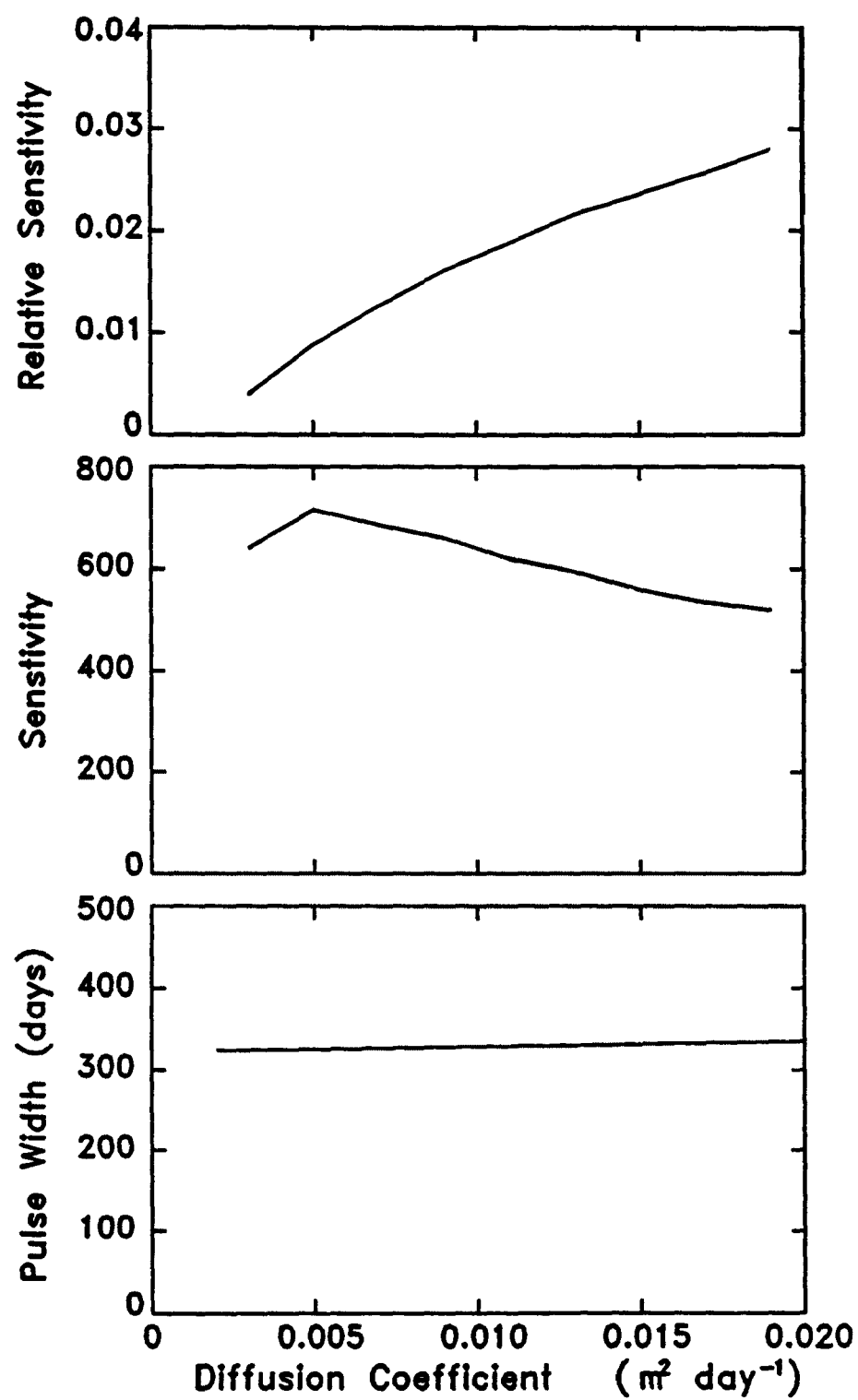Figure 8.34. Sensitivity of pulse width to dispersivity.

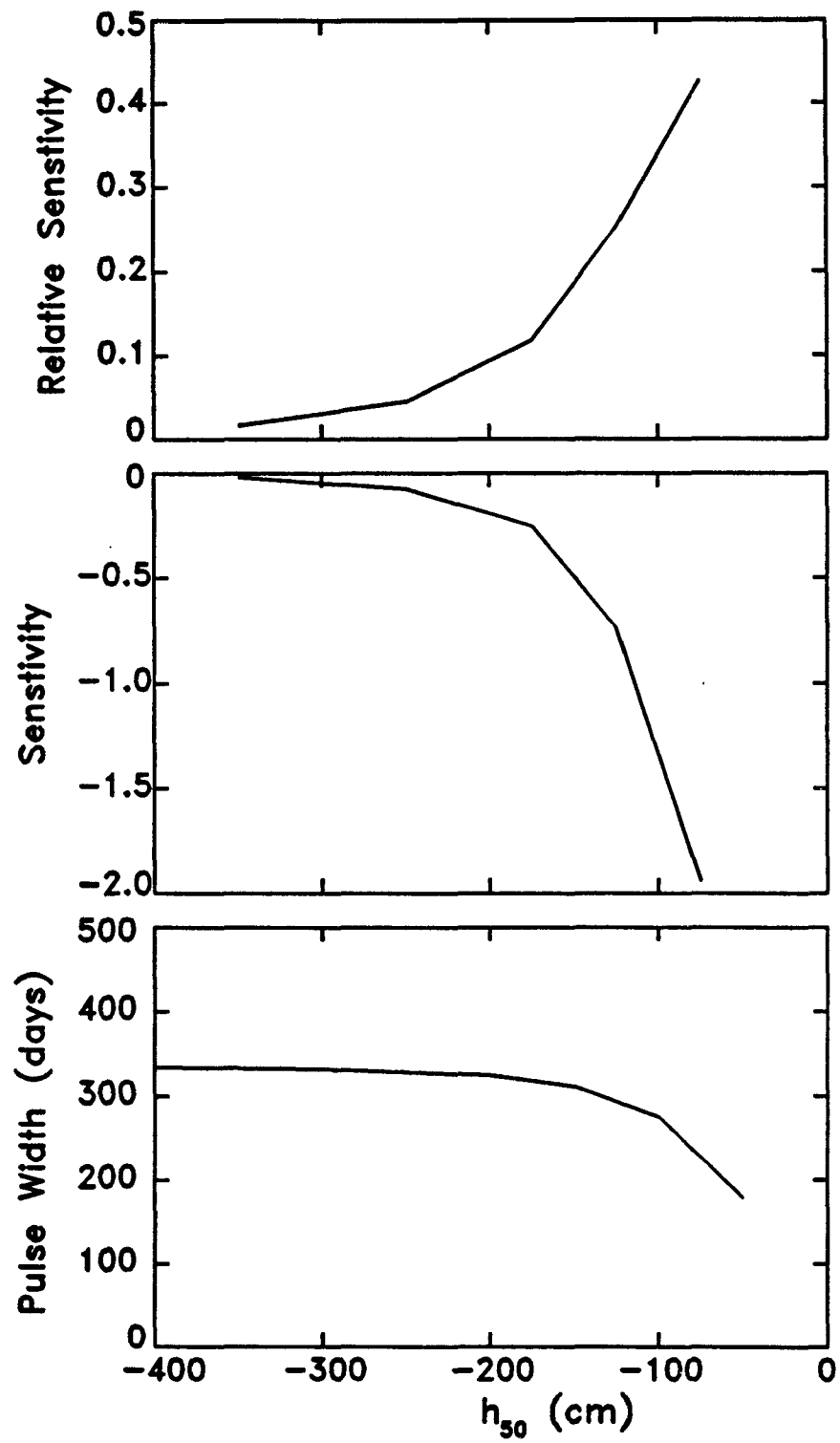Figure 8.35. Sensitivity of pulse width to diffusion coefficient.

156

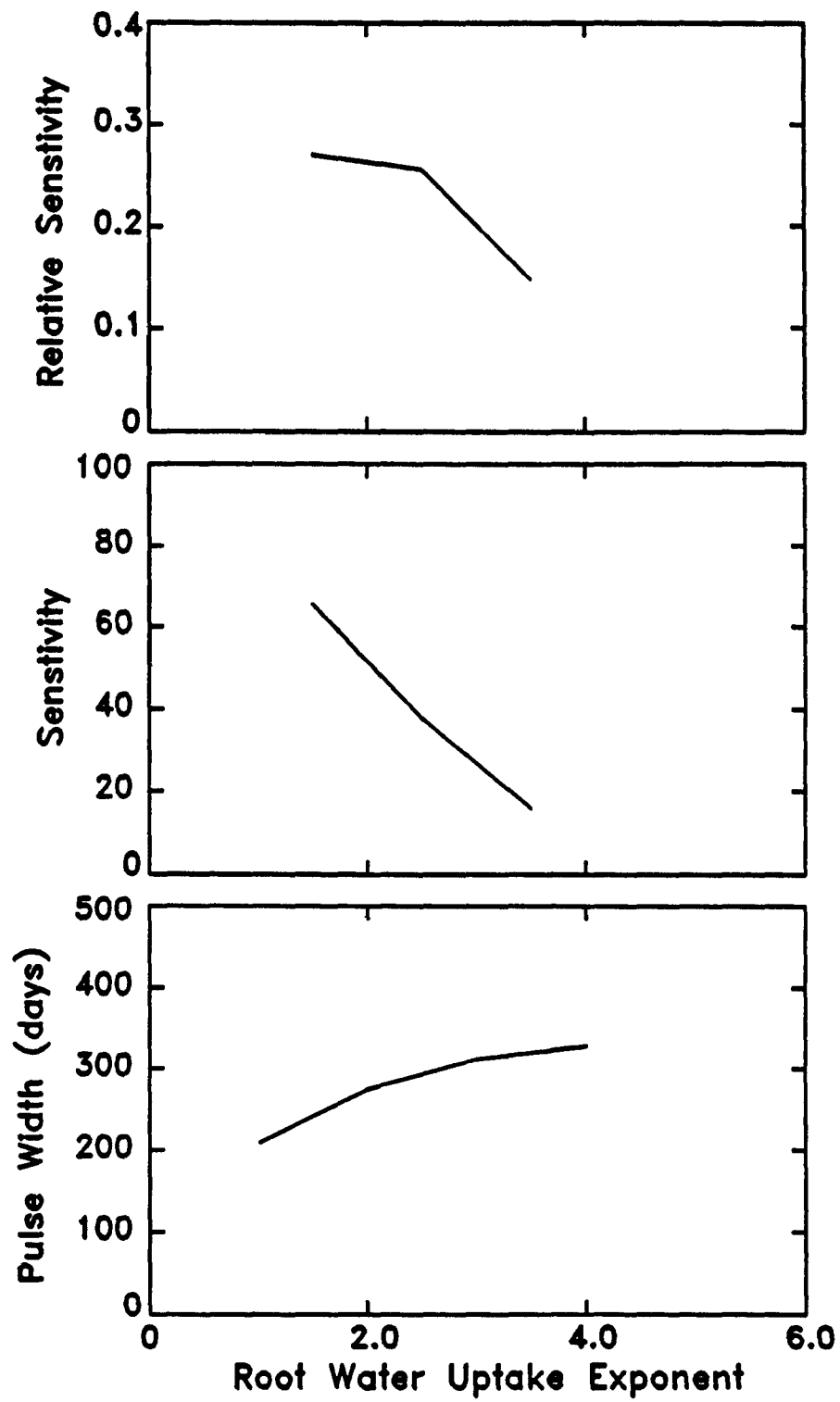Figure 8.36. Sensitivity of pulse width to root uptake potential, $h_{50}$.

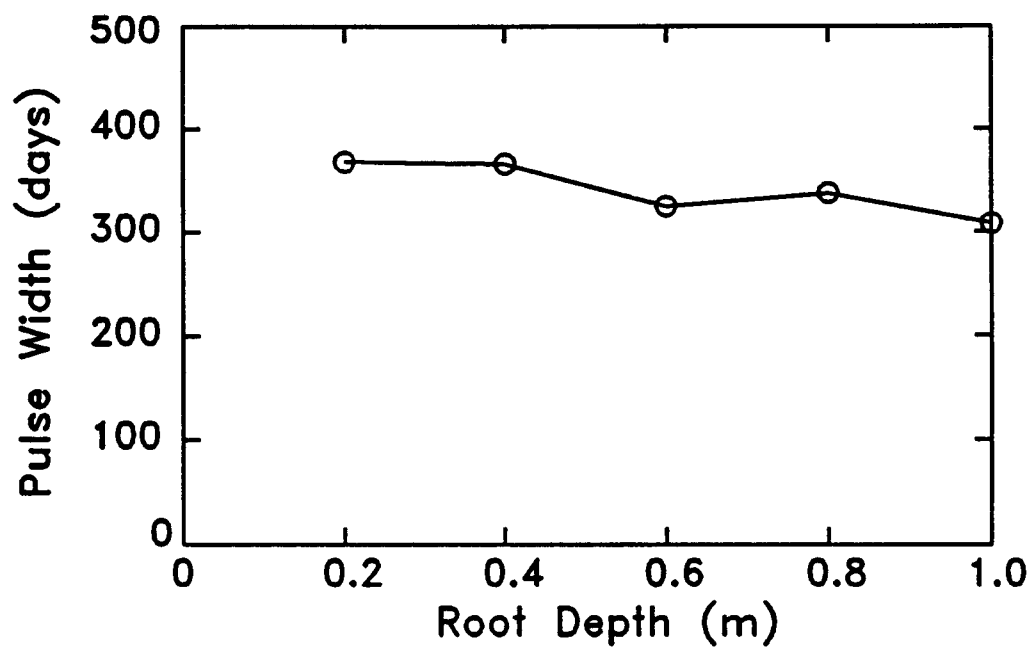Figure 8.37. Sensitivity of pulse width to root uptake exponent.

Figure 8.38. Pulse width of pollutant at 2-m depth as a function of root depth.
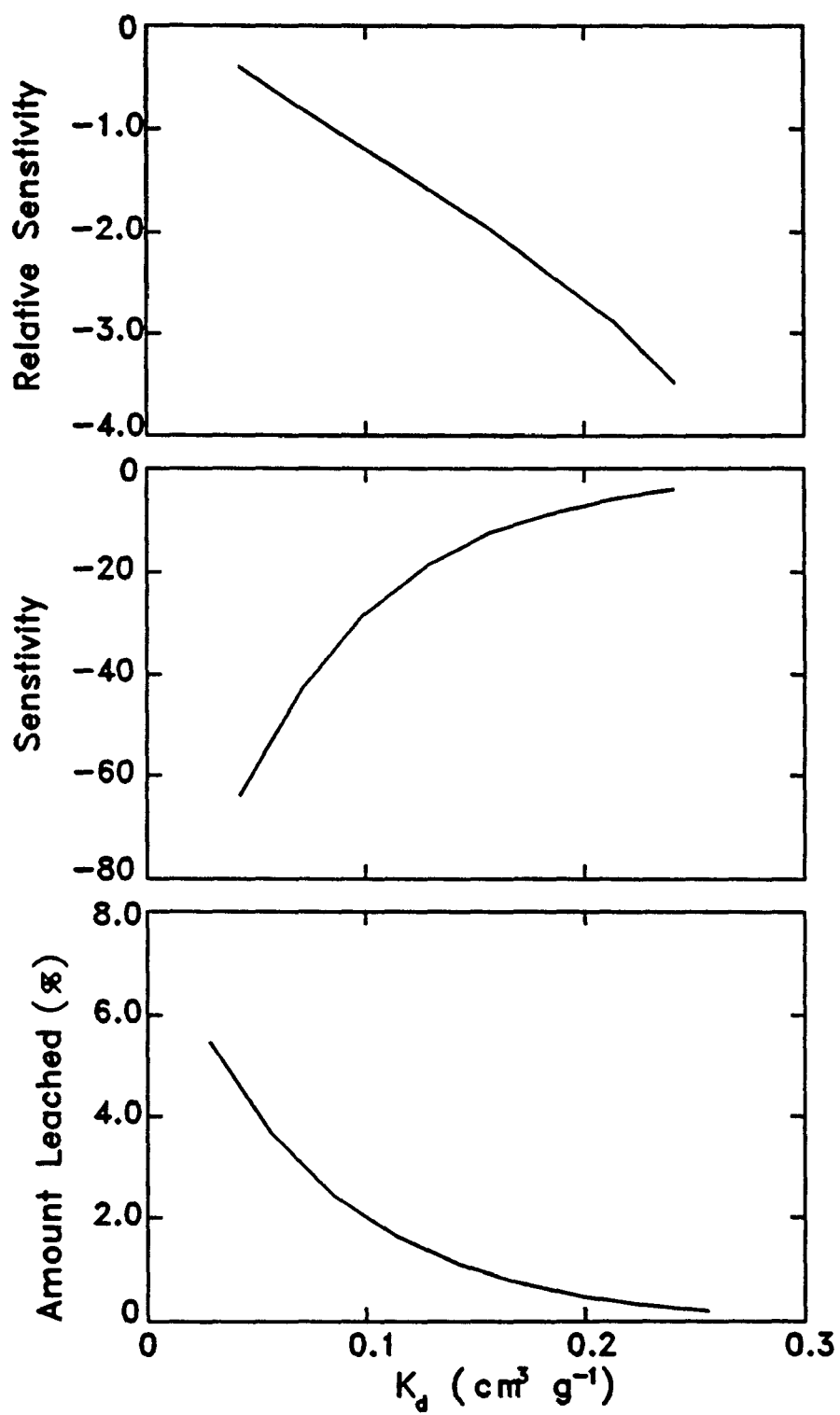
Figure 8.39. Sensitivity of amount leached to partition coefficient.
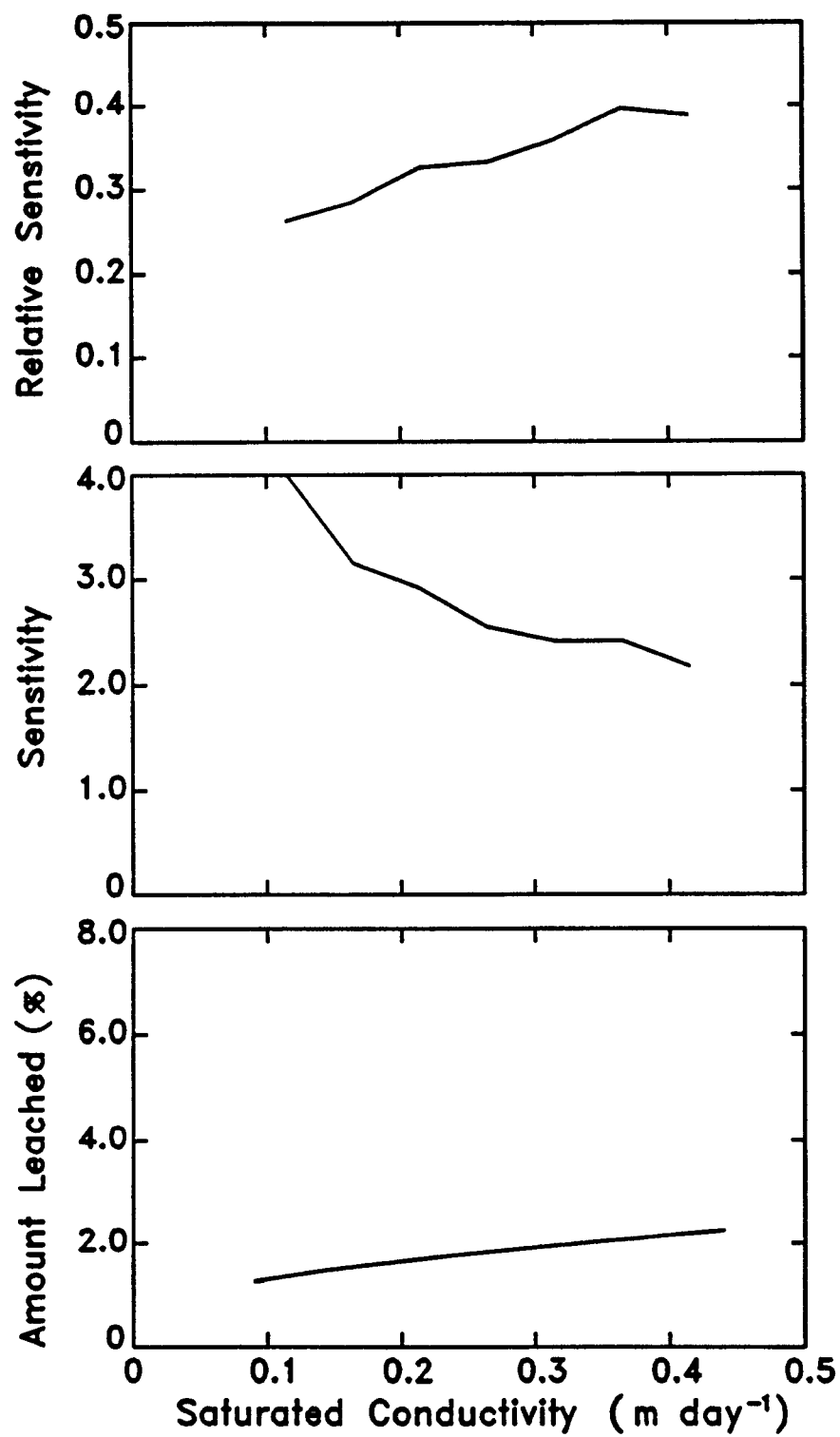
Figure 8.40. Sensitivity of amount leached to saturated hydraulic conductivity.
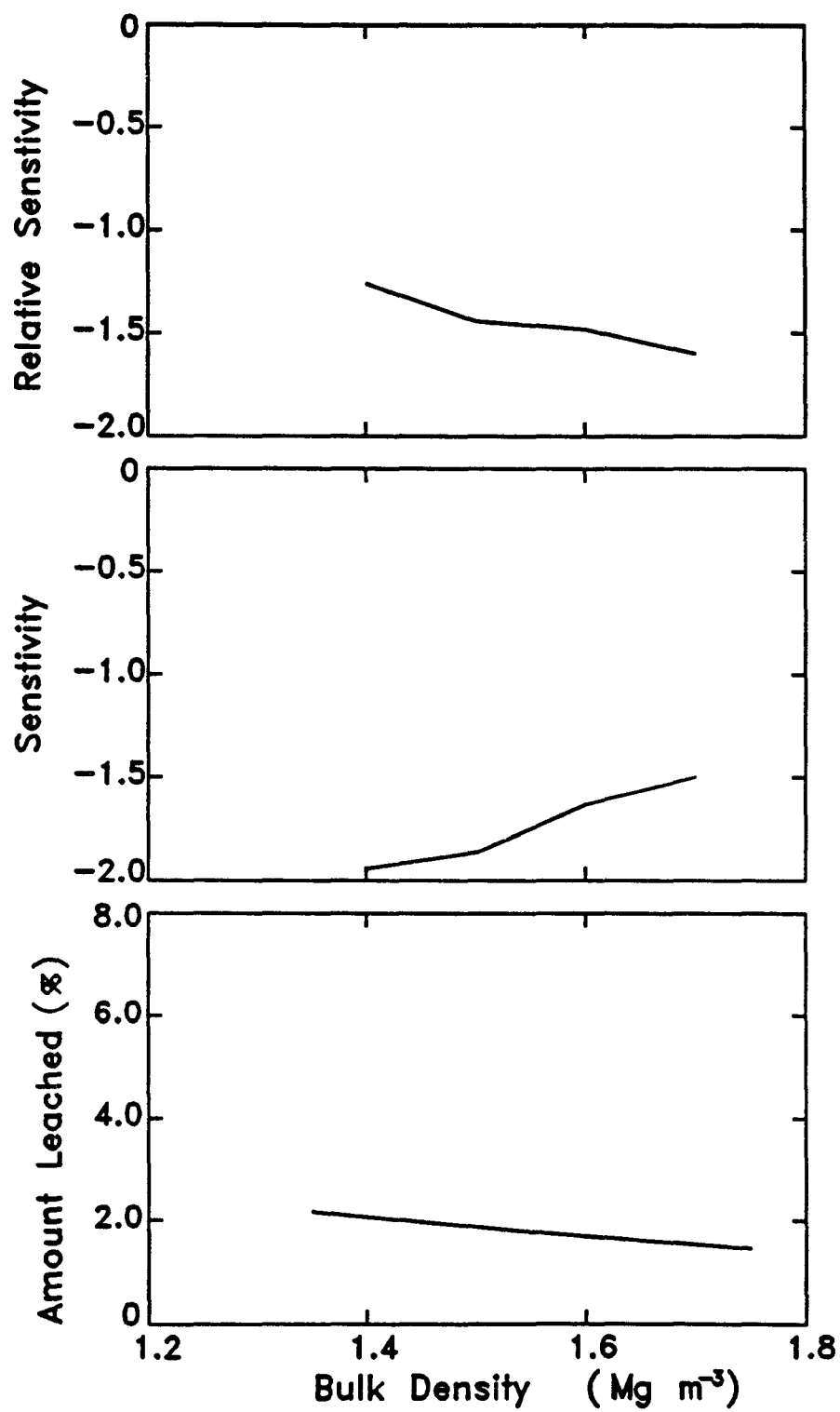
Figure 8.41. Sensitivity of amount leached to bulk density.
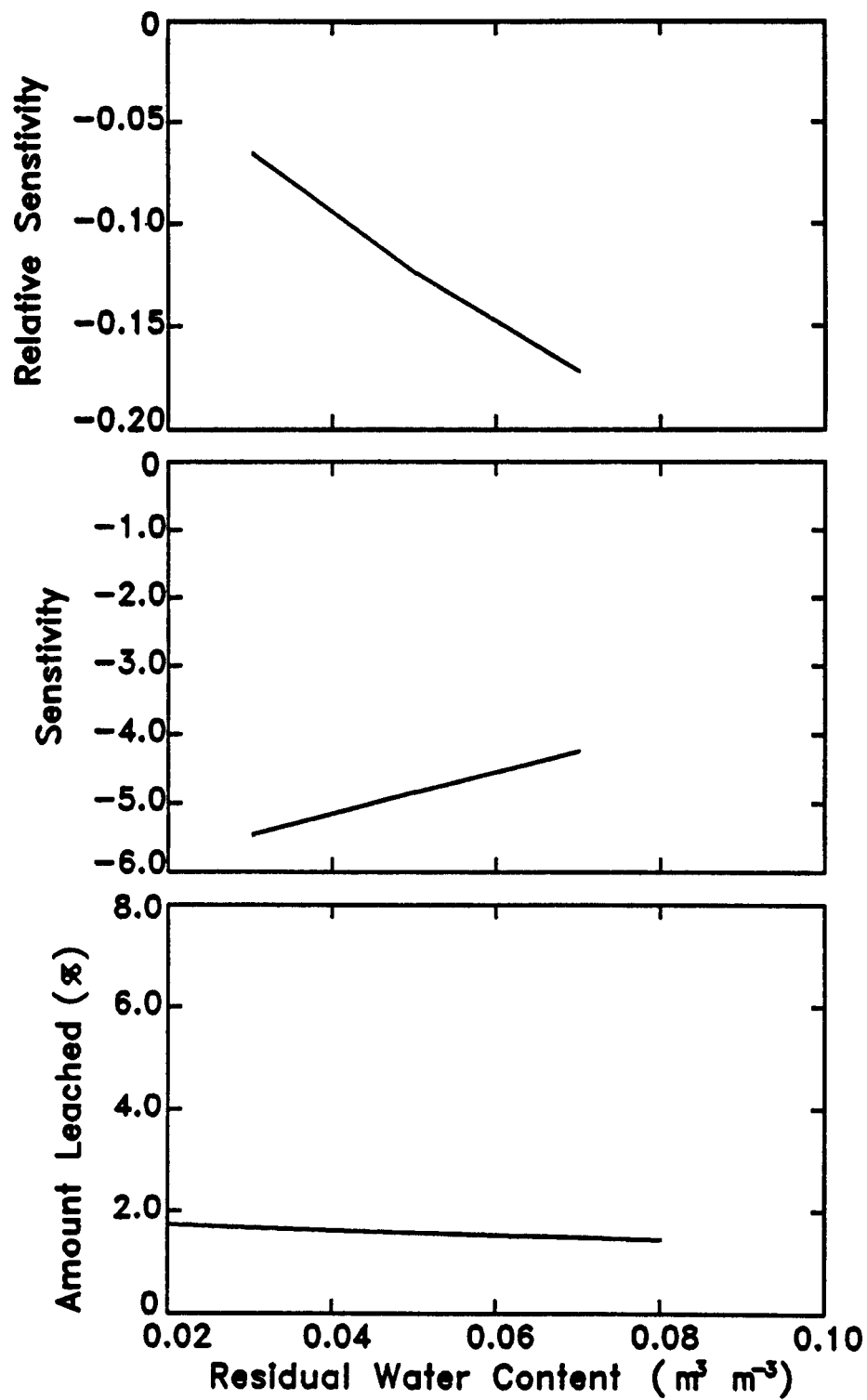
Figure 8.42. Sensitivity of amount leached to residual water content.
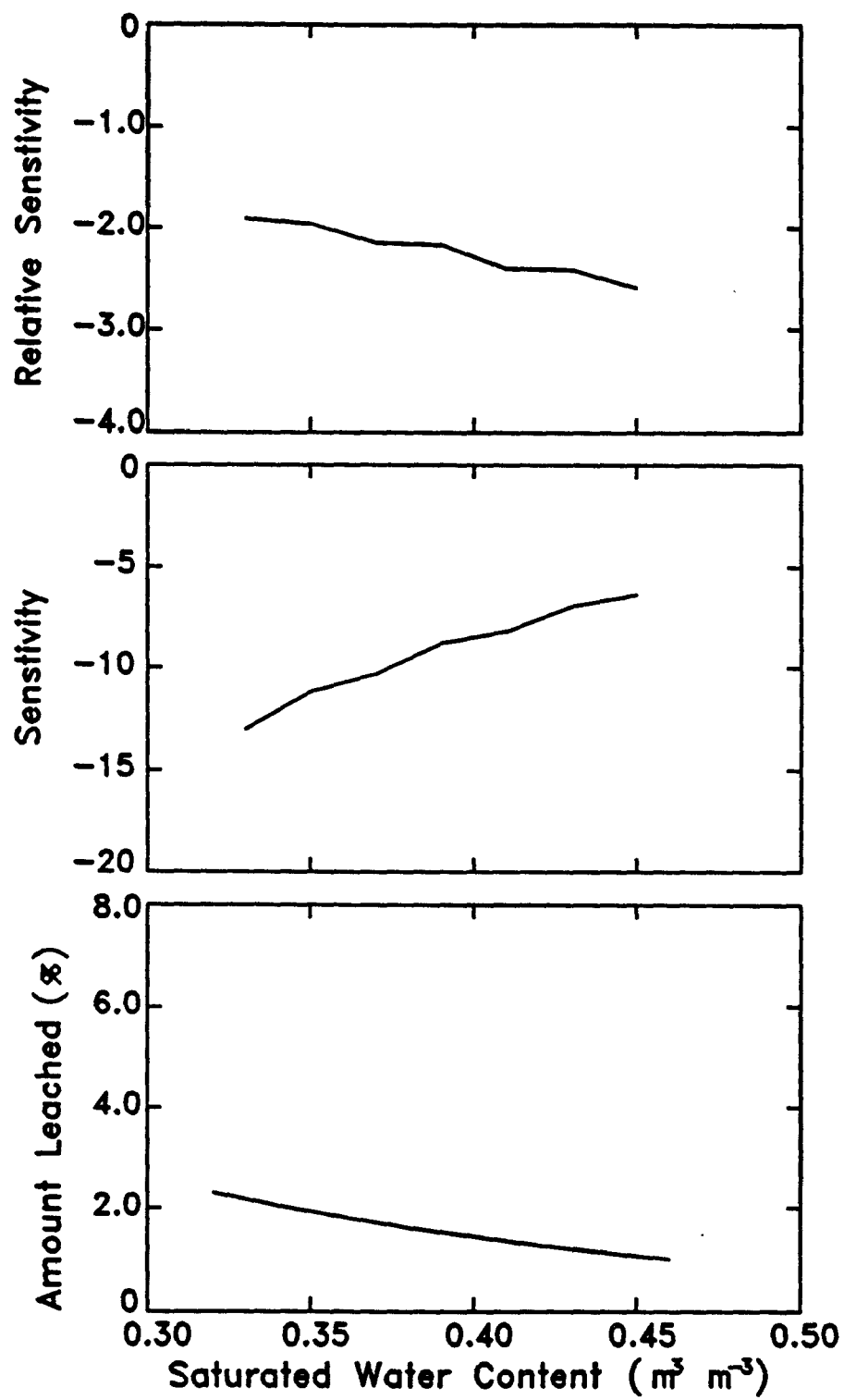
Figure 8.43. Sensitivity of amount leached to saturated water content.
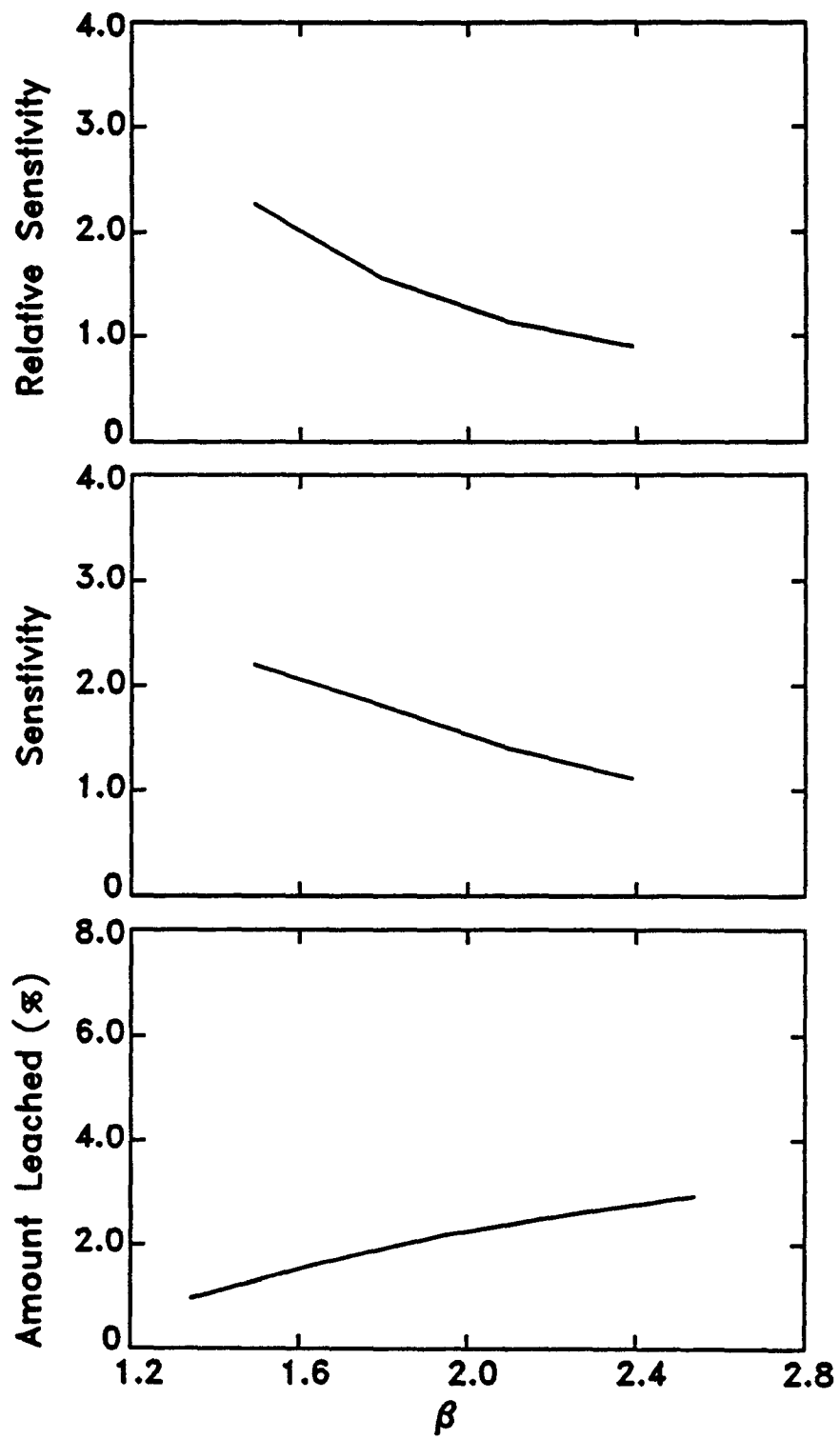
Figure 8.44. Sensitivity of amount leached to the van Genuchten $\beta$ parameter.
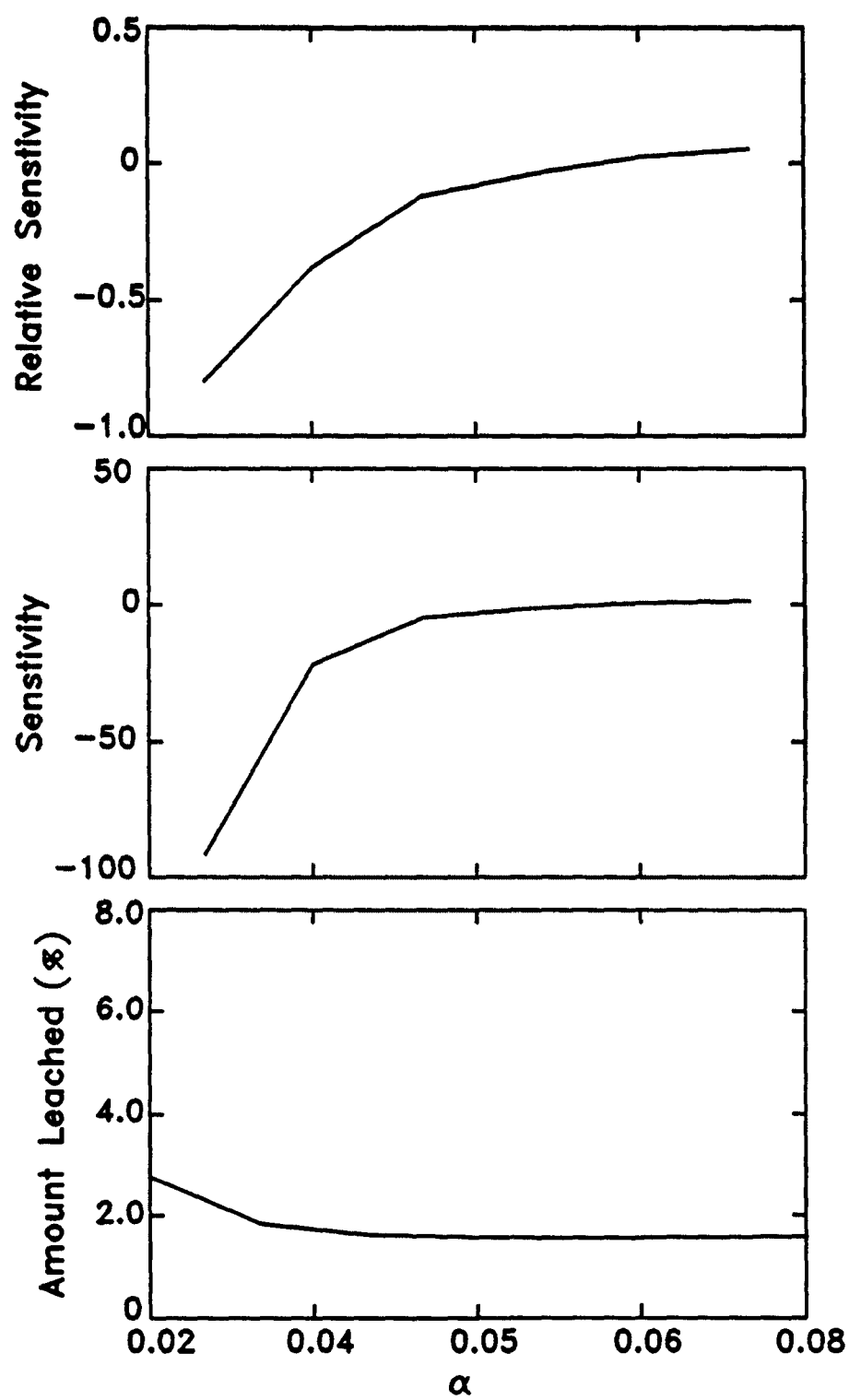
Figure 8.45. Sensitivity of amount leached to the van Genuchten α parameter.

Figure 8.46. Sensitivity of amount leached to dispersivity.

Figure 8.47. Sensitivity of amount leached to diffusion coefficient.

Figure 8.48. Sensitivity of amount leached to root uptake potential, $h_{50}$.
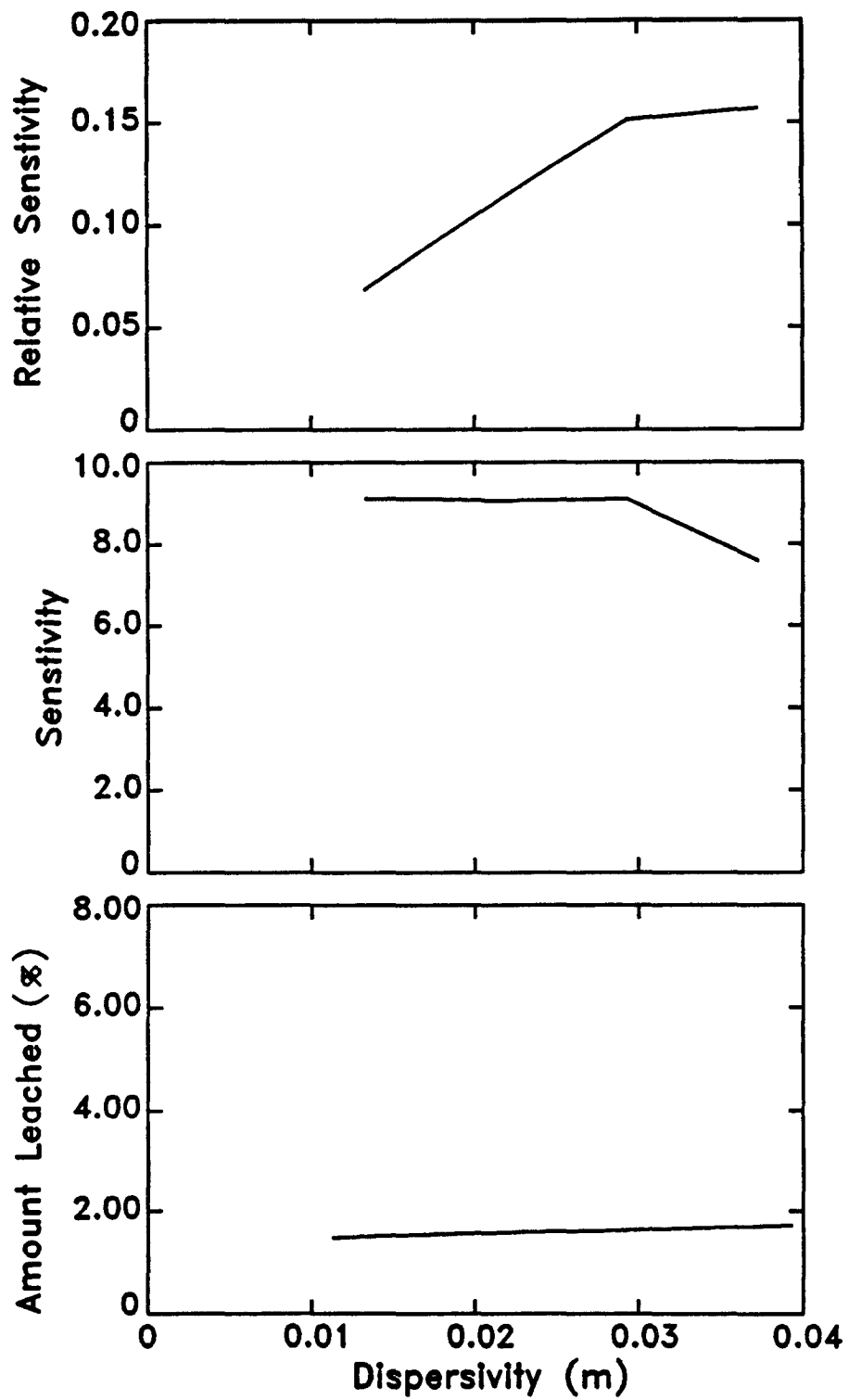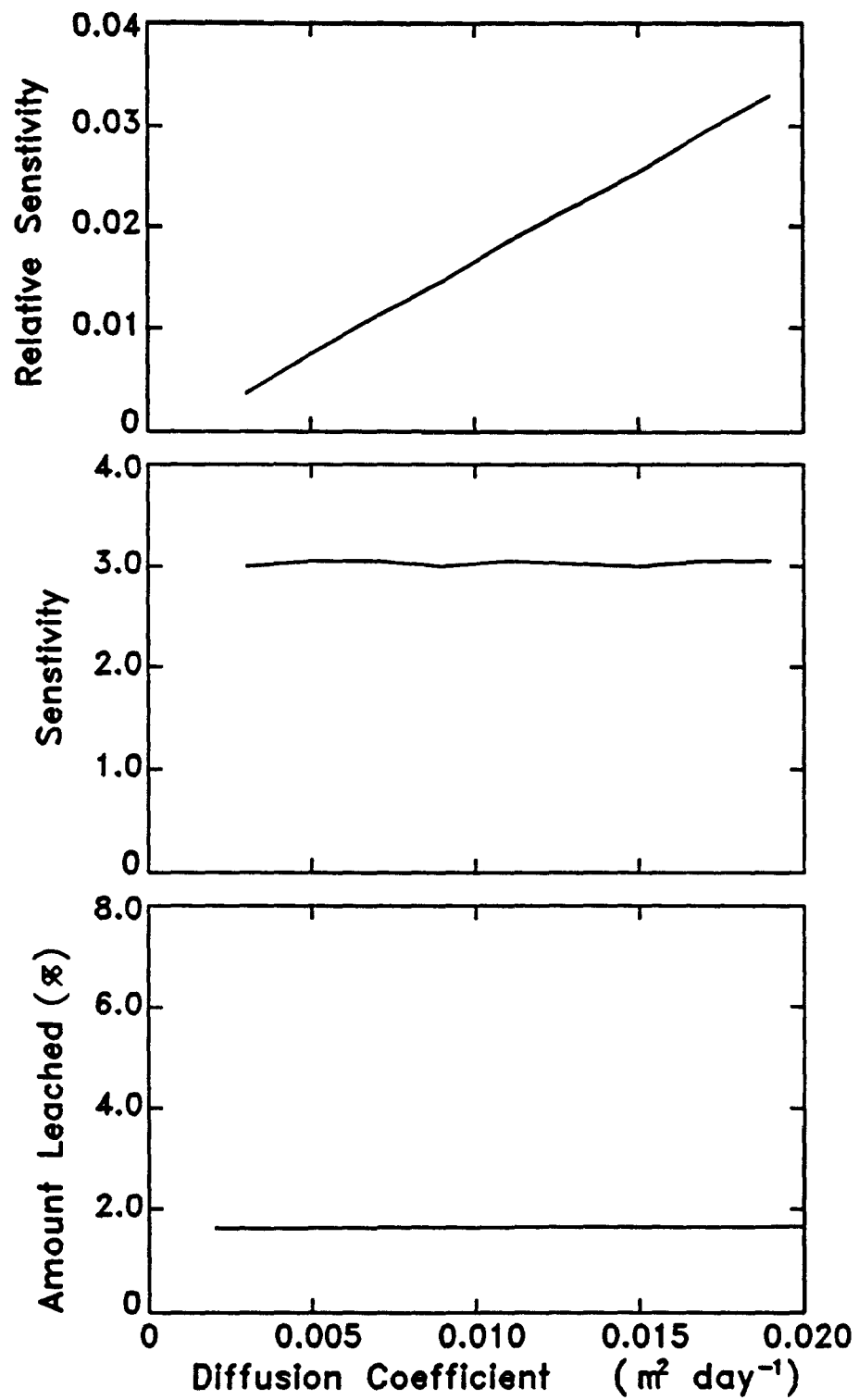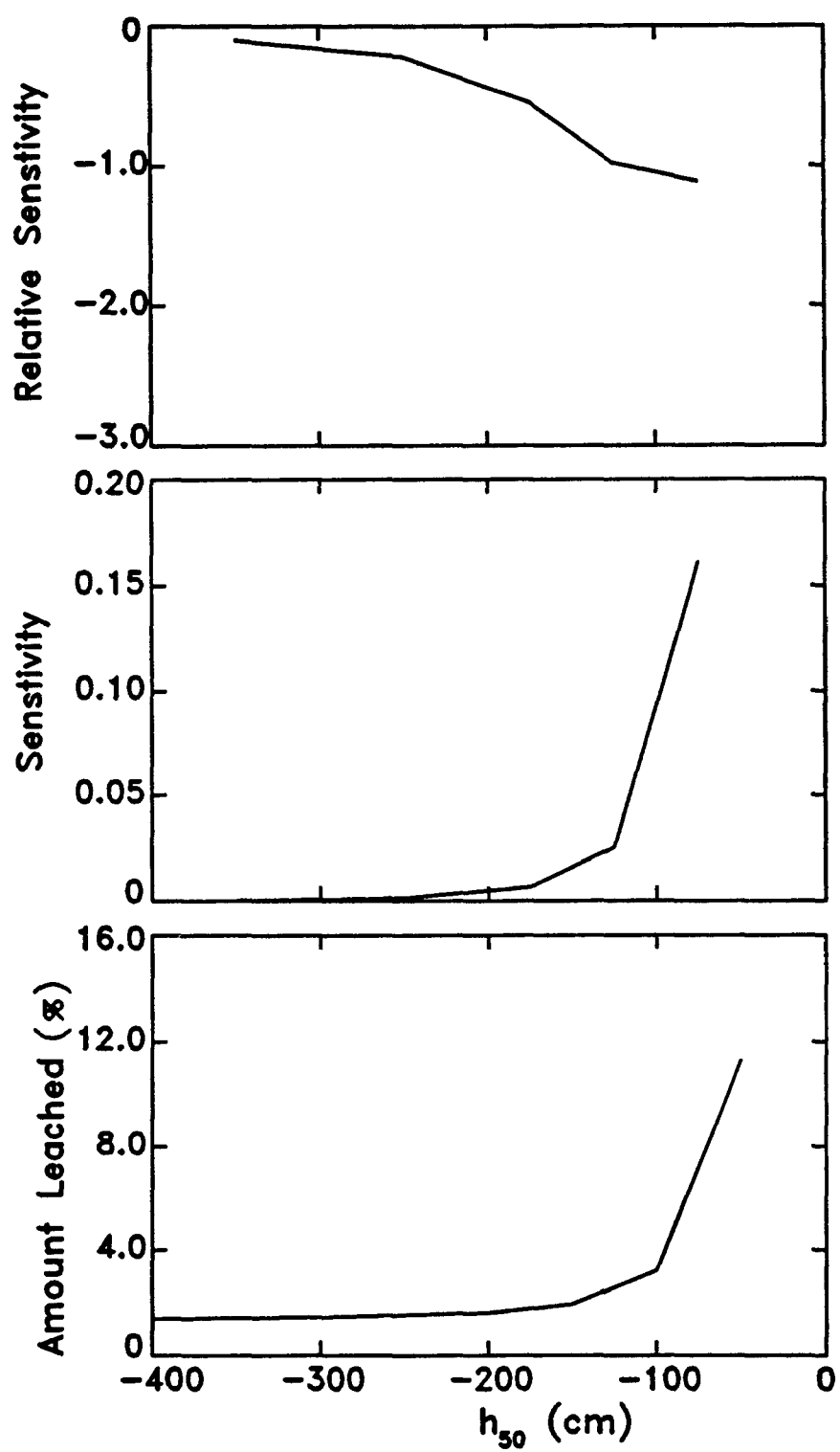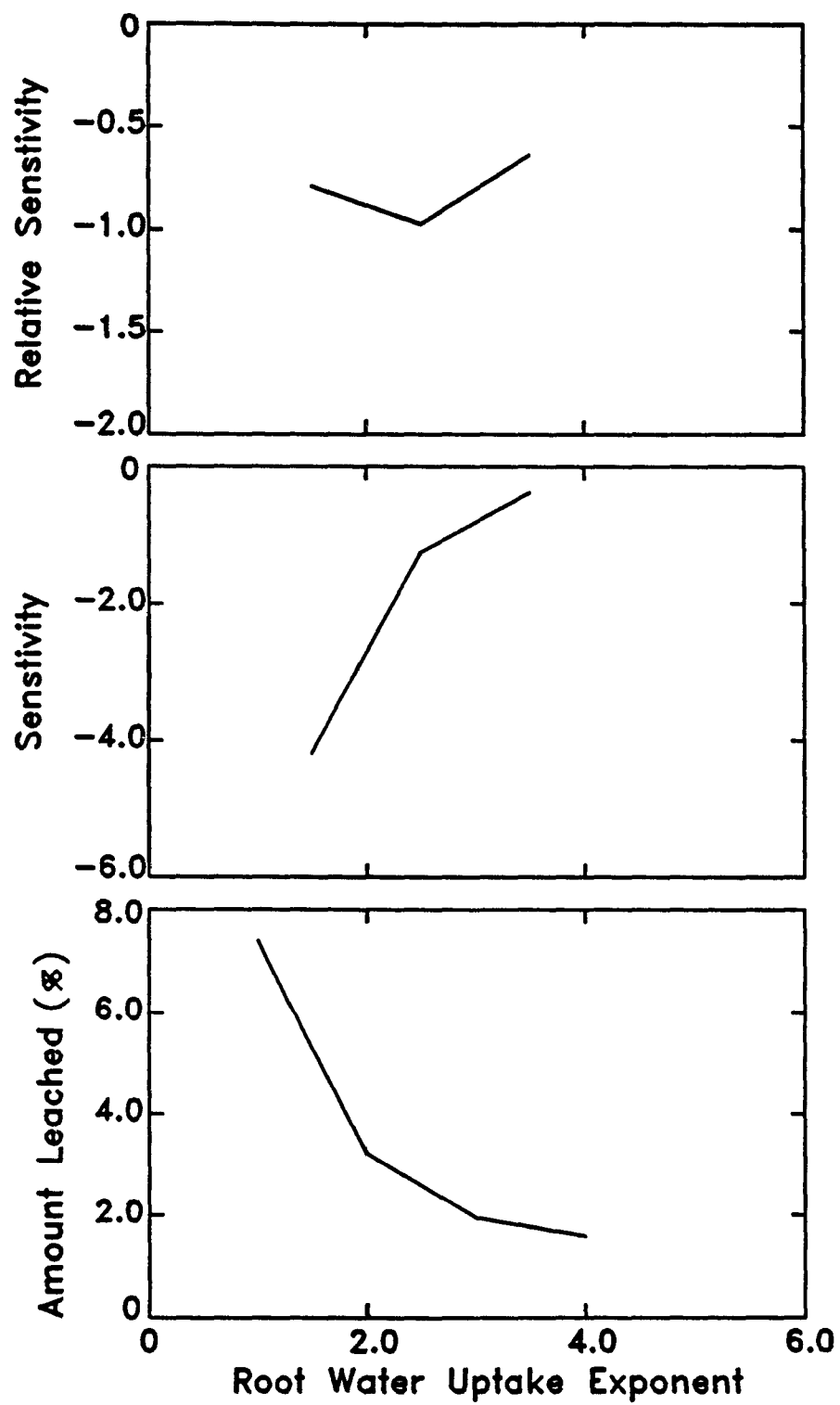
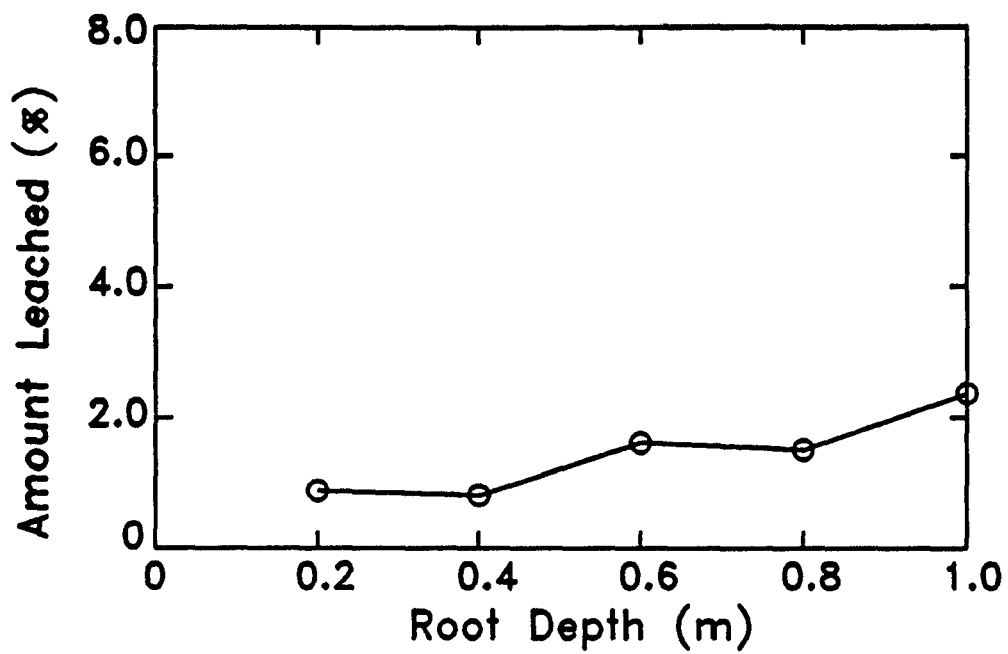Figure 8.49. Sensitivity of amount leached to root uptake exponent.

Figure 8.50. Amount of pollutant leached below 2-m depth as a function of root depth.

# SECTION 9

## UNCERTAINTY ANALYSIS

The first part of this report deals with the sensitivity of model output to changes in single input parameters. This section will show overall model uncertainty due to combined uncertainty in model parameters. Monte Carlo techniques were used in this analysis. This approach characterizes model uncertainty by making many simulations with the model using different input parameters selected at random from distributions of the real parameters. This results in many model outputs which can then be summarized probabilistically to provide insight on model uncertainty. The technique can be applied to any model, but it requires many computations. This section includes results for RITZ. Figures 7.5 to 7.13 show uncertainty in travel time due to uncertainty in weather for CMLS.

## Uncertainty Analysis for RITZ Model

In order to conduct Monte Carlo simulations for estimating model uncertainty, we need to generate many sets of model input parameters with means, standard deviations, and correlations characteristic of the actual distributions for these parameters. A multivariate data generating procedure using principle components (Haan, 1977; Zhang et al., 1993) was used.

Since a uniform soil profile is assumed in RITZ, the depth weighted average soil properties for the Norfolk soil were used. The probability distributions of the soil parameters were determined using soil data from 87 soil profiles and ten soil series of sand from Florida. The bulk density, saturated conductivity, organic carbon content, saturated water content, and Clapp-Hornberger constant were best described by a log normal distributions. The means and standard deviations of soil properties from the analysis are given in Table 9.1. Statistics for bulk density, saturated water content, and Clapp-Hornberger constant for Norfolk sand obtained from undisturbed soil cores (Quisenberry et al., 1987) are included in Table 9.1 along with values from Jury (1986). The depth weighted saturated hydraulic conductivity values from in-situ field data show a large variability with a coefficient of variation of 2.07. This variability includes variability across depths and sites as well as experimental error.

The range of values for the partition coefficient and half-life of benzene are also shown in Table 9.1. A wide range of values for these properties were found in the literature. Normal distributions were assumed for these two parameters.

The statistical characteristics of the soil and chemical parameters used in the Monte Carlo analysis are shown in Table 9.2. Soil properties and chemical properties were assumed to be uncorrelated. If the generated saturated water content exceeded the soil porosity based on the generated bulk density, the set of generated parameters was rejected and another set was generated. One hundred sets of input parameters were generated for Monte Carlo simulation.

Results of incorporating the variability and uncertainty of soil parameters into RITZ for the standard scenario defined in Table 5.1 are shown in Figure 9.1. This figure shows the concentration of the pollutant in water as a function of time for three probability levels. Consider the curve labeled 95% probability. At any instant of time, the predicted concentration of pollutant at the 2-m depth was less than the plotted value for 95% of the simulations. Likewise, the predicted concentration of the pollutant in water was less than the plotted values for 50% and 5% of the simulations for the lines labeled 50% probability and 5% probability, respectively. These curves indicate that the maximum concentration has values in the range of 0.06 to 0.64 g $m^{-3}$ for 90% of the simulations. Five percent of the predicted values are greater than 0.64 g $m^{-3}$ and 5% are less then 0.06 g $m^{-3}$. Figure 9.2, 9.3, and 9.4 are cumulative probability plots for travel time, pulse width, and amount leached below the 2-m depth. Figure 9.2 shows the probability that the travel time will be less than

172

Table 9.1. Variability of soil properties.

| Parameter | Mean | CV | Source |
|---|---|---|---|
| Bulk Density (Mg m$^3$) | 1.59 | 0.05-0.06 | Florida soils[1] |
| Bulk Density (Mg m$^3$) | 1.20-1.67 | 0.03-0.26 | Jury, 1986 |
| Bulk Density (Mg m$^3$) | 1.38-1.47 | 0.08-0.20 | Staffer, 1988 |
| Bulk Density (Mg m$^3$) | 1.64 | 0.02 | Norfolk sand,undisturbed Quisenberry et. al., 1987 |
| Saturated Conductivity (m day$^{-1}$) | 0.67-14.3 | 0.73-14.9 | Florida soils[1] |
| Saturated Conductivity (m day$^{-1}$) | 0.04-3.16 | 0.48-3.20 | Jury, 1986 |
| Saturated Conductivity (m day$^{-1}$) | 1.5-2.56 | 1.10-1.30 | Staffer, 1988 |
| Saturated Conductivity (m day$^{-1}$) | 0.26 | 2.07 | Norfolk sand,in-situ Quisenberry et. al., 1987 |
| Organic Carbon (%) | 0.21-1.23 | 0.30-0.74 | Florida soils[1] |
| Organic Carbon (%) | 0.04-2.59 | 5.75-0.60 | Staffer, 1988 |
| Saturated Water Content (m$^3$ m$^{-3}$) | 0.36-0.47 | 0.04-0.11 | Florida soils[1] |
| Saturated Water Content (m$^3$ m$^{-3}$) | 0.38 | 0.03 | Norfolk sand,undisturbed Quisenberry et. al., 1987 |
| Saturated Water Content (m$^3$ m$^{-1}$) | 0.35 | 0.05 | Norfolk sand,in-situ Quisenberry et. al., 1987 |
| Porosity | 0.37-0.53 | 0.11-0.07 | Jury, 1986 |
| Clapp-Hornberger Constant | 2.06-4.69 | 0.08-0.17 | Florida soils[1] |
| Clapp Hornberger Constant | 11.6 | 0.19 | Norfolk sand, undisturbed Quisenberry et. al., 1987 |

**Table 9.1. Continued.**

| Parameter | Mean | CV | Source |
|---|---|---|---|
| Koc ($cm^3 g^{-1}$) | 19000 | 0.65 | Pyrone in sand sediments Karickhoff and Brown, 1979 |
| Koc ($cm^3 g^{-1}$) | 23000 | 0.73 | Methoxychlor in sand fraction Karickhoff and Brown, 1979 |
| Koc ($cm^3 g^{-1}$) | 120000 | 0.00 | Pyrone in clay fraction Karickhoff and Brown, 1979 |
| Koc ($cm^3 g^{-1}$) | 83000 | 0.16 | Methoxychlor in clay fraction Karickhoff and Brown, 1979 |
| Koc ($cm^3 g^{-1}$) | 83,92,107 | $0.11^2$ | Benzene in soils Karickhoff and Brown, 1979 Rogers et al., 1980 Chen et al., 1992 |
| Half Life (days) | 104,106 | -- | benzene in solution Zoetman et al., 1981 Goldsmith and Balderson, 1988 |
| Half Life (days) | 231 | -- | benzene in soil Rifai et al., 1988 |
| $K_d$ ($cm^3 g^{-1}$) | 2.01 | 0.31 | Jury, 1986 |

1. Ten Florida soil series are: Albany sand, Blanton sand, Bonifay fine sand, Chobee sandy loam, Manatee sandy loam, Myakka sand, Orangeburg sandy loam, Pomona sand, Wauchula sand, and Winder loamy sand.

2. Calculated from three values at the left.

Table 9.2. Statistics of parameters used in RITZ uncertainty analysis

| | $\rho$ | $K_s$ | OC | $\theta_s$ | CH | $K_{oc}$ | $t_{1/2}$ |
|---|---|---|---|---|---|---|---|
| Mean | 1.65 | 0.19 | 0.14 | 0.378 | 4.9 | 80 | 104 |
| Coef. of Variation, CV | 0.05 | 2.00 | 0.40 | 0.05 | 0.14 | 0.20 | 0.20 |
| Log mean | 0.4995 | -2.465 | -2.040 | -0.974 | 1.580 | - | - |
| Log CV | 0.10 | 0.593 | -0.189 | -0.051 | 0.088 | - | - |

Correlation Matrix[1]

| | $\rho$ | $K_s$ | OC | $\theta_s$ | CH | $K_{oc}$ | $t_{1/2}$ |
|---|---|---|---|---|---|---|---|
| Bulk Density, $\rho$ | 1.00 | | | | | | |
| Sat. Conductivity, $K_s$ | -0.761 | 1.00 | | | | | |
| Organic Carbon, OC | -0.189 | 0.012 | 1.00 | | | | |
| Sat. Water Content, $\theta_s$ | -0.872 | 0.572 | 0.227 | 1.00 | | | |
| Clapp-Hornberger Const, CH | 0.726 | -0.731 | -0.374 | -0.695 | 1.00 | | |
| Partition Coefficient, $K_{oc}$ | 0.0 | 0.0 | 0.0 | 0.0 | 0.0 | 1.00 | |
| Pollutant Half-life, $t_{1/2}$ | 0.0 | 0.0 | 0.0 | 0.0 | 0.0 | 0.0 | 1.00 |

1. Correlation matrix for soil properties was obtained from log transformed data of Blanton Sand, FL.

the travel time plotted. The figure indicates that the travel time for the pollutant ranges from approximately 940 to 1460 days with 90% of the values falling in the 980 to 1370 day range. Figure 9.3 shows the probability that the pulse width will be less than the pulse width plotted. The computed pulse width varies from 950 to 1050 days with 90% of the values in the between 960 and 1020 days. Figure 9.4 shows the probability that the amount leached will be less than amounts plotted. The predicted leaching varies from 0.009% to 0.2% of the amount applied with 90% of the values in the range of 0.02% to 0.2% of the amount applied. Clearly, there is a large uncertainty in model predictions due to only soil properties.

Figures 9.5, 9.6, 9.7, and 9.8 show results of the uncertainty analysis due to uncertainty in the partition coefficient and half-life of the pollutant. The maximum concentrations on the 95%, 50%, and 5% probability curves are 0.7, 0.21, and 0.008 g m$^{-3}$, respectively. This range is slightly larger than those for soil properties. Figure 5.6 shows that the travel time varies from 970 to 1310 days for these simulations with 90% of the values in the range of 1050 to 1220 days. Pulse width takes on values of 950 to 1010 days due to uncertainty in these chemical properties. Ninety percent of the values are in the range of 970 to 1000 days. The amount leached varies over more than 4 orders of magnitude with 90% of the leaching amounts in the range of 0.004 to 0.4 % of the amount applied (Figure 9.8). In this case the uncertainty in amount leached due to chemical properties exceeds that due to soil properties.

Simulations for systems incorporating uncertainty in both soil and chemical properties produced results shown in Figures 9.9, 9.10, 9.11, and 9.12. The ranges of values predicted here exceed those for soil and chemical properties individually. Large differences in predicted concentrations are shown in Figure 9.9 with nearly 150-fold differences in concentration between the 5% and 95% lines. Travel times take on values from 950 to 1540 days with 90% of the values in the 960 to 1350 day range. Pulse widths vary from 950 to 1060 days with 90% of the simulations between 955 to 1020 days. Calculated amounts leached beyond the 2-m depth have values of 0.0003 to 0.8%. Ninety percent of the values lie in the range of 0.004 to 0.5%.

## Summary

The uncertainties presented come as a result of uncertainties in soil properties, organic carbon partition coefficient, and half-life of the pollutant. These uncertainties would increase if all of the chemical properties, oil properties, and site characteristics were included in the analysis. One site characteristic with a large degree of uncertainty is the weather and hence the infiltration and evapotranspiration at a site. Results shown for CMLS (Figures 7.2 to 7.13) and for HYDRUS (Figure 8.1) indicate the significance of weather uncertainty on the predictions. Haan and Nofziger (1991) presented the results of a detailed simulation study that evaluated the impact of variations in weather sequences on the transport of a solute through the soil profile. They demonstrated that large differences in the times required for a solute to reach a given depth in the soil profile and in the concentrations of the solute that at that depth exist due entirely to differences in weather sequences at the specific site. Zhang et al (1993) presents an analysis of uncertainty for CMLS as well as implications of this uncertainty for model use and soil sampling. They suggest that results from field experiments and modeling studies involving only one weather sequence are of little value in making decisions about future behavior of a chemical in a soil system.

The fact that these uncertainties exist must be incorporated into our use of models. It is more realistic to think in terms of the probability that a certain type of behavior will take place rather than attempting to say whether or not that behavior will occur. Moreover, the fact that soil properties vary spatially within a mapping unit must be acknowledged. We will be better served to simulate movement in that unit for the many different sets of properties expected and to summarize the model predictions than to attempt to derive some representative set of parameters for the region hoping that the model output for that set will describe the entire region. By simulating results for many sets of parameters expected in the area, we can determine the contaminant leaching for the area and gain knowledge of the likely range of leaching possible. All of this

information can then be used in the decision-making process. Uncertainties must also be included when validating models experimentally.

Finally, the uncertainty in model predictions due to uncertainty in input parameters represents only part of the overall uncertainty. This analysis does not incorporate uncertainty due to model simplifications of real phenomena, errors in understanding that phenomena, or errors in solving the simplified problem.
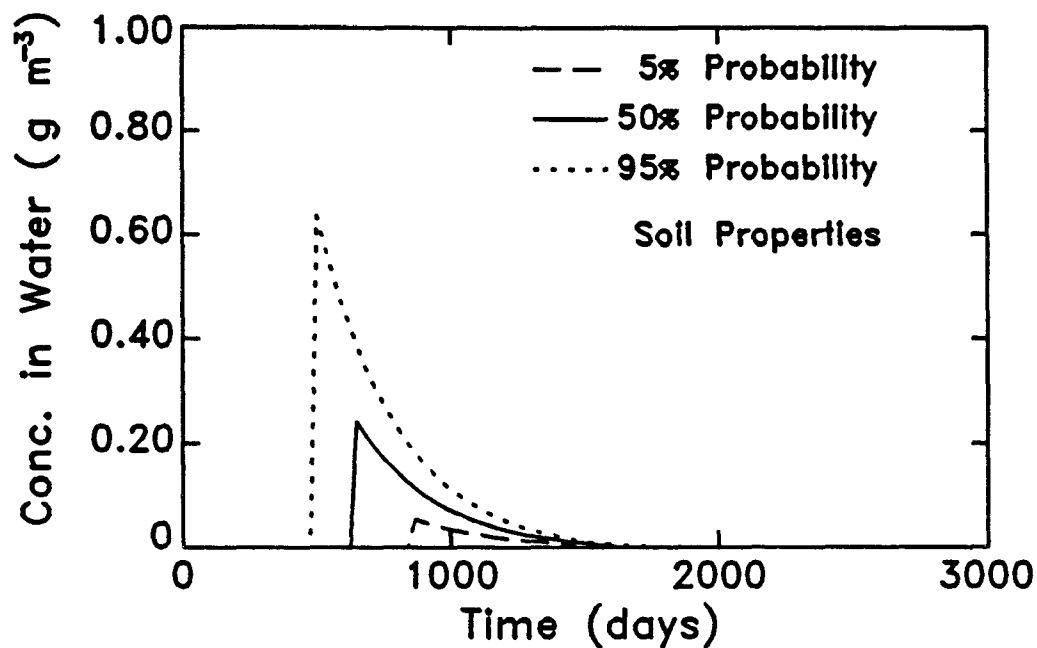
Figure 9.1. Concentration of pollutant at the 2-m depth which is not exceeded for 5%, 50%, and 95% of the simulations which incorporate uncertainty in soil properties.
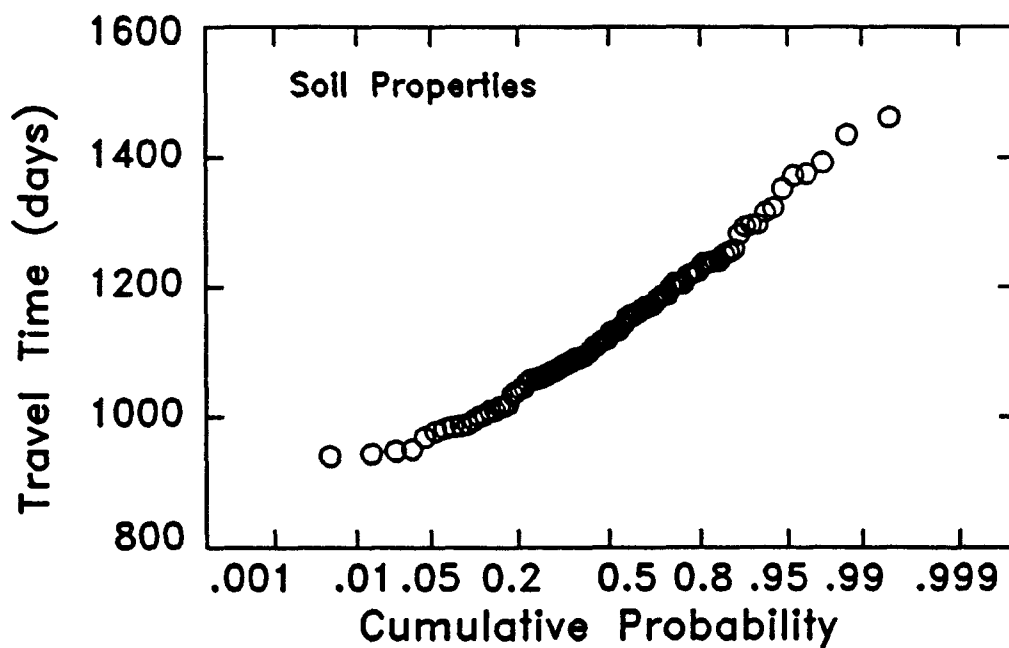


Figure 9.2. Probability that different travel times will not be exceeded based on uncertainty in soil properties.
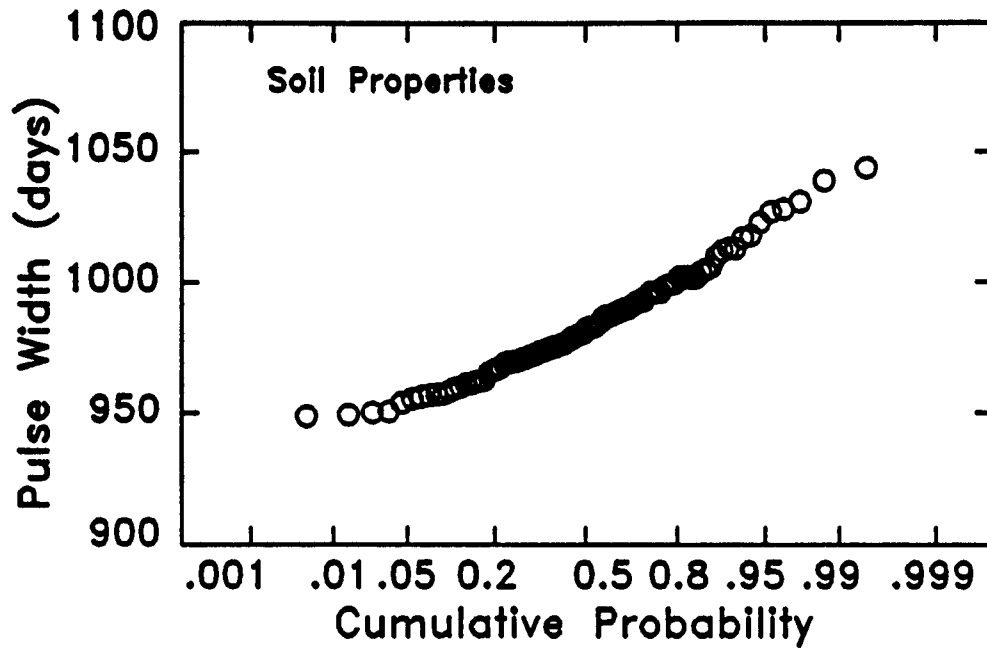
178

Figure 9.3. Probability that different pulse widths will not be exceeded based on uncertainty in soil properties.
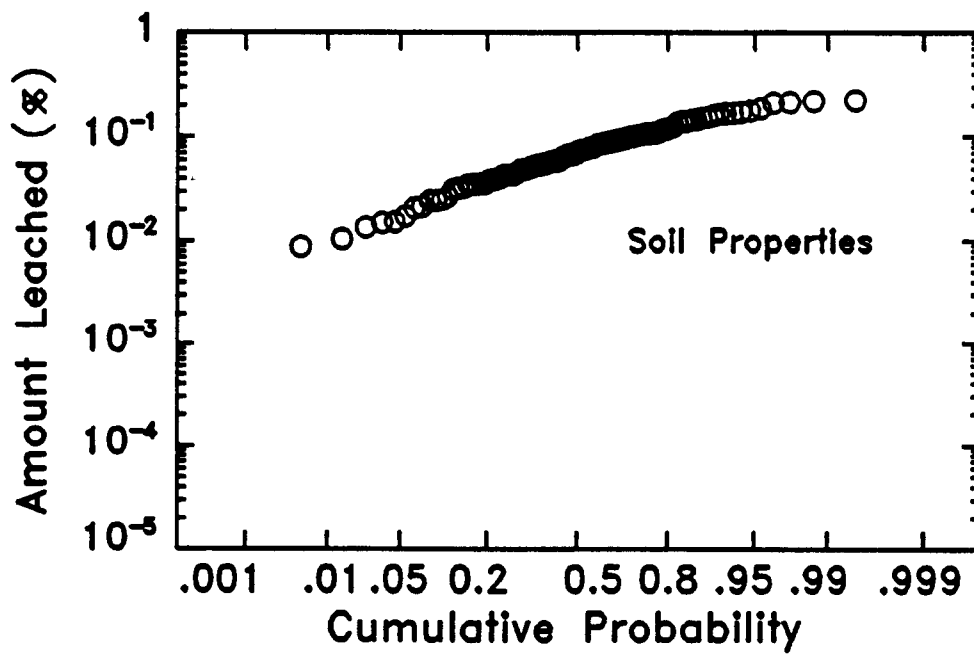


Figure 9.4. Probability that different amounts leached will not be exceeded based on uncertainty in soil properties.

179

Figure 9.5. Concentration of pollutant at the 2-m depth which is not exceeded for 5%, 50%, and 95% of the simulations which incorporate uncertainty in selected chemical properties.



Figure 9.6. Probability that different travel times will not be exceeded based on uncertainty in selected chemical properties.

Figure 9.7. Probability that different pulse widths will not be exceeded based on uncertainty in selected chemical properties.



Figure 9.8. Probability that different amounts leached will not be exceeded based on uncertainty in selected chemical properties.
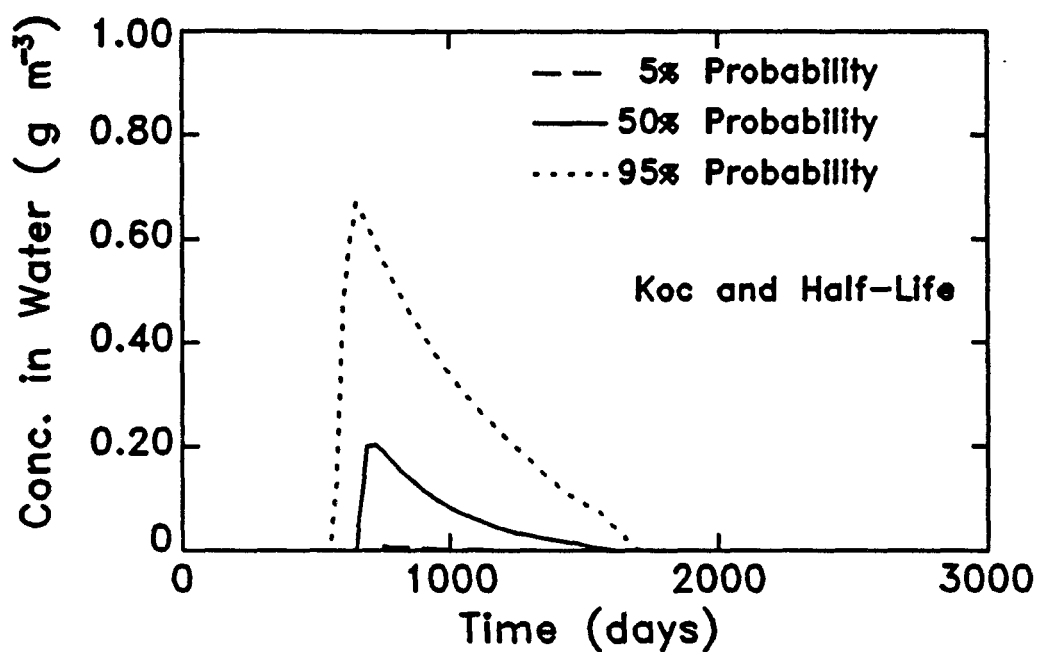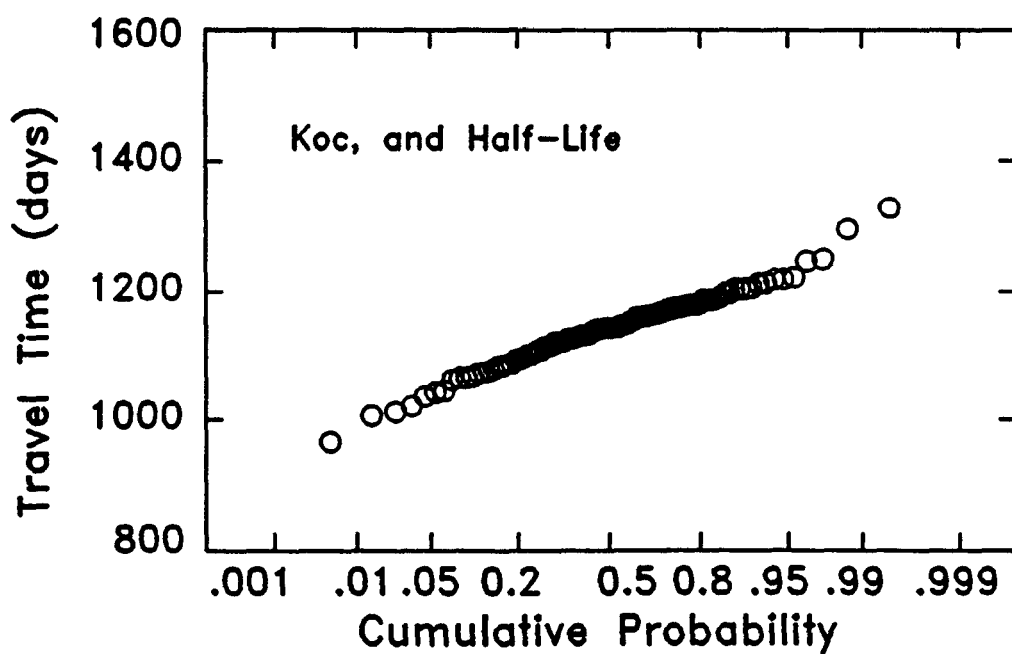
Figure 9.9. Concentration of pollutant at the 2-m depth which is not exceeded for 5%, 50%, and 95% of the simulations which incorporate uncertainty in soil and chemical properties.



Figure 9.10. Probability that different travel times will not be exceeded based on uncertainty in soil and chemical properties.
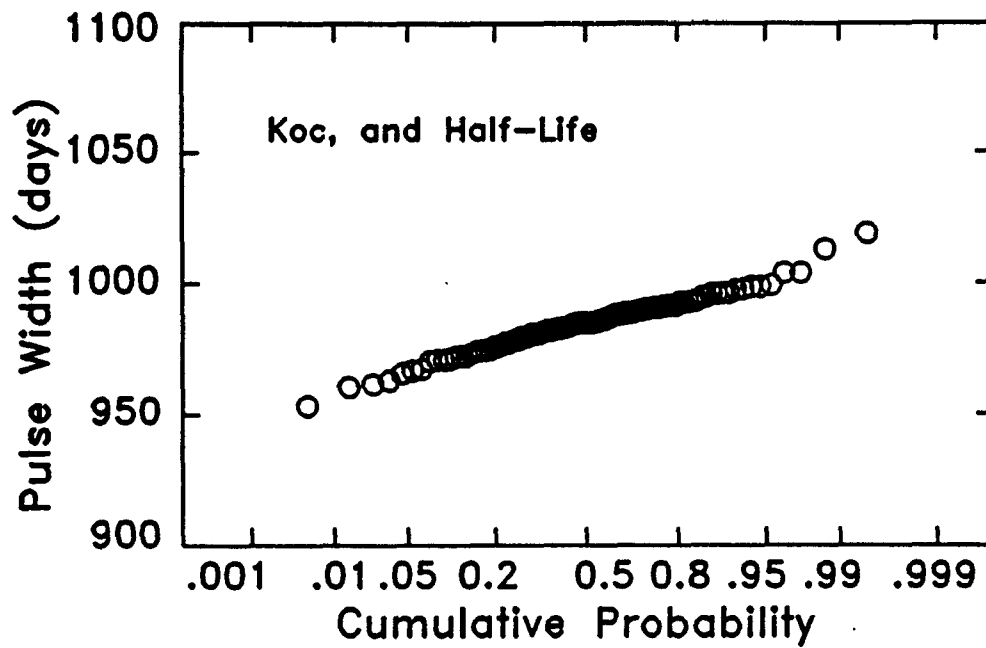
Figure 9.11. Probability that different pulse widths will not be exceeded based on uncertainty in soil and chemical properties.
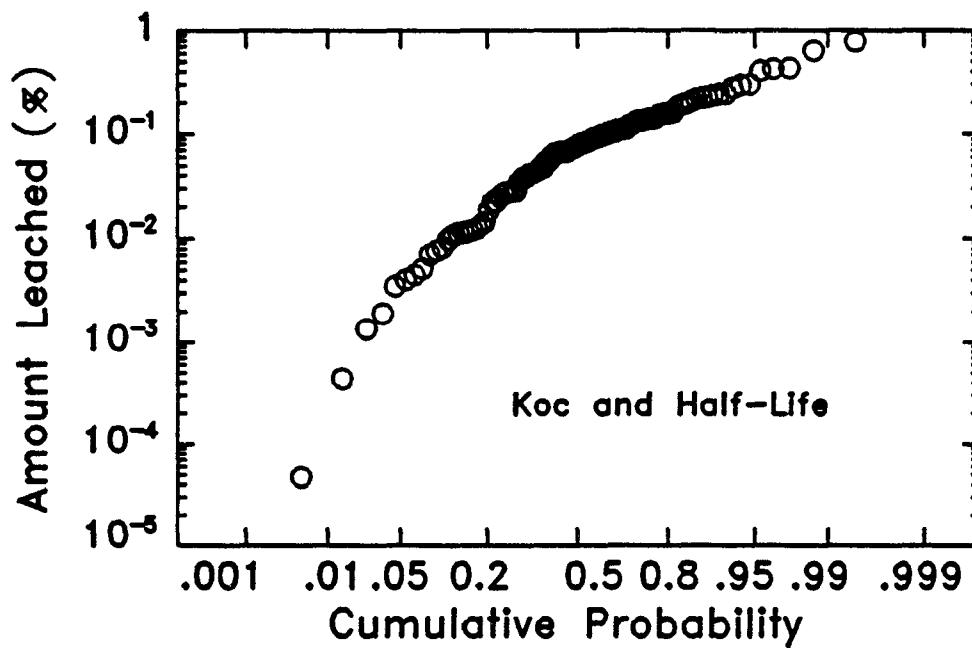


Figure 9.12. Probability that different amounts leached will not be exceeded based on uncertainty in soil and chemical properties.
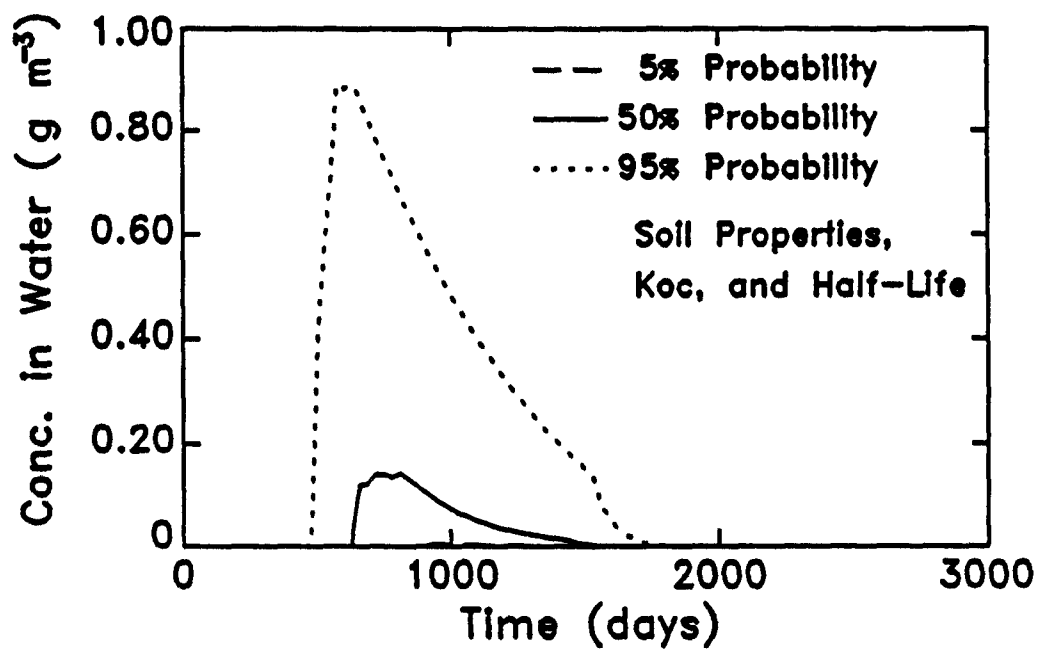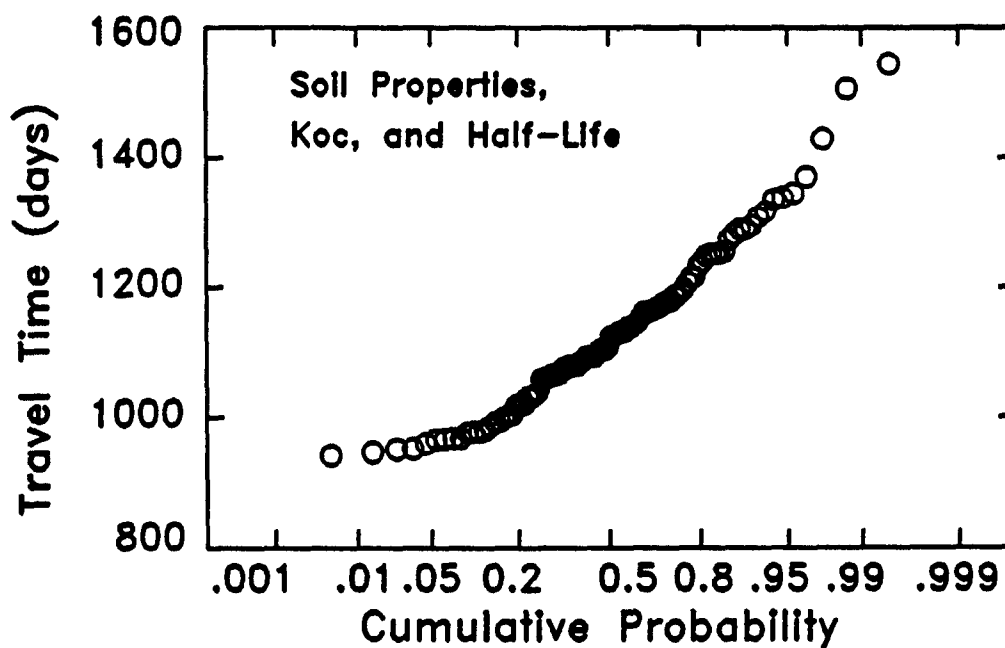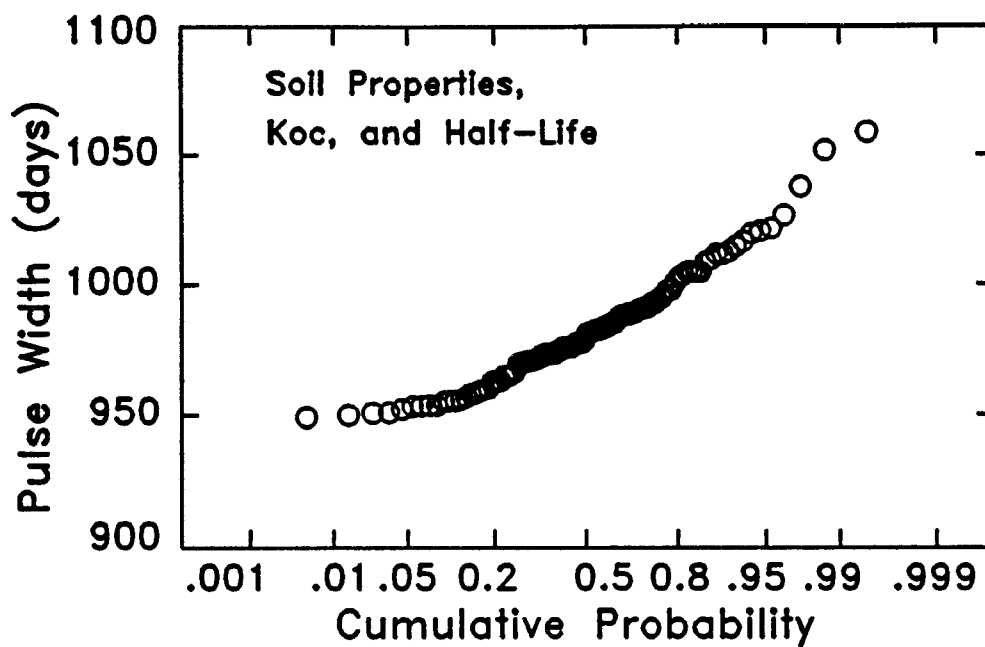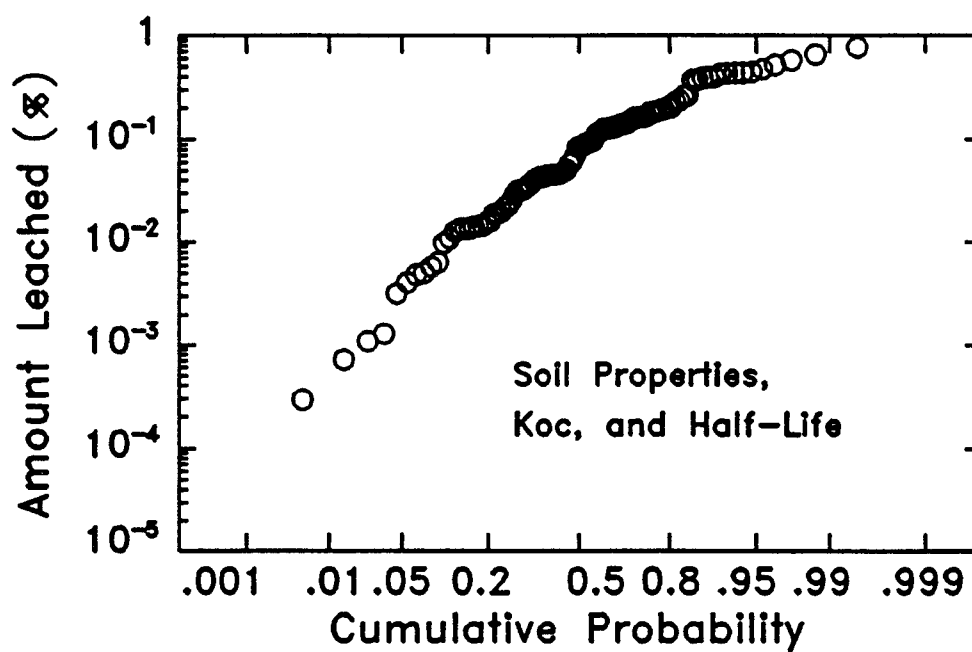
# REFERENCES

Alvarez, P.J.J., and T.M. Vogel. 1991. Substrate interaction of benzene, toluene and para-xylene during microbial degradation by pure cultures and mixed culture aquifer slurries. Appl. Environ. Microbiol., 57:2981-2985.

Blaney, H.F., and W.D. Criddle. 1962. Determining consumptive use and irrigation water requirements. USDA Tech. Bull. 1275. 59pp.

Bond, W.J., and I.R. Phillips. 1990. Approximate solutions for cation transport during unsteady, unsaturated soil water flow. Water Resour. Res. 26:2195-2205.

Burges, S.B., and D.P. Lettenmaier. 1975. Probabilistic methods in stream quality management. Water Resour. Bull. 11(1):115-130.

Cawlfield, J.D., and M.-C. Wu. 1993. Probabilistic sensitivity analysis for one-dimenstional reactive transport in porous media. Water Resour. Res. 29:661-672.

Chen, Y.-M., L.M. Abriola, P.J.J. Alvarez, P.J. Anid, and T.M. Vogel. 1992. Modeling transport and biodegradation of benzene and toluene in sandy aquifer material: comparison with experimental measurements. Water Resour. Res. 28:1833-1847.

Clapp, R.B., and G.M. Hornberger. 1978. Empirical equations for some soil hydraulic properties. Water Resour. Res. 14:601-604.

Dettinger, M.D., and J.L. Wilson. 1981. First order analysis of uncertainty in numerical models of groundwater flow. Part 1. Mathematical development. Water Resor. Res. 17:149-161.

Goldsmith, C.D. Jr., and R.K. Balderson. 1988. Biodegradation and growth kinetics of enrichment isolates on benzene, toluene, and xylene. Water. Sci. Tech. 20:505-507.

Haan, C.T. 1977. Statistical methods in hydrology. Iowa State Univ. Press, Ames, Iowa.

Haan, C.T., and. D.L. Nofzifer. 1991. Characterizing chemical transport variability due to natural weather sequnces. Agronomy Abstract. p.220.

Jarvis, N. 1991. MACRO- A model of water movement and solute transport in macroporous soils. Dept. of Soil Sci., Swedish Univ. of Agric. Sci., Uppsala, Sweden.

Jury, W.A. 1986. Spatial variability of soil properties. p. 245-269. In S.C. Hern and S.M. Melancon (ed.) "Vadose Zone Modeling of Organic Pollutants", Lewis Publ. Inc., Michigan.

Karickhoff, S.W., and D.S. Brown. 1979. Sorption of hydrophobic pollutants on natural sediments. Water Research 13:241-248.

Knopman, D.S. and C.I. Voss. 1987. Behavior of sensitivities in the one-dimensional advection-dispersion equation: implications for parameter estimation and sampling design. Water Resour. Res. 23:253-272.

Knopman, D.S., and C.I. Voss. 1988. Further comments on sensitivities, parameter estimation, and sampling design in one-dimensional analysis of solute transport in porous media. Water Resourc. Res. 24:225-238.

184

Kool, J.B., and M.Th. van Genuchten. 1991. HYDRUS: One-dimensional variably saturated flow and transport model, including hysteresis and root water uptake. U.S. Salinity Lab., USDA-ARS, Riverside, California.

Loague, K., R.E. Green, T.W. Giambelluca, T.C. Liang, and R.S. Yost. 1990. Impact of uncertainty in soil, climatic, and chemical information in a pesticide leaching assessment. J. Contam. Hydrol. 5:171-194.

McCuen, R.H. 1973. The role of sensitivity analysis in hydrologic modeling. J. Hydrol. 18:37-53.

Newman, S.P. 1980. A statistical approach to the inverse problem of aquifer hydrology. 3. Improved solution method and added perspective. Water Resour. Res. 16:331-346.

Nichols W.E., and M.D. Freshley. 1993. Uncertainty analysis of unsaturated zone travel time at Yucca Mountain. Ground Water 31:293-301.

Nofziger, D.L., and A.G. Hornsby. 1986. A microcomputer-based management tool for chemical movement in soil. Applied Agric. Research 1:50-57.

Nofziger, D.L. and A.G. Hornsby. 1988. Chemical movement in layered soils: user's manual. Department of Agronomy, Oklahoma State University. Computer Software Series CSS-30 and University of Florida. IFAS. Cir. 780, 44 pp.

Nofziger, D.L., J.R. Williams, and Thomas E. Short. 1988. Interactive simulation of the fate of hazardous chemicals during land treatment of oily wastes: RITZ user's guide. Report No. EPA/600/8-88-001, U.S. Environmental Protection Agency. 61 pp.

Quisenberry, V.L., D.K. Cassel, J.H. Dane, and J.C. Parker. 1987. Physical characteristics of soils of the southern region Norfolk, Dothan, Wagram, and Goldsboro series. Southern Cooperative Series Bulletin 263. South Carolina Agricultural Experiment Station, Clemson University.

Richardson, C.W., and D.A. Wright. 1984. A model for generating daily weather variables. U.S. Department of Agriculture, Agricultural Research Service, ARS-8, 83p.

Rifai, H.S., P.B. Bedient, J.T. Wilson, K.M. Miller, and J.M. Armstrong. 1988. Biodegradation modeling at aviation fuel spill site. J. Environ. Eng. 114:1007-1029.

Rogers, R.D., J.C. McFarlane, and A.J. Cross. 1980. Adsorption and desorption of benzene in two soils and montmorillonite clay. Environ. Sci. Technol. 14:457-460.

Short, E.S. 1985. Movement of contaminants from oily wastes during land treatment. Proceedings of Conference on Environmental and Public Health Effects of Soils Contaminated with Petroleum Products, Univ. of Massachusetts in Amherst, Massachusetts, Oct. 30-31, 1985.

Staffer, M.J. 1988. Estimating confidence bands for soil-crop simulation models. Soil Sci. Soc. Am.J. 52:1782-1789. Sensitivity of RITZ to Henry's constant and diffusion coefficient of chemical in air:

Stevens, D.K., W.J. Grenney, and Z. Yan. 1989. VIP: A model for the evaluation of hazardous substances in the soil. Civil and Environmental Engineering Department, Utah State University, Logan, Utah.

Stuart, B.J., G.F. Bowlen, and D.S. Kosson. 1991. Competitive sorption of benzene, toluene, and the xylenes onto soil. Environ. Progress. 10:104-109.

Swartzendruber, Dale. 1960. Water flow through a soil profile as affected by the least permeable layer. J. of Geophysical Research 65:4037-4042.

USDA-SCS. 1972. National engineering handbook. Hydrology section 4, Ch.4-10. USDA. Washington, DC.

van Genuchten, M.Th. 1980. A closed-form equation for predicting the hydraulic conductivites of unsaturated soils. Soil Sci. Soc. Am. J. 44:892-898.

van Genuchten, M.Th., F.J. Leij, S.R. Yates, and J.R. Williams. 1991. The RETC codes for quantifying the hydraulic functions of unsaturated soils. United States Environmental Protection Agency. EPA/600/2-91/065.

Zhang, H., C.T. Haan, and D.L. Nofziger. 1993. An approach to estimating uncertainties in modeling transport of solutes through soils. J. Contaminant Hydrol. 12:35-50.

Zoetman B.C.J, E. De Greef, and F.J.J. Brikmann. 1981. Persistency of organic chemicals in ground water, lessons from soil pollution incidents in the Netherlands. Sci. Tot. Environ. 21:187-202.

# APPENDIX

## Problems Encountered in Using Models

This section describes some problems we encountered in using the computer programs. We did our best to verify that these problems are real and are not just the result of our inability to correctly use the models.

## VIP

VIP is distributed as an executable interactive program. To facilitate the many simulations we needed to make for this analysis we requested and obtained source code for a batch version of the program. This was compiled into a batch program. We found the batch version produced results in agreement with the interactive version when the oil content of the sludge was zero, but it failed when oil was present. With oil present, degradation rapidly decreased to zero and oxygen became limiting even though parameter values defined a system in which oxygen was not limiting. This suggests that the source code provided was not the latest version and included errors not present in the interactive program.

An error was detected in the source code where the definition of subroutine OUT did not include the same number of parameters as the code calling this subroutine. This did not produce a compiler error, but it could produce unexpected results at run time. We cannot determine if this error exists in the interactive code.

The VIP manual states that advection of air is included in the model and an input parameter is provided for the advection velocity in the unsaturated pore space. Our examination of the source code revealed that this component is not implemented and this variable is not used. Also no differences in output from the interactive program were observed for a wide range of values of this input parameter.

Because of the first problem mentioned, we were forced to use the interactive program for our analysis. This program worked as intended, but our efforts were hampered in two ways. First, the program supports a maximum of 150 nodes on the space grid. This limited the size of the grids we could use (See Figure 6.1). The interactive code also limits the number of times at which results can be generated to 50. This was a problem in our analysis since we did not know in advance what times to specify. These limitations may be more evident to us than to general VIP users due to the analysis we were performing.

Finally, we would like to know if the gradual decline in concentration shown in Figure 6.1 is a result of discretization error or if it represents the true solution to the problem. In addition, we would like to know why the concentration decreases more rapidly than that predicted by RITZ (See Figure 6.1 and the discussion of it). Possibly an error exists in RITZ or VIP.

## HYDRUS

HYDRUS supports upper boundary conditions which change in a step-wise manner in time, but only 50 changes can be made during a simulation. This limitation prevents changing boundary conditions on a daily basis if the duration of the time simulated exceeds 50 days. This is a significant limitation for long-term fate studies.

HYDRUS supports different types of boundary conditions at the upper soil surface. We attempted to use a constant flux boundary condition to simulate infiltration of daily rainfall amounts. HYDRUS solved

the flow equation satisfactorily when the specified flux density did not exceed 15% of the saturated conductivity. When this value was exceeded, the model would not converge and would stop. To simulate these daily rainfall amounts, it was necessary to preprocess the rainfall data to guarantee that the flux on any day did not exceed 15% of the saturated conductivity. If the rainfall exceeded that amount, the excess was carried over to the following days.

When making the sensitivity analysis, we often encountered combinations of parameters for which the program would terminate abnormally even though the parameter values appeared to be reasonable and physically consistent.